MOLECULAR MECHANISMS UNDERLYING CARDIAC RYANODINE RECEPTOR DYSFUNCTION IN SUDDEN CARDIAC DEATH

N.L. THOMAS

A thesis submitted in candidature for the degree of Philosophiae Doctor

August 2005

Department of Cardiology
Wales Heart Research Institute
Cardiff University

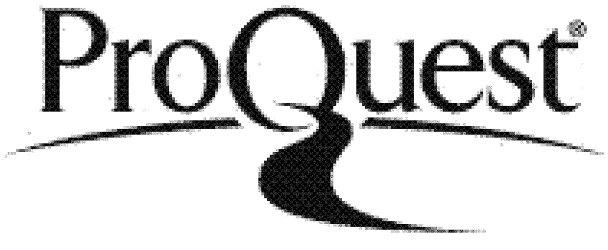

ProQuest LLC
789 East Eisenhower Parkway
P.O. Box 1346
Ann Arbor, MI 48106-1346

DECLARATION

This work has not previously been accepted in substance for any degree and is not being concurrently submitted in candidature for any degree.

Signed Lowri Thomas (candidate)

Date 26/08/05

STATEMENT 1

This thesis is the result of my own investigations, except where otherwise stated. Other sources are acknowledged by footnotes giving explicit references. A bibliography is appended.

Signed Lowri Thomas (candidate)

Date 26/08/05

STATEMENT 2

I hereby give consent for my thesis, if accepted, to be available for photocopying and for inter-library loan, and for the title and summary to be made available to outside organisations

Signed Lowri Thomas (candidate)

Date 26/08/05

Acknowledgements

I would like to thank some people, without whom the work in this thesis would never have been completed.

Firstly, I would like to thank Professor Tony Lai for giving me the opportunity to work as part of his group at the Wales Heart Research Institute.

I am especially grateful to my supervisor Dr Chris George for his guidance at every step of the way through my PhD, from helping me out in the lab to teaching me how to have more confidence in my data – if it wasn't for him, I would've started a career in hotel catering some years ago. Though there is still time for that.

I would also like to thank all of my colleagues on the second floor of the WHRI, especially Dr Debbie Reynolds for her friendship and for being some kind of comedy genius, Dr Chris Saunders for his help and pub quiz knowledge, and Hala Jundi for being a friend, my IT guru and for always giving me a lift home. Thanks also to Dr Spyros Zissimopoulos for letting me steal his bench space and for being in the lab every time I came in on the weekend, and to Dr Lynda Blayney and Michail Nomikos for their company at the UK Ca^{2+} signalling conferences. I must also thank everyone at Medical Microscopy for letting me use their lab twice a week.

Thank you Karolina Taylor and Tom Clarke for asking me if I'd finished my thesis every two weeks since January and to Peter, Wendy and Jan on the ground floor of the WHRI for letting me be their incompetent receptionist for a few months while I was writing up.

Thanks to all my family and friends for putting up with my absence or my whingeing while I was writing up, and especially to my partner Will who has taken most of the strain, and has listened patiently to me whitter on about this thesis every day for the past few months; I couldn't have done it without his moral support.

Publications

Thomas, N.L., George, C.H. and Lai, F.A. (2004) Functional heterogeneity of ryanodine receptor mutations associated with sudden cardiac death. *Cardiovascular Research* **64**; 52-60

George, C.H., Jundi, H., Thomas, N.L., Scoote, M., Walters, N., Williams, A.J. and Lai, F,A. (2004) Ryanodine receptor regulation by intramolecular interaction between cytoplasmic and transmembrane domains. *Molecular Biology of the Cell* **15(6)**; 2627-38.

Thomas, N.L., Lai, F.A. and George, C.H. (2005) Differential Ca^{2+} sensitivity of RyR2 mutations reveals distinct mechanisms of channel dysfunction in sudden cardiac death. *Biochemical and Biophysical Research Communications* **331**; 231-238

George C.H., Thomas N.L. and Lai F.A. (2005) Ryanodine receptor dysfunction in arrhythmia and sudden cardiac death. *Future Cardiology* **1(4)**; 1-11

Abstracts

Thomas N.L., George C.H. and Lai F.A. (2004) Molecular mechanisms underlying RyR2 (Ca^{2+} release channel) dysfunction in stress-induced VT. *Biophysical Journal (Annual Meeting Abstracts)* **86 (1)**; 49A-49A

George, C.H., Jundi, H., Thomas, N.L., and Lai, F.A. (2004) Altered intra-RyR interaction associated with stress-induced ventricular tachycardia. *Biophysical Journal (Annual Meeting Abstracts)* **86 (1)**: 49A-50A

George, C.H., Walters, N., Thomas, N.L., Yeung, W.Y., Reynolds, D.F. and Lai F.A. (2005) Visualisation of intr-RyR2 interactions in HL-1 cardiomyocytes: novel FRET probes reveal a structural basis for Ca^{2+} channel dysfunction in arrythmogenesis. *Biophysical Journal (Annual Meeting Abstracts)* **88 (1):** 92A-92A

Thomas N.L., George C.H. and Lai F.A. (2005) In situ characterisation of the Ca^{2+} sensitivity of cardiac RyR mutations reveals multiple mechanisms of channel dysfunction in sudden death. *Biophysical Journal (Annual Meeting Abstracts)* **88 (1);** 308A-309A

Summary

Ca^{2+} release via the cardiac ryanodine receptor (RyR2) is a fundamental event in excitation-contraction coupling. Point mutations in the gene encoding RyR2 are associated with arrhythmogenic right ventricular dysplasia type 2 (ARVD2), a disease likely characterised by abnormal release of Ca^{2+} that may result in sudden death. GFP-tagged RyR2 mutants ($R^{176}Q/T^{2504}M$, $L^{433}P$ and $N^{2386}I$) were generated and expressed in a human embryonic kidney (HEK) cell model, enabling profiling of the amplitude and temporal characteristics of caffeine-evoked Ca^{2+} release through homotetrameric channels using confocal microscopy. Mutants were functionally heterogeneous and demonstrated profound differences in Ca^{2+} release when compared with WT channels, including the novel observation that one of the mutants ($L^{433}P$) exhibited reduced sensitivity to caffeine activation. The molecular basis of this heterogeneity was investigated by determining the sensitivity of the mutant channels to cytoplasmic Ca^{2+}. This was achieved by evaluation of caffeine-induced Ca^{2+} release from WT or mutant channels in streptolysin-O permeabilised HEK cells, where the cytoplasmic Ca^{2+} concentration was clamped. Although resting ER Ca^{2+} store and cytoplasmic Ca^{2+} levels were comparable in all cells, RyR2 mutants were characterised by a profound loss of Ca^{2+}-dependent inactivation. We also investigated whether these mutations disrupted the interaction between RyR2 and accessory proteins involved in normal channel function. cDNA encoding mutation susceptible regions were constructed and screened against a human cardiac cDNA library using a yeast two hybrid system. The $N^{2386}I$ mutation abolished association of the RyR2 domain with two cardiac proteins, which robustly occurred with the corresponding WT domain. These findings demonstrate that ARVD2-linked RyR2 mutations critically affect channel activation and suggest that differential sensitivity to cytoplasmic Ca^{2+} may be a causative mechanism in the pathogenesis of this disease. Defective interaction between RyR2 and accessory proteins may also be an important component of ARVD2 pathogenesis, suggesting that there is unlikely to be a common mechanism underlying channel dysfunction in sudden cardiac death.

Contents

List of Figures and Tables

Chapter 1

General Introduction

1.1. Ca^{2+} signalling

1.1.1. The diversity of Ca^{2+} signalling

Ionized Ca^{2+} is an ubiquitous cellular signal, responsible for controlling numerous diverse cellular processes, such as muscle contraction, neurotransmission, secretion, proliferation and fertilization (Clapham, 1995; Berridge et al., 2003). This versatility emerges from its use of an extensive repertoire of signalling components and the fact that it can be sequestered from the cytoplasm into the organelles, mainly the endo/sarcoplasmic reticulum (ER/SR). Elevation of the intracellular Ca^{2+} concentration, either by Ca^{2+} influx or release from an intracellular store acts as a trigger to switch numerous cellular processes "on" and Ca^{2+} removal from the cytosol serves to turn them "off". In practice this depends on the complex interplay between numerous channels, pumps and exchangers, in theory however, the Ca^{2+} signalling network can be divided into four functional units (Berridge, 2000):

- The generation of Ca^{2+}-mobilising signals: Signalling is triggered by a stimulus (normally acting via a plasma membrane receptor) that generates various Ca^{2+}-mobilising signals (e.g. inositol-1,4,5-trisphosphate, cyclic ADP ribose, nicotinic acid dinucleotide phosphate).
- ON mechanisms: These are mechanisms which feed Ca^{2+} into the cytosol, which can occur either by the entry of external Ca^{2+} via plasma membrane channels or by release from the internal stores.
- Ca^{2+}-sensitive processes: The resultant Ca^{2+} signal activates various Ca^{2+} binding proteins (e.g. troponin C in muscle), which undergo conformational change thereby modulating downstream processes.
- OFF mechanisms: Once Ca^{2+} has carried out its signalling functions it is rapidly removed from the cytoplasm by these processes. This occurs by extrusion via the plasma membrane or sequestration into storage organelles to restore the resting condition. (See Figure 1.1.)

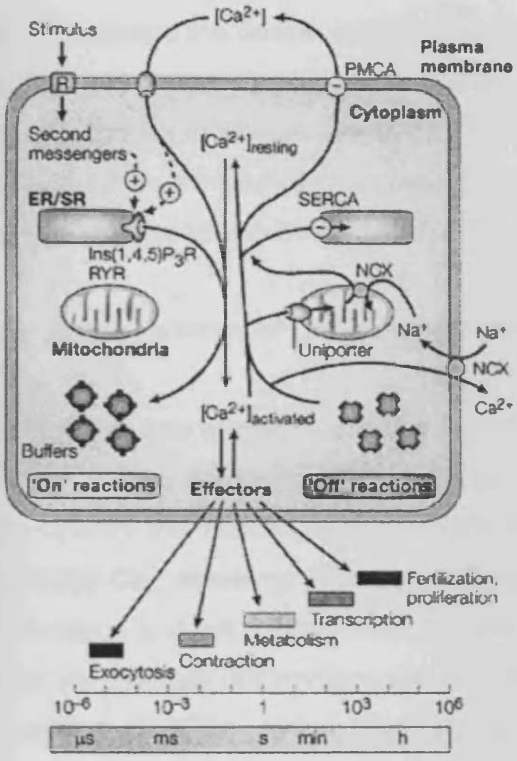

Figure 1.1. The Ca^{2+} signalling network (from Berridge, 2003). Stimuli induce both the entry of external Ca^{2+} and the formation of second messengers that release Ca^{2+} stored within the endoplasmic/sarcoplasmic reticulum (ER/SR) via the ryanodine receptor (RyR) or the inositol-1,4,5-trisphosphate receptor ($Ins(1,4,5)P_3R$). A small proportion of this Ca^{2+} (shown as dark circles) bind to effectors that activate various cellular processes that operate over a wide temporal spectrum (shown beneath the figure), while most is buffered in the cytoplasm. Ca^{2+} is removed from the cell by extrusion via the Na^+/Ca^{2+} exchanger (NCX) and the plasma membrane Ca^{2+} ATPase (PMCA), or can otherwise be sequestered back into the ER/SR by the sarco(endo)plasmic reticulum Ca^{2+} ATPase (SERCA), or into the mitochondria via the uniporter. Cell survival is dependent on Ca^{2+} homeostasis, whereby the Ca^{2+} fluxes during the "off" reactions exactly match those during the "on" reactions.

1.1.2. The complexity of Ca^{2+} signalling: spatio-temporal regulation

Additional levels of complexity in the Ca^{2+} signal are encoded by the precise spatial and temporal patterns in its release. Some of these signals result in highly localized brief bursts of Ca^{2+}, while others produce longer-lasting global increases, and the specific response elicited by the Ca^{2+} signal is mediated by this kind of encryption (Berridge, 1997; Dolmetsch et al., 1998; Lewis, 2001). Release from internal stores is mediated by various channels, of which the ryanodine receptor (RyR) and inositol-1,4,5-trisphosphate receptor (IP_3R) have been most extensively studied (Clapham, 1995). Elementary Ca^{2+} release via a single RyR (quark) or IP_3R (blip) can activate highly localised cellular processes, or initiate more complex Ca^{2+} signalling events resulting from the coordinated opening of clusters of RyRs or IP_3Rs, known as sparks or puffs, respectively (Cheng et al., 1993; Lipp & Nigli, 1998; Bootman et al., 1997; Berridge, 1997). Sparks and puffs contribute to Ca^{2+} waves and oscillations, which are global Ca^{2+} release events.

Ca^{2+} signals are usually presented as brief spikes (known as transients), and in some cases this is sufficient to activate a response such as muscle contraction or neurotransmitter release (Berridge et al., 2000). During prolonged stimulation, these Ca^{2+} transients need to be repeated to set up regular oscillations such as those known to activate the oocyte at fertilization (Ozil & Swann, 1995). Cells respond to

known to activate the oocyte at fertilization (Ozil & Swann, 1995). Cells respond to such oscillations using highly sophisticated mechanisms, including the ability to interpret changes in frequency. Such frequency-modulation is responsible for such multi-faceted responses as exocytosis (Tse et al., 1993) and optimization of gene transcription (Dolmetsch et al., 1998; Li et al., 1998).

1.1.3. Dysregulation of Ca^{2+} signalling is a pathological event

Although Ca^{2+} has a major signalling function in most cells, it is highly toxic in sustained or high concentrations and is involved in triggering apoptosis (Berridge, 2000). It is for this reason, along with the fact that Ca^{2+} cannot be metabolised, that intracellular Ca^{2+} levels need to be carefully regulated. Dysregulated Ca^{2+} release, sequestration and influx have been implicated in diseases including cardiac and skeletal myopathies (for reviews see Pogwizd et al, 2001; George et al., 2005; Benkusky et al., 2004), kidney, liver and pancreatic dysfunction (Vassilev et al., 2001; Shibao et al., 2003; Matsuda et al., 2001), infertility (Watnick et al.,2003), neuropathology (Tang et al., 2003; Mattson et al., 1998; Verkhratsky, 2005) and cancer (van den Abeele et al., 2002). Although the precise mechanisms by which Ca^{2+} signalling dysfunction leads to cellular and tissue pathology remain largely unknown, it is likely that defects in Ca^{2+} homeostasis are causative.
This is reflected by the fact that many cell systems utilize Ca^{2+} signalling to control specialized processes, for example the triggering of neurotransmitter release in the nervous system, the control of enzyme secretion in the pancreas and the activation of T-lymphocytes by an antigen. Perhaps the most specialized mechanism of Ca^{2+} handling is in muscle, in particular cardiac muscle where Ca^{2+} fluxes regulate contraction of the heart. The remainder of this section discusses these cardiac specific mechanisms of Ca^{2+} homeostasis.

1.2. Ca^{2+} signalling in the heart

Ca^{2+} signalling is a vital component of the normal physiological function of the heart since it controls the electrical as well as the contractile activity that combines to produce the heartbeat. Ca^{2+} fluxes achieve a synchronised cellular depolarisation and subsequent activation of the contractile proteins, via the physiological mechanism of excitation-contraction (EC) coupling (Bers, 2002). To maintain this process, intracellular Ca^{2+} homeostasis must be carefully regulated to synchronise depolarisation and contraction during systole (i.e. the time at which ventricular contraction occurs) and that relaxation occurs fully during diastole (i.e. the time at which ventricular relaxation occurs) before the start of the next cycle. This regulation of Ca^{2+} release and sequestration is further complicated by its reliance on the integration of other ionic fluxes i.e. changes in the concentrations of $Na^+/K^+/Cl^-$ can affect intracellular Ca^{2+} and vice versa. This interdependence emphasises the importance of Ca^{2+} homeostasis in the heart, defects in which have been implicated in the pathogenesis of both heart failure and cardiac arrhythmias, the latter being the main focus of the work presented in this thesis.

1.2.1. Cardiac myocyte contractile machinery

The human myocyte is typically mononucleate, 10-20 μm in diameter and 50-100 μm long. The cell is sometimes branched and is attached to adjacent cells in an end-to-end fashion forming what is known as the intercalated disc, which has a characteristic profile in cross section (see Figure 1.2.). Each individual cardiomyocyte is packed with long contractile bundles called myofibril-like units. Each myofibril is composed of smaller units called sarcomeres, these are the basic units of contraction and contain two types of interdigitating filament: a thick filament made of the protein myosin and a thin filament composed chiefly of actin, which overlap each other (Berne & Levy, 1993). The myocyte also contains an internal network of endoplasmic reticulum, known as the sarcoplasmic reticulum (SR), which is not continuous with the outer sarcolemmal membrane of the cell, yet closely associates with it, particularly within the surface sarcolemmal invaginations characteristic of cardiomyocytes, referred to as the transverse (t) tubules. Contraction of a myocyte is caused by shortening of its sarcomeres, which occurs as a result of an increase in the overlap between the actin and myosin myofilaments by the sliding filament mechanism. At the molecular level, this movement is initiated by the binding of myosin head units to actin; a process known as cross-bridge formation.

At rest, the actin sites, with which the myosin heads would react, are blocked by tropomyosin. Contraction at systole is initiated by a sudden rise in the concentration of free intracellular Ca^{2+} due to release from the SR, which acts as an internal Ca^{2+} store for this process. This causes Ca^{2+} to bind to the troponin C subunit of the troponin complex, which then undergoes a conformational change, displacing tropomyosin and allowing the interaction of actin and myosin. Force and movement is produced by a subsequent change in the angle of this cross-bridge, after which the head disengages and the process repeats itself. The energy for contraction is provided by molecules of adenosine trisphosphate (ATP), which bind to the myosin head units and on hydrolysis yield the energy for cross-bridge movement. Hence this is an ATP-expensive process, explaining the numerous mitochondria present in myocytes. The onset of relaxation and diastole is subsequently initiated by the removal of Ca^{2+} from the cytosol, which can occur by extrusion via the sarcolemmal pumps and exchangers as well as by re-uptake of Ca^{2+} into the SR.

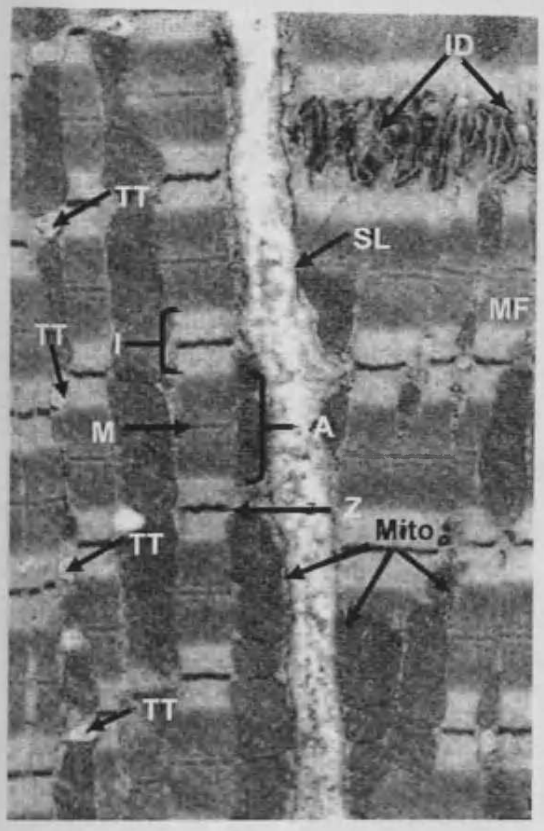

Figure 1.2. Electron micrograph of monkey ventricular cells showing details of ultrastructure (adapted from Berne & Levy, 1993). The sarcolemma (SL) is the boundary of the muscle cells and is extensively folded where the cells meet at the intercalated disc (ID) region. The prominent myofibrils (MF) show distinct banding patterns, including the A band (A), dark Z lines (Z), I band regions (I), and M lines (M) at the centre of each sarcomere unit. Mitochondria (Mito) occur either in rows between myofibrils or in masses just underneath the sarcolemma. Regularly spaced t-tubules (TT) appear at the Z line levels of the myofibrils. Bar represents 1 μm.

1.2.2. The Cardiac Action Potential

The initiating event in cardiac excitation-contraction coupling is the action potential (AP). The AP causes an abrupt reversal of the membrane potential to a positive value which is determined by the complex interplay of many ion channels and

transporters and results in the genesis of a Ca^{2+} transient. The AP is also responsible for propagation of the excitation from cell to cell in the heart and allows the heart to function as a syncytium (Bers, 2001). The AP has a characteristic form in the heart with distinct phases, each corresponding to a specific or predominant ion flux, as outlined in Figure 1.3. The resting cardiac myocyte membrane is preferentially permeable to K^+, and it is this efflux of K^+ along an electrochemical gradient that dictates the negative membrane potential. Rapid depolarisation occurs due to the opening of voltage-dependent Na^+ channels, causing a rapid influx of Na^+ ions; this represents the upstroke of the AP (Phase 0). Early repolarisation (Phase 1) is then caused by an outward current of K^+ ions through transiently opened K^+ channels. The plateau that follows early repolarisation (Phase 2) is the result of the inward current of Ca^{2+} ions caused by the opening of the $Ca_v1.2$. The process of final repolarisation (Phase 3) starts at the end of the plateau phase when the efflux of K^+ from the myocyte begins to exceed the influx of Ca^{2+}. The excess Na^+ that had entered the cell rapidly during depolarisation is removed by the actions of the Na^+/K^+-ATPase. Similarly, most of the excess Ca^{2+} is eliminated by the Na^+/Ca^{2+} exchanger (NCX) and plasma membrane Ca^{2+}-ATPase (PMCA) as well as being pumped back into the store to restore the resting potential.

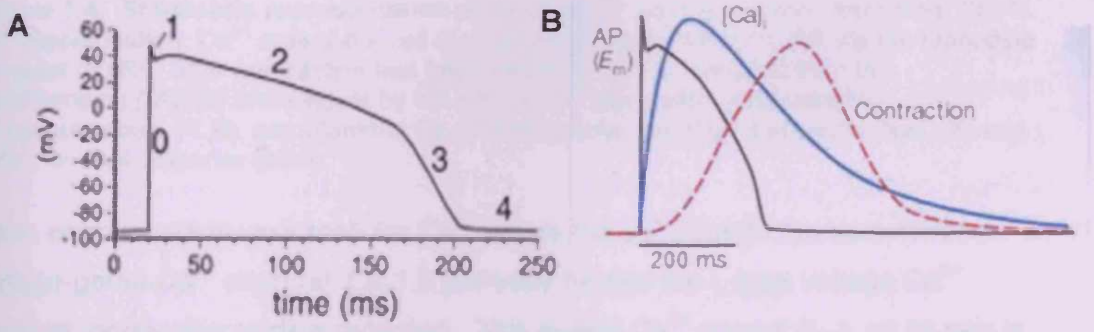

Figure 1.3. Schematic representations of the cardiac action potential (AP) in a ventricular myocyte, showing timing and morphology (adapted from Keating & Sanguinetti, 2001 and Bers, 2002). A) The various phases (0-4) are mediated by ion fluxes, summarized as follows: **Phase 0** - rapid depolarisation caused by an inward Na^+ current, signalling the onset of systole; **Phase 1** – early repolarisation, mediated by a transient outward K^+ current and closure of the Na^+ channels; **Phase 2** – the $Ca_v1.2$ current contributes to the long plateau duration; **Phase 3** – many outward K^+ currents and Na^+ and Ca^{2+} efflux contributes late repolarisation and the restoration of the resting membrane potential, seen in **Phase 4**. Thus, the coordinated opening and closing of cardiac ion channels is responsible for cardiac excitability. B) The time course of an AP, Ca^{2+} transient and contraction measured in a rabbit ventricular myocyte at 37°C.

1.2.3. Cardiac Excitation-Contraction (EC) coupling

EC coupling is the process by which electrical stimulation of the myocyte, in the form of membrane depolarisation, is translated into contraction (Fabiato & Fabiato 1979, Bers & Peres Reyes 1999, Bers 2002, Eisner et al, 2003). EC coupling occurs in all contractile muscle (skeletal, cardiac and smooth), however only cardiac EC coupling will be discussed here (see Figure 1.4.).

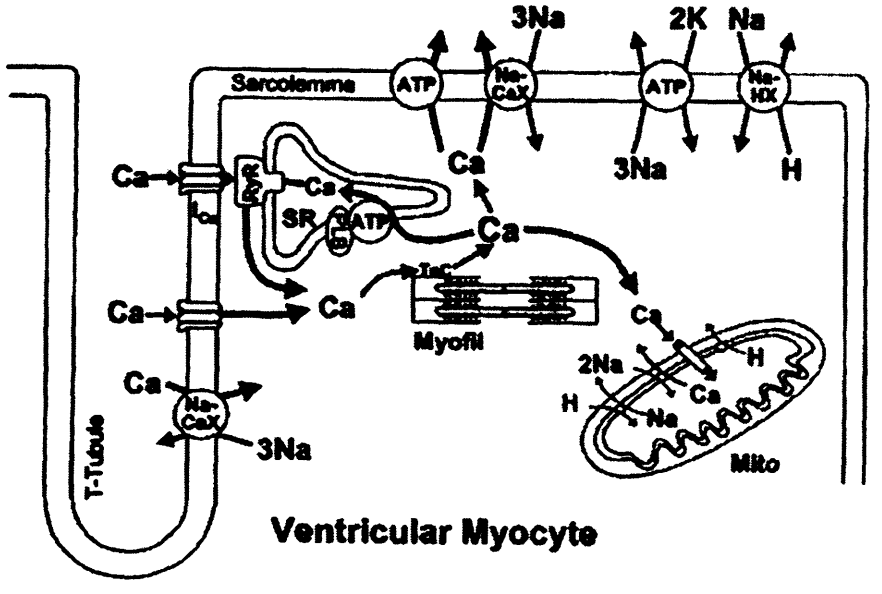

Figure 1.4. Schematic representation of cardiac EC coupling (taken from Bers, 2001). On depolarisation, Ca^{2+} enters the cell (I_{Ca}), eliciting release from the SR via the ryanodine receptor (RyR). After contraction has been initiated, Ca^{2+} is removed from the myofilaments (Myofil) and cytosol by the SR Ca-ATPase pump (modulated by phospholamban, PLB), sarcolemmal Ca-ATPase pump, Na^+/Ca^{2+} exchange (NaCaX) and mitochondrial uniporter (Mito).

Upon depolarisation, extracellular Ca^{2+} enters the cell through the sarcolemmal voltage-gated Ca^{2+} channel, $Ca_v1.2$ (formerly termed the L-type voltage Ca^{2+} channel, or dihydropyridine receptor). This inward Ca^{2+} current (I_{Ca}), on its own is insufficient to bring about the required conformational change in troponin needed for contraction to occur (Scoote & Williams, 2002). The additional Ca^{2+} required is obtained by release from the SR Ca^{2+} store via the cardiac ryanodine receptor (RyR2) (Coronado et al., 1994). I_{Ca} acts as a trigger for this process, in which Ca^{2+} release is propagated from one population of RyR2s (known as a 'Ca^{2+} release unit' (CRU)) to another - a phenomenon called 'calcium-induced calcium release' (CICR) (Fabiato, 1983; Fabiato, 1989). To facilitate CICR, individual populations of RyR2s (or CRUs) localise in areas of the SR membrane which are adjacent to $Ca_v1.2$ channels within the t-tubules of the sarcolemma (Franzini-Armstrong et al., 1999). Such structures are referred to as the terminal cisternae, and this region is known as

the junctional SR. Ca^{2+} itself is the ligand that activates RyR2; hence the influx of Ca^{2+} (called a 'sparklet') activates a population of these channels causing a synchronised release of Ca^{2+} known as a Ca^{2+} spark (Cheng et al., 1993). Multiple Ca^{2+} sparks, acting in concert increase the concentration of free Ca^{2+} within the cytosol from ~100nM to ~1000nM during systole (Bers, 2001), which then brings about contraction. For this increase in cytosolic Ca^{2+} concentration to be achieved, the amount of Ca^{2+} entering the cytoplasm (either by influx or SR release) must be of the order of 100μM. This is due to the high buffering capacity of the cytosol, which contains numerous Ca^{2+} binding proteins (e.g. troponin, calmodulin, ATP) (Berlin et al., 1994; Bers, 2001).

For relaxation to occur, Ca^{2+} release through RyR2 must terminate and this is achieved by the rapid removal of cytosolic Ca^{2+} either by re-uptake into the SR via the SR Ca^{2+}-ATPase (SERCA) (Bassani et al., 1994a), or by extrusion via the sarcolemmal NCX (Bassani et al., 1994b). These two actions balance the Ca^{2+} influx/release at systole such that there is no net loss or gain of Ca^{2+} with each cycle. However, it is because of this inter-reliant nature of the processes involved in EC coupling that a defect/mutation in any one of its components could lead to abnormal Ca^{2+} handling, resulting in arrhythmia. Table 1.1 summarizes these defects.

1.2.4. The β-adrenergic (catecholaminergic) pathway regulates EC coupling

Sympathetic stimulation controls the inotropic (increase in contractility), lusitropic (relaxation or decrease or contractility) and chronotropic (influencing the heart rate) states of the heart, enhancing myocardial performance. This is achieved by perhaps the most well characterised signal amplification cascade in the heart: the β-adrenergic cascade, which alters the phosphorylation status of many of the components of EC coupling, thus altering their function *in vivo* (Bers, 2002). The signalling pathway begins with the activation of the β-adrenergic receptor by neurally released norepinephrine or catecholamines (Kapiloff, 2002), and is summarized in Figure 1.5. In this way the activity of cardiac EC coupling can be rapidly modified by adrenergic input, regulating what is known as the "fight or flight" response in the heart (Koch et al., 2000).

The functional consequences of phosphorylation can be grouped into inotropic and lusitropic effects. Inotropic effects include: 1) A 2-4 fold greater influx of Ca^{2+} through the phosphorylated $Ca_v1.2$ channel for any given excitation (Tsien et al., 1986; McDonald et al., 1994). 2) Phosphorylation of the RyR2 increases the

Protein	Function	Genetic mutation	Phenotype	Functional effects	References
$Ca_v1.2$	Depolarisation activated Ca^{2+} channel which mediates I_{Ca}	$G^{406}R$, *de novo* mutation in alternatively spliced exon 8A, encoding transmembrane segment S6	Timothy Syndrome: multisystem pathology, lethal arrhythmia and autism	Maintained inward Ca^{2+} currents due to ablation of voltage-dependent inactivation	Splawski et al., 2004, 2005
PLN	Phospho-regulated inhibitor of SERCA activity	R^9C, $L^{39}stop$	Inherited form of dilated cardiomyopathy and HF respectively	R^9C: phosphorylation deficient, resulting in increased SERCA inhibition, leading to a reduced store. $L^{39}stop$: possible constitutive inhibitor of SERCA or null mutation	Haghighi et al., 2003, 2004; Schmitt et al., 2003; Chien et al., 2003
Troponin T	Myofilament protein which mediates Ca^{2+}-dependent contraction	Many, $I^{79}N$ most prevalent	Familial cases of HOCM - increased risk of arrhythmia and SCD	Increased Ca^{2+} sensitivity and cardiac contractility, slower decay of the intracellular Ca^{2+} transient	Watkins et al., 1995; Varnava et al., 2001; Knollmann et al., 2003
CSQ2	Intra-SR Ca^{2+} buffering protein; lumenal Ca^{2+} sensor for RyR2	$D^{307}H$ and three nonsense mutations	CPVT - increased risk of arrhythmia and SCD	Disrupts Ca^{2+} binding ability or result in non-functional protein. Decreased intra-lumenal Ca^{2+} buffering and abnormal lumenal Ca^{2+} dependent RyR2 regulation	Lahat et al., 2001; Postma et al., 2002; Terentyev et al., 2003; Vitachenko-Karpinski et al., 2004

Table 1.1. Ca^{2+} handling defects and cardiopathology. Summary of how mutation in the various proteins involved in EC coupling can lead to a disease phenotype. Abbreviations: PLN, phospholamban; SERCA, sarco/endoplasmic reticulum Ca^{2+} ATPase; CSQ2, the cardiac isoform of calsequestrin; HF, heart failure; SCD, sudden cardiac death; HOCM, hypertrophic obstructive cardiomyopathy; CPVT, catecholaminergic polymorphic ventricular tachycardia.

channel's sensitivity to activation by Ca^{2+} (Valdivia et al, 1995; Marx et al., 2000) and so this directly increases SR Ca^{2+} release. Lusitropic effects include: 1) Greater SR Ca^{2+} re-uptake through SERCA (due to phosphorylation of its regulatory protein phospholamban) so that a larger SR load is expected. 2) A decrease in myofilament Ca^{2+} sensitivity (due to phosphorylation of troponin), but the dramatic increase in Ca^{2+} transients more than compensates for this (Bers, 2001). 3) Enhanced NCX activity due to its phosphorylation and hence an increase in Ca^{2+} efflux, again increasing the rate of relaxation. These lusitropic effects are important in ensuring that there is sufficient SR Ca^{2+} available for the next cycle of release, since if they are impaired cardiac output will also be reduced (Scoote & Williams, 2002).

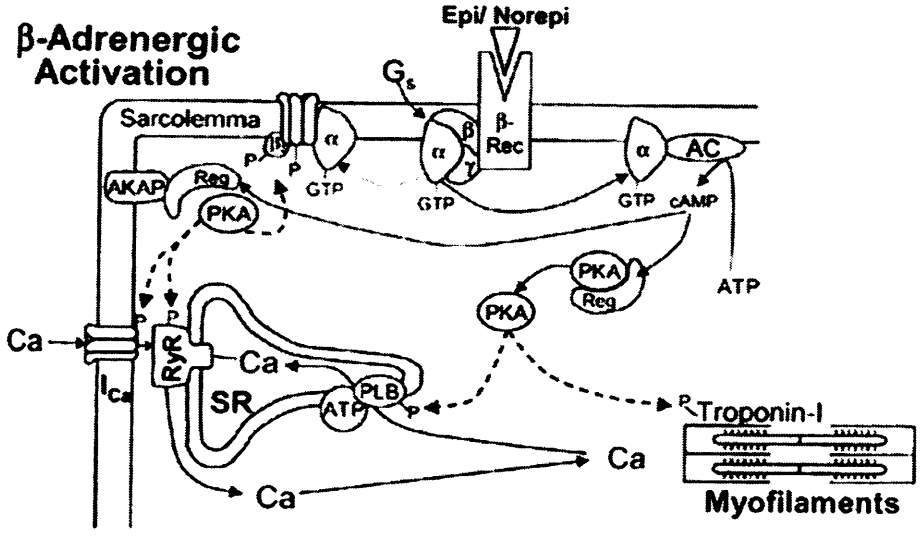

Figure 1.5. Schematic representation of the β-adrenergic pathway (from Bers, 2001). Binding of catecholamines (Epi = epinephrine, Norepi = norepinephrine) to the β-adrenergic receptor (β-Rec) leads to stimulation of adenylyl cyclase (AC, via activation of the α subunit of the GTP binding protein G_s), allowing the generation of cyclic adenosine monophosphate (cAMP), resulting in dissociation of the regulatory (Reg) and catalytic subunits of cAMP-dependent protein kinase (PKA). Activation of this enzyme leads to phosphorylation of the various EC coupling components. Another minor pathway is via a direct effect of the activated α subunit of G_s on $Ca_v1.2$.

The effects of β-adrenergic activation are therefore complex, with the function of many proteins being affected by PKA mediated phosphorylation. Defective phosphorylation of these EC coupling components is thought to play a role in cardiac pathology (see section 1.5.2.).

It is obvious from Figures 1.4. and 1.5. that RyR2 is a central mediator of EC coupling, integrating $Ca_v1.2$ activation, coordinating SR Ca^{2+} release and having a role in regulation of the SR status. Dysregulation of RyR2 is therefore a pathological event, and the molecular mechanisms which underlie aberrant channel functionality are the focus of this project.

1.3. The Ryanodine Receptor

The ryanodine receptor (RyR) is a large transmembrane SR Ca^{2+} release channel that regulates the release of stored Ca^{2+} from the SR lumen during Ca^{2+} signalling processes, including EC coupling. Ryanodine receptors were initially observed in electron micrographs as large, electron dense bridging structures between the sarcolemmal t-tubule and the junctional SR called "feet" by Franzini-Armstrong (1970) (see Figure 1.6.).

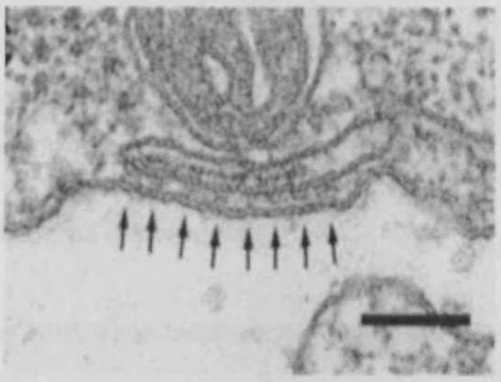

Figure 1.6. Transverse section of chick embryo heart with junctional complexes showing the presence of 'feet' (on the opposite side of the junctional SR membrane from the tips of the arrows), taken from Sun et al. (1995). Bar represents 0.1μm.

Caldwell & Caswell (1982) later showed biochemical evidence for a high molecular weight protein which could represent these junctional feet. The isolation and molecular identification of this SR Ca^{2+}-release channel was greatly accelerated by the recognition that the neutral plant alkaloid ryanodine is a selective and specific ligand for the channel (hence its name, the ryanodine receptor) (Pessah et al., 1985). Ryanodine is found naturally in the stems and roots of the South American shrub *Ryania speciosa*, which was originally used as a pesticide (Sutko et al., 1997). However, it was later found to cause irreversible contracture of skeletal muscle and progressive decline in cardiac muscle twitches (Jenden & Fairhurst, 1969; Sutko & Willerson, 1980), and it was then observed that ryanodine appeared to bind specifically to the junctional regions of the SR, where these "feet" were located (Flucher & Franzini-Armstrong, 1996). Incorporation of the ryanodine binding protein complex into artificial planar lipid bilayers revealed that this structure was an ion channel (Fill & Copello, 2002; Hymel et al., 1988; Imagawa et al., 1987; Lai et al, 1987; Smith et al., 1988). Ryanodine binds to the RyR with high affinity and specificity when it is in the open configuration, thus allowing it to act as a marker of channel activation (for further discussion on the methods by which RyR activity can

be measured, see Chapter 4). The development of [^{3}H]ryanodine binding as a research tool allowed the purification and identification of RyRs in skeletal (Inui et al., 1987a; Lai et al., 1987) and cardiac muscle (Lai et al., 1988a; Inui et al., 1987b). The RyR protein was found to be a tetramer (Lai et al., 1989) and is so large (560kDa for the monomer, Takeshima et al., 1989) that it can be seen at the electron microscopic level (as "feet" - Lai et al., 1988b; Saito et al., 1988; Wagenknecht et al., 1989). In addition, it was demonstrated that the RyRs were organised in a distinct pattern on the SR in close association with the L-type Ca^{2+} channels (Franzini-Armstrong et al., 1999) and a typical cardiac couplon may have about 100 RyR2s and 10-25 L-type channels (Bers, 2001). Furthermore, we now know that the spatial distribution of these two Ca^{2+} channels is key to the efficient signal transduction process that underlies EC coupling.

1.3.1. RyR isoforms and distribution

The genes encoding RyR have been identified and sequenced in invertebrates, fish, amphibians, birds and mammals (Franzini-Armstrong and Protasi, 1997; Sutko and Airey, 1996). In mammals, the three RyR isoforms are encoded by different genes, despite this RyR1 and RyR2 are 66% identical and RyR3 is 67-70% identical to RyR1 and RyR2 (Franzini-Armstrong & Protasi, 1997; Sutko & Airey, 1996). They are thought to have different physiological roles, which is reflected by their tissue-specific expression. Table 1.2. summarizes the main differences between the three isoforms, highlighting their relative importance in Ca^{2+} signalling and development.

1.3.2. Structure of the Ryanodine Receptor

The RyR is the largest ion channel known with a total molecular mass of about 2.2MDa. The protein exists as a homotetramer, based on its quatrefoil appearance (Lai et al., 1988b; Wagenknecht et al., 1989), gel permeation chromatography characteristics (Inui et al., 1987a) and stoichiometry of ryanodine binding (Lai et al., 1988b; 1989). Each subunit contains about 5000 residues (Franzini-Armstrong and Protasi, 1997; Williams et al., 2001) ~80-90 % of which is located in the cytoplasm and is essential for the regulation of the channel pore (Franzini-Armstrong and Protasi, 1997; Mackrill, 1999). This large cytoplasmic N-terminal acts as a scaffold for various accessory proteins and as a target for many physiological and pharmacological modulators (Mackrill, 1999).

RyR isoform	Chromosome	Splice variants	Distribution	Divergent regions	Knock-out phenotype	Defect	References
Skeletal (RyR1)	19q13.1	At 10 441 bp (+15 bp), and at 11 591 bp (+18 bp)	Skeletal muscle, various tissues including smooth muscle and brain	D1: 4254-4631 aa D2: 1342-1403 aa D3: 1872-1923 aa	Perinatal death	Skeletal muscle failure, lack of contractile response, no EC coupling	MacLennan et al., 1989; Takeshima et al., 1989; Zorzato et al., 1990; Phillips et al., 1996; Takeshima et al., 1994
Cardiac (RyR2)	1q42.1-q43	At 4437 bp (+30 bp) and 11 145 (+24 bp)	Cardiac muscle, brain	D1: 4210-4562 aa D2: 1353-1397 aa D3: 1852-1890 aa	Embryonic death	Morphological abnormalities in the heart tube	Nakai et al., 1990; Otsu et al., 1990; Tunwell et al., 1996; Takeshima et al., 1998
'Brain' (RyR3)*	15q14-q15	At 11 569 bp (-82 bp).	Diaphragm, central nervous system and various tissues including smooth muscle, in conjunction with RyR1	D1: 4100-4400 aa	No gross abnormalities. Increased locomotor activity	Impaired hippocampal synaptic plasticity	Hakamata et al., 1992; Sonnleitner et al., 1998; Leeb & Brenig, 1998; Takeshima et al., 1996; Fugatsugi et al., 1999

Table 1.2. The three mammalian RyR isoforms. Each isoform is encoded by genes on different chromosomes and have structurally distinct splice variants, the functional significance of which is not known. Splice variants of the human isoforms only are detailed here, though many others have been discovered in the isoforms of other species (notably rabbit RyR3, see Jiang et al., 2003), + and – indicate base pair (bp) insertions and deletions respectively. Divergent regions represent residues that do not show considerable identity with the other isoforms and may impose the functional differences seen. The embryonic lethality of the RyR2 knock-out emphasises the vital role of RyR2 in cardiac development and Ca^{2+} homeostasis. * RyR3 was initially termed the 'brain' isoform as it was initially sequenced from this organ, however RyR1 and 2 are also expressed in the brain and may also have a role there.

The three-dimensional structure of the tetramer of all three RyR isoforms has been determined at a resolution of 25-30 Å, and recently the RyR1 structure has been resolved at 14 Å, using cryo-electron microscopy (cryo-EM) of frozen-hydrated, detergent solubilised individual isolated channels in conjunction with single-particle image processing (see Figure 1.7. - Wagenknecht et al., 1989; Radermacher et al., 1994; Sharma et al., 1998; Sharma et al., 2000; Wagenknecht & Radermacher, 1995; Serysheva et al., 2005; Samso et al., 2005). For all three isoforms, the three-dimensional reconstructions showed an overall mushroom shape consisting of two major components: a large, quatrefoil cytoplasmic assembly (290 Å x 290 Å x 130 Å) composed of at least ten distinct interconnected globular domains (including the assemblages which form the corners of the cytoplasmic structure (clamps) and connecting structures, termed handles (Radermacher et al., 1994), and a differentiated small transmembrane assembly (120 Å x 120 Å x 70 Å) (see Figure 1.7.). The cytoplasmic domain of the RyR is a very open structure with clearly identifiable structural regions and solvent accessible spaces (Williams et al., 2001). The structure of RyR1 has also been determined in both closed and open conformations (Orlova et al., 1996; Samso & Wagenknecht, 1998), revealing structural differences (described in Figure 1.7.B). Although all three isoforms have been purified from natural sources, more recently an alternative source of RyRs is from expression systems in which recombinant wild type or genetically modified RyR proteins can be produced from cDNAs. A notable advantage of using cloned receptors for quantitative EM study is that genetic manipulations can be made that effectively create sequence-specific labels such as GFP, so that the positions of various residues can be located on the three-dimensional structure (see Figure 1.8., Liu et al., 2001, 2004; Zhang et al., 2003b). A similar approach was used to localise the binding sites of various ligands (including calmodulin and the FK506 binding protein) on RyR1, using difference maps of free RyR and RyR-ligand complexes (Wagenknecht et al., 1997).

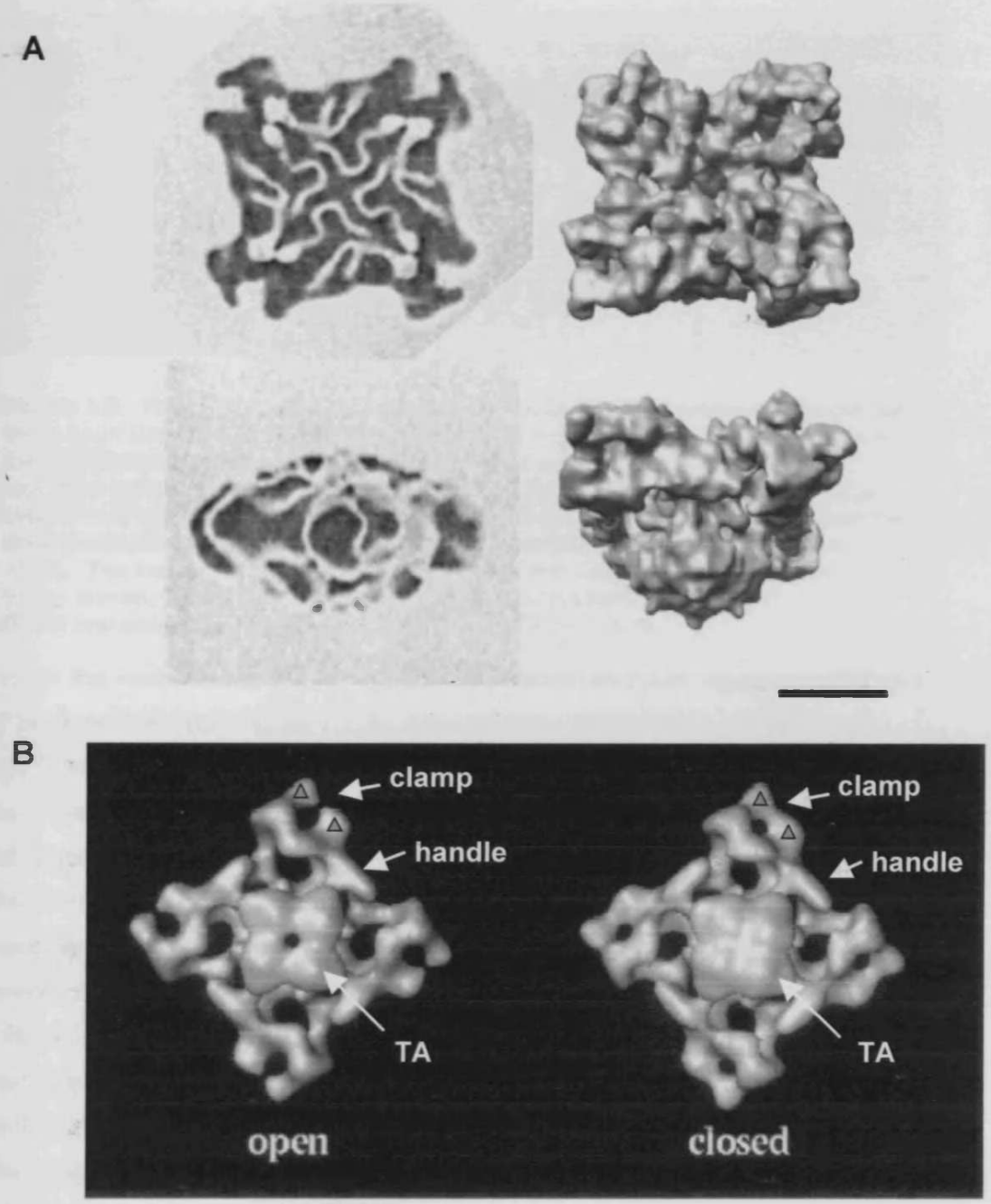

Figure 1.7. The three dimensional structure of RyR. A) Progress in resolving the three dimensional structure of RyR. This was initially achieved at 37 Å (left -Wagenknecht et al., 1989), and more recently 14 Å (right - Serysheva et al., 2005) for RyR1. Both were determined by single-particle image processing of individual channels (280 particles for the 37 Å resolution image and ~22 000 for the 14 Å resolution image), visualised by electron microscopy. Scale bar represents 100 Å. Top images: structure from the cytoplasmic side, bottom images: side view, with the cytoplasmic side facing upwards. The improved map clearly shows more structural detail including the membrane spanning pore region, the globular domains of the cytoplasmic assembly (see Figure 1.8.), and the central channel itself. This should allow better defined docking of computationally predicted structural domain folds and help to resolve structure-function relationships. B) Three-dimensional reconstruction of RyR1 in the open and closed state (resolved to 25 Å, from Samso and Wagenknecht, 1998), viewed from the sarcoplasmic reticulum lumen. Noticeable conformational differences include the presence of a central aperture in the transmembrane assembly (TA) of the open channel, connecting lumenal and cytoplasmic sides. In addition, the open form is characterised by an "opening" of the clamp domains (marked with triangles) relative to the closed form. Though not seen in this figure, the channel in the open state is slightly taller relative to that of the closed channel and cytoplasmic assemblies appear to undergo a relative rotation of about 4°.

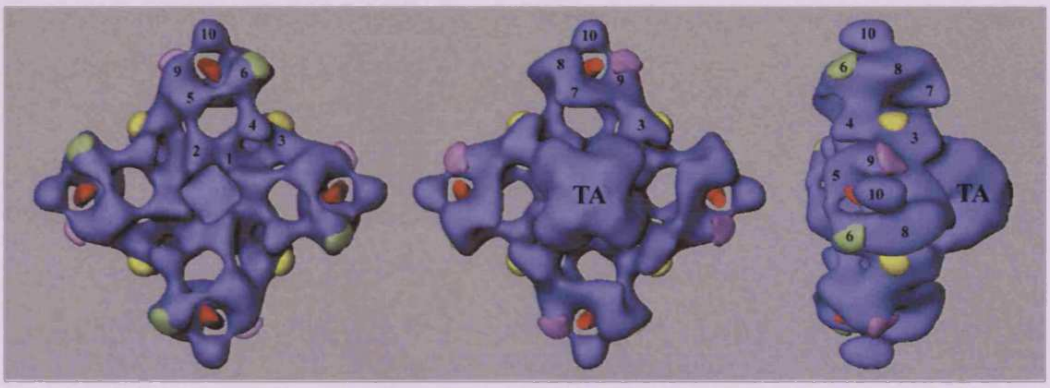

Figure 1.8. Three-dimensional structure of RyR2, detailing various regions that have been located using difference maps (from Liu et al., 2004). Left, top view from the cytoplasmic surface; middle, bottom view that would face the sarcoplasmic reticulum lumen; right, side view that shows that RyR2 has a small TA and a large cytoplasmic assembly. The numerals 1–10 on the cytoplasmic assembly indicate the distinguishable domains, according to earlier nomenclature (Radermacher et al., 1994). The location of the N-terminus (shown in red) was delineated using a GST fusion protein, whereas all three divergent regions (shown in yellow (DR1), green (DR2) and purple (DR3)) were mapped using GFP insertions.

Although the resolution of the RyR three-dimensional structure using cryo-EM gets ever more refined (see Figure 1.7.A), determination of the exact nature of the protein's conformation is only likely to be achieved by atomic resolution. This has already been achieved for other smaller ion channels and pumps (Toyoshima et al., 2000; Doyle et al., 1998), however the progression from the intrinsic organization of RyRs into two-dimensional arrays (see Figure 1.10.) to the formation of three-dimensional crystals that are suitable for use in X-ray diffraction studies is proving to be more complex than previously anticipated (George et al., 2005). It is possible that the atomic structure of the RyR will have to be resolved by studying partial fragments encompassing discrete regions of the protein and then assembling the information to reconstruct the architecture of the intact molecule, as has been achieved for portions of the inositol 1,4,5-trisphosphate Ca^{2+} release channel (Bosanac et al., 2002). Atomic resolution would be particularly useful in determining the precise structure of the membrane spanning regions of the C-terminal, these are the most important elements in the structure of an ion channel because they delineate the pore, and by anchoring the protein into the membrane, constrain the structure of the entire molecule (Dulhunty & Pouliquin, 2003; Williams et al., 2001). The transmembrane portion contains several compact hydrophobic domains, the precise number of which is still debated. Models with 4 (Takeshima et al., 1989), 6 (Tunwell et al., 1996) 10 (Zorzato et al., 1990) and 12 (Brandt et al., 1992) transmembrane domains have been proposed, based on hydropathy plot analyses (see Figure 1.9 A). However, hydropathy profiles can be misleading because strong hydrophobicity peaks can be formed by hydrophobic pockets within soluble proteins and do not necessarily

correspond to parts of the protein that are embedded in the membrane (Dulhunty & Pouliquin, 2003; Williams et al., 2001). The model of Brandt et al appears incorrect due to the findings of Du et al (2002) who, using tagged fusion constructs suggested a 6TM model starting at residue 4557, with an ambiguous hairpin loop between residues 4277-4363 (See Figure 1.9.B).

Further evidence for this model has emerged from mutational analyses and analogies with better characterised ion channels, such as the inositol 1,4,5-trisphosphate receptor (IP_3R) and the bacterial KcsA channel (MacKinnon, 2003; Ramos-Franco et al., 1999), which are all tetrameric and structurally homologous.

It has been put forward that the sequence linking the last two hydrophobic C-terminal segments (M3/4 of 4TM model, M8/10 of the 10TM model, M5/6 of the 6TM model) consists of a pore loop (P-loop) (Williams et al., 2001; Gao et al., 2000). It is this region, which shows limited sequence homology in all three channels that forms the conductance pathway. Part of the loop forms a pore-helix and selectivity filter, with partial negative charges pointing into the pore. Exposed negative charges at the mouth of the pore concentrate cations and contribute to selectivity, whereas negative charges at the opposite end of the pore facilitate the movement of ions through the channel (Dulhunty & Pouliquin, 2003; Doyle et al., 1998).

Evidence that the C-terminal portion of the RyR forms the pore comes from studies of truncated channels. Heterologous expression of a deletion mutant of RyR1 encompassing the first 182 N-terminal and the last 1030 C-terminal amino acids yielded an ion channel with a conductance comparable to that of full-length RyR1 (Bhat et al., 1997b). However, this truncated channel required higher concentrations of Ca^{2+} for activation, was insensitive to Ca^{2+} dependent inactivation and was also insensitive to caffeine activation.

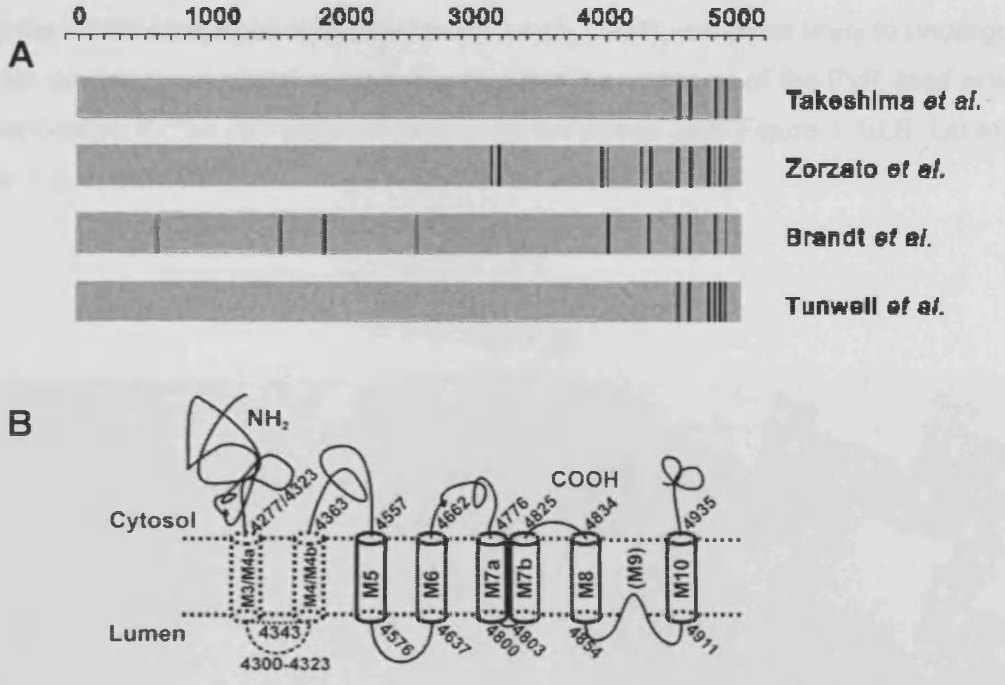

Figure 1.9. Models that have been proposed for the location of transmembrane segments of the RyR. A) The linear sequence of amino acids in the RyR is indicated in the upper scale. The grey bars represent the RyR, with putative transmembrane segments as vertical bars. The source of each model is given on right hand side of the figure (adapted from Dulhunty & Pouliquin, 2003). B) Proposed membrane topology of RyR1 with 6 TM domains from Du et al (2002). Dashed lines indicate the tentative nature of the first predicted helical hairpin loop. The numbers inside each transmembrane sequence (M3-M10) are those proposed by Zorzato et al (1990). The proposed selectivity filter is designated "(M9)" even though it is not a transmembrane sequence.

1.3.3. RyR intra-molecular interactions and their functional effects

RyRs form two-dimensional ordered arrays (see Figure 1.10.) in both skeletal and cardiac muscle, as observed by electron microscopy of sectioned or freeze-fractured muscle, and of isolated SR vesicles (Block et al., 1988; Protasi et al., 1996). In arrays, the cytoplasmic assembly of each RyR interacts along the edges of the clamp domain with the corresponding regions of its nearest neighbours such that the edges of adjoining RyRs overlap by ~12 nm (Saito et al., 1988). Recently, it was shown that tetramer lattice formation is an intrinsic property of the RyR since purified channels are capable of self-assembling *in vitro* into large two-dimensional arrays (Yin & Lai, 2000; Yin et al., 2005). It has been proposed that inter-tetramer contact in this array formation is mediated by an accessory protein (the FK506 binding protein (FKBP)) and that these interactions could be responsible for the concerted opening and closing of channels seen *in vivo* (Marx et al., 1998). However, three-dimensional

modelling of these arrays suggests that domains 6 and 10, which are spatially distinct from the FKBP binding site (Wagenknecht et al., 1997), are most likely to undergo protein-protein interactions, suggesting that it is the structure of the RyR itself which is responsible for the formation of these ordered arrays (see Figure 1.10.B, Liu et al., 2004; Yin et al., 2005).

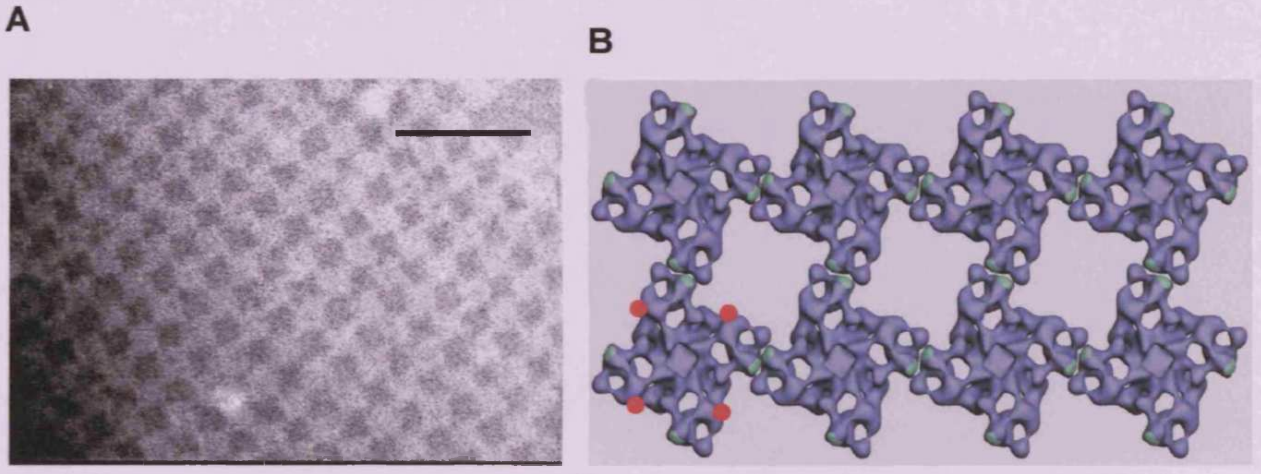

Figure 1.10. Two-dimensional lattice formation of RyR. A) Electron micrograph of a negatively stained RyR1 2D crystallline array from rabbit skeletal muscle, formed on positively charged lipid membranes. Scale bar = 120 nm. B) Model of a two-dimensional array which is consistent with the available experimental data (from Liu et al., 2004, but also see Yin et al., 2005), showing that the cytoplasmic assembly of each RyR interacts along the edges of its clamps (through domains 6 and 10) with the corresponding regions of its nearest neighbours. Interacting regions are distinct from the FKBP12 binding site (shown as red circles, Wagenknecht et al., 1997), indicating that 'coupling' of tetramers is unlikely to be mediated by this accessory protein.

As well as being involved in inter-tetramer interactions, regions of the cytoplasmic domain of RyR1 and RyR2 have also been implicated in inter-domain interactions within the tetrameric channel, and it is these interactions which are thought to mediate the global conformational change associated with Ca^{2+} release. Using a peptide probe approach, Ikemoto and colleagues demonstrated that the N-terminal and central domains of the RyR (in both cardiac and skeletal muscle isoforms) are closely associated in the inactive channel state and in fact stabilize the closed conformation, while loosening of this interaction ('unzipping') by mutation/competitive binding of a peptide produced the active conformational state (Yamamoto et al., 2000; El-Hayek et al., 1999). Further discussion of this mechanism can be found in sections 1.5.1.1. and 1.5.2.2.2.

2000; El-Hayek et al., 1999). Further discussion of this mechanism can be found in sections 1.5.1.1. and 1.5.2.2.2.

Additional work using site-specific antibodies has also shown that these N-terminal (590-609 a.a.) and central domain (2442-2477 a.a.) regions undergo domain-domain interaction (Kobayashi et al., 2004). Binding of antibodies targeted to these sequences enhanced channel activation, as shown by ryanodine binding and agonist induced Ca^{2+} release in RyR1, and fluorescence quenching studies showed that the antibodies produced the domain 'unzipping' postulated previously.

It is also known that the extreme C-terminus of the RyR is capable of self-association (Stewart et al., 2003), and indeed is a molecular determinant of oligomerization since deletion of the final 15 amino acids from RyR1 resulted in an inactive channel, attributed to impaired assembly of a tetrameric complex (Gao et al., 1997).

1.3.4. RyR ion conductance and channel gating

Since intracellular membrane channels are not amenable to standard whole cell patch clamp recording techniques, RyR channels must be incorporated into an artificial membrane system such as a planar phospholipid bilayer (Williams, 1995; Favre et al., 1999). This method enables the precise measurement of currents through a single RyR, and permits determination of the biophysical properties of the channel, under activating and inhibitory conditions. This powerful and widely used technique will be discussed in greater detail in Chapter 4.

Despite its physiological role as a Ca^{2+} release channel, RyR is permeable to a range of divalent and monovalent cations (Lindsay et al., 1991; Tinker & Williams, 1992), but not to anions (Lindsay & Williams, 1991). The ion selectivity of the channel is in part compromised due to the fact that its conductance is extremely high allowing high rates of cation translocation across the SR lumen (Williams et al., 2001), without having an effect on function. This relatively non-selective nature of RyR conductance (see Table 1.3.) seems to relate, in part to the relatively wide width of the selectivity filter portion of the pore, compared to other ion channels. This region, along with the short pore length and a large capture radius ensures high rates of ion entry and underlie the high conductance of the channel. However, in line with its role as a Ca^{2+} channel, the relative permeability of divalent cations (i.e. Ca^{2+}, Mg^{2+}, Ba^{2+} and Sr^{2+}) is at least six times greater than that of monovalent ions such as K^+ (Williams et al., 2001).

The precise gating mechanism of RyR is still speculative, though the gate is believed to be near the cytosolic side of the pore. A possible mechanism is that a specific

helical region in the pore undergoes conformational change, rotating each monomer subunit, in a similar manner to the opening and closing of a camera aperture (Wagenknecht & Radermacher, 1997). A frequently observed phenomenon with reconstituted RyRs in bilayers is the appearance of sub-conductance states (Meissner, 1994; Williams et al., 2001). These sub-conductance states, which in many cases correspond to ¼, ½, and ¾ of the main conductance (see Figure 1.11. for an example of a single channel recording) are thought to be due to the uncoordinated gating of the four separate monomers within the tetramer (Kaftan et al., 1996; Marks, 1996). However, the existence of substates as genuine RyR phenomena is controversial. In addition, it is now known that Ca^{2+} release through a single RyR *in vivo* is quantal in its nature (Wang et al., 2004), suggesting that release is an all-or-nothing event.

The high capacity and conductance, and low selectivity of RyRs are important properties of the channel with regard to its physiological role in EC coupling, where a large amount of Ca^{2+} needs to be released very quickly. Another important consideration however, is that the channel should be closed during diastole in order that the SR store can be replenished, which requires a termination mechanism.

Cation	Conductance (pS)	pX^+/pK^+	pX^{2+}/pK^+	pX^{2+}/pBa^{2+}
K^+	720	1	-	-
Na^+	445	1.15	-	-
Cs^+	460	0.61	-	-
Rb^+	620	0.87	-	-
Li^+	215	0.99	-	-
Ba^{2+}	200	-	5.8	1
Sr^{2+}	165	-	6.7	1.1
Ca^{2+}	135	-	6.5	1.1
Mg^{2+}	90	-	5.9	1.1

Table 1.3. Single channel properties of RyR2 (modified from Williams et al., 2001). Conductances were calculated from the slope of the current-voltage relationships in symmetrical 210mM solutions for monovalent cations, and in bi-ionic conditions with K^+ at the cytosolic face of the channel for divalent cations. pX^+/pK^+ : permeability ratio of monovalent cations relative to K^+. pX^{2+}/pK^+ : permeability ratio of divalent cations relative to K^+. pX^{2+}/pBa^{2+} : permeability ratio of divalent cations relative to Ba^{2+}.

1.3.5. Termination of Ca^{2+}-Induced Ca^{2+}-Release

Since CICR is an intrinsically self-reinforcing process, it would be expected that the released Ca^{2+} would trigger further release events, leading to an explosive positive feedback process that would release all the Ca^{2+} in the store (Stern & Cheng, 2004).

However, this is not the case, implying that there must be a mechanism by which this process can be terminated. There are many candidate mechanisms:

- *Inactivation* (Stern, 1992): This can be Ca^{2+} or opening dependent. Produces stable EC coupling in simulations but is yet to be demonstrated in bilayers, suggesting that it may depend on the presence of an absent regulatory protein e.g. sorcin (Farrell., 2003).
- *Adaptation* (Györke & Fill, 1993): This is the term for spontaneous closing of channels after activation by a rapid increase in cytosolic Ca^{2+} comparable to that during the cardiac AP (simulated by uncaging Ca^{2+} by flash photolysis). Following adaptation, channels were not in a refractory state and could be re-activated by a larger Ca^{2+} stimulus. Adaptation has been shown to occur faster at physiological Mg^{2+} concentrations (Valdivia et al., 1995).
- *Stochastic attrition* (Stern, 1992): Because there are a finite number of RyRs in a cluster, and their openings are stochastic, there is always a chance that they will all close simultaneously. However, data from mathematical modelling predicts that, except for when the open probability is low, the time for attrition is too long for this to be the sole termination mechanism.
- *Lumenal Ca^{2+} effects* (Shannon et al., 2003; Györke & Györke, 1998): Local depletion of SR Ca^{2+} does not terminate release by reducing the unitary conductance since the rate of intralumenal diffusion is sufficient to quickly replace that which has been released. However, RyR gating can be modulated by lumenal Ca^{2+}, suggesting that this could also be a mechanism of termination.
- *Amplitude dependent termination* (Wang et al., 2004): Elementary Ca^{2+} release events (sparks) can be decomposed into 'quantal units', with a single quantum representing the unitary release current of a single RyR. Sparks of larger amplitude (i.e. composed of many quanta/channels) terminated earlier. In this model, local Ca^{2+} released from open RyRs prevents others from opening, thereby limiting the degree of recruitment.
- *Coupled gating* (Marx et al., 1998; Laver, 2005): See section 1.4.2.1. FBKP-mediated coupled gating is an unlikely mechanism since these accessory proteins may not mediate inter-tetramer interactions (see sections 1.3.3. and 1.4.2.1.), and termination is known to occur in their absence (Stern & Cheng, 2004). However, coupled gating has recently been proposed to be regulated by lumenal Ca^{2+} (Laver, 2005), and termination by this mechanism remains to be investigated.

1.4. RyR modulation

The precise gating of RyR2 is vitally important in the maintenance of EC coupling and thus the co-ordinated contraction of the heart, and is achieved partly through modulation of the channel by various physiological effectors, cellular processes, and accessory proteins. RyR thus integrates a diverse array of cellular inputs to effect the appropriate Ca^{2+} release. The channel is also modulated and several pharmacological agents, used clinically in treating RyR-linked diseases (e.g. dantrolene) or those used to investigate RyR function *in vitro* (e.g. caffeine, ryanodine).

1.4.1. Modulation of RyR function by small molecule effectors

1.4.1.1. Cytosolic Ca^{2+}

Ca^{2+} ions are by far the most important effectors of RyR, and their action on the channel is complex. Ca^{2+} activates, deactivates and conducts the current through the channel, and its presence is often required in order that the RyR can be activated by other factors. In the absence of other effectors such as Mg^{2+} and ATP, a bell–shaped Ca^{2+} activation/inactivation curve has been demonstrated by RyR using Ca^{2+} efflux, single channel and ryanodine binding studies. The RyR channels are activated by low Ca^{2+} concentrations (1-10μM), reaching a broad maximum near 100μM and inhibited by high Ca^{2+} concentrations (1-10mM) (Chen et al., 1997a; Chu et al., 1993; Copello et al., 1997; Laver et al., 1995; Li & Chen, 2001). This bimodal Ca^{2+} dependence of RyR suggests the presence of high affinity activating and low affinity inhibitory Ca^{2+} binding sites (see Figure 1.16.), the location and nature of which will be discussed in Chapter 5. There are differences in the Ca^{2+} regulation of the three RyR isoforms, with RyR2 channels generally requiring lower levels of Ca^{2+} for peak activation and higher levels for inactivation compared to the other isoforms (Rousseau & Meissner, 1989; Chen et al., 1997b; Jeyakumar et al., 1998; Murayama et al., 1999; Sonnleitner et al., 1998; Li & Chen, 2001). This increased sensitivity to activation by Ca^{2+} reflects the physiological role of RyR2 in cardiac EC coupling, where Ca^{2+} release is initiated by CICR, rather than physical coupling. However, it is unlikely that the substantially higher Ca^{2+} levels required for RyR2 inactivation are ever reached in cells implying that other physiological factors may be involved in

release termination. However, regulation of RyR gating by Ca^{2+} is complex, being mediated at the lumenal as well as the cytoplasmic side of the channel.

1.4.1.2. Lumenal Ca^{2+}

The influence of cytosolic Ca^{2+} on RyR2 has long been recognized, however Ca^{2+} binding to the lumenal surface of RyR2 may also regulate the channel (Sutko & Airey, 1996; Zucchi & Ronca-Testoni, 1997). In single channel recordings, RyR2 activity is decreased in sub-millimolar luminal (trans) Ca^{2+} levels, while it is enhanced in high millimolar concentrations. It was proposed that this was due to Ca^{2+} diffusing through the pore and binding to sites on the cytosolic side of the channel (Tripathy & Meissner, 1996; Xu & Meissner, 1998). However, more compelling evidence from trypsin digestion experiments now exists to suggest the existence of a specific regulatory Ca^{2+} binding site on the SR luminal side of RyR1 (Ching et al., 2000). A study by Györke & Györke (1998) demonstrated that elevated luminal Ca^{2+} enhanced the sensitivity of RyR2 to activating cytosolic Ca^{2+}. This occurred irrespective of whether the electrochemical gradient for Ca^{2+} supported a cytosolic-to-luminal or a lumenal-to-cytosolic flow of Ca^{2+} through the channel, ruling out the possibility that the lumenal Ca^{2+} was acting by interaction with cytosolic activation sites, suggesting the presence of distinct Ca^{2+}-sensitive binding sites at the lumenal face of the protein. This means that the magnitude of Ca^{2+} release for any given trigger is not simply a function of SR load, instead as SR load increases there is increased Ca^{2+} binding site mediated activation of RyR2. Recently, it was demonstrated that arrhythmia-linked mutants of RyR2 had an increased sensitivity to luminal Ca^{2+} activation (Jiang et al., 2004), suggesting that disruption of luminal Ca^{2+} sensing is a pathological process. It must be noted however, that due to the interplay between cytosolic and lumenal Ca^{2+} pools it is almost impossible to separate their respective effects. In addition, luminal Ca^{2+} effects are also mediated, at least in part, by associated proteins like calsequestrin (Beard et al., 2002; Szegedi et al., 1999) or junctin (Zhang et al., 2001) which will be discussed in section 1.4.2.6.

1.4.1.3. ATP, Mg^{2+} and cADPr

Cytosolic ATP and other adenine nucleotides activate RyRs (Copello et al., 2002; Sonnleitner et al., 1997; Coronado et al., 1994; Smith et al., 1985; Xu et al., 1996). Mg^{2+}, however is a potent RyR channel inhibitor at millimolar concentrations (Copello et al., 2002, Coronado et al., 1994, Laver et al., 1997; Xu et al., 1996). In the cytosol

most ATP is in its Mg^{2+} bound form (Fill & Copello, 2002), yet it is free ATP that binds to and stimulates the channel (Sonnleitner et al., 1997), by allegedly sensitising it to Ca^{2+} activation (Meissner et al., 1997). Indeed it is thought that ATP mediated activation counteracts the inhibition which occurs as the result of exposure to Mg^{2+} in the mM range (Meissner, 1984). The order of potency is adenosine 5'-(β,γ-methylene)-trisphosphate (AMP-PCP, a non-hydrolysable analogue of ATP) > cAMP > ADP > AMP. The action of ATP and Mg^{2+} on RyRs is also isoform specific, with RyR1 being substantially more sensitive to the action of both ligands than either RyR2 or RyR3 (Copello et al., 2002).

The mechanistic basis for Mg^{2+} inhibition is thought to be due to direct competition between Mg^{2+} and Ca^{2+} ions for the Ca^{2+} activation sites, shifting the Ca^{2+} sensitivity of the channel. Since the estimated cellular free Mg^{2+} concentration is ~1mM, this inhibitory effect may be a significant mechanism for closing RyRs (discussed in more detail in paragraph 1.3.6.).

Cyclic ADP-ribose (cADPr) is a metabolite of β-nicotinamide adenine dinucleotide (NAD), is present in myocytes at 20-200nM, but is thought to play a more important role in many non-muscle systems (Lee, 1997; Guo et al., 1996). It has been found to be a powerful intracellular Ca^{2+} release agent in sea urchin eggs (Galione et al., 1991; Lee, 1997), an action mediated by RyR2, but not RyR1 (Meszaros et al., 1993; Galione et al., 1993). Sitsapesan et al. (1994) showed that NAD, cADPr and its metabolite ADP ribose were all capable of RyR2 activation, but not at physiological ATP levels. They concluded that these molecules compete weakly with the ATP site, but cannot serve as physiological modulators of SR Ca^{2+} release.

1.4.1.4. Redox Status

The purified RyR2 contains ~84 free cysteines (21 per monomer), which are suitable for modification by oxidants (Xu et al., 1998). In the myocardium a large number of thiols are likely to be in a reduced state because cells maintain a reducing environment through reducing compounds such as glutathione (in its reduced state, GSH) and NADH. There is evidence that oxidizing and reducing agents affect single RyR channel function (Marengo et al., 1998). Oxidizing conditions, simulated by oxidized glutathione (GSSG), affected the Ca^{2+} sensitivity of RyR2 and its affinity for the regulatory protein calmodulin (CaM) (Balshaw et al., 2001). Furthermore, RyR2 is modulated by NADH oxidase (Cherednichenko et al., 2004) with reduced activity seen with NAD^+ and increased activity seen with NADH (Zima et al., 2003).

Moreover, an N-terminal region of RyR1 (residues 41-420) was found to have structural homology with the oxidoreductase enzyme, isocitrate dehydrogenase. Consistent with this it was also shown that RyR1 binds NAD^+, however the binding properties suggested that this serves more of a regulatory role, rather than an enzymatic one (Baker et al., 2002). Therefore, this region might in some manner control the redox status and hence the activity of the channel.

Nitric oxide (NO) has also been proposed to be an important physiological modulator of cardiac muscle EC-coupling (Kelly et al., 1996; Eu et al., 1999; Petroff et al., 2001; Ziolo et al., 2001). NO is known to affect cellular functions involving S-nitrosylation and oxidation of free thiols (Stamler & Hausladen, 1998), and RyR2 is endogenously S-nitrosylated (Xu et al., 1998). In *in vitro* studies, NO and NO-related molecules activated (Stoyanovsky et al., 1997; Xu et al., 1998) or inactivated (Zahradnikova et al., 1997) RyR2s. Moreover, channel activation has been correlated with the number of thiols modified by NO. Xu et al (1998) demonstrated that the physiological NO donors, S-nitrosoglutathione (GSNO) and S-nitrosocysteine (CysNO) activated RyR2 in a concentration dependent manner, and that this was attributed to inter-subunit cross-linking. Moore et al (1999) found that a residue of RyR1 which was protected by CaM (Cys-3635), was required for this cross-linking. Indeed, mutation of this cysteine residue to an alanine resulted in channels which were not responsive to NO modulation, suggesting that the effect of NO is mediated by this residue (Sun et al., 2001).

1.4.1.5. Phosphorylation status

Initially, RyR2 was proposed to have a single phosphorylation site (Ser2809 - rabbit RyR2, Ser2808 – human/mouse RyR2) for the Ca^{2+}-Calmodulin dependent protein kinase (CaMKII). This site was also phosphorylated by cAMP dependent protein kinase (protein kinase A; PKA), but to a lesser extent (Witcher et al., 1991), though phosphorylation by both kinases is thought to modulate RyR activity.

How does PKA dependent RyR2 phosphorylation alter channel gating?

Valdivia et al (1997) found that PKA slightly decreased basal open probability (P_0) at 100nM Ca^{2+}, but greatly increased peak P_0 during rapid photolytic release of Ca^{2+}. In more intact cellular systems, PKA dependent RyR2 phosphorylation increased the frequency of resting Ca^{2+} sparks only when phospholamban was phosphorylated (i.e. when the SR load was increased) (Li et al., 2002). Thus effects of PKA-dependent

RyR2 phosphorylation at rest may be modest, but the situation may differ during EC coupling (Bers, 2004).

In contrast, Marx et al (2000) found that PKA dependent phosphorylation at Ser2809 enhanced the open probability of RyR2s, and destabilised the channel promoting substates (for an example of a single channel recording showing the presence of these substates see Figure 1.11.). This was attributed to PKA-dependent phosphorylation causing displacement of FKBP12.6, though confusingly, CaMKII phosphorylation of this site did not produce these effects.

The role of RyR2 phosphorylation has been evaluated using mutants that mimic constitutively phosphorylated ($S^{2809}D$) and de-phosphorylated ($S^{2809}A$) channels in lipid bilayers (Reiken et al., 2003a; Wehrens et al., 2003). $S^{2809}D$ channels displayed increased activity and substates similar to those observed with native, PKA-hyperphosphorylated RyRs, which coincided with a loss of FKBP12.6 binding. Loss of this accessory protein appeared to account for the observed changes in channel gating, since binding of a mutant FKBP12.6 ($D^{37}S$) – thought to have a greater affinity for RyR2 than the WT, restored RyR2-$S^{2809}D$ function to normal.

In contrast, co-immunoprecipitation and Western blot analysis carried out by Stange et al. (2003) found that the extent of FKBP12.6 binding was unaffected in constitutively phosphorylated mutants, with WT and mutant RyR2s also having essentially identical functional properties in single channel experiments. In agreement with this Xiao et al. (2004) found that FKBP12.6 could bind to both Ser2808 PKA phosphorylated and nonphosphorylated forms of RyR2, as identified using site-specific, phosphorylation-specific antibodies. Moreover, complete phosphorylation by exogenous PKA disrupted neither recombinant nor native FKBP12.6-RyR2 complex. Currently, different experimental conditions are suggested to underlie these discrepancies. For example, it was noted by Stange et al that the solubilization conditions used by Marx et al were insufficient to solubilize RyRs from membranes.

In addition, Xiao et al (2005) have recently identified a novel PKA phosphorylation site at Ser2030 using phospho-peptide mapping. They found that this site was phosphorylated only after catecholaminergic stimulation of rat myocytes, whereas Ser2808 was constitutively phosphorylated in unstimulated cells – and that phosphorylation of either site did not alter the FKBP12.6-RyR2 interaction. These data indicate that Ser2030 is the major PKA phosphorylation site of RyR2 which responds to catecholaminergic stimulation, but the effects of this phosphorylation are not mediated by FKBP12.6. However, the functional role of phosphorylation at Ser2030 has not yet been evaluated.

CaMKII mediated phosphorylation also alters RyR2 activity

Direct phosphorylation at Ser2809 by CaMKII was shown to activate the channel (Witcher et al., 1991). Additional studies have confirmed RyR2 phosphorylation by CaMKII in lipid bilayers (Hain et al., 1995; Takasago et al., 1991), but the effects on the channel are mixed, with either increases (Witcher et al., 1991; Hain et al., 1995; Wehrens et al., 2004a) or decreases (Lokuta et al., 1997) in RyR2 opening reported. In intact cells, transgenic overexpression of CaMKII-δ increased diastolic spark frequency and fractional Ca^{2+} release during EC coupling, despite a reduced SR load – probably caused by the increased diastolic leak (Maier et al., 2003). Adenovirus infected adult rabbit myocytes overexpressing CaMKII and permeabilised myocytes exposed to pre-activated CaMKII exhibited the same activating effects on sparks and SR Ca^{2+} release (Maier et al., 2003). Overall, it appears that CaMKII-dependent RyR2 phosphorylation strongly activates Ca^{2+} release during both diastole and systole (Bers, 2004).

Until recently, it was assumed that Ser2809/8 was the only target for CaMKII mediated RyR2 phosphorylation. However, the presence of additional sites is likely since many conserved potential phosphorylation sequences have been identified in the protein sequence (Takeshima, 1993). Functional studies and peptide mapping comparing the effects of endogenous and exogenous kinases support the presence of several RyR phosphorylation sites (Takasago et al., 1991; Hain et al., 1995). Rodriguez et al. (2003) showed that CaMKII phosphorylates RyR2 to a four fold higher stoichiometry than does PKA, suggesting that sites in addition to Ser2809 are CaMKII targets, a finding substantiated by the fact that two Ser2809 mutants ($S^{2809}D$ and $S^{2809}A$) incorporated ^{32}P in metabolic labelling experiments (Stange et al., 2003). Wehrens et al (2003) have identified a CaMKII site on RyR2 at Ser2815, which upon phosphorylation strongly activates the channel in bilayer experiments. This study however suggests a lower CaMKII to RyR2 phosphorylation stoichiometry (1.5) than Rodriguez et al. (2003).

These findings suggest there is more than one phosphorylation site on RyR2 for both PKA and CaMKII. However, even though both enzymes are driven either directly, or as a consequence of the elevated Ca^{2+} transients produced by stimulation of the ß-adrenergic pathway, the effect of phosphorylation at these different sites may be more complex than previously anticipated.

1.4.2. Modulation of RyR2 function by protein regulators

RyR2 exists as part of a huge macromolecular complex, serving as a scaffold for a number of accessory proteins that regulate various aspects of channel function. Most ligands interact with the vast cytosolic N-terminal portion of the molecule (e.g. FKBPs, calmodulin, PKA), while a few bind to the luminal side (e.g. junctin, triadin, calsequestrin) in order to modulate Ca^{2+} release (Mackrill, 1999). Thus, although the channel exhibits marked auto-regulation, its association with these accessory proteins appears to add another layer of versatility and complexity to Ca^{2+} release modulation. Several strategies, including biochemical approaches and more recently high-resolution electron microscope image reconstruction and difference maps have been used to determine protein binding sites on RyR.

1.4.2.1. The FK506-binding proteins

FK506 and rapamycin are immunosuppressant drugs that bind to immunophilin target FK-binding proteins (FKBPs). In T-lymphocytes Ca-CaM normally activates calcineurin (also known as protein phosphatase 2B) which dephosphorylates the nuclear transcription factor NFAT (the nuclear factor of activated T-cells) allowing its entry into the nucleus where it stimulates interleukin-2 transcription, a lymphokine which promotes T-cell proliferation. The FKBP-FK506 complex binds to calcineurin, preventing its action, thereby suppressing the immune response (Schreiber & Crabtree, 1992; Marks, 1996). FKBPs also catalyse peptidylprolyl-*cis-trans*-isomerization, a function believed to be involved in protein folding, but their isomerase activity is not essential for RyR effects (Mackrill, 1999; Kay, 1996; Marks, 2000). FKBPs bind to and co-purify with RyRs (Marks et al., 1989; Jayaraman et al., 1992; Timerman et al., 1993, 1994, 1996): FKBP12 binds tightly to RyR1, - and while the heart expresses both FKBP12 and 12.6, the latter preferentially associates with RyR2, due to a much higher affinity (x600, Timerman et al., 1996). The molar ratio of FKBP to RyR is 1:1 i.e., one FKBP protein is bound to each of the four subunits of the RyR channel complex (Timerman et al., 1993, 1996). The binding site for FKBP12.6 on RyR2 was initially proposed to be in the central domain of the protein (2361-2496 amino acids), which was identified using yeast two-hybrid analysis (Marx et al., 2000). This region corresponded to that in RyR1 which interacts with FKBP12 (Cameron et al., 1997; Bultynck et al., 2001;Gaburjakova et al., 2001). However, recently loci for FKBP12.6 binding have been mapped to the N- and C-termini as well (Masumiya et al., 2003; Zissimopoulos & Lai, 2005).

Nonetheless, due to the complexity of the tetrameric RyR2 structure and the fact that this domain was assigned functionality on the basis of the study of fragments of the RyR2 rather than the full length protein, it is entirely feasible that all of these loci contribute to the single FKBP12.6 binding site in the intact molecule (George et al., 2005).

Removal of FKBP12.6 from the RyR2 (using FK506 or rapamycin) activates the channel (possibly by increasing Ca^{2+} sensitivity of the channel) and inhibits adaptation (Kaftan et al., 1996; Xiao et al., 1997). Studies in intact myocytes showed that removal of FKBP12.6 by FK506 increased the resting spark frequency and enhanced Ca^{2+} transients (McCall et al., 1996). Others report that FKBP12.6 removal has very little impact on RyR2 channel function (Barg et al., 1997; Timerman et al., 1996; Xin et al., 2002). Several groups have shown that FKBP12/12.6 removal promotes the appearance of subconductance states in single channel experiments (Ahern et al., 1994; Ahern et al., 1997; Brillantes et al., 1994; Kaftan et al., 1996; Marx et al., 2000). This observation led to the suggestion that FKBP binding stabilizes the coordinated gating of the four channel monomers and in doing so stabilizes the structure of the permeation pathway so that openings go from the fully closed to the fully open state (see Figure 1.11.).

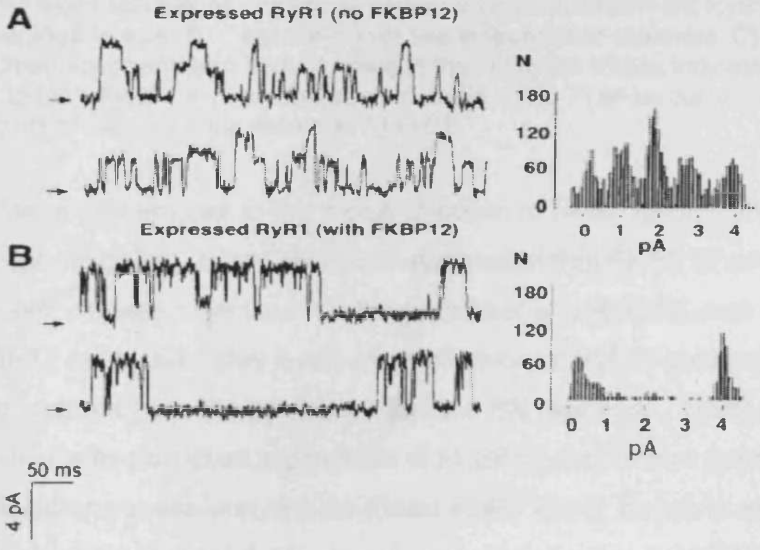

Figure 1.11. Single channel recordings of RyR1 which appear to exhibit subconductance states (adapted from Marks, 1996). A) Subconductance states corresponding to conductances of 0, 1, 2, 3, 4 pS appear in the absence of FKBP12. B) (A) Addition of FKBP12 reduced the frequency of these subconductance states, and the channel was either fully closed or fully opened (4 pS). The charge carrier for these experiments was Ca^{2+}. Channel openings are in the upward direction; the arrows (left) indicate the closed state of the channel.

Marx et al. (1998) suggested that FKBPs may also be involved in physical 'coupling' between RyR tetramers. They proposed that this could be a mechanism allowing simultaneous opening and coordinated closure of channels *in vivo* (see Figure 1.12.). Although recent evidence shows that synchronous RyR opening does occur (Wang et al., 2004), it is unlikely to be mediated by FKBPs since the region which mediates inter-tetrameric interaction (encompassing domains 6 and 10) is spatially distinct from the FKBP12 binding site (see Figure 1.10.B and Yin et al., 2005).

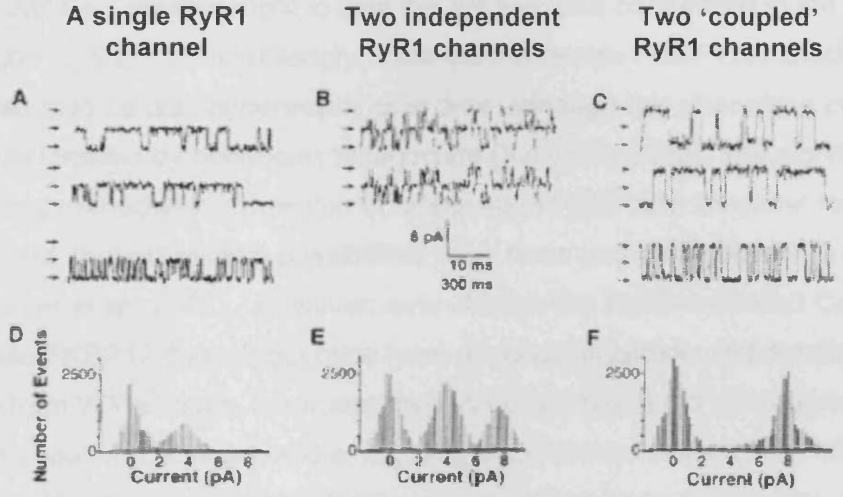

Figure 1.12. Coupled gating of RyR1 tetramers, co-expressed with FKBP12 (adapted from Marx et al., 1998). A) shows a single recombinant RyR1 channel with openings to 4pA. B) Recording from two independent channels. C) Coupled RyR1 channels opening to 8pA. Arrows at the left of the traces indicate (from bottom to top), the 0-, 4-, and 8pA current levels. D) to F) show current amplitude histograms of the channels shown in A) to C).

There is some uncertainty as to the mode of action of FKBP12 on RyR1. As well as stabilizing channel gating, it has also been suggested that FKBP12 could be a physical coupler between the $Ca_V1.1$ voltage sensor and RyR1 (Lamb & Stevenson, 1996). FKBP12 might also play a role in rectification of RyR1, preventing retrograde movement of cations from the cytoplasm into the SR (Ma et al., 1995). Surprisingly, transgenic mice with disrupted expression of FKBP12 showed no functional or structural alterations in skeletal muscle (Shou et al., 1998), however major developmental multisystem defects were detected, indicating that FKBP12 ablation caused many RyR independent effects. Nonetheless, animals having a skeletal muscle-specific FKBP12 knockout (Tang et al., 2001) displayed abnormal muscle contraction, suggesting that FKBP12 has a fundamental role in maintaining muscle structure integrity.

There are reports that suggest that FKBP12.6 is critical to normal RyR2 channel operation in the heart (Kaftan et al., 1996; McCall et al., 1996). It has even been suggested that abnormal FKBP12.6-RyR2 interactions, occurring as a result of channel hyperphosphorylation may be implicated in heart failure (Marks, 2000; Marx et al., 2000; Ono et al., 2000; Yano et al., 2000). Marx et al. (2000) demonstrated that RyR2 is hyperphosphorylated at Ser2809 in human heart failure, with channels showing multiple conductances and increased overall flux (i.e. the FKBP12.6 depleted phenotype). This hyperphosphorylation was proposed to cause a persistent diastolic SR Ca^{2+} leak, thought to limit the SR load and contraction in the failing heart (see section 1.5.2.1.). Interestingly, male but not female FKBP12.6 knockout mice developed mild cardiac hypertrophy over time, although this phenotype could be induced in females by oestrogen antagonism (Xin et al., 2002). The significance of this oestrogen-mediated protection in response to FKBP12.6 knockout remains unexplained, though several possibilities have been proposed (Nelson & Herrera, 2002; Pelzer et al., 2001). However, even though the RyR2-mediated Ca^{2+} sparks from these FKBP12.6 knockout mice have a higher amplitude and duration compared to those from WT animals, the males' hypertrophied hearts do not progress to more severe myopathies or heart failure, implying that decreased cytosolic FKBP12.6 per se, may not be the primary culprit in the generation of these pathologies (Fill & Copello, 2002). Thus the impact of FKBP12.6 on RyR2 function and dysfunction in pathology is not yet clearly established.

1.4.2.2. Calmodulin

Calmodulin (CaM) is an ubiquitous 16.7kDa cytosolic protein that is thought to participate in the regulation of many ion channels including the L-type Ca^{2+} channel and some Ca^{2+}-activated K^+ channels, thereby acting as an intracellular Ca^{2+} sensor (Levitan, 1999). CaM also influences SR Ca^{2+} release through a direct interaction with RyRs as well as other proteins that regulate Ca^{2+} release. The CaM protein consists of two pairs of EF hands linked by a flexible hinge region (Mackrill, 1999) and can interact with RyRs even in its Ca^{2+} free form (apoCaM).
In contrast to its actions on RyR1 and RyR3 (stimulatory at low [Ca^{2+}], inhibitory at [Ca^{2+}] > 1 μM (Fuentes et al., 1994; Rodney et al., 2000)), CaM inhibits RyR2 activity at all [Ca^{2+}] (Balshaw et al., 2001; Yamaguchi et al., 2003), although not all investigators have found inhibition at low [Ca^{2+}] (Fruen et al., 2000). CaM achieves this inhibition by shifting the Ca^{2+} dependence of RyR2 activation to a higher [Ca^{2+}]

(Balshaw et al., 2001; Xu & Meissner, 2004), altering the Ca^{2+}-dependent activation of the RyR (Bers, 2004).

One CaM molecule binds with nanomolar affinity to each RyR1 monomer at both low and high [Ca^{2+}]. One CaM binds per RyR2 monomer at 200μM [Ca^{2+}], but at 100nM [Ca^{2+}] there may be less than one CaM per RyR2 monomer (Fruen et al., 2000; Balshaw et al., 2001; Yamaguchi et al., 2003). Thus, higher [Ca^{2+}] may increase CaM:RyR2 stoichiometry.

Trypsin and alkylation protection assays, sulphydryl oxidation and ligand overlay experiments have demonstrated a single CaM binding site on RyR (residues 3553-3662) (Moore et al., 1999; Yamaguchi et al., 2001). However, the apoCaM/CaM binding location is Ca^{2+} dependent and is mediated by interaction with the lobe domains of the protein (Rodney et al., 2001; Xiong et al., 2002; Zhang et al., 2003c). It has also been suggested that the C-terminal lobe of CaM binds to amino acids 3630-37, while the N-terminal lobe of CaM binds in the 1982-1999 region in a nearby position in the 3D structure. In fact cryo-microscopy studies of the 3D structure of RyR1 suggests that Ca^{2+} binding causes an approximately 32 Å shift of the channel CaM binding site (Wagenknecht et al., 1994). Therefore, long range conformational changes are thought to be involved in the modulation of RyR2 activity by CaM (Meissner, 2004). Functionally, there may be a role for CaM in the termination of SR Ca^{2+} release. However, CaM binds to and dissociates from RyR2 on a time scale of seconds to minutes (Balshaw et al., 2001), and so is unlikely to regulate the channel on a beat to beat basis. It is now thought that this function is most likely carried out by another protein, namely sorcin (Farell et al., 2005).

1.4.2.3. Sorcin

Unlike CaM, sorcin (**so**luble drug **r**esistance related **c**alcium binding prote**in**) could regulate RyR with appropriate kinetics, suggesting that it may be a physiological modulator of the channel during the cardiac cycle. Sorcin is a 22kDa Ca^{2+} binding protein with five EF hands which has been reported to be associated with RyR2 in cardiomyocytes (Meyers et al., 1995), though the exact location of the binding site is not yet known. Sorcin can rapidly reduce RyR2 open probability in bilayer studies and decreases ryanodine binding (Lokuta et al., 1997) though this inhibition was reduced by PKA phosphorylation of sorcin (Lokuta et al., 1997; Farell et al., 2003; 2005). Sorcin binds to RyR2 only at elevated [Ca^{2+}] (EC_{50} ~ 200 μM, Farrell et al.,

2003) suggesting that β-adrenergic stimulation decreases sorcin-mediated inhibition of RyR2, allowing for increased Ca^{2+} release during EC coupling.
Adenoviral overexpression of sorcin in myocytes caused reduced Ca^{2+} transients and a decrease in Ca^{2+} spark frequency due to an increase in Ca^{2+} extrusion via the Na^{+}/Ca^{2+} exchanger, resulting in a decreased SR load (Seidler et al., 2003). Recent studies of *in vivo* sorcin over-expression gave contrasting results: Meyers et al. (2003) found decreased Ca^{2+} transients and contraction, while Suarez et al. (2004) found that both these parameters were increased. The reasons for these differences is unexplained, however the general consensus is that sorcin may serve as an endogenous inhibitor of SR Ca^{2+} release, where this effect can be relieved at low $[Ca^{2+}]$ or by PKA-dependent phosphorylation.

1.4.2.4. PKA, protein phosphatases 1 and 2A and their anchoring proteins

The RyR2 macromolecular complex includes protein kinases and phosphatases which are anchored to specific domains of the channel by adaptor/anchoring proteins, markedly augmenting the localized signalling capacity. Marx et al. (2001, 2000) showed that PKA is anchored to RyR2 via muscle A kinase anchoring protein (mAKAP). Residues 3003-3039 of RyR2 participate in a leucine zipper interaction with mAKAP which in turn binds to the regulatory subunit of PKA. PP1 and PP2A are thought to participate in dephosphorylation of RyR2. PP1 associates via a leucine zipper motif on spinophilin. This adaptor protein also targets PP1 to RyR1 and RyR2 (residues 554-588). PP2A associates with the targeting protein PR130 which interacts with RyR2 (but not RyR1) via leucine zipper motifs (residues 1603-1631) (Marx et al., 2000). Notably, this study demonstrated that the CaM-activated phosphatase, calcineurin (PP2B), was not part of this macromolecular complex. CaMKII also co-immunoprecipitates with RyR2 (Zhang et al., 2003c), but the molecular site of interaction has not yet been elucidated (even though it is known to phosphorylate at Ser2815 (Wehrens et al., 2004a)), though alphaKAP is known to anchor this kinase to the SR in skeletal muscle (Bayer et al., 1998). Thus, the requisite molecular machinery for both phosphorylation and dephosphorylation are anchored directly to the protein resulting in highly localized control over the phosphorylation state of the channel.

1.4.2.5. $Ca_v1.2$

$Ca_v1.2$ (also known as the L-type voltage operated Ca^{2+} channel or dihydropyridine receptor (DHPR) or $Ca_v1.1$ in skeletal muscle) is a plasma membrane Ca^{2+} channel that senses depolarisation of the surface membrane and initiates the process of EC coupling in muscle (Franzini-Armstrong & Protasi, 1997; Mackrill, 1999). In skeletal muscle, the $\alpha 1$ subunit of $Ca_v1.1$ interacts with RyR1 after it detects depolarisation, and it is this direct mechanical interaction that is the basis of EC coupling in skeletal muscle. Of particular importance in this physical coupling is the region of the loop between the second and third domain of the $\alpha 1$ subunit of $Ca_v1.1$ (i.e. the II-III loop) and residues 951-1112 and 1837-2168 of RyR1 (Leong & MacLennan, 1998a&b; Proenza et al., 2002). It is probable that $Ca_v1.1$ makes contact with RyR1 near the clamp structures (see Figure 1.7., Franzini-Armstrong et al., 1999; Block et al., 1988). In cardiac muscle, EC coupling is known to be mediated by CICR, with no physical coupling of the two Ca^{2+} channels (Piacentino et al., 2000; Trafford & Eisner, 2003), despite highly homologous $Ca_v1.1/2$ and RyR proteins (Mikami et al., 1989). This may explain why the specific location of $Ca_v1.1/2$ channels relative to RyRs differs in skeletal and cardiac muscle. In skeletal muscle, $Ca_v1.1$s are clustered in groups of four, or tetrads, which are positioned so that each channel is located immediately above one of the RyR subunits to facilitate direct interaction (Block et al., 1988; Franzini-Armstrong & Kish, 1995). In cardiac muscle, there is a less ordered array of $Ca_v1.2$ channels over RyR2 junctions where they are concentrated at couplons, albeit not as tetrads (Franzini-Armstrong & Protasi, 1997). There is also a 4-10 fold excess of RyR2s over $Ca_v1.2$ in the heart, implying that at most 10-25% of the RyR2s could possibly interact with a $Ca_v1.2$ (Bers & Stiffel, 1993).

1.4.2.6. Calsequestrin, triadin and junctin

Calsequestrin (CSQ) is a high-capacity Ca^{2+} binding protein, which localizes to the junctional SR membrane and whose primary function appears to be buffering of intra-luminal Ca^{2+} (Yano & Zarain-Herzberg, 1994; Franzini-Armstrong et al., 1987). Cardiac CSQ is a highly acidic protein of ~45kDa with 119 Glu and Asp residues that permit it to bind 40-50 Ca^{2+} ions per molecule (MacLennan & Wong, 1971; Scott et al., 1988; Yano & Zarain-Herzberg, 1994). Triadin (~35kDa) and junctin (~26kDa) are integral SR proteins which physically couple CSQ to the RyR2 via 'polar zippers' formed between 'KEKE' motifs present in their primary structures and acidic moieties

near the inner mouth of the RyR channel domain (Zhang et al., 1997; Lee et al., 2004), forming a quaternary complex (Caswell et al., 1991; Jones et al., 1995; Zhang et al., 1997; Mackrill, 1999).

CSQ is also known to aggregate in the presence of Ca^{2+} (Maurer et al., 1985) forming regular arrays that appear crystalline in the lumen of the SR (Franzini-Armstrong et al., 1987). This polymerisation of CSQ provides a highly charged surface onto which Ca^{2+} can be adsorbed (MacLennan et al., 2002). It has also been suggested that assembly and disassembly of these CSQ arrays could be instrumental in the regulation of Ca^{2+} release from beat to beat (Ikemoto et al., 1991; Launikonis et al., 2005). This idea is reinforced by a study in which Gyorke et al (2004) suggest that CSQ itself participates actively in RyR2 regulation. They showed that the open probability of RyR2 (with triadin and junctin) is inhibited by CSQ at low luminal [Ca^{2+}], but that this inhibition is relieved at high luminal [Ca^{2+}]. Thus, it is possible that CSQ contributes to the luminal sensing of Ca^{2+} by RyR2 (Bers, 2004). Transgenic mice in which CSQ had been overexpressed >10 fold developed cardiac hypertrophy (Jones et al., 1998; Sato et al., 1998). Cardiomyocytes from these mice display a 10 fold increase in the amplitude of caffeine induced Ca^{2+} release compared to controls, as would be expected for cells possessing a greater level of intra-SR Ca^{2+} buffer. Conversely, these cells exhibited a decreased spontaneous RyR2 activity, which was explained by a decrease in free SR Ca^{2+}. More moderate levels of adenoviral CSQ expression (2-4 fold) in adult ventricular myocytes resulted in enhanced Ca^{2+} transient and spark amplitude (Terentyev et al., 2003). These results indicate that cardiac CSQ plays pivotal roles both in Ca^{2+} storage and in regulation of Ca^{2+} release via RyR2. It was not surprising therefore, when mutations in the CSQ gene were found to be associated with an inherited arrhythmia syndrome. The mutations ($D^{307}H$ and three nonsense mutations) result in an autosomal recessive form of catecholaminergic ventricular tachycaridia (CPVT –the autosomal dominant form of which is associated with mutations in RyR2- see section 1.5.2.2.) (Lahat et al., 2001; Postma et al., 2002). The missense mutation disrupts the negatively charged region of the protein, affecting its ability to bind Ca^{2+}, whereas the nonsense mutations result in the complete absence of the protein, - both situations have been shown to lead to a decrease in Ca^{2+} buffering which could result in SR Ca^{2+} overload or have a direct effect on RyR2 activity, (Terentyev et al., 2003; Viatchenko-Karpinski et al., 2004) which could lead to arrhythmogenesis.

The function of triadin and junctin beyond that of anchoring CSQ to the RyR is not precisely known. Isoproterenol stimulation of myocytes overexpressing triadin resulted in intracellular Ca^{2+} disturbances similar to those seen with CSQ mutant

overexpression (Terentyev et al., 2005). Conversely, overexpression of a triadin mutant lacking the KEKE domain had no effect on Ca^{2+} cycling, suggesting that the interaction between these proteins is important in the regulation of Ca^{2+} release. Mice overexpressing triadin 1 show some hypertrophy and those overexpressing junctin show altered Ca^{2+} handling, notably impaired relaxation, implying that junctin overexpression might in some way slow termination of CICR (Kirchhefer et al., 2003).

1.4.3. Modulation of RyR2 function by pharmacological agents

Many exogenous substances have been reported to modulate RyR function but their actions are often complex, for example, several modulators may either stimulate or inhibit Ca^{2+} release depending on concentration or incubation time. Many of these have been useful as experimental tools to investigate RyR function *in vitro* (e.g. ryanodine, caffeine), while others have been used therapeutically in the treatment of RyR-related diseases (e.g. dantrolene) or cause adverse RyR-mediated effects (e.g. anaesthetics, cardiac and aminoglycosides)

1.4.3.1. Ryanodine

Ryanodine is an ester of pyrrole-α-carboxylic acid with ryandolol, and modulation of cardiac and skeletal muscle function by this compound has been known for many years (Jenden & Fairhurst, 1969). In bilayer studies, it has been shown that ryanodine (1nM-10μM) locks RyR in an open state, corresponding to about 40-60% of normal channel conductance (Rousseau et al., 1987). However, higher ryanodine concentrations (in the millimolar range), caused complete blockade of the channel which was irreversible, at least within the timescale of the experiments (Rousseau et al., 1987; Lai et al., 1989; Bull et al. 1989; Buck et al. 1992). The interpretation of these results is that the interaction of ryanodine with its high-affinity binding site stabilizes the open state of the channel, but the decreased conductance may be due to partial physical occlusion of the channel by the ryanodine molecule. At higher concentrations, ryanodine binds to three low-affinity sites (Lai et al., 1989), which causes further reduction in channel conductance, up to complete blockade (Buck et al., 1992, Zucchi & Ronca-Testoni, 1997). However, the theory that ryanodine acts as a direct channel pore blocker has not been directly tested, and recent studies have suggested an alternate mechanism whereby ryanodine binds to sites that allosterically induce substantial conformational changes in the RyR which make the

conformational changes associated with channel opening energetically unfavourable (Fessenden et al., 2000).

Channel inactivation is also observed after prolonged incubation with lower (100 nM) concentrations of ryanodine (Zucchi & Ronca-Testoni, 1997). Covalent labelling of RyR with a photo-activatable derivative of ryanodine suggested that this channel inactivation was associated with the development of stable, virtually irreversible interactions between RyR monomers (Bidasee et al., 1995).

Furthermore, it has been observed that ryanodine binding can only occur when the channel is in the open configuration (making it a marker of channel activation – see Chapter 3), hence the consensus opinion is that the ryanodine binding sites are located somewhere within the channel pore which have been localised to the C-terminal 76kDa fragment of the protein, by two independent studies using different approaches (Callaway et al., 1994; Witcher et al., 1994). Further evidence for this comes from expression studies of C-terminal truncated RyR proteins, which formed functional channels upon incorporation into lipid bilayers, the gating of which were modified by ryanodine (Bhat et al., 1997b; Xu et al., 2000).

It has also been demonstrated that ryanodine sensitises the RyR to Ca^{2+} activation with ryanodine-modified RyR2 channels being half-maximally activated by 100-1000-fold less Ca^{2+} than unmodified channels (Masumiya et al., 2001; Du et al., 2001c).

1.4.3.2. Methylxanthines

Caffeine and other methylxanthines activate both the cardiac and skeletal RyR, with cardiac RyR being more sensitive (Rousseau & Meissner, 1989; Rousseau et al., 1988; Liu & Meissner, 1997). The order of potency of methylxanthines has been determined as: 1,7-dimethylxanthine > theobromine > theophylline > caffeine. Caffeine appeared to shift the Ca^{2+}-dependence of RyR gating to ~10 times lower [Ca^{2+}], so that significant Ca^{2+} release was seen even at nanomolar [Ca^{2+}]. Single channel studies showed that low concentrations (0.5-2mM), caffeine had a Ca^{2+}-sensitizing effect, and channel activation required the presence of submicromolar Ca^{2+}. Higher concentrations (>5 to 10 mM) however, were capable of channel activation even at picomolar levels of Ca^{2+} (Sitsapesan & Williams, 1990). Channels activated by caffeine were still characteristically modified by ryanodine, ATP, Mg^{2+} and ruthenium red.

In binding experiments, caffeine (1-30mM) favoured ryanodine binding by increasing the sensitivity of the binding reaction (Pessah et al., 1987; Chu et al., 1990; Holmberg & Williams, 1990; Hernandez-Cruz et al., 1995). The action of caffeine is

extremely rapid and is quickly reversible, even in intact myocytes. This makes it a very useful experimental tool in measuring RyR activation (and is used for this purpose in Chapter 4) and in some cases the SR load (Smith et al., 1988).
In general, the effect of caffeine was thought to be similar to that of adenine nucleotides. However, it has been suggested that caffeine and adenine nucleotides act on different, albeit interacting sites, since they have synergistic effects on channel gating and ryanodine binding (Ogawa & Hararfuji, 1990).

1.4.3.3. Cardiac glycosides

Digoxin is one of the few drugs used in clinical cardiology which has a well characterised effect on RyR2. Digoxin is known to increase cardiomyocyte cytosolic [Ca^{2+}] via its established action on the Na^+-K^+-ATPase (Reuter et al., 2002), whereby the resulting [Na^+] increase is removed from the cell by the NCX, resulting in an inward Ca^{2+} flux. However, cardiac glycosides directly activate RyR2 as well, and thus their inotropic effect and tendency to induce Ca^{2+}-dependent arrhythmias may, also reflect their direct effect on RyR2 (McGarry & Williams, 1993; Sagawa et al., 2002).

1.4.3.4. Anaesthetics

Volatile anaesthetics e.g. halothane, isofluorane and enflurane increase both RyR1 and RyR2 activity in a Ca^{2+}-dependent manner, with a maximum occurring at 1-10 μM Ca^{2+} (Zucchi & Ronca-Testoni, 1997). This effect of halogenated volatile anaesthetics on RyR1 is important in individuals who suffer from malignant hyperthermia (MH) or central core disease (CCD). Mutation of RyR1 has been implicated in the pathogeneisis of these conditions which are triggered by the administration of halogenated volatile anaesthetics, causing muscle rigidity and hypermetabolism among other symptoms (see section 1.5.1.).
Conversely, local anaesthetics such as tetracaine and procaine have been shown to inhibit skeletal muscle SR Ca^{2+} release, ryanodine binding and single channel open probability without affecting unitary conductance(with tetracaine being the most potent of the two). These effects are likely to be mediated by a high-affinity binding site, corresponding to, or interacting with the Ca^{2+} binding and adenine nucleotide binding sites (Zucchi & Ronca-Testoni, 1997).

1.4.3.5. 4-Chloro-m-cresol

4-Chloro-m-cresol (4-cmc) and the related compound 4-chloro-m-ethylphenol, induced Ca^{2+} release from skeletal SR at a concentration of ~300 μM (Hermann-Frank et al., 1996; Zucchi & Ronca-Testoni, 1997), and it is used diagnostically to distinguish between normal and MH-susceptible muscles. In bilayer experiments, 4-chloro-m-cresol increased channel open probability, an effect which was more pronounced when applied to the luminal (trans) chamber. 4-Chloro-m-cresol exhibits isoform specificity since it activates RyR1 and RyR2 (Wong & Pessah, 1996), but not RyR3 (Fessenden et al., 2000). Further to this, residues 4007-4180 of RyR1 were determined as being essential for 4-cmc-mediated activation of the channel (Fessenden et al., 2003).

1.4.3.6. Dantrolene

Dantrolene is the hydantoin derivative, 1-((5-(p-nitrophenyl)furfurylidine) amino)hydantoin sodium. It acts as a postsynaptic muscle relaxant and is the chief drug used in the prevention and treatment of MH (Zucchi & Ronca-Testoni, 1997). Single channel studies using human RyR1 showed a bi-phasic activation-inactivation response to dantrolene (Nelson et al., 1996), effects also observed in cardiac muscle, but the relative sensitivity to dantrolene was lower (Zucchi & Ronca-Testoni, 1997).

1.4.3.7. Aminoglycosides

Aminoglycoside antibiotics, especially neomycin are highly positively charged and inhibit caffeine induced SR Ca^{2+} release (Palade, 1987). Neomycin inhibited ryanodine binding to both RyR1 and RyR2, with higher concentrations needed for RyR2 inhibition (Zimanyi & Pessah, 1991; Mack et al., 1992; Wang et al., 1996). It has also been suggested that high concentrations of neomycin irreversibly inactivate RyRs (Mack et al., 1992). Assays performed after trypsin treatment confirmed that the neomycin binding site was located in a 76 kDa fragment, corresponding to the carboxyl part of the protein (Wang et al., 1996).

1.4.3.8. Ruthenium red

Ruthenium red is a polycationic dye with a structure that includes 14 amino groups, and has been shown to inhibit SR Ca^{2+} release, both in cardiac and skeletal muscle. This effect has also been shown using ryanodine binding and single channel studies, with inhibitory concentrations ranging from 10 nM to 20 μM, with activated channels requiring higher concentrations for inhibition. In bilayer experiments, micromolar ruthenium red produced irreversible channel closure (Smith et al., 1985) in an asymmetrical and voltage-dependent manner (Ma, 1993). On the basis of these results, it was suggested that the binding site is located close to the pore of the channel, and that ruthenium red cannot permeate the open channel. However, Ca^{2+} release, single channel and ryanodine binding studies of skeletal and cardiac channels concluded that ruthenium red modifies RyRs by at least two different mechanisms, involving binding to both cytosolic and luminal sites (Xu et al., 1999). Ruthenium red induces substates in RyR single channel conductance via undefined mechanisms, reducing the effectiveness of this compound as an inhibitor of RyR channel activity.

1.5. RyR and pathology

The finely co-ordinated process of EC coupling involves a number of exquisitely regulated protein components. Alteration of these proteins, or the environment which regulates their function, is known to result in impaired contraction and/or pathological cellular consequences. A number of inherited or acquired muscle and cardiac diseases appear to result from RyR dysfunction, which is commonly manifested as enhanced Ca^{2+} release at rest. Mutations in RyR1 have been found to result in the skeletal muscle myopathies, malignant hyperthermia and central core disease, whereas the arrhythmogenic conditions catecholaminergic polymorphic ventricular tachycardia and arrhythmogenic right ventricular dysplasia type 2 have been associated with point mutations in RyR2. In addition, altered regulation of RyR2 may be involved in the pathogenesis of heart failure.

1.5.1. Skeletal muscle diseases resulting from defects in RyR1

Mutations in the skeletal muscle ryanodine receptor are known to result in malignant hyperthermia (MH), a pharmacogenetic disease triggered by inhalational anaesthetics (Mickelson & Louis, 1996). These mutations are generally thought to result in excessive mobilization of Ca^{2+} from the SR. Susceptible individuals anaesthetized with halothane or other halogenated anaesthetics suddenly develop an unusual metabolic reaction characterized by muscle rigidity and acidosis, arrhythmias and rapid rise in body temperature. The onset of MH can be fatal unless the SR leak is prevented by the administration of dantrolene, which specifically blocks RyR1 (Zhao et al., 2001). Diagnosis of the MH phenotype is made using an *in vitro* contracture test (IVCT), where augmented sensitivity to caffeine and halothane contractile responses in muscle biopsies is a marker for MH susceptibility (Ellis & Harriman, 1973; Larach, 1989).

Central core disease (CCD) is a distinct but related disorder, also caused by mutations in RyR1 (Matthews & Moore, 2004). This is a congenital myopathy, which displays considerable phenotypic variability. Thus, proximal muscle weakness, hypotonia and motor deficiencies are present in most, but not all CCD patients and certain CCD individuals may also be MH susceptible (Lyfenko et al., 2004). This disorder derives its name from the finding of amorphous central areas or cores that lack mitochondria in the skeletal muscle fibres of affected individuals. A possible explanation for this is that the mutant, leaky channels would cause an elevation in the cytoplasmic [Ca^{2+}], which would be removed efficiently by Ca^{2+} extrusion

mechanisms in the sarcolemmal regions of the cell, however central areas would be more likely to retain higher Ca^{2+} levels, causing central mitochondria to undergo Ca^{2+} overload and death (Benkusky et al., 2004).

More than 40 missense mutations have been identified as potential culprits of MH and CCD (for review see Brini, 2004 and McCarthy et al., 2000), as well as several in-frame deletions that result in the removal of one to three amino acids (Sambuughin et al., 2001; Monnier et al., 2001) or of seven amino acids (and insertion of a Tyr residue) (Zorzato et al., 2003). Interestingly, these mutations appear clustered in three regions of the RyR1; namely, near the N-terminal (C^{35}- R^{614}), the central (D^{2129}-R^{2458}), and near the C-terminal (V^{4214}- A^{4942}) domains of the channel (Brini, 2004, see Figure 1.13.). The relevance of this clustering points towards the mechanisms by which RyR1 dysfunction causes the disease phenotype: mutations in the N-terminal and central domains may disrupt the interactions which are thought to stabilize the closed and open states of the channel (Ikemoto and Yamamoto, 2000; El-Hayek et al., 1999), and mutations in the C-terminus may directly affect ion permeation through the pore (Avila et al., 2003).

1.5.1.1. Functional effects of MH and CCD mutations in RyR1

Ikemoto and colleagues showed that a peptide corresponding to residues 2442-2477 of RyR1 (called DP4) enhanced ryanodine binding and Ca^{2+} release in isolated SR, by competing with the corresponding region of RyR1 in binding to the N-terminal domain (Yamamoto et al., 2000). Moreover, these stimulatory effects were lost when DP4 contained a MH mutation ($R^{2458}C$). These results suggest that the interactions between these domains of RyR1 may be involved in the channel regulation mechanism, and that MH-linked mutation causes the closed state of the channel to be unstable, causing hypersensitisation effects.

Hypersensitisation effects were also seen in a pig model of MH which also results from a point mutation in RyR1 ($R^{615}C$) (Gillard et al., 1991). Porcine MH muscle exhibits increased sensitivity to caffeine and halothane (Allen et al., 1990) and decreased sensitivity to inhibition by Mg^{2+} (Owen et al., 1997). Mutant channels also exhibit longer mean open times and decreased Ca^{2+} dependent inactivation in single channel experiments (Fill et al., 1990). This resultant increase in Ca^{2+} mobilisation is thought to elevate intracellular Ca^{2+} levels (though reports on this have shown conflicting data), triggering pathological processes, for example, an increased rate of

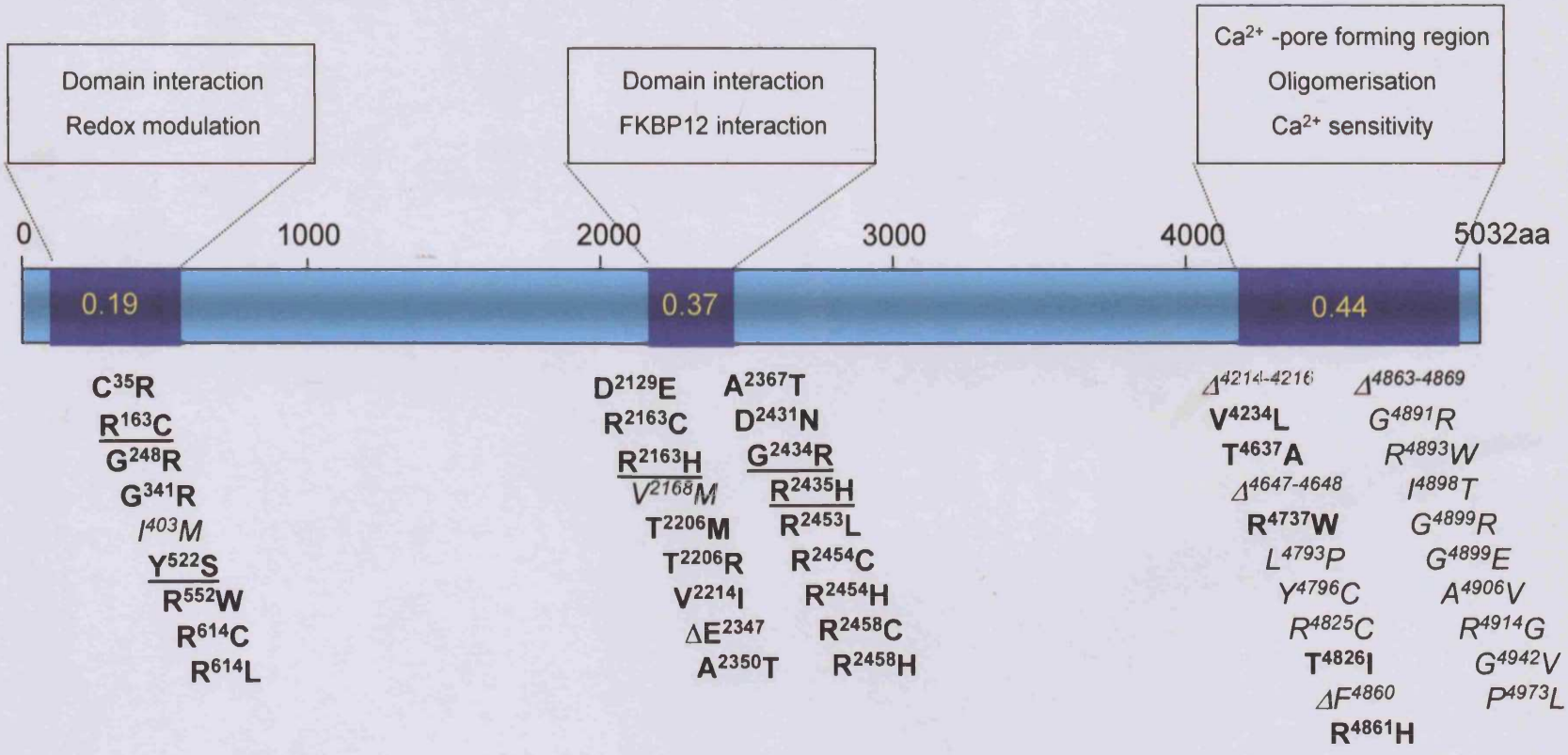

Figure 1.13. Mutations in RyR1 which cause the skeletal muscle disorders. Those associated with Malignant Hyperthermia are shown in bold (Gillard et al., 1991; Manning et al., 1998; Brandt et al., 1999; Sambuughin et al., 2001) and those linked with Central Core Disease in italics (Zhang et al., 1993; Quane et al., 1993; Monnier et al., 2001; Tilgen et al., 2001; Zorzato et al., 2003; Robinson et al., 2002). The five underlined mutations cause MH but are also associated with CCD. The mutations segregate to three distinct regions of discrete functionality as shown, and the numerical values relate to the relative distribution of mutations within these clusters.

ATP hydrolysis by upregulated Ca^{2+} pumps is thought to be responsible for the rise in body temperature seen (Benkusky et al., 2004).

Functional evaluation of 15 MH and CCD mutants recombinantly expressed in HEK293 cells found that all mutant channels exhibited an increased sensitivity to activation by caffeine, compared to WT (Tong et al., 1997). Expression of CCD mutant proteins also increased resting cytoplasmic Ca^{2+} levels and decreased ER stores, whereas these parameters were unaltered in cells expressing mutants that result in MH alone. Investigations have been carried out in several laboratories on different cell models expressing mutant RyR1 cDNAs and on muscle biopsies of MH individuals. These studies again found that the mutant channels exhibited hypersensitivity to agonists (Otsu et al; 1994), altered Ca^{2+} release (Treves et al., 1994; Censier et al., 1998), enhanced Ca^{2+} sensitivity (Tong et al., 1999b) and a decreased sensitivity to Mg^{2+} inhibition (Duke et al., 2002). However, they failed to categorically document that the main effect of RyR1 mutation was to augment basal cell Ca^{2+}. These studies have nevertheless suggested that the variable pathophysiological responses seen with MH and CCD could depend on differences in the properties of the different RyR1 mutants, and that this could depend on the mutational loci. It has been observed that MH patients who lack clinical myopathies are more likely to have mutations at the N-terminus of RyR1, while clinical myopathies exhibit a C-terminal bias (Matthews & Moore, 2004).

Some C-terminal RyR1 mutations lie in the putative selectivity filter of the channel pore (Gao et al., 2000), and are thought to cause disruption of the Ca^{2+} permeation pathway. Such mutations result in the abolition of agonist induced responses when expressed as homotetramers, and in decreased responses when expressed as mutant-WT heterotetramers – an effect attributed to a decreased ER load (Lynch et al., 1999). Voltage-gated Ca^{2+} release was absent in skeletal myotubes expressing such ($I^{4898}T$) mutant channels suggesting that sarcolemmal excitation was functionally uncoupled from the SR. Hence the term "EC uncoupled" was coined to describe this mechanism (Avila et al., 2003).

Thus, it appears that CCD-linked RyR1 mutation can result in two different mechanisms of channel dysfunction: the "leaky channel hypothesis" proposes that mutations cause channels to be hyperactivated, causing a depletion in the Ca^{2+} store, leading to impaired muscle function, whereas the "EC uncoupling hypothesis" proposes a loss of voltage-gated Ca^{2+} release. Results obtained from functional studies so far suggest that both these mechanisms are in operation and may not necessarily be mutually exclusive (Brini et al., 2004).

1.5.2. Cardiomyopathies resulting from defects in RyR2

1.5.2.1. Heart Failure

Changes in intracellular Ca^{2+} handling also play a crucial role in the defective contractility observed in heart failure. In its simplest terms, heart failure (HF) is a condition where the heart is unable to provide sufficient cardiac output to supply the metabolic demands of the organism because the contractile function of the heart is depressed (Bers, 2001). The physiological process that determines contractile performance is EC coupling, and so it is appreciated that detrimental alteration of the proteins involved in this process is a potential factor in the pathogenesis of HF. Individual components have been studied in detail and one consistent finding in many models of HF is a decreased SR Ca^{2+} load (Lindner et al., 1998; Pieske et al., 1999; Hobai & O'Rourke, 2001). The Ca^{2+} transient required to initiate contraction is dependent on a sufficient Ca^{2+} store and so when the store is depleted, SR Ca^{2+} release will be curtailed and as a result reduced contractile force is generated (Lindner et al., 1998).

Two states that appear to bring about reduced SR Ca^{2+} loading in HF are down-regulation in the expression and a decrease in the activity of SERCA (Hasenfuss et al., 1994), resulting in reduced loading of the SR with Ca^{2+}, and the up-regulation of the sarcolemmal NCX (Hasenfuss, 1998) which promotes the removal of vital Ca^{2+} from the cell. Both these states could impair the restoration of SR Ca^{2+} stores during diastole, hindering the cells ability to make available the required Ca^{2+} for the next wave of depolarisation. This is believed to be the primary factor in the defective EC coupling seen in HF (Lindner et al., 1998). Traditionally, RyR2 has not been considered to have a direct role in this process, however more recently work has been published that does suggest a central role for RyR2 in HF. Expression levels of functional RyR2 channels in HF, as measured by ryanodine binding have shown conflicting results. These measurements have shown the levels of RyR2 to be unchanged (Nimer et al., 1995), increased (Sainte Beuve et al., 1997) and decreased (Vatner et al., 1994) in a variety of animal HF models. Other studies suggest that the number of RyR2s relative to DHPRs is reduced, causing a functional uncoupling of the two channels, resulting in reduced SR Ca^{2+} release (Milnes & MacLeod, 2001). Work by Yamamoto et al (1999) implied that RyR2 activity is increased to compensate for the reduced SR load and Ca^{2+} release seen in HF. This compensatory modulation of RyR2 may come as the result of catecholaminergic stimulation. Decreased cardiac output activates the compensatory effects of the

sympathetic nervous system and HF is described as a hypercatecholaminergic state (Scoote & Williams, 2002). Indeed levels of circulating catecholamines are closely correlated with severity and prognosis of HF (Cohn et al., 1984; Cohn, 1995). In response to this, the function of various EC coupling components, including the RyR2 is augmented by β-adrenergic dependent increases in phosphorylation (Scoote & Williams, 2004, Marx et al., 2000). In a series of experiments, Marks and co-workers have shown that RyR2 becomes hyperphosphorylated at Ser2809 in chronic HF (see section 1.4.1.5., Marx et al., 2000; Reiken et al., 2003a). The consequences of this are dissociation of FKBP12.6 and hence a loss of coupled gating, an increase in the open probability of the channel and the appearance of sub-conductance states. This functional change in RyR2 is thought to allow a diastolic SR Ca^{2+} leak which would further deplete the SR Ca^{2+} store and serve as a substrate for ventricular arrhythmias and sudden death (Marks et al., 2002a; Marks et al., 2002b). They propose that although phosphorylation of RyR2 occurs as a compensatory response in failing hearts, its continuation for a prolonged period will eventually become counterproductive to cardiac function (see Figure 1.14.). This represents an attractive model that superficially explains many of the mechanisms underlying HF. However, major inconsistencies have emerged from several laboratories that appear to fundamentally challenge the validity of this model. For example:

- Xiao et al (2004) demonstrated that PKA phosphorylation of RyR2 at Ser2808 (as identified by using site- and phosphorylation specific antibodies) did not cause dissociation of FKBP12.6 in either recombinant or native systems.
- WT and phosphomimetic 2809 RyR2 mutants exhibited equivalent FKBP12.6 binding and channel function (Stange et al., 2003).
- Xiao et al (2005) identified Ser2030 as the physiological target of β-adrenergic stimulation, whereas Ser2808 was constitutively phosphorylated. However, phosphorylation at either of these residues did not affect the RyR2-FKBP12.6 interaction. Furthermore, the phosphorylation status of RyR2 at Ser2809 and Ser2030 was similar in failing and non-failing canine hearts.
- RyR2 is thought to be phosphorylated by both PKA and CaMKII at Ser2809 and both of these enzymes can be stimulated either directly, or indirectly by stimulation of the β-adrenergic signalling pathway (Marks, 2001; Zhang et al., 2003a). It is therefore difficult to envisage how phosphorylation by PKA but not CaMKII can result in an increase in channel activity.

- EC coupling gain was not affected in FKBP12.6 null mice and none developed HF (Xin et al., 2002), though those created in another strain were prone to arrhythmogenic death, but not HF (Wehrens et al., 2003).
- Li et al (2002) reported that the PKA mediated increase in spark frequency seen in non-failing hearts was entirely attributable to phospholamban phosphorylation and enhanced SR Ca^{2+} loading, with RyR2 phosphorylation having no effect on this parameter. This work suggests that although RyR2 phosphorylation may increase channel activity, it's significance as a mechanism for regulating SR Ca^{2+} load is minimal, with SERCA being the more important regulatory component (Eisner et al., 1998; Eisner & Trafford, 2000).
- Some studies also suggest that RyR2 does not exhibit altered functionality in HF. Holmberg & Williams (1989) showed that RyR2s from end-stage failing hearts did not exhibit any functional differences compared to WT RyR2s from normal sheep hearts, and more recently Jiang et al (2002a) demonstrated that despite an abnormal SR Ca^{2+} release in HF, RyR2 function was normal.
- A recent study by Oda et al (2005) demonstrated that defective interdomain interactions within the structure of the RyR2 is the primary cause of RyR dysfunction in HF and that FKBP12.6 dissociation can occur as a result of this. This suggests that FKBP12.6 dissociation is the consequence rather than the cause of RyR instability in HF.

It is also important to highlight that there are numerous downstream protein targets of the β-adrenergic pathway - all of which are responsible for the regulation of Ca^{2+} cycling in myocytes (see Figure 1.5.), and as such it is difficult to attribute the resultant pathological phenotype to one of these proteins.

Despite this, evidence for the hyperphosphorylation hypothesis has been provided by observations that β-blockers reverse this phenomenon and restore the stoichiometry of the RyR2: FKBP12.6 complex and normal RyR2 activity (Reiken et al., 2001; Doi et al., 2002; Reiken et al., 2003b). Other studies have shown that FKBP12.6 levels were decreased in HF animal models (Yano et al., 2000; Ono et al., 2000) leading to a greater SR Ca^{2+} leak. Thus, it appears that FKBP12.6 serves to modulate channel function and prevent excessive non-physiological opening of the channel (Scoote & Williams, 2002), a theory consistent with the fact that FKBP12.6 null mice exhibit an increased duration and amplitude of RyR2-mediated Ca^{2+} sparks (Xin et al., 2002).

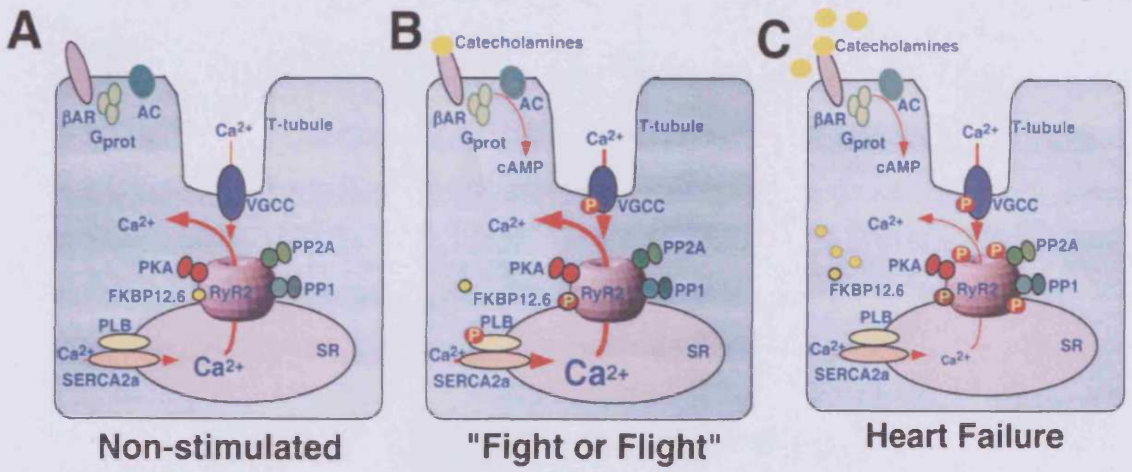

SR Ca^{2+}	"normal"	"normal/increased"	"decreased"
Peak Ca^{2+} release	"normal"	"increased"	"decreased"
Aberrant diastolic Ca^{2+} release	none	none/minimal	increased

Figure 1.14. Physiological and proposed pathophysiological regulation of RyR2 by PKA phosphorylation (adapted from Marks, 2002). A) In the non-stimulated heart, RyR2 is relatively non-phosphorylated by PKA. B) Physiological stimulation via the sympathetic nervous system (fight-or-flight) results in increased circulating catecholamine levels, and PKA substrates are phosphorylated, increasing EC coupling gain. C) In the failing heart, long-term stimulation by elevated serum catecholamines results in PKA hyperphosphorylation of RyR2, thought to cause dissociation of FKBP12.6, resulting in pathological hypersensitivity to activation by cytosolic Ca^{2+}, which could lead to arrhythmia. These effects are summarised underneath the figure.

More recently, defects in RyR1 associated with hyperphosphorylation have also been identified in HF (Reiken et al., 2003b). This suggests that HF induces a generalised EC coupling myopathy which impairs both cardiac and skeletal muscle function, which may underlie the generalised muscle weakness and reduced exercise tolerance associated with HF.

Although controversy still remains regarding the importance of RyR2 phosphorylation under normal physiological conditions, it may still play a role in generating triggered arrhythmias. Ca^{2+} induced arrhythmias are thought to occur during SR Ca^{2+} overload, making the idea of them occurring in HF seem paradoxical since this condition is associated with a decreased store content. However, Pogwizd et al (2001) showed that the residual β-adrenergic receptor responsiveness was sufficient to load the SR with enough Ca^{2+} to reach the threshold needed to initiate spontaneous Ca^{2+} release. As NCX is upregulated in HF, for every given SR Ca^{2+} release there is a greater efflux of Ca^{2+} via NCX and an inward arrhythmogenic Na^{+} current, which could cause delayed afterdepolarisations.

Hyperphosphorylation of RyR2, leading to a diastolic leak of SR Ca^{2+} has been proposed to be the cause of ventricular arrhythmias seen in HF (Marks et al., 2002a; Marks et al., 2002b) and that protection from cardiac arrhythmia can be achieved through stabilization of the FKBP12.6: RyR2 complex using pharmacological agents (Yano et al., 2003; Kohno et al., 2003). In particular, a benzothiazepine derivative known as JTV519 is thought to achieve this by increasing the affinity of FKBP12.6 for RyR2 (Wehrens et al., 2004b – in this paper FKBP12.6 is referred to as calstabin2), though a more recent report suggests that this drug prevents Ca^{2+} leak with no effect on RyR2-bound FKBP12.6 (Oda et al., 2005).
Recent work has also suggested that PKA hyperphosphorylation of RyR2 and its effects can be directly prevented by treatment with the angiotensin II antagonist valsartan (Okuda et al., 2004). Furthermore, this drug also resulted in restoration of functional SERCA expression and thus SR Ca^{2+} uptake.

1.5.2.2. Ca^{2+}-dependent arrhythmia syndromes caused by genetic mutations in RyR2

The identification of genes underlying inherited arrhythmia syndromes such as Long QT and Brugada syndromes (caused by genetic defects in cardiac K^+ and Na^+ channels) has underlined the importance of the role of ion channel dysfunction in the development of malignant arrhythmia and cardiopathology (Marban, 2002; Keating & Sanguinetti, 2001). These diseases of ion channel dysfunction are referred to as "channelopathies", some of which are summarized in Table 1.4. Defects in ion channel function cause arrhythmia, because it is their coordinated opening and closing that mediates the cardiac action potential, and thus cardiac excitability.
To date, 43 mutations in RyR2 are known to be associated with two inherited forms of arrhythmia leading to sudden cardiac death (SCD – see Figure 1.15.). Both conditions; catecholaminergic polymorphic ventricular tachycardia (CPVT) and arrhythmogenic right ventricular cardiomyopathy/dysplasia type 2 (ARVC/D2) are autosomal dominant cardiomyopathies exhibiting exercise- and stress-induced fatal ventricular arrhythmias. They have both been mapped to the RyR2 chromosomal loci 1q42-43 (Swan et al., 1999; Rampazzo et al., 1995).

Disease	Mode of inheritance	Gene encoding protein/ion channel	Normal function	Mechanism of mutant ion channel/protein dysfunction	Phenotype
LQT1	Autosomal dominant*	*KVLQT1 (KCNQ1)* encodes $I_{Ks}K^+$ (α subunit)	Slowly activating delayed rectifier K^+ current	Loss-of-function (mutation leads to a truncated, non-functional protein) or dominant-negative** mechanism	Prolonged QT interval, predisposition to fatal stress/exercise (especially swimming) induced arrhythmias
LQT2	Autosomal dominant	*HERG (KCNH2)* encodes $I_{Kr}K^+$ (α subunit)	Rapidly activating delayed rectifier K^+ current	Loss-of function (mutation leads to a truncated, non-functional protein) or dominant negative mechanism	Prolonged QT interval, predisposition to fatal arrhythmias linked to auditory stimuli or while at rest
LQT3	Autosomal dominant	*SCN5A* encodes Na^+ channel (α subunit)	Inward Na^+ current	Gain-of-function; increased Na^+ flux and incomplete inactivation of the channel	Prolonged QT interval, predisposition to fatal arrhythmias while at rest
LQT4	Autosomal dominant	*ANK2* encodes Ankyrin B	Membrane adaptor protein targeting and anchoring ion channels/pumps	Loss-of-function; mutation abolishes protein-protein interactions	Atypical compared to other LQTS, sinus bradycardia, polyphasic T waves and atrial fibrillation. Predisposition to fatal stress/exercise induced arrhythmias
LQT5	Autosomal dominant	*mink (KCNE1)* encodes $I_{Ks}K^+$ (β subunit)	Regulates the slowly activating delayed rectifier current	Loss or reduction-of-function via shifted voltage dependence of activation	Prolonged QT interval. Predisposition to fatal stress/exercise induced arrhythmias
LQT6	Autosomal dominant	*MiRP1 (KCNE2)* encodes $I_{Kr}K^+$ (β subunit)	Regulates the rapidly activating delayed rectifier current	Loss or reduction-of-function; mutants channels exhibit slowed opening and rapid closing, diminishing the K^+ current	Prolonged QT interval. Predisposition to fatal stress/exercise induced arrhythmias
LQT7 or Andersen Syndrome	Autosomal dominant	*KCNJ2* encodes Kir2.1, the inward rectifier (I_{K1}) K^+ channel	Outward K^+ current	Dominant-negative mechanism, leading to an unstable resting membrane potential	Prolonged QT interval. Predisposition to fatal stress/exercise induced arrhythmias, associated with multi-system pathology
JLNS	Autosomal recessive	*KVLQT1 (KCNQ1)* or *minK (KCNE1)* encode $I_{Ks}K^+$ (α and β subunits)	Slowly activating delayed rectifier K^+ current	Loss-of-function; homozygous mutation leads to K^+ current ablation	Prolonged QT interval. Predisposition to fatal stress/exercise induced arrhythmias, also associated with deafness
IVF	Autosomal dominant	*SCN5A* encodes Na^+ channel (α subunit)	Inward Na^+ current	Loss or reduction-of-function; mutant channels show accelerated inactivation	In most cases no ECG abnormalities are found, and otherwise healthy individuals suddenly undergo fatal ventricular fibrillation
Brugada syndrome or SUNDS	Autosomal dominant	*SCN5A* encodes Na^+ channel (α subunit)	Inward Na^+ current	Loss or reduction-of-function; mutant channels show delayed reactivation and enhanced inactivation, with loss/reduction of Na^+ current	Predisposition to fatal arrhythmia via incomplete or complete bundle branch block
CPVT and ARVD2	Autosomal dominant	*RyR2* encodes the ryanodine receptor	Channel which mediates Ca^{2+} release from the SR	Gain-of-function; mutant channels result in excessive SR Ca^{2+} release	No ECG abnormalities, predisposition to fatal stress/exercise induced arrhythmias
CPVT	Autosomal recessive	*CSQ2* encodes calsequestrin	Intra-SR Ca^{2+} buffering protein; lumenal Ca^{2+} sensor for RyR2	Loss -of-function; decreased intra-lumenal Ca^{2+} buffering and abnormal lumenal Ca^{2+} dependent RyR2 regulation	No ECG abnormalities, predisposition to fatal stress/exercise induced arrhythmias
Timothy Syndrome	*De novo*	*CACNA1A* encodes $Ca_v1.2$	Depolarisation activated Ca^{2+} channel which mediates I_{Ca}	Gain-of-function; maintained inward Ca^{2+} currents due to ablation of voltage-dependent inactivation	multisystem pathology, lethal arrhythmia and autism

*Long QT syndromes that are inherited in an autosomal dominant fashion are sometimes referred to as Romano-Ward syndrome (Romano et al., 1963; Ward, 1964).
**Dominant negative mechanism: whereby a mutant subunit corrupts the normal function multimeric channels

Table 1.4. Summary of known ion channelopathies. Defects in ion channel function cause arrhythmias because it is their coordinated gating which shapes the action potential (AP). It should be noted that all of these channelopathies (apart from ARVD2) occur within a structurally normal heart, implying that the defect is purely

electrical in origin. Even though phenotypes of patients have been given here it should be noted that there is extensive variability among known mutation carriers, suggesting that the environment in which the mutant genes are expressed is important in determining the severity of the condition.
Abbreviations: LQT – Long QT syndrome; JLNS - Jervell and Lange-Nielsen syndrome; IVF - Idiopathic ventricular fibrillation; SUNDS - Sudden Unexpected Nocturnal Death Syndrome; CPVT – catecholaminergic polymorphic ventricular tachycardia; ARVD2 – arrhythmogenic right ventricular dysplasia type 2.
References: Wang et al., 1995; Dumaine et al., 1996, 1999; Splawski et al., 1997, 2000, 2004, 2005; Keating & Sanguinetti, 2001; Towbin, 2001; Priori et al., 2001b, 2003; Marban, 2002; Sanguinetti, 1999; Hoppe et al., 2001; Mazhari et al., 2001; Mohler et al., 2003, 2004; Abbot et al., 1999; Plaster et al., 2001; Tristani-Firouzi et al., 2002; Jervell & Lange-Nielsen, 1957; Neyroud et al., 1997; Duggal et al., 1998; Krishnan & Antzelevitch, 1991; Brugada & Brugada, 1992; Rook et al., 1999; Vatta et al., 2002; Tiso et al., 2001; Laitinen et al., 2001; George et al., 2005; Lahat et al., 2001; Postma et al., 2002.

ARVD is an acronym used to describe at least six genetically distinct forms of cardiomyopathy (Rampazzo et al., 1994, 1997, 2000; Ahmad et al., 1998; Li et al., 2000) that are characterized by structural and functional abnormalities in the right ventricle wall whereby this part of the myocardium becomes progressively degenerated (by apoptotic mechanisms (Valente et al., 1998)) and replaced with fibrous and fatty tissue, and usually presents with arrhythmias of right ventricular origin (Marcus et al. 1982; Gemayel et al., 2001). Linkage studies have identified at least six candidate chromosomal loci in different families affected by the disease (Marcus et al., 2003). ARVD2 was first described by Nava et al. (1988) and is distinct from the other forms because it is associated with exercise/stress-induced ventricular tachycardia (VT) and SCD. Additionally, ventricular dysplasia was less pronounced in the ARVD2 affected individuals identified by Tiso et al. (2001). Conversely, CPVT is characterised by the fact that arrhythmia occurs in a structurally normal heart, as with Long QT or Brugada syndrome (Viskin et al., 1998). In contrast to these syndromes however, CPVT patients exhibit a normal resting ECG that gives way to ventricular arrhythmias at times of adrenergic activation (i.e. physical /emotional stress) (Leenhardt et al., 1995).

Despite the morphological differences, these two conditions are allelic – they are caused by mutation of the same gene and share a common pre-disposition to effort induced VT, suggesting that they could belong to a single clinical entity with a broad range of phenotypic variability influenced by other genetic or epigenetic factors. However, as with MH and CCD, these cardiomyopathies could be distinct but related conditions. Strikingly, ARVD2/CPVT mutations appear to cluster in regions of RyR2 which correspond to those associated with MH/CCD mutations in RyR1. This finding could indicate that these regions are important for modulation of channel function, and indeed these regions do include domains that have been assigned specific functionality (see Figure 1.16.). On the other hand, the lack of mutations in other regions of the channel may reflect the fact that such mutations are not tolerated (i.e.

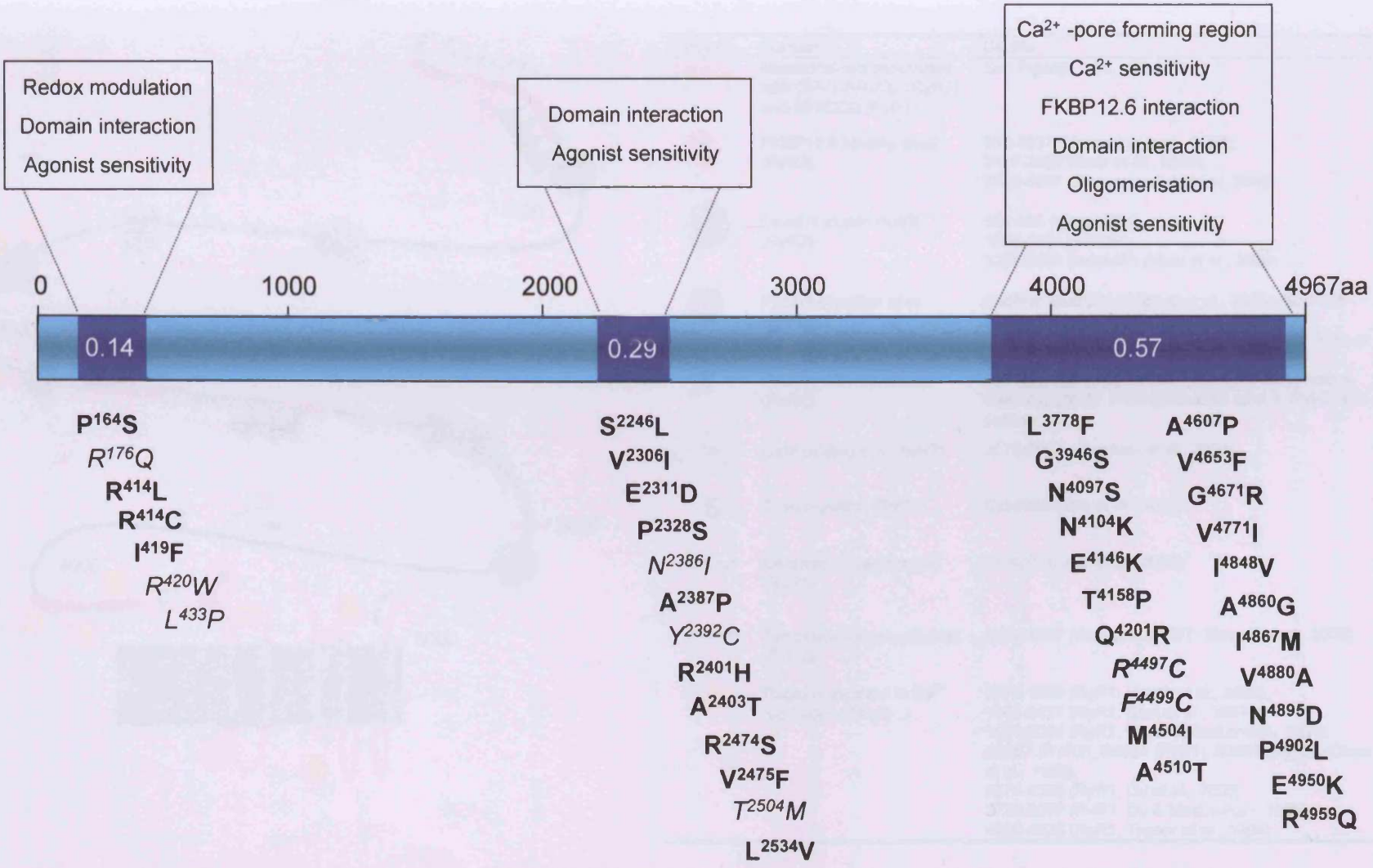

Figure 1.15. RyR2 mutations associated with CPVT/ARVD2. Forty-three RyR2 mutants, occurring in discrete domains have been identified (Laitinen et al., 2001, 2003; Tiso et al., 2001; Priori et al., 2001, 2002; Bauce et al., 2002; Tester et al., 2004; Choi et al., 2004; Bagattin et al., 2004; Hasdemir et al., 2004; Aizawa et al., 2005). The numerical values relate to the relative distribution of mutations within clusters. CPVT- and ARVC2 associated mutations are represented by bold and italic font, respectively. ARVC2 mutations have only been identified in amino-terminal and central domains. The functionality attributed to each mutational cluster in shown. A more detailed map of RyR2 domain functionality is shown in Figure 1.16.

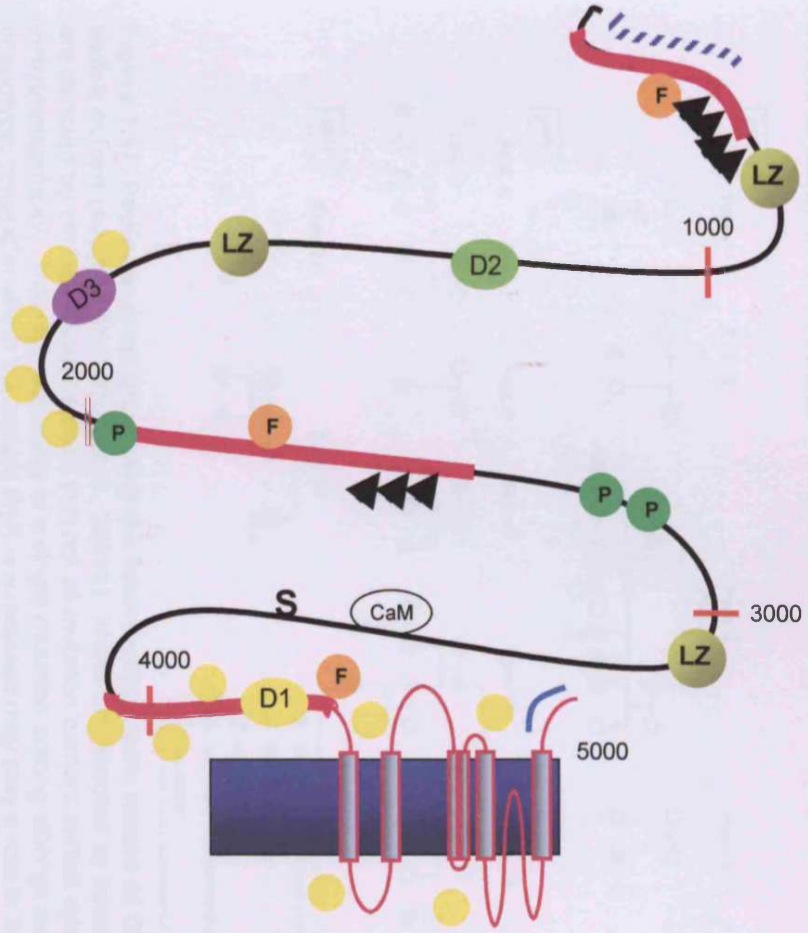

Symbol	Domain	Details
	Mutational loci associated with CPVT/ARVD2 (RyR2) and MH/CCD (RyR1)	See Figures 1.13. and 1.15.
F	FKBP12.6 binding sites (RyR2)	305-1937 (Masumiya et al., 2003); 2427-2428 (Marx et al., 2000); 3788-4967 (Zissimopoulos & Lai, 2005)
LZ	Leucine zipper motifs (RyR2)	554-588 (spinophilin), 1603-1631 (PR130), 3003-3039 (mAKAP) (Marx et al., 2000)
P	Phosphorylation sites (RyR2)	CaMKII: Ser2809 (Witcher et al., 1991), Ser2815 (Wehrens et al., 2003), PKA: Ser2809 (Marx et al., 2000), Ser 2030 (Xiao et al., 2005)
	Interdomain interaction (RyR2)	590-639 interacting with 2460-2492 (Yamamoto & Ikemoto, 2002). Analogous sites exist in RyR2, see section 1.5.1.
CaM	CaM binding site (RyR2)	3578-3595 (Balshaw et al., 2001)
S	S-nitrosylation (RyR1)	Cys3635 (Sun et al., 2001)
	Oxidoreductase domain (RyR1)	41-420 (Baker et al., 2002)
	Tetrameric oligomerisation (RyR2)	4952-4967 (Gao et al., 1997; Stewart et al., 2003)
	Regions involved in Ca^{2+} regulation of RyR	1872-1923 (RyR1, Hayek et al., 2000), 1641-2437 (RyR1, Bhat et al., 1997a), 1861-2094 (RyR1, Chen & MacLennan, 1994), E3987 (RyR2), E4032 (RyR1), E3885 (RyR3) (Chen et al., 1998), 4274-4535 (RyR1, Du et al., 2000) 3720-5037 (RyR1, Du & MacLennan, 1999), 4830-4625 (RyR1, Treves et al., 1994)

Figure 1.16. Ryanodine receptor domain functionality. The most relevant domains and sites of interaction are shown as symbols, explained in the key above. Numbers correspond to the appropriate residues of RyR2 or RyR1 (for domains which have not yet been characterised in the cardiac isoform). Divergent regions are shown in the colours which indicate their position in the three dimensional reconstructions shown in Figure 9; DR1 (yellow), DR2 (green), DR3 (purple). The arrangement of transmembrane domains is from the model of Du et al., 2002.

are embryonic lethal) and so have not survived in the genome (Marks et al., 2002a). This may be a reason why the incidence of these CPVT/ARVD2 individuals in the population is likely to be grossly underestimated, as is the proportion of deaths attributable to RyR2 mutation. Another reason for this is that difficulties in the clinical diagnosis of CPVT in particular can hinder its identification, for example exercise stress-testing does not always elicit VTs in CPVT patients who had displayed syncopal episodes (Allouis et al., 2005), and CPVT may also be misdiagnosed as LQT1 (in as much as ~30% of cases) (Choi et al., 2004). Additionally, the size of the RyR2 gene (105 exons, spanning approximately 800 kilobases) precludes economical and straightforward diagnostic screening of RyR2 mutations in all susceptible individuals, - which in some cases may be difficult to discover due to the sporadic (non-inherited) nature of a few of the mutations (see Figure 1.17., Priori et al., 2001a&b).

The first report of RyR2 genotyped CPVT individuals showed a distinct male bias and an early age of onset (8 ± 2 years) (Priori et al., 2002). However, this was not seen in other patient groupings, where there was equal male/female prevalence and a broader range of age of onset (Laitinen et al., 2001; Choi et al., 2004), in agreement with the phenotypic manifestation of ARVD2 (Tiso et al., 2001; Bauce et al., 2002). Consequently, the small number of cases analysed could skew the reported gender/age bias reported for CPVT, and data from much larger populations is needed to clarify these matters.

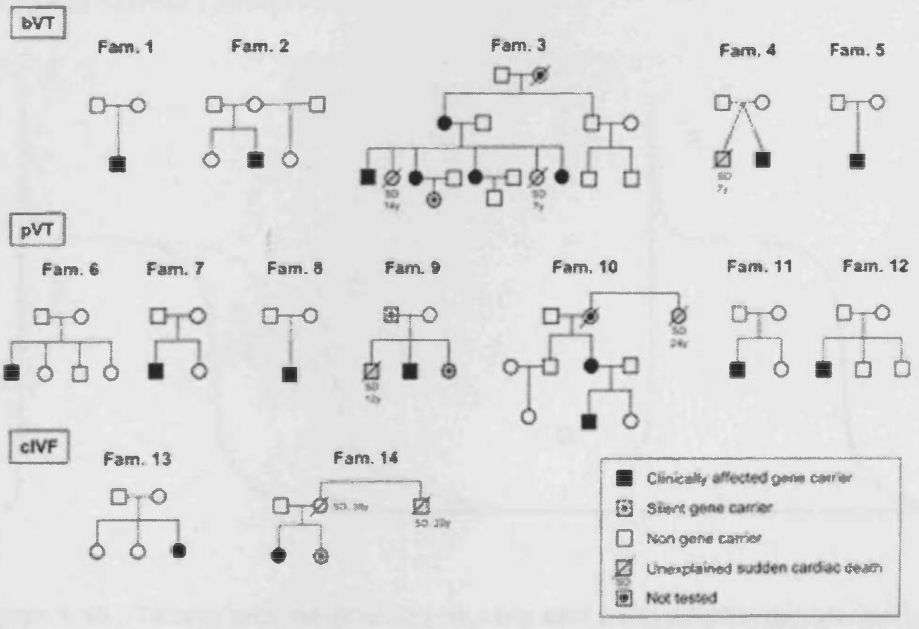

Figure 1.17. Pedigree chart displaying the inherited/sporadic nature of CPVT in an Italian cohort (adapted from Priori et al., 2001b). Males are denoted by squares, and females are denoted by circles. It can be seen that not all mutation carriers exhibit symptoms/ arrhythmogenicity. This high variability of a single mutation among siblings suggests that the phenotypic context in which the mutant RyR is expressed may play a role in the lethality of the condition. It should be noted that although this cohort shows a male bias and early age of onset, this is not always seen as discussed in section 1.5.2.2.

1.5.2.2.1. Mechanism of arrhythmogenesis in CPVT/ARVD2

Cardiac arrhythmias can arise due to a variety of mechanisms including re-entry, automaticity and triggered activity (Wit & Rosen, 1983). Re-entry describes the situation in which the activating impulse succeeds in re-exciting regions of the myocardium after the refractory period has subsided and can cause continuous circulation of APs, and it normally arises from myocardial damage causing a disturbed pattern of conductance. Automaticity and triggered activity are representative mechanisms of de novo abnormal impulse generation within individual myocytes and 3D mapping suggests that most VT in non-ischaemic HF is initiated by such mechanisms (Pogwizd et al., 1998; Janse, 2004; Pogwizd & Bers, 2004). Automaticity refers to the ability of myocardial cells to initiate spontaneous depolarisation during the diastolic interval, however it is triggered activity which is thought to be most closely linked to Ca^{2+}-mediated arrhythmogenesis. Triggered activity is so called because the impulse can only occur if it follows a previous AP (Cranefield & Wit, 1979) and arises from the generation of sub-threshold membrane depolarisations, termed afterdepolarisations, which follow the previous AP. These afterdepolarisations can occur during the repolarisation of the previous impulse (these are termed early afterdepolarisations – EADs), or they can occur after repolarisation is complete (where they are known as delayed afterdepolarisations – DADs). Figure 1.18. shows a graphical representation of these phenomena with respect to the normal cardiac AP.

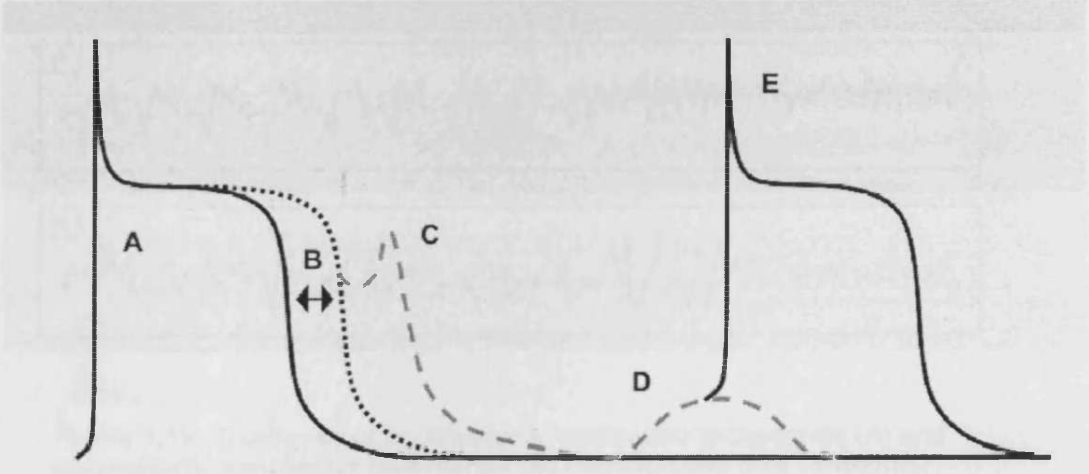

Figure 1.18. Timing and morphology of early and delayed afterdepolarisations (taken from Scoote and Williams, 2004). A normal action potential: (A) may be extended in duration (B) such that an early afterdepolarisation is generated (C) during the repolarisation phase. A delayed afterdepolarisation (D) only occurs after a normal action potential (A) is completed and the cell has returned to the resting membrane potential. If the DAD is of sufficient magnitude to reach a depolarising threshold, a new action potential (E) can occur which itself can initiate a triggered arrhythmia.

Arrhythmias associated with CPVT take the form of bi-directional and/or polymorphic VT (Figure 1.19 shows examples of these phenomena on an ECG), both of which are capable of degenerating into ventricular fibrillation and SCD (Swan et al., 1999; Priori et al., 2001b; 2002; Leenhardt et al., 1995; Marks et al; 2002a). Bi-directional VT is a rare and unusual arrhythmia, normally associated with digoxin toxicity (Ma et al., 2001). The mechanism by which cardiac glycosides such as digoxin cause arrhythmia is known to be via Ca^{2+} overload and DAD generation within cardiomyocytes (Rosen & Danilo, 1980; Hauptman & Kelly, 1999) and there is now evidence from isoproterenol induction of arrhythmia in CPVT that DADs occur as a result of this stimulus and do indeed culminate in the generation of bi-directional VT (Nakajima et al., 1997). These observations suggest that bi-directional VT is a triggered arrhythmia resulting from DADs, secondary to intracellular Ca^{2+} overload and spontaneous SR Ca^{2+} release. DADs are believed to result from a transient Ca^{2+}-activated inward current evoked by spontaneous Ca^{2+} release from the SR under conditions that favour accumulation of intracellular Ca^{2+} (Pogwizd & Bers, 2004). The role of SR Ca^{2+} release via RyR2 is emphasised by studies using ryanodine which blocks DAD formation (Marban et al., 1986). The transient inward depolarising current is from the NCX (Pogwizd & Bers, 2004; Fedida et al., 1987). Upon release of SR Ca^{2+}, NCX removes excess Ca^{2+} in exchange for an inward depolarising movement of Na^{+}. If this inward Na^{+} movement is sufficient to cause a DAD amplitude in excess of the threshold potential of the cell, a depolarisation will occur, which may propagate through the heart causing extrasystoles and VT.

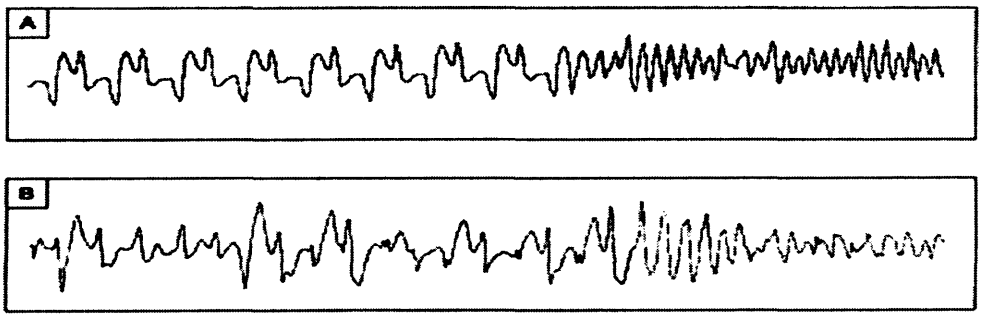

Figure 1.19. Examples of bi-directional ventricular tachycardia (A) and polymorphic ventricular tachycardia (B) degenerating into ventricular fibrillation in patients with CPVT (taken from Priori et al., 2002). Bi-directional VT is characterized by a beat-to-beat alternation of the QRS axis, while polymorphic VT has an irregularly variable axis of the QRS.

1.5.3.2.2. Functional characterisation of RyR2 mutants

There is clearly a need to carry out a functional evaluation of CPVT/ARVD2-linked RyR2 mutants in appropriate experimental systems since, as can be seen in Table 1.4., it is possible for arrhythmia to arise via different mechanisms of channel dysfunction (e.g. gain-, reduction-, or loss-of-function, dominant negative mechanisms etc). Functional characterisation of RyR2 mutants is at an early stage, however considerable data are available concerning the characterisation of RyR1 mutants associated with MH and CCD. These studies appear to favour two mechanisms for RyR mediated dysfunctional Ca^{2+} regulation: 1) mutation leads to increased channel activation or, 2) mutation leads to RyRs deficient in the skeletal muscle EC coupling mechanism (see section 1.5.2.1.). The latter mechanism could not apply to cardiac muscle since it relies on a different EC coupling system (see section 1.4.2.5.). However, pre-existing observations concerning bi-directional VT and DADs, points to the former mechanism being responsible for arrhythmogenesis linked to RyR2 mutations. In other words, CPVT/ARVD2 result from 'gain-of-function' mutations, which alter channel properties making them more sensitive to opening stimuli and mediating excessive SR Ca^{2+} release, in particular during diastole when the channel would normally be closed. This 'gain-of-function' could be amplified by catecholaminergic drive during stress or exercise. A model that could possibly fit this description has been proposed by Marks (2001) and is an extension of the maladaptive hyperphosphorylation proposed to occur in HF (Marks et al., 2002a&b, see section 1.5.2.1.), with increased sympathetic drive during stress/exercise, leading to FKBP12.6 dissociation and channel activation. Mutation of the channel could lower the threshold for activation of RyR2 by phosphorylation, bringing about a transient set of conditions that would allow DADs to develop. Wehrens et al. (2003) demonstrated that PKA- (but not CaMKII) mediated RyR2 phosphorylation at Ser 2809 led to increased SR Ca^{2+} release during exercise. Importantly, their recombinantly expressed RyR2 mutants ($S^{2246}L$, $R^{2474}S$, $R^{4497}C$) demonstrated reduced affinity for FKBP12.6 when compared with the WT channel in an *in vitro* binding study, and an increased open probability in single channel experiments following PKA phosphorylation. Interestingly, three other mutants ($P^{2328}S$, $Q^{4201}R$, $V^{4653}F$) which exhibited decreased binding of FKBP12.6 (referred to as calstabin 2, Lehnart et al., 2004), also showed significantly decreased Mg^{2+} inhibition, leading to increased channel activity (see section 1.4.1.3.) - a mechanism also thought to be involved in RyR1 dysregulation in MH/CCD (Duke et al., 2002). Decreased Mg^{2+} levels have also been shown to increase the propensity for ventricular arrhythmias

and sudden cardiac death (Mela et al., 2002; Wei et al., 2002), suggesting that decreased sensitivity to Mg^{2+} inhibition via an undefined mechanism may have a role in arrhythmogenesis.

However, both these studies (Wehrens et al., 2003, Lehnart et al., 2004) support an FKBP12.6 dependent mechanism of arrhythmogenesis, which is currently controversial since many different studies have challenged the validity of this model (see section 1.5.2.1.). In particular the first CPVT transgenic mouse ($R^{4497}C$) exhibited exercise induced bi-directional VT (Cerrone et al., 2005), which was absent in both FKBP12.6 null mouse models (Wehrens et al., 2003; Xin et al., 2002).

A later study characterised two of the last three mutants ($S^{2246}L$, $R^{4497}C$) with an additional pore mutant ($N^{4104}K$), in a cardiomyocyte cell line (HL-1; George et al., 2003a). In agreement with the clinical phenotype, the resting properties of cells expressing mutant RyR2s were not altered compared to those expressing the WT, including equivalent interaction between mutant and WT RyR2 with FKBP12.6. Following activation with RyR2 specific agonists (caffeine and 4-cmc), mutants exhibited augmented Ca^{2+} release, though the levels of WT and mutant phosphorylation were the same. Catecholamine stimulation resulted in equivalent disruption of the association with FKBP12.6 in both WT and mutant RyR2-expressing myocytes. This indicates that selective FKBP12.6 dissociation from mutant RyR2 cannot underlie the augmented Ca^{2+} release demonstrated in this study.

The pore mutant $R^{4497}C$ was also investigated by Jiang et al. (2002b) in HEK293 cells, -a cell line widely used for this purpose since it does not endogenously express RyR. This mutant was found to have a higher open probability than WT channels in bilayer experiments, especially at low [Ca^{2+}], when the channel should normally be closed. This increased basal activity was also evident as spontaneous cytoplasmic Ca^{2+} oscillations in these cells. Again, such data are consistent with a gain-of-function model. More recently, this group investigated three pore mutants; $N^{4104}K$, $R^{4497}C$ and $N^{4895}D$ (Jiang et al., 2004). They observed abnormal luminal Ca^{2+} activation of these mutants, based on the fact that they had a lower ER Ca^{2+} threshold for spontaneous release (a process they refer to as store-overload-induced Ca^{2+} release (SOICR)). Single channel experiments demonstrated that the mutants had an increased sensitivity to activation by luminal Ca^{2+}, and the authors proposed that this might be a unifying mechanism for RyR2 mutant dysfunction in CPVT. However, this work was based on the characterisation of only three of the forty-three known mutations (all three of which were located in the C-terminal region), and so this suggestion may represent an over-simplification since characterisation of the mutants is at such an early stage. Moreover, the size and complexity of the RyR2,

together with the fact that domains of this protein have been assigned discrete functionality (George et al., 2005) would argue against there being a common mechanism whereby all mutations could lead to RyR2 dysfunction. In addition, it is possible that the locus of mutation is important in determining the mechanistic basis of the disease. This has been considered for MH/CCD, where N-terminal and central domain mutations are thought to destabilize RyR1 leading to a gain-of-function and where pore mutations are thought to disrupt the Ca^{2+} permeation pathway (as discussed in section 1.5.1.1.).

Disruption of intra-RyR interactions by mutant residues is considered a plausible pathogenic mechanism for CPVT/ARVD2 as well as for MH/CCD. Yamamoto & Ikemoto (2002) showed that domain peptides corresponding to portions of the N-terminal (residues 590-639) and central domain (residues 2460-2495) of RyR2 enhanced ryanodine binding and Ca^{2+} release from cardiac SR. These peptides were also shown to sensitize the channel to activating Ca^{2+}, causing hyperactivation effects similar to those seen in CPVT (Priori et al., 2001b). These effects were attributed to competitive binding of the central domain peptide to the N-terminal of the channel (and conversely, binding of the N-terminal peptide to the central domain of the channel), disrupting the intra-molecular interactions that would normally stabilize the resting state. These effects were abolished by introducing a CPVT mutation ($R^{2474}S$) into the central domain peptide, indicating that the mutated residue was essential for interaction with the N-terminus and thus channel regulation, and that defective interaction between these domains may represent a pathological mechanism by which defective RyR2 function could result in arrhythmia generation (Yamamoto & Ikemoto, 2002). Structural instability of the RyR2 has also recently been implicated in the pathogenesis of HF (Oda et al., 2005).

As with MH/CCD, CPVT/ARVD2 are two conditions caused by mutations of the same gene, leading to the question of how this is possible. Clues to this may lie in the mutational locus: most MH mutations cluster in the N-terminal and central domain, while mutations causing CCD, tend to be in the C-terminus of RyR1. Similarly, mutations in the N-terminus of RyR2 have only been demonstrated in ARVD2 families, while mutations in the C-terminus have been reported only in conjunction with CPVT. Since N and C-terminus are thought to be functionally distinct, it could be envisaged that mutations in these different regions would produce different phenotypes.

Interestingly, mutation in the central domain leads to both phenotypes, implying that the different phenotypes produced could depend on the type of amino acid change or even the genetic background in which it is expressed. Another possibility is that

families with ARVD2 and CPVT are exposed to different environmental influences, which lead to the different phenotypes. The distinction between CPVT and ARVD2 has been addressed in a study by Tiso et al. (2002), which demonstrated that ARVD2/CPVT mutants exhibited opposite affinity for FKBP12.6, with ARVD2 mutants having a reduced affinity for FKBP12.6. They proposed that the increased channel activity that would result from this would lead not only to arrhythmia but would also induce Ca^{2+}-activated apoptosis, leading to the myocardial damage seen in ARVD2. A relationship between RyR2 activation and cell death has been demonstrated (Mariot et al., 2000; George et al., 2003b) and this, together with the fact that these effects can be prevented by co-expression of FKBP12.6 (George et al., 2003b) suggests that abnormal RyR2-mediated Ca^{2+} handling could mediate the morphological derangements seen in ARVD2.
Clearly, the mechanistic basis of triggered Ca^{2+} leak in CPVT/ARVD2 remains unresolved and highly controversial, in particular, none of the studies to date have addressed the characterisation of ARVD2 RyR2 mutants, especially those in the N-terminus, in a mammalian cell context, hence this subject is intended to be the focus of investigation in this thesis.

1.5.2.2.3. Treatment of CPVT/ARVD2

Currently, chronic administration of β-blockers and/or implantable cardioverter defibrillators (ICD) are used in the management of CPVT/ARVD2, although these do not represent optimal therapeutic strategies (Priori et al., 2001a; Marks et al., 2002a). International guidelines agree on the success of ICD therapy in all patients predisposed to arrhythmia (Priori et al., 2002), but it poses a tremendous cost implication, and a strategy of widespread implantation is not feasible even in more developed countries. The overwhelming benefits of β-adrenergic blockade in the context of CPVT/ARVD2 are substantial (Priori et al.,2002), although the efficacy of this treatment ranges from complete protection against cardiac VT (Bauce et al., 2002) to a persistent recurrence of tachyarrhythmias (Priori et al., 2002), with the latter group becoming candidates for ICD therapy. The precise effect of β-adrenergic blockade on RyR2 function remains controversial; in spite of this their action in reducing arrhythmogenic sudden death may be partially explained by a general reduction in heart rate, which is itself protective against DAD generation (Scoote & Williams, 2004; Priori et al., 1988). Interestingly, it has been shown that β-blockers can restore normal levels of PKA phosphorylation and binding of FKBP12.6 to RyR2

in failing hearts (Reiken et al., 2001, 2003b; Doi et al., 2002). However, β-blockers are unlikely to affect RyR2 only as they act at the beginning of a signalling cascade, and would be expected to affect most EC coupling components.

Clearly, the development of an optimal treatment means that elucidating the underlying molecular events of RyR2-dependent pathogenesis is essential. A major consideration in developing such a therapy would be that Ca^{2+} channel function must be preserved under resting conditions since CPVT/ARVD2 affected individuals are characterised by normal resting cellular Ca^{2+} homeostasis. An experimental drug, JTV519 is thought to represent a promising advance in this area. This drug was proposed to stabilise the RyR2:FKBP12.6 complex, thereby normalising cardiac function (Wehrens et al., 2003; Yano et al., 2003). However, JTV519 is a derivative of the benzothiazepine class of voltage-gated Ca^{2+} channel blockers, and lacks specificity for RyR2 and recent work which suggests that the mode of action of the drug does not directly involve binding of FKBP12.6 to the channel agrees with this (Oda et al., 2005). Intriguingly, it is feasible that the beneficial effects of JTV519 may be attributable to its lack of specificity, as is the case with Verapamil, a phenylalkylamine $Ca_v1.2$ channel antagonist found to reduce the frequency of stress-induced arrhythmia in CPVT patients, which was also found to interact with RyR2 and the cAMP-dependent signalling cascade (Swan et al., 2005).

Evidently, the complexities of myocardial Ca^{2+} signalling predict a wide variety of pharmacologic targets, and it is anticipated that more efficient therapies to combat CPVT/ARVD2 will emerge in the near future. However, as discussed previously the complexity of RyR2 is likely to preclude a unifying mechanism of channel dysfunction and so broad-spectrum therapies may not be applicable, since what prevents arrhythmia in one patient may promote channel aberrant function in another. Hence, it is hoped that characterisation of individual mutants using appropriate experimental models, will contribute to the development of future therapeutic strategies.

1.6. Aims of this thesis

Currently, the precise mechanistic basis of RyR2 dysregulation in the pathogenesis of ARVD2/CPVT remains to be fully resolved and only eight out of the 43 identified arrhythmogenic RyR2 mutants have been functionally characterised in various studies (Wehrens et al., 2003; George et al., 2003; Lehnart et al., 2004; Jiang et al., 2002, 2004), all of which are associated with CPVT and exhibited gain-of-function channel characteristics. In light of this, the general aim of this thesis was to investigate the functional characteristics of the four ARVD2-linked mutations; $R^{176}Q/T^{2504}M$ (found on the same allele, co-segregating with the affected phenotype), $L^{433}P$ and $N^{2386}I$ (Tiso et al., 2001). The intention of this approach was to gain an insight into the mechanism by which aberrant Ca^{2+} handling leads to the disease phenotype of ARVD2, and also to establish whether these mutants exhibited a different functionality to previously characterised CPVT-linked mutants. The experimental strategy centred around recombinant expression of engineered mutants in a cell line devoid of RyR, thereby avoiding difficulties in the interpretation of results due to channel heterotetramerisation with endogenous RyR2. Channel functionality will be examined within this living cell context using agonist-induced Ca^{2+} release, before further investigation of channel sensitivity to activating and deactivating cytosolic Ca^{2+} using a novel, more physiological approach (in which the channels could be maintained in a more physiological environment).

The effect of mutation on the interaction of cardiac accessory/regulatory proteins with the channel will also be investigated, since the loss of these interactions may represent a mechanism of arrhythmogenesis.

Thus, it is anticipated that this strategy should reveal some of the cellular implications of ARVD2-linked RyR2 mutation, and aid our understanding of channel dysfunction in this cardiopathology.

Chapter 2

Materials and Methods

2.1. Materials

2.1.1. General laboratory reagents and chemicals

All reagents and chemicals were of analytical grade and were obtained from Sigma or Calbiochem unless otherwise stated. All reagents and equipment for polyacrylamide gel electrophoresis were obtained from BioRad, unless otherwise stated. All reagents were dissolved in dH_2O and stored at room temperature unless otherwise stated. All filter sterilization was through 0.2μM filters (Sartorius).

2.1.2 Molecular biology reagents

- *EDTA, 0.5 M*: a stock solution of Na_2EDTA (sodium ethylene-diamine-tetraacetate) was prepared, the pH was adjusted to 11.0 for the solid to go into solution, then adjusted to 8.0 with HCl.
- *Tris, 2 M*: a stock solution was prepared and the pH was adjusted to 8.0 with HCl.
- *TAE, 50x stock*: 2 M Tris, 2 M acetic acid, 50 mM EDTA.
- *DNA loading buffer, 2x stock*: 2x TAE, 50% (v/v) glycerol, 0.25% (w/v) orange G.
- *Resuspension solution*: 50 mM Tris, 10 mM EDTA, 100 μg/ml RNAase A, pH adjusted to 7.5 with HCl. Filter sterilised.
- *Lysis solution*: 0.2 M NaOH, 1% (w/v) sodium dodecyl sulphate (SDS). Filter sterilised.
- *Neutralisation solution*: 4.09 M Guanidine-HCl, 0.759 M CH_3COOK, pH adjusted to 4.2 with glacial CH_3COOH. Filter sterilised.
- *Sodium acetate, 3 M*: a 3 M solution of CH_3COONa was prepared and the pH was adjusted to 4.8 with glacial CH_3COOH and then filter sterilised.
- *Column equilibration buffer (QBT)*: 750 mM NaCl; 50 mM MOPS, pH 7.0; 15% (v/v) isopropanol, 0.15% (v/v) Triton® X-100.
- *Medium salt column wash buffer (QC)*: 1 M NaCl, 50 mM MOPS, 15% (v/v) isopropanol, pH 7.
- *Column elution buffer (QF)*: 1.25 M NaCl, 50 mM Tris, 15% (v/v) isopropanol, pH 8.5.
- *Guanidine thiocyanate, 5 M*: a stock solution was prepared and filter sterilised.
- *4/40 wash solution*: 40% (v/v) isopropanol, 4.2 M guanidine-HCl, filter sterilised.
- *DNA modifying and restriction enzymes*: all enzymes and appropriate buffers were obtained from Amersham-Pharmacia, Promega, Roche and Stratagene.

- *Molecular weight DNA markers*: obtained from Invitrogen.
- *Sequencing kit*: BigDye terminator v5, obtained from Applied Biosystems.

2.1.3. Bacterial cell culture reagents

All growth media and antibiotics were obtained from Sigma, sterile plastic and glassware were from Greiner and Fisher. All glassware was washed in detergent-free water and autoclaved (135°C, 4 bars, 90 minutes). Growth media were autoclaved under the same conditions prior to the addition of antibiotics. Aseptic technique was employed in all protocols and surfaces were swabbed with 70% (v/v) ethanol before and after use.

- *LB medium*: 10 g/L tryptone, 5 g/L yeast extract, 5 g/L NaCl, 15 g/L agar (for plates only), autoclaved. Medium was allowed to cool to ~ 50°C before adding the appropriate antibiotic.
- *Ampicillin 100 mg/ml stock*: filter sterilised and stored -20°C, used at a working concentration of 100 μg/ml.
- *Kanamycin 30 mg/ml stock*: filter sterilised, stored at -20°C, used at a working concentration of 30 μg/ml.
- *NZY medium*: 16 g/L NZ, 5 g/L yeast extract, autoclaved.
- *SOC medium*: 20 g/L tryptone, 5 g/L yeast extract, 0.5 g/L NaCl, 0.18 g/L KCl, 0.95 g/L $MgCl_2$, autoclaved. Medium was allowed to cool to ~ 50°C before adding glucose at 2% (w/v) final concentration from the stock solution.
- *Glucose, 20% (w/v)*: a stock of glucose was prepared and filter sterilised.
- *Ethanol, 80%(v/v)*: an 80% stock of ethanol was prepared and filter sterilised.
- *Freezing down medium*: 50 % (v/v) LB medium, 50 % (v/v) glycerol, autoclaved.

2.1.4. Yeast cell culture reagents

All growth media and reagents were obtained from Sigma and sterile plastic and glassware from Fisher or Greiner. All glassware was treated as for bacterial cell culture. All growth media were autoclaved and aseptic technique was employed in all protocols as before.

- *Glucose, 20% (w/v)*: a stock solution was prepared and filter sterilised.

- *YPD medium*: 20 g/L peptone, 10 g/L yeast extract, 20 g/L agar (for plates only), autoclaved. Medium was allowed to cool to ~ 50°C before adding glucose at 2% (w/v) final concentration from the stock solution.
- *YNB, 10x*: 67 g/L YNB (Yeast Nitrogen Base), autoclaved. Stored at 4°C and used within 2 months.
- *DO (drop-out) supplements, 10x*: DO supplement stock solutions were prepared (10x DO/-Leu, 16 g/L, 10xDO/-Trp, 19 g/L, 10x DO/-His, 19 g/L, 10x DO/-Leu-Trp, 16 g/L, 10x DO/-Leu-Trp-His, 16 g/L (+ 0.2 g/L uracil)), autoclaved. Stored at 4°C and used within 2 months.
- *SD (selective drop-out) minimal medium*: 1x YNB, 1x DO supplement as appropriate, 20g/L agar (for plates only), autoclaved. Medium was allowed to cool to ~50°C before adding glucose at 2% (w/v) final concentration of the stock solution.
- *3-amino-1,2,4-triazole (3-AT) 1 M*: a stock solution of 3-AT was freshly prepared, filter sterilised and added to autoclaved, cooled SD/-Leu-Trp-His medium to give a final concentration of 15 mM.
- *Polyethylene glycol (MW: 3350 i.e. PEG 3350), 50% (w/v)*: stock solution was prepared and filter sterilised.
- *TE, 10x*: 100 mM Tris, 10 mM EDTA, pH adjusted to 7.5 with HCl. Filter sterilised.
- *Lithium acetate (LiAc), 10x*: a 1 M stock solution was prepared and adjusted to pH 7.5 with dilute acetic acid, filter sterilised.
- *PEG/LiAc solution*: 40% (w/v) PEG 3350, 1x LiAc, 1x TE, added from the stock solutions, always freshly prepared.
- *LiAc/TE solution*: 1x LiAc, 1x TE, always freshly prepared.
- *5-bromo-4-chloro-3-indoyl-β-D-galactopyranoside (X-gal)*: a 20 mg/ml stock solution was prepared in N,N-dimethylfprmamide (DMF) and stored in the dark at -20°C.
- *Z buffer*: 100 mM Na_2HPO_4, 40 mM NaH_2PO_4, 10 mM KCl, 1 mM $MgSO_4$, pH adjusted to 7.0, autoclaved.
- *Z buffer/X-gal solution*: 1.67 ml of X-gal stock solution (0.33 mg/ml final concentration) and 270 µl of β-mercaptoethanol (0.27% (v/v) final concentration) was added to 100 ml Z buffer, always freshly prepared.
- *Yeast protein extraction (cracking) buffer*: 8 M urea, 4% (w/v) SDS, 0.5 M ammonium sulphate, 50 mM tris, 1 mM EDTA, 0.01% (v/v) β-mercaptoethanol, pH adjusted to 6.8 with HCl. Filter sterilised.

- *Yeast plasmid extraction buffer*: 4% (w/v) SDS, 1x LiAc, 1x TE, filter sterilised and always freshly prepared.
- *Chloroform: phenol: isoamyl alcohol (25:24:1):* used in a fume hood, stored at 4°C.

2.1.5. Plasmid vectors

2.1.5.1. Mammalian expression vector

The mammalian expression vector containing the full-length hRyR2 which was tagged at the N-terminus with eGFP (pcDNA3-GFP-hRyR2) was obtained from Dr. Chris George. The generation and characterisation of eGFP-hRyR2 has been reported (George at al., 2003c). Briefly, overlapping cDNA clones comprising the complete coding sequence of the hRyR2 (Tunwell et al., 1996) were assembled to create a single cDNA encoding the entire open reading frame (ORF) of hRyR2 (George et al., 2003c). The complete cDNA sequence (-121 to 15335 bp) was transferred into pcDNA3 (Invitrogen) using *NotI-XhoI* restriction sites, generating plasmid pcDNA3-hRyR2 encoding the hRyR2 ORF (14904bp) (George et al., 2003c). A fragment of peGFP-C3 (Clontech) (35 to 1330bp) was amplified by PCR, digested with *MluI/SpeI*, and inserted into *MluI/SpeI* digested pcDNA-hRyR2. This strategy placed eGFP at the N-terminus of hRyR2 separated by a four amino acid spacer (Thr-Ser-Gly-Ser). In mammalian cells, transcription is initiated by the cytomegalovirus (CMV) promoter (P_{CMV}) and terminated by the stop codon (TAA) inherently encoded by the RyR2 sequence. pcDNA3 replicates autonomously in both *E.coli* and in mammalian cells from the ColE1 and SV40 origin, respectively. The vector also encodes β-lactamase for selection by ampicillin resistance in bacteria (See Figure 2.1.)

2.1.5.2. Shuttle/ intermediate vector

The pSL1180 superlinker vector (Amersham) was used to clone fragments of RyR2 used in site-directed mutagenesis, this was purely for the purpose of DNA manipulation and propagations; no protein expression was initiated from this vector. The pSL1180 superlinker is small vector derived from pUC118, which replicates in bacteria from the pUC origin. It is widely used as a shuttle vector for cloning

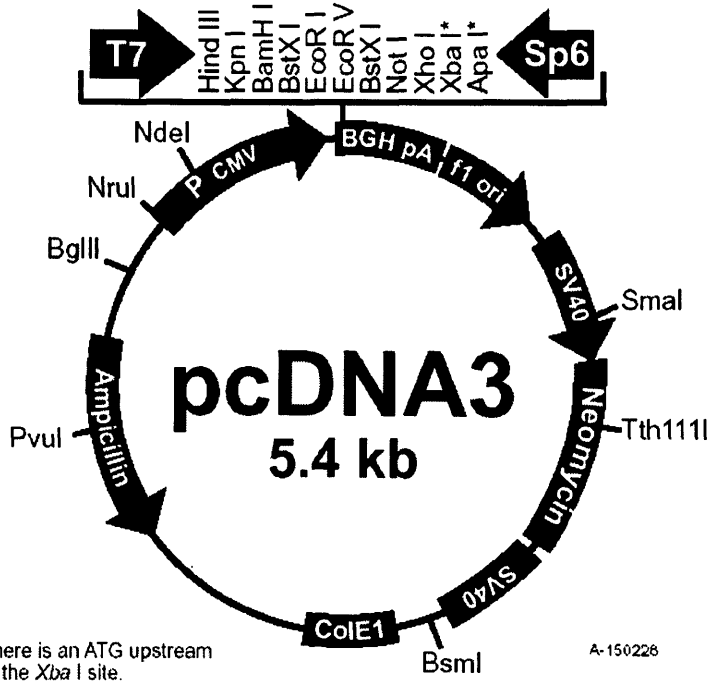

Figure 2.1. Mammalian expression vector pcDNA3. eGFP-hRyR2 was constructed in the mammalian expression vector pcDNA3. Expression was driven by a CMV promoter.

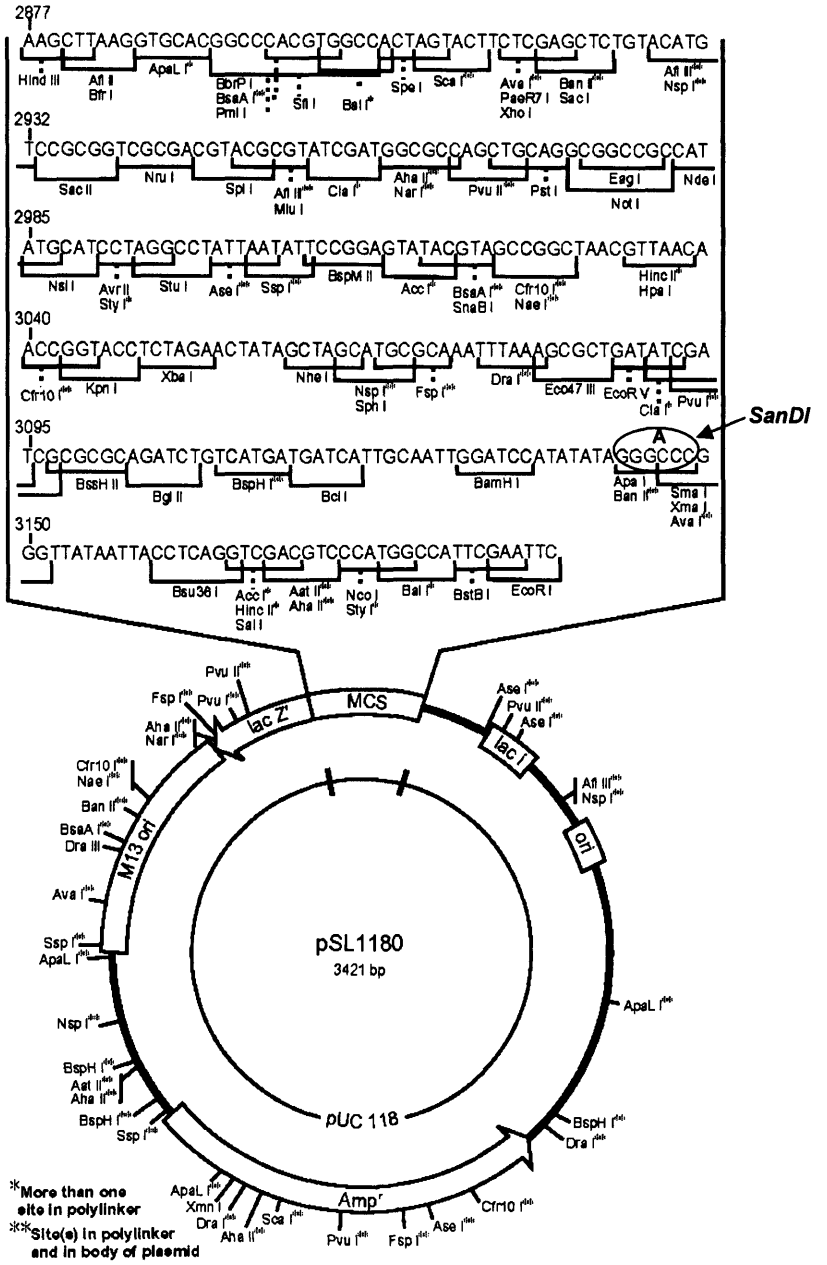

Figure 2.2. pSL1180 superlinker. This was used as an intermediate vector in the mutagenesis of RyR2 DNA fragments due to the fact that it's MCS contains many unique restriction enzyme sites, though a *SanDI* site (GGGACCC) had to be introduced by site directed mutagenesis at the position shown. Proteins were not expressed from this vector.

purposes due to its extensive multiple cloning site (MCS), containing the majority of commercially available restriction enzyme recognition sites (see Figure 2.2.).

2.1.5.3. Yeast expression vectors

Yeast two hybrid vectors and control plasmids were obtained form Clontech (see Figure 2.3.):

- pGBKT7: used to generate fusions of the bait protein with the GAL4 DNA-binding domain (Figure 2.3.A). It confers kanamycin resistance on transformed bacteria and tryptophan prototrophy on transformed yeast. It also contains a c-myc epitope tag.
- pACT2: used to generate fusions of the target protein (or a collection of random, unknown proteins) with the GAL4 activation domain (Figure 2.3.B). It confers ampicillin resistance on transformed bacteria and leucine prototrophy on transformed yeast. It also contains a HA epitope tag.
- pCL1: positive control plasmid. It encodes the full-length GAL4 protein.
- pVA3: positive control plasmid used with pTD1. It encodes a DNA-BD/murine p53 fusion protein.
- pTD1: positive control plasmid used with pVA3. It encodes an AD/SV40 large T-antigen fusion protein.
- pLAM5: negative control plasmid used with pTD1. It encodes a DNA-BD/human laminin C fusion protein.

2.1.6. Oligonucleotides

Custom oligonucleotide primers were ordered from Sigma Genosys, and were obtained as lyophilised pellets. Pellets were resuspended in an appropriate volume of deionised H_2O to give a stock concentration of ~250 µM according to the manufacturers instructions. Primer concentration (in µM) was confirmed by spectrophotometric quantification of a 1:100 dilution (in duplicate), determined by measuring the absorbance at 260 nm (A_{260}) in a quartz cuvette using a Perkin-Elmer MBA2000 spectrophotometer. Given the nucleotide sequence, the molecular weight and the melting temperature, the concentration was automatically calculated (taking into account that A_{260} = 1 corresponds to ~20-39 µg/ml of ssDNA, depending on the base composition, with ~ 33 µg/ml taken on assumption of an equal mixture of the

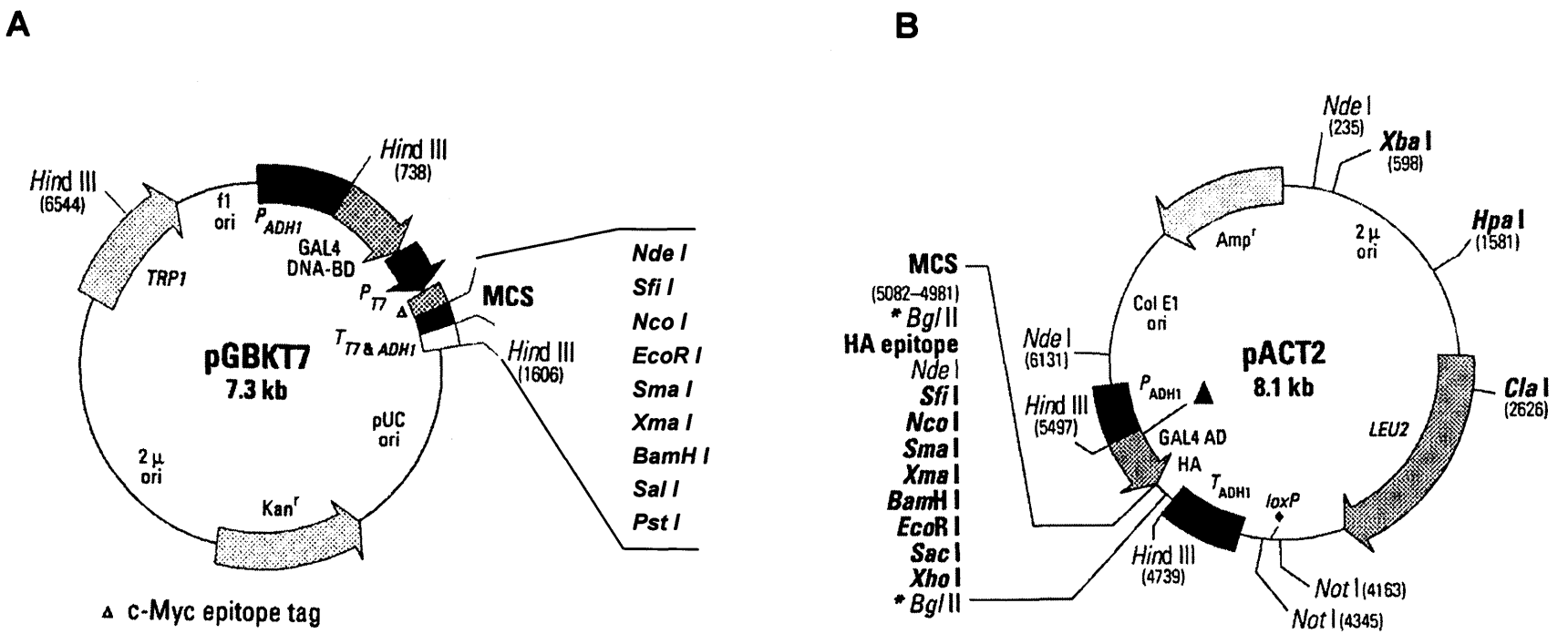

Figure 2.3. Yeast expression vectors. A) The pGBKT7 vector (bait) expresses proteins fused to the GAL4 DNA-binding domain (BD). In yeast, fusion proteins are expressed from the constitutive ADH1 promoter (P_{ADH1}); transcription is terminated by the T7 and ADH1 transcription termination signals ($T_{T7\ \&\ ADH1}$). pGBKT7 also contains the T7 promoter, a c-myc tag and a multiple cloning site (MCS). pGBKT7 replicates autonomously in both *E.coli* and *S.cerevisiae* from the pUC and 2µ ori, respectively. The vector carries the kanamycin resistance gene for selection in *E.coli* and the *TRP1* nutritional marker for selection in yeast. B) The pACT2 (target or library) vector generates a fusion of the GAL4 Activation Domain (AD) and a protein of interest (or a protein encoded by a cDNA in a fusion library) cloned into the MCS in the correct orientation and reading frame. The hybrid protein is expressed in yeast host cells from the constitutive ADH1 promoter (P_{ADH1}); transcription is terminated at the ADH1 transcription termination signal (T_{ADH1}). The protein is targeted to the yeast nucleus by the nuclear localization signal from the SV40 T-antigen, which has been cloned into the 5' end of the GAL4 AD sequence. pACT2 replicates autonomously in both *E.coli* and *S.cerevisiae* from the ColE1 and 2µ ori, respectively. The vector carries the ampicillin resistance gene for selection in *E.coli* and the *LEU2* nutritional marker for selection in yeast.

four bases). Working concentrations of 20 µM or 3.2 pmol/µl were prepared and primers were stored at -20°C. A list of all the primers used in this study is given in Appendix I.

2.1.7. Human Embryonic Kidney (HEK) 293 cell line culture reagents

HEK293 cells (ATCC number CRL-1573) derive from human embryonic kidney cells immortalized by adenovirus 5 DNA infection (Graham et al. 1977). They are adherent, and exhibit typical epithelial cell morphology (see Chapter 3, Figure 3.6.-3.7. and .3.9.).

All growth media and reagents were supplied by Gibco/Invitrogen and all chemicals were from Sigma unless otherwise stated. Sterile culture flasks and bottles were supplied by Nunc (Fisher) or Greiner. Class I cell culture containment hoods (Microflow biological safety cabinets) were employed for all procedures.

- *Dulbecco's Modified Eagle Medium* (DMEM) supplemented with 10% (v/v) foetal calf serum, 2 mM glutamine and 100 µg/ml penicillin/streptomycin (all filter sterilised). Stored at 4°C.
- *Trypsin-EDTA*, 1x in HBSS without calcium or magnesium, stored at – 20 °C.
- *Poly-L-lysine, 0.1% solution*: used to coat coverslips (150 µl/coverslip). Stored at 4°C.
- *Freezing down medium*: 10% (v/v) dimethyl sulphoxide (DMSO) in foetal calf serum, filter sterilised and stored at 4°C.
- *Saline solution*, 0.9% (w/v) supplied by Baxter Medical Supplies.
- *Phosphate buffered saline (PBS)*: 137 mM NaCl, 2.7 mM KCl, 4.3 mM Na_2HPO_4, 1.4 mM KH_2PO_4, pH adjusted to 7.4 using HCl, filter sterilised.
- *Cell fixing solution*: 4% (w/v) paraformaldehyde in PBS, always freshly prepared.
- *Cell permeabilising solution*: 0.1% (v/v) Triton X-100 in PBS, always freshly prepared.
- *alamarBlue™ reagent*: obtained from Biosource and used as a 10% (v/v) solution in complete DMEM. Stored at 4°C.
- *Hepes buffered saline (HBS) 2x*; 280 mM NaCl, 10 mM KCl, 1.5 mM Na_2HPO_4, 10 mM glucose, 50 mM Hepes, pH adjusted to 7.05, filter sterilised and stored in aliquots at -20°C.
- *Calcium chloride, 2 M*: a 2 M stock of $CaCl_2.6H_2O$ was prepared, filter sterilised and stored in aliquots at -20°C.

2.1.8. Calcium imaging reagents and agonists

- *Krebs-Ringer-Hepes (KRH) buffer*: 120 mM NaCl, 25 mM Hepes, 4.8 mM KCl, 1.2 mM KH_2PO_4, 1.2 mM $MgSO_4$, 1.3 mM $CaCl_2$ (omitted when making KRH-Ca^{2+}), pH adjusted to 7.4. Filter sterilised and stored at 4°C.
- *Calcium dyes*: fluo-3 and calcium orange acetoxymethyl esters (AM) was obtained from Molecular Probes and dissolved in a solution of 20% (w/v) pluronic acid in DMSO to obtain a stock concentration of 3.2 mM, which could be stored at –20 °C but were usually freshly prepared. For use, this was then diluted 1/300 in serum free DMEM to obtain a working concentration of 10 µM.
- *Caffeine, 100 mM*: stock solution prepared in KRH, diluted 1/10 to prepare a 10 mM stock, always freshly prepared.
- *Thapsigargin, 1 mM*: stock solution prepared in DMSO, stored in aliquots at -20°C.
- *Ionomycin, 1M*: stock solution prepared in DMSO, diluted 1/10 to prepare a 100 µM stock, stored in aliquots at – 20 °C.
- *EGTA, 100mM*: a stock solution of Na_2EGTA (ethylene glycol-bis (β-aminoethylether)-N,N,N',N'-tetraacetic acid) was prepared, the pH was adjusted to 10.0 with KOH for the solid to go into solution, then adjusted to 7.0 with HCl, stored at 4 °C.
- *CaEGTA, 100mM*: a stock solution of EGTA was prepared as described as above to which 96 mM $CaCO_3$ was added, before adjusting to the pH to 7.0 with HCl.
- *Minimum free Ca^{2+} buffer (0.1 nM, 10E)*: 10 mM EGTA, 100 mM KCl, 1 mM $MgCl_2$, 20 mM HEPES (N-2-hydroxypiperazine-N'-2-ethanesulphonic acid), adjusted to pH 7.0 with HCl, filter sterilised and stored at 4 °C.
- *Maximum free Ca^{2+} buffer (61 µM, 10CaE)*: 10 mM CaEGTA, 100 mM KCl, 1 mM $MgCl_2$, 20 mM HEPES, adjusted to pH 7.0 with HCl, filter sterilised and stored at 4 °C.
- *Streptolysin-O, 5 mg/ml*: a stock solution was prepared corresponding to an activity of 25 U/µl, stored in aliquots at –80 °C.
- *4-chloro-m-cresol, 1 M*: stock solution prepared in HPLC grade methanol, serially diluted to prepare 100 mM, 10 mM and 1 mM stocks, always freshly prepared.
- *Carbamyl choline (Carbachol), 100 mM*: stock solution prepared in KRH, always freshly prepared.

2.1.9. Protein biochemistry reagents

- *Tris, 1.5 M*: a 1.5 M solution of Tris was prepared and pH was adjusted to 8.8 with HCl, stored at 4°C.
- *Tris, 0.5 M*: a 0.5 M solution of Tris was prepared and pH was adjusted to 6.8 with HCl, stored at 4°C.
- *Ammonium persulphate, 10% (w/v):* always freshly prepared.
- *Running buffer, 1x*: 25 mM Tris, 250 mM glycine, 0.1% (w/v) SDS.
- *SDS-gel loading buffer, 2x*: 100 mM Tris pH 6.8, 20% (v/v) glycerol, 4% (w/v) SDS, 0.2% (w/v) bromophenol blue, 10% (v/v) β-mercaptoethanol, filter sterilised and always freshly prepared.
- *Transfer buffer ('Wet Blot' – for GFP-hRyR2 constructs)*: 25 mM Tris, 192 mM glycine, 0.01% (w/v) SDS.
- *Transfer buffer (Semi-dry – for Y2H constructs):* 48 mM Tris, 39 mM glycine, 0.037% (w/v) SDS, 20% (v/v) methanol.
- *Molecular weight markers*: pre-stained (Kaleidoscope), obtained from Bio-Rad.
- *Hypo-osmotic HEK cell lysis buffer*: 1x protease inhibitor cocktail tablet (obtained from Roche) dissolved in a 25 ml solution of 20 mM Tris, 5 mM EDTA and 0.05% (v/v) Triton-X-100, pH adjusted to 7.4 with HCl.
- *Tris-buffered saline (TBS), 1x*: 20 mM Tris, 137 mM NaCl, pH adjusted to 7.6 with HCl.
- *TBS-T 1x*: 1x TBS, 0.1% (v/v) Tween-20.
- *Blocking solution*: 5% (w/v) non-fat dried milk in TBS-T.
- *Membrane stripping buffer*: 62.5 mM Tris, 2% (w/v) SDS, 100mM β-mercaptoethanol, pH adjusted to 6.7 with HCl.
- *Coomassie blue stain*: 40% (v/v) methanol, 10% (v/v) glacial acetic acid, 0.25% (w/v) brilliant blue.
- *Coomassie destain*: 40% (v/v) methanol, 10% (v/v) glacial acetic acid.

2.1.10. Antibodies

- *Ab-cMyc*, mouse monoclonal, raised against residues 410-419 (QKLISEEDL) of the human cMyc protein (9E10, Santa Cruz), used at 1:1000 dilution for Western blotting.

- *Ab-GFP* (B-2), mouse monoclonal IgG, raised against the entire Green Fluorescent Protein of *Aequoria Victoria,* though cross reacts with enhanced GFP. Obtained from Santa Cruz. Used at 1:5000 dilution for western blotting.
- *pAb-129*, rabbit polyclonal anitserum, raised to unique residues 4673-4697 of the cardiac ryanodine receptor (KAALDFSDAREKKKPKKDSSLSAV), and does not cross react with RyR1. Used 1:1000 dilution for Western blotting, 1:100 for immunocytochemistry.
- *pAb-1093*, rabbit polyclonal antiserum, rased to residues 4515-4564 of the cardiac ryanodine receptor (EDKGKQKLRQLHTHRYGEPEC), and does not cross react with RyR1. Used 1:500 dilution for Western blotting, 1:100 for immunocytochemistry.
- *Anti-SERCA antibody* (2A-A1), mouse monoclonal IgG2a, raised against purified canine cardiac SR vesicles. Obtained form Affinity Bioreagents. Used 1:10,000 for Western blotting.
- *Anti-calreticulin antibody*, rabbit polyclonal antiserum raised against the entire recombinant protein (Roderick et al, 1997), provided by Dr. D. Llewellyn, Cardiff University. Used 1:1000 for Western blotting.
- *Anti-calsequestrin antibody* (pAb3516), rabbit polyclonal IgG, raised to purified native canine cardiac calsequestrin. Obtained from Abcam, used 1:2500 for Western blotting.

2.1.11. Computer software and data analysis

Numerical data was stored in spreadsheets and plotted in graphical form using Excel (Microsoft), where data was expressed as means ± the standard error. Standard curves for protein concentration standards were generated in Minitab (Minitab Inc.) using linear regression analysis. EC_{50} curves were obtained in GraphPad Prism v3.02 (GraphPad Software Inc.) using a sigmoidal dose-response curve fit with variable slope. Ca^{2+} sensitivity curves were fitted on Origin v7 (OriginLab Corporation) using a Gaussian curve fit equation (see individual chapters for algorithm equations).

Western blots were scanned at 300dpi using a densitometer (GS-700, Bio-Rad), and image processing was undertaken using Photoshop (Adobe) and PowerPoint (Microsoft). Densitometric analysis was performed on 'raw data' images using Quantity One software (Bio-Rad). All measurements were calibrated against an area of the blot containing no protein.

DNA and protein sequence analysis was done using software contained within the Genetic Computing Group package (GCG, University of Wisconsin, USA) or JEMBOSS, both of which can be accessed via the MRC website (http://www.hgmp.mrc.ac.uk) or using software available at the NCBI website (http://www.ncbi.nlm.nih.gov).

2.1.12. Health and Safety

All reagents were handled and stored as recommended by manufacturer's safety sheets. All experiments were carried out in accordance with COSHH regulations and local college regulations. All genetic manipulation was registered and carried out in accordance with local GMAG guidelines. All bacteria, yeast and mammalian cell culture waste were disinfected with Actichlor (Adams) at 1000ppm available chlorine (1 tablet per litre of waste) prior to disposal.

2.2. Methods

General molecular biology, biochemical and cell culture techniques were employed according to procedures in Molecular Cloning: a Laboratory Manual (Sambrook et al., 1989) and Short Protocols in Molecular Biology (Ausubel et al., 1997). Yeast two-hybrid techniques were carried out according to the MatchMaker GAL4 User Manual (Clontech) and Yeast Protocols Handbook (Clontech).

2.2.1. Molecular biology techniques

2.2.1.1. Agarose gel electrophoresis

DNA fragments were analysed by agarose gel electrophoresis and compared against DNA molecular weight markers. An agarose gel was prepared by dissolving the appropriate amount of agarose (ultra-pure, Eurogentec) (see Table 2.1) in TAE (1x) buffer and heating in a microwave oven. The solution was allowed to cool to below 50°C before addition of ethidium bromide to a concentration of 0.1 µg/ml, and poured into a gel tray which was assembled according to the manufacturers instructions (Bio-Rad). Once the gel was set, DNA samples in DNA loading buffer (1x) were loaded onto the gel alongside a DNA molecular weight marker (Invitrogen). Electrophoresis was carried out at constant voltage, typically at 5-10 V per cm of gel, until the dye front had migrated approximately two thirds the length of the gel. Gels were visualized with UV transillumination and imaged using a gel documentation system (Bio-Rad) with Hamamatsu camera and Quantity One software.

Table 2.1. Agarose Concentrations for DNA Electrophoresis

% Agarose	Effective range of resolution of linear DNA (kb)
0.7	0.8 – 12
1.0*	0.5 – 10
1.2	0.4 – 10
1.7	0.2 – 3
2.0*	0.1 – 2

* Typically, 1% was used for products >1kb, 2% was used for products <1kb.

Table reproduced from *Short Protocols in Molecular Biology* (Ausubel et al. 1997)

2.2.1.2. Cloning of DNA fragments

Plasmid DNA (usually 1-2 µg) was digested with the appropriate restriction enzymes (typically 5-10 U per 20 µl reaction) for 2 hours at 37°C, according to the manufacturers instructions. For double digests with incompatible buffers, the two enzymes were employed sequentially, in their specific buffer. The first digest was confirmed by agarose gel electrophoresis followed by excision and purification with the QIAEX II gel extraction kit (Qiagen), according to the manufacturers instructions. Briefly: agarose gel slices were dissolved in a high salt buffer, containing DNA-binding beads at 50°C for 5 minutes. The beads were sedimented by centrifugation at 14,000 *x*g for 30 seconds (Microfuge R, Beckman) and then washed once with high salt buffer, followed by two washes with a 70% ethanol buffer. DNA was eluted from the beads in 30 µl 10 mM Tris pH 8.5.

PCR products with engineered restriction sites at their 5' termini were digested overnight, 10% of the PCR reaction was analysed by gel electrophoresis and the remainder purified using the QIAquick PCR purification kit (Qiagen). Reaction mixtures were added to a DNA-binding spin-column, centrifuged at 14,000 *x*g for 1 minute before washing twice with an 80% ethanol buffer, DNA was eluted in 30 µl nuclease-free water.

Ligation was carried out using the Rapid DNA ligation kit (Roche), according to the manufacturer's instructions. The insert to be ligated was mixed with the plasmid vector (50 ng) in a 3:1 molar ratio, together with T4 DNA ligase and ligase buffer. This mixture was incubated at 4°C for 16 hours before being used to transform competent bacteria.

Where DNA fragments were to be cloned into TOPO® conjugated vectors (Invitrogen), 4.5 µl of the agarose gel extracted/purified product (typically approximately 100 – 200 ng) was added to 0.5 µl of vector and 1 µl of 6X salt buffer. The reaction was incubated at room temperature for 5 minutes and the whole reaction mix immediately transformed into *E. Coli* TOP10F as described below.

2.2.1.3. Bacterial cell culture

Two strains of *Epicurian coli* were used in this study: XL-10 Gold (Stratagene), Xl-1 Blue (Stratagene), and two strains of *Escherichia coli*: TOP10F (Invitrogen) and electrocompetent DH5α (Invitrogen). Bacteria were cultured at 37°C (except XL-10 Gold cells, transformed with full length RyR2 constructs that were grown at 30°C)

under aseptic conditions in LB medium, either in suspension with shaking at 225rpm (Innova 4300 shaker, New Brunswick) or on solid medium on LB-agar plates (plate incubator, Heraeus). For transformed bacteria, the growth medium contained ampcillin at 100 µg/ml or kanamycin at 30 µg/ml, for appropriate plasmid selection.
For long term storage of transformed bacteria, frozen glycerol stocks were prepared from 0.5 ml overnight liquid culture mixed with sterile glycerol in a 1:1 ratio. These were stored at -80°C. Bacteria were revived by streaking ~10 µl of the frozen stock onto an LB-agar plate (containing antibiotic). Glycerol stocks of bacteria transformed with the full length RyR2 were not made as they cannot be revived with the plasmid intact (George et al., 2003c; Bhat et al., 1999; Du & MacLennan, 1999).

2.2.1.4. Preparation of competent bacteria

XL-10 Gold ultracompetent cells are optimised for transformation of large DNA molecules (8-35 kb) with high efficiency (~5 x 10^9/µg pUC18 plasmid DNA) and were obtained from Stratagene, as were the XL-1 Blue supercompetent cells, used for transforming single-stranded mutagenised plasmids. Chemically competent TOP10F cells were prepared in our laboratory by Dr. S. Rogers using the $CaCl_2$ treatment method (Hanahan, 1983) and were stored in 100 µl aliquots at -80°C for up to 6 months. Electrocompetent DH5α were prepared in our lab by Dr. S. Zissimopoulos (Dower et al., 1988) and stored at -80°C for up to one month.

2.2.1.5. Transformation of competent bacteria

For transformation of full length GFP-RyR2 constructs: XL-10 Gold ultracompetent cells (25 µl) were thawed on ice and treated with 1 µl ß-mercaptoethanol (0.5 M, provided with the cells) for 10 minutes before adding 30 ng of ligation mix (if ligation mix was not very concentrated, 50 µl of XL-10 cells were used) or 15 ng plasmid for re-transformation and mixing gently. Cells were incubated on ice for 30 minutes before heat-shock treatment at 42°C for 30 seconds in a water bath and immediate transfer to ice for 2 minutes. NZY medium (800 µl) was then added to the cells and they were incubated at 37°C for 1 hour with shaking at 225rpm. Two unequal volumes of the cell suspension were subsequently plated onto LB-agar plates containing the appropriate antibiotic (this was to ensure two different densities of colony growth, avoiding lawn growth so that distinct colonies could be picked). Plates were incubated overnight at 30°C until colonies appeared. Plates were not

stored at 4°C, since this resulted in recombination of the RyR2 sequence, or gross plasmid degradation (George et al., 2003c; Bhat et al., 1999; Du & MacLennan, 1999).

Site directed mutagenesis products (5 µl) were transformed into XL-1 Blue supercompetent cells (25 µl) by a similar method as that employed for transformation of XL-10s, though ß-mercaptoethanol treatment was not included in this protocol.

Yeast two hybrid constructs and TOPO ligations (10 ng) were transformed into chemically competent TOP10F cells (100 µl), according to the manufacturers instructions (Invitrogen). The DNA was mixed with the cells and incubated on ice for 30 minutes, before heat shocking as previously, adding 300 µl SOC medium and incubating at 37°C with shaking at 225rpm. Plates from these transformations were incubated at 37°C overnight and subsequently stored at 4°C for up to 4 weeks.

Plasmid DNA obtained from yeast was transformed into DH5α cells by electroporation as follows: The cells (50 µl) were thawed on ice and up to 5 µl of the plasmid DNA solution was added to the cells and mixed gently. Cells were incubated on ice for 5 minutes and they were then transferred to a pre-chilled, sterile electroporation cuvette (0.2 cm electrode gap, Bio-Rad). Cells were electroporated for 5-10 msec in a Genepulser II electroporator (Bio-Rad) set at 25 µF (capacitance), 200 Ω (resistance) and 2.5 kV (voltage). Cells were then suspended in 800 µl SOC medium and incubated at 37°C with shaking at 225rpm. Two unequal volumes were plated onto two LB-agar plates containing the appropriate antibiotic (again in order to obtain two different densities of colony growth so that distinct colonies could be picked) and incubated overnight at 37°C.

2.2.1.6 Small scale plasmid isolation ('miniprep')

Colonies were screened for the presence of recombinant plasmid by the following method: LB-broth (5 ml) cultures containing the appropriate antibiotic were prepared by inoculation with a single colony and incubation over night at 30°C (for full length GFP-hRyR2 constructs) or 37°C with shaking at 225rpm, 3 ml of each culture was subsequently pelleted at 13,000 *x*g for 2 minutes (Microfuge R, Beckmann). Plasmid DNA was purified from these cell pellets by the alkaline lysis method employed by the Wizard® SV Miniprep plasmid purification kit (Promega). Bacterial pellets were resuspended in 250 µl resuspension solution (which contains RNase A, ensuring that liberated RNA is digested) and lysed in 250 µl Lysis solution, which contains SDS which solubilises phospholipid and protein components of the cell membrane leading to release of cell contents. This buffer also contains sodium hydroxide which creates

alkaline conditions that denatures chromosomal DNA and proteins. The lysate is then neutralised by the addition of 350 µl of Neutralisation solution. The high salt concentration results in precipitation of potassium dodecyl sulphate (KDS), which also causes precipitation of all cell debris (co-precipitated in insoluble salt-detergent complexes) which was subsequently removed by centrifugation at 13,000 *x*g for 10 minutes. The cleared lysate was then applied to a spin column containing a silica-gel DNA binding membrane and centrifuged again for a further 1 minute at 13,000 *x*g. The membrane was washed twice with an 80% ethanol buffer and the DNA eluted in 50 µl 10mm Tris pH 8.5. Recombinant plasmids were then analysed as in paragraph 2.2.1.7. before being prepared on a larger scale (paragraph 2.2.1.8.)

2.2.1.7. Analysis of recombinant plasmids

Recombinant plasmids were confirmed by restriction enzyme mapping, single digests were usually sufficient for full length GFP-hRyR2 constructs since most commercially available enzymes produce a diagnostic pattern of restriction fragments (See Chapter 3, Figure 3.2.). For all other constructs double digests were normally used, with the two enzymes each cutting at a single site, one within the insert and one within the vector sequence. Verified recombinant transformants were then confirmed by direct DNA sequencing using the BigDye™ terminator cycle sequencing kit (ABI Prism) and ABI Prism 377 sequencer (Perkin-Elmer) according to the manufacturer's instructions. After verification, plasmids were prepared on a large scale (see paragraph 2.2.1.8).

2.2.1.8. Large scale plasmid isolation

Sequence verified transformant cultures (1 ml) were inoculated into 250 ml cultures and grown overnight at 30°C (for full length GFP-hRyR2 constructs) or 37°C with shaking at 225rpm. The resulting bacterial suspension was pelleted by centrifugation (8000 x*g*, 20 minutes, 4°C, JLA16.250 (fixed-angle rotor), Avanti J-25, Beckman) and larger scale plasmid preparation was the carried out using either the Qiagen maxi prep kit (GFP-hRyR2 constructs) which uses an ion-exchange resin method, or the Wizard® PureFection kit, which employs DNA-binding magnetic beads for purification. The Qiagen kit was chosen for use in isolating the full length GFP-hRyR2 because it was found to preserve the integrity of the recombinant hRyR2 plasmid, which is extremely fragile and prone to non-specific recombination. This protocol is based on a modified alkaline lysis procedure, followed by binding of plasmid DNA to QIAGEN®

Anion-Exchange Resin under appropriate low-salt and pH conditions. The bacterial pellets underwent alkaline lysis using the same reagents as previously. Samples were incubated on ice for 20 minutes, and insoluble cell matter was removed by centrifugation (20,000 x*g*, 30 minutes, 4°C, JA 25.50 (fixed angle rotor), Avanti J-25, Beckman). The supernatant was applied to a Qiagen-tip 500 which has been equilibrated using Column equilibration buffer (QBT). The plasmid DNA was then washed twice with medium salt column wash buffer (QC), then eluted with Buffer QF (15 ml). Plasmid DNA was precipitated using isopropanol (0.7 volumes) overnight at –20°C. Following centrifugation (15 000 x*g*, 30 minutes, 4°C), the DNA pellet was washed in 70% ethanol (5ml) and further centrifuged (15 000 x*g*, 10 minutes, 4°C). The plasmid DNA was dissolved in 500 µl nuclease-free dH_2O at 37°C for 5 minutes. Plasmids which did not contain full length GFP-hRyR2 were prepared using the Wizard® PureFection kit, according to the manufacturer's instructions. Bacterial pellets underwent alkaline lysis, and cell debris was removed as described previously. The supernatant was then transferred to a different tube and was mixed with 5 ml guanidine thiocyanate (5 M) before adding 3.75 ml Magnesil™ paramegnetic particles. This mixture was incubated for 3 minutes at room temperature in order for the plasmid DNA to bind to the particles. The tube was then placed on a magnetic stand which collected the particles so that they could be washed once with 4/40 wash solution and then three times with 80% ethanol. The DNA was eluted off of the magnetic particles using 6 ml nuclease-free dH_2O and precipitated using isopropanol (0.7 volumes) and sodium acetate (0.1 volumes) at -20°C. The DNA was collected, washed and resuspended in 500 µl dH_2O as with those prepared using the Qiagen kit.

Plasmids were quantified, verified by restriction digest and agarose gel electrophoresis before being stored at -20°C.

2.2.1.9. DNA quantification

DNA concentration (in µg/ml) was determined by spectrophotometric quantification of a 1:50 dilution sample (in duplicate) by measuring the absorbance at 260 nm (A_{260}, the wavelength at which DNA exhibits peak light absorption) in a quartz cuvette using a Perkin-Elmer MBA2000 spectrophotometer. The concentration was calculated taking into account that an A_{260} value of 1 corresponds to 50 µg/ml of double stranded DNA. Plasmid purity was also quantified by measuring the ratio of A_{260}/A_{280}, with values ≥ 1.8 indicating highly purified preparations. Contamination by proteins, which have a peak absorption at 280 nm will lower this ratio.

2.2.1.10. In vitro *site-directed mutagenesis*

This technique of mutagenesis utilizes complementary oligonucleotide primers as a means for the exchange of DNA base pairs and requires that the dsDNA plasmid template be completely amplified by a DNA polymerase (see Figure 2.4.). It is for this reason that mutation cassettes of RyR2 were created and inserted into the shuttle vector pSL1180 (Amersham), ensuring that the template to be amplified was > 9 kb (see Chapter 3, section 3.2.1.).

Mutation of recombinant DNA constructs was carried out using the QuikChange® Site-Directed Mutagenesis Kit (Stratagene) according to manufacturer's instructions (see Figure 2.4.) and complementary primers were designed (see Appendix I) and purified by high-pressure liquid chromatography (HPLC) (Sigma-Genosys). When designing the mutagenic oligonucleotide primers for use in this technique, care must be taken to ensure that:

1. Both mutagenic primers should contain the desired mutation and anneal to the same sequence on opposite strands of the plasmid.
2. Primers should be between 25 and 45 bases in length to ensure complete and correct annealing. The melting temperature (T_m) of the primers should be ≥ 78°C, and they should terminate in one or more C or G bases for primer stability.
3. The desired mutation should be at the centre of the primer with 10-15 flanking bases of correct sequence.
4. Primers must have a high level of purity (hence the use of HPLC for purification). A low level of purity would result in a significant decrease in mutation efficiency.

A reaction mixture containing the appropriate oligonucleotide primers was set up as in Table 2.2. below. This mixture then underwent the thermal cycling conditions outlined in Table 2.3.

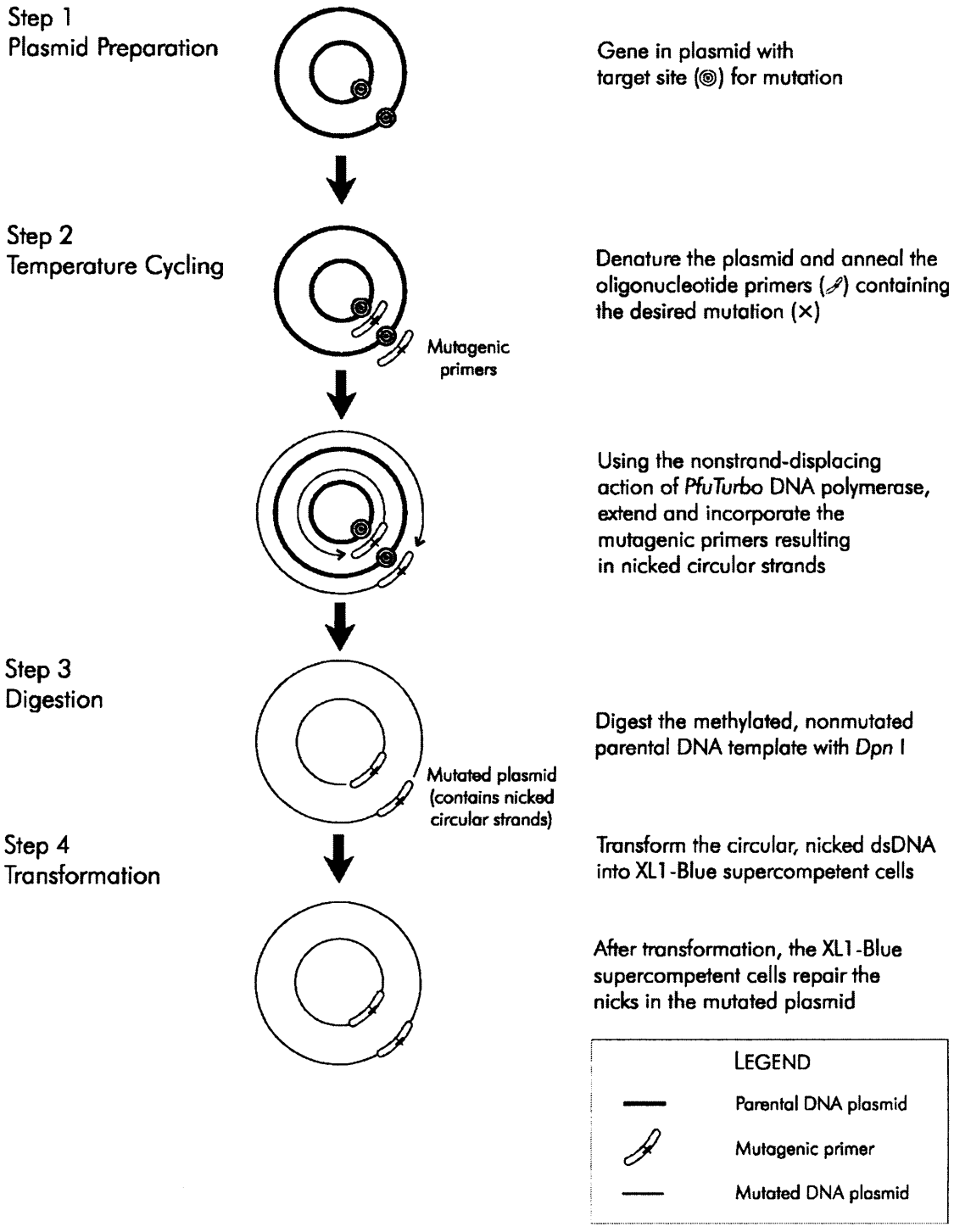

Figure 2.4. Overview of the *in vitro* site directed mutagenesis method (adapted from the Quickchange® kit, Stratagene).

Table 2.2. Typical reaction mix for in vitro site-directed mutagenesis

Reagent	Final concentration	Volume
Reaction buffer	1X	5 µl of 10X stock
DNA plasmid template	5-50 ng total	1 µl of 30 ng/µl stock
Forward primer	150 ng total	1 µl of 150 ng/µl stock
Reverse primer	150 ng total	1 µl of 150 ng/µl stock
dNTP mix	0.2 mM	1 µl of 10 mM stock
Pfu Turbo	2.5 u total	1 µl of 2.5 u/µl stock
Nuclease free H_2O	To 50 µl	40 µl

Table 2.3. Thermal cycling conditions for in vitro site-directed mutagenesis

Step	Temperature	Time	Number of cycles
Initial denaturation	95°C	30 seconds	1
Denaturation	95°C	30 seconds	12-18
Annealing	55°C	1 minute	
Extension*	68°C	7 -18 minutes	
Store	4°C	indefinite	1
* 2 minutes per kb to be amplified			

Following thermal cycling 10 U (1 µl) of *DpnI* endonuclease was added to the products and incubated at 37°C for 90 minutes. The *DpnI* endonuclease (target sequence: 5'-Gm^{6}ATC-3') is specific for methylated and hemimethylated DNA and is used to digest the parental DNA template and to select for mutation-containing synthesized DNA. DNA isolated from almost all *Escherichia coli* strains is *dam* methylated and therefore susceptible to *DpnI* digestion. The nicked vector containing the desired mutation was then transformed into XL1-Blue supercompetent cells as described in paragraph 2.2.1.5.

2.2.1.11. PCR amplification of DNA

PCR reactions were carried out using a Perkin-Elmer GeneAmp system 2400 thermal cycler. *Pfu* DNA polymerase (Promega) was used for generation of high fidelity products for cloning, since this enzyme possesses a 3'→5' exonuclease (proofreading) activity, resulting in excision of any base misinsertions that may occur during polymerisation. However, Pfu DNA polymerase-generated PCR products are blunt-ended, and so *Taq* polymerase (Promega) was used to generate A overhangs

on *Pfu* amplified constructs for TA cloning. A typical example of the reaction mixture and thermal cycling conditions is given in Table 2.4. and 2.5. respectively. PCR products were verified by agarose gel electrophoresis (see paragraph 2.2.1.1.) and purified using the QIAquick PCR purification kit (Qiagen), which employs a DNA binding column, according to the manufacturers instructions

Table 2.4. Typical PCR reaction

Reagent	Final concentration	Volume
DNA template	50-100 ng total	0.5 µl of 200 ng/µl stock
Forward primer	20 pmol total	1 µl of 20 µM stock
Reverse primer	20 pmol total	1 µl of 20 µM stock
PCR buffer	1x	5 µl of 10x stock
$MgCl_2$*	2.5 mM	2.5 µl of 50 mM stock
dNTP mix	0.2 mM	0.5 µl of 20 mM stock
DNA polymerase	1 U total	0.5 µl of 2 U/ul stock
Nuclease-free H_20	Up to 50 µl	39 µl

*$MgCl_2$ was included in the *Pfu* PCR buffer

2.5. Typical thermal cycling conditions

Step	Temperature	Time	Number of cycles
Initial denaturation	95°C	2 minutes	1
Denaturation	95°C	1 minute	25-35
Annealing*	50-65°	30 seconds	
Extension**	72°C	30 seconds-5 minutes	
Final extension	72°C	5 minutes	1
Storage	4°C	Indefinite	1

* Annealing temperature was dependent on the Tm of the primers.

** Extension time was dependent on the size of the PCR product to be amplified, and the DNA polymerase employed. For Pfu, 2 minutes per kb was allowed.

2.2.2. Yeast two-hybrid techniques

2.2.2.1. Yeast cell culture

The yeast strains used were Y190 and CG-1945 (Clontech) which have the ability to regulate the expression of both the *LacZ* and *HIS3* reporter genes. In CG-1945, expression of the *LacZ* reporter is driven by a weaker promoter and so this strain cannot be used in liquid β-galactosidase assays. Regulation of expression of the *HIS3* reporter gene in the Y190 strain is 'leaky', and background growth needs to be suppressed by at least 20 mM 3-amino triazole (3-AT), in CG-1945 the *HIS3* promoter has been replaced by the *GAL1* promoter leading to tighter regulation of the reporter gene, and background growth is suppressed by 5 mM 3-AT.

Yeast was cultured in aseptic conditions at 30°C in YPD medium, either in suspension with shaking (Innova 4300 shaker incubator, New Brunswick) or on solid YPD-agar plates (plate incubator Heraeus). Transformed yeast was grown in SD minimal medium.

For long term storage of transformed yeast, frozen glycerol stocks were prepared as follows: 2-3 isolated fresh colonies were taken from an agar plate and thoroughly resuspended by vortexing in a 1:1 solution of the appropriate SD minimal medium and sterile glycerol. Yeast was revived by streaking ~10µl of the frozen stock on a SD-agar plate to produce individual colonies.

The cell number of growing cultures was estimated by measuring the absorbance at 600nm (A_{600}) of an approximately diluted cell suspension (in order for A_{600} to be in the range of 0.1-1). Cell density was calculated using the formula: 1 A_{260} unit/ml approximates to 3 x 10^7 cells/ml.

2.2.2.2. Yeast Transformation

Competent cells were made by the lithium acetate method as follows: 50 ml of YPD medium was inoculated with 2-3 colonies and incubated at 30°C overnight with shaking at 250 rpm to saturation (i.e. A_{600}>1.5). The culture was then refreshed to early log phase (A_{600}= 0.2-0.3) by an appropriate dilution in 250 ml of fresh YPD, and incubated further for approximately 2.5 hours, until the A_{600} reached 0.5-0.6 (mid-log phase). Cells were collected by centrifugation at 1000 *x*g for 5 minutes (Allegra 6R, Beckman) and washed once in sterile dH_2O. The final cell pellet was resuspended in 1.5 ml LiAc/TE solution. Competent cells were used immediately after preparation.

100 µl of yeast competent cells were used for each transformation, together with 100 ng of plasmid DNA and 100 µg of herring testes carrier DNA. For double transformations the two plasmids were introduced simultaneously, using 200 ng of each. PEG/LiAc (600 µl) was added to the cells before incubation at 30°C for 30 minutes with shaking at 200 rpm. DMSO (70µl – 10% v/v of the final volume) was added and mixed by gentle inversion. Cells were subjected to heat shock treatment for 15 minutes at 42°C in a water bath, before immediate transfer to ice for 2 minutes. Cells were then collected, again by centrifugation at 13,000 *x*g for 1 minute (Microfuge R, Beckman), and the cell pellet was resuspended in 200 µl TE buffer. This cell suspension (100 µl) was plated onto the appropriate SD-agar plates and incubated at 30°C until colonies appeared (3-5 days).

2.2.2.3. Yeast two-hybrid library screening

The library plasmid was introduced into CG1945 yeast strain (pre-transformed with the bait construct) essentially as described in paragraph 2.2.2.2., with the appropriate scale up. Competent cells pre-transformed with the bait construct were prepared in SD/-Trp medium in order to maintain selective pressure on the plasmid. 175 µg of the human cardiac library plasmid (50 µg for every million independent clones, with the library used here containing 3.5×10^6 independent clones), together with 4 mg of herring testes carrier DNA was introduced to 1 ml of competent cells. The yeast transformation procedure was then continued as in paragraph 2.2.2.2. After heat shock treatment here however, the cells were collected, resuspended in YPD medium and incubated at 30°C with shaking for 1 hour in order to enrich the culture. The transformed cells were then collected by centrifugation (1000 *x*g for 5 minutes, Allegre 6R, Beckman) and resuspended in TE buffer (8 ml). 400 µl of the suspension was plated onto 20 x 200 mm diameter SD/-Leu-Trp-His agar plates in order to select for interacting proteins. A competitive inhibitor of the HIS3 protein: 3-amino-1,2,4-triazole (3-AT, 5 mM), was included in the agar plates in order to suppress background growth. 100 µl of 1:10, 1:100 and 1:1000 dilutions were plated on SD/-Leu-Trp agar plates in order to determine transformation efficiency. Plates were incubated at 30°C for up to 14 days to allow slower growing colonies (i.e. weak interactions) to appear. Reddish-brown HIS^+ colonies that grew to >2 mm diameter were considered positives. HIS^+ colonies were preserved by making a glycerol stock which was stored at -80°C. The transformation efficiency (colonies/µg of DNA) and the number of clones screened were calculated from the following formulae:

$$\frac{\text{Number of colonies x suspension volume (8000µl)}}{\text{Volume plated (400µl) x dilution factor x amount of DNA used (µg)}} = \text{colonies/µg DNA}$$

colonies/ µg DNA x amount of library plasmid DNA used (µg) = number of clones screened

2.2.2.4. Yeast protein extraction

Total yeast protein was extracted as follows: 2-3 isolated fresh colonies were used to seed a 10ml overnight culture in the appropriate SD medium. The culture was then refreshed to early-log phase (A_{600} of 0.2-0.3) by an appropriate dilution in 50 ml of fresh SD medium, and incubated further for approximately 4 hours, until the A_{600} reached 0.5-0.6 (mid-log phase). Cells were harvested by centrifugation at 1000 *x*g for 5 minutes (Allegre 6R, Beckman) and washed once in sterile H_2O. The cell pellet was then resuspended in the appropriate volume of warm (60°C) cracking buffer containing 1x complete protease inhibitor cocktail (Roche). The volume of cracking buffer used was dependent on the number of A_{600} units of cells collected and 100 µl of cracking buffer was used for every 7.5 A_{600} of cells, for example: a culture of 45 ml at A_{600} = 0.6 would require 0.6 x 40 x 100/7.5 = 320 µl cracking buffer. The cell resuspension was then transferred to another tube containing 80 µl of glass beads (425-600 microns, Sigma) per 7.5 A_{600} units and incubated at 70°C for 10 minutes before vortexing vigorously for 1 minute. Cell debris was pelleted at 14,000 *x*g for 5 minutes at 4°C (Microfuge R, Beckman). The supernatant containing the soluble yeast proteins stored at -80°C.

2.2.2.5. β-galactosidase colony lift assay

This assay was employed for investigating the presence of β-galactosidase activity produced as a result of interaction between bait and prey constructs and yields qualitative results only. Yeast colonies assayed for β-galactosidase activity was always fresh (never more than 5 days old). A disc of sterile filter paper (Whatman No.5) was pre-soaked in Z buffer/X-gal solution while a second, dry filter paper was placed over the surface of the agar plate to allow colonies to attach (~ 2 minutes). The filter paper was then completely submerged in a pool of liquid nitrogen for 10 seconds in order to lyse the attached yeast colonies. After complete freezing, the

filter paper was removed from the liquid nitrogen and allowed to thaw at room temperature. It was then placed on the pre-soaked filter (colony side-up), and incubated at 30°C for 8 hours for the blue staining to appear.

2.2.2.6. Yeast plasmid isolation

A crude, yeast plasmid DNA extract was prepared as follows: 2-3 isolated fresh colonies were seeded to prepare a 10 ml overnight culture in the appropriate SD medium. The culture was refreshed to early log phase (A_{600} ~0.2-0.3) by a suitable dilution in 50 ml of SD and incubated further for ~4 hours until the culture reached mid-log phase (A_{600}~0.5-0.6). Cells were collected by centrifugation (1000 *x*g for 5 minutes, Allegra 6R, Beckman) and washed once in sterile H_20. The cell pellet was then resuspended in 500 µl of Yeast Plasmid Extraction buffer together with 250 µl of glass beads (425-600 microns, Sigma) and vortexed vigorously for 2 minutes. Cell debris was pelleted at 10,000 *x*g for 5 minutes (Microfuge R, Beckman) at 4°C and the supernatant was removed to another tube and prepared by phenol-chloroform extraction as follows: The DNA solution was mixed with an equal volume of phenol-chloroform-isoamyl alcohol (25:24:1) and vortexed for 1 minute. The mixture was centrifuged at 14,000 *x*g for 5 minutes at 4°C and the DNA-containing aqueous phase transferred again to a new tube. This was repeated three times before precipitating the DNA by adding one volume of isopropanol and 0.2 volumes of 3 M sodium acetate pH 5.3. The precipitation solution was mixed well before centrifugation at 14,000 *x*g for 20 minutes at 4°C. The DNA pellet was washed with 70% v/v ethanol and re-centifuged at 14,000 *x*g for 10 minutes at 4°C. The resultant collected DNA was dried at 95°C for 1 minute before resuspension in 20 µl sterile H_2O.

2.2.2.7. Analysis of library screen positives

HIS^+ colonies were revived by streaking from the frozen glycerol stock onto SD/-Leu-Trp plates as well as on SD/-Leu-Trp-His (containing 5mM 3-AT), and plates were incubated at 30°C until colonies appear. β-galactosidase colony-lift assay was carried out on the colonies growing on the SD/-Leu-Trp to verify the positive interaction. If the β-galactosidase assay was negative, this particular HIS^+ colony was no longer considered a true positive interaction, whereas if it was positive, the HIS^+ colony was processed further for isolation of the library plasmid. Several isolated fresh colonies form the SD/-Leu-Trp-His (with 5 mM 3-AT) plate were

seeded to prepare a 10ml overnight culture in SD/-Leu-Trp-His (with 5 mM 3-AT) medium. The culture was then refreshed to early log phase (A_{600} of 0.2-0.3) by an appropriate dilution in 50 ml of SD, and this "saturation-refresh" cycle was repeated twice more in order to keep selective pressure on the interacting library plasmid, while ensuring the loss of any other non-interacting plasmids potentially harboured within the original HIS^+ colony. Plasmid DNA was then extracted from 50 ml of mid-log phase culture (A_{600} of 0.5-0.6) as described in paragraph 2.2.2.6.
As the plasmid DNA extracted for yeast was not of sufficient yield and purity for further manipulation, it was therefore immediately transformed (5 µl) into electrocompetent *E.coli*, from which high quality plasmid DNA was isolated. Transformed bacteria were plated on ampicillin containing LB agar plates in order to select for the AD-library plasmid (pACT2). The approximate length of the interacting sequence was estimated by digesting the isolated plasmids with HindIII (which cuts either side of the pACT2 multiple cloning site, leaving an excess of 750 base pairs), and then subjecting the resulting fragments to agarose gel electrophoresis. The plasmid DNA then underwent automatic cycle sequencing, and the sequence obtained was compared against all sequences in the GenBank nucleotide databases using the BLAST software program available at the NCBI website (http://www.ncbi.nlm.nih.gov).

2.2.3. Protein biochemistry techniques

2.2.3.1. Preparation of protein samples for SDS-PAGE

HEK cells (~2 x 10^7) were harvested by trypsinisation and pelleted (1000 *x*g, 5 minutes, Allegra 6R, Beckman), and then resuspended in a suitable volume of hypo-osmotic buffer (75 µl for every 1 x 10^6 cells harvested). Cells were homogenised through a needle (26 G) and were lysed with 5-6 cycles of freeze-thaw waterbath sonication. Nuclei were removed by centrifugation (1000 *x*g for 10 minutes, Microfuge R, Beckman) and the post-nuclear supernatant (containing membrane and soluble fractions) was concentrated to approximately ~200 µl by vacuum centrifugation (Savant).
Protein concentration was estimated with the use of a micro BCA assay kit (Pierce) according to the manufacturer's instructions. The method is based on the reduction of Cu^{2+} to Cu^+ by protein (in an alkaline medium) and subsequent chelation of the cuprous ion by bicinchoninic acid (BCA) to produce a purple coloured complex. Sample measurements were taken in duplicate for two appropriate dilutions and

compared against a standard curve produced by the linear regression of the absorbance against the known concentration of bovine serum albumen (BSA) samples (ranging from 10-200 µg/ml).

2.2.3.2. SDS-Polyacrylamide gel electrophoresis (SDS-PAGE)

Proteins were analysed by SDS-PAGE. RyR2 proteins were run on large gels (Hoefer), all other protein preparations were separated using mini-gels (ATTO). Briefly, a separating gel of appropriate concentration was prepared according to Table 2.6. The polymerisation mixture was poured into the appropriate gel casting system, which was assembled according to the manufacturer's instructions, and covered with a thin layer of water. Once the separating gel was set the water layer was carefully removed with filter paper. The stacking gel mixture (4% - prepared as for the separating gel except with 0.5 M Tris pH 6.8 bufffer) was then poured on top of the separating gel and the comb was inserted to form the wells. Once the stacking gel was set, protein samples were loaded alongside protein molecular weight markers (Bio-Rad). Electrophoresis was carried out at constant current (typically 40 mA, or 12 mA if running the gel overnight for RyR2 preparations) until the dye front had run off of the gel, or that all apart from the uppermost two markers had run off of the gel (when detecting RyR2).

Table 2.6. Separating acrylamide gel formulation

Reagent	**Final concentration**	**Typical volumes (µl)**			
acrylamide % in gel (X)		**4%***	**10%****	**12%****	**15%****
Acrylamide/bis-acrylamide (37.5:1), 40%	X	3000	5000	6000	7500
Tris, 1.5M, pH 8.8	25% (v/v)	7500	5000	5000	5000
SDS, 10% (w/v)	1% (v/v)	300	200	200	200
Ammonium persulphate, 10% (w/v)	0.5% (v/v)	200	100	100	100
TEMED	0.05 (v/v)	15	10	10	10
dH_2O	Up to final volume	18,978	9690	8690	7190
Where X is dependent on the % of acrylamide required, according to the sizes of the proteins separated					
* Used for running RyR2 proteins on large (Hoeffer) gels (total volume = 30 ml)					
**Used with ATTO mini-gel apparatus for all other proteins (total volume = 20 ml for 2 gels)					

2.2.3.3. *Transfer of proteins onto a membrane*

Proteins from SDS-PAGE gels were transferred onto a polyvinylidene difluoride (PVDF) membrane (Immobilon-P, Millipore) using a high power wet-blotting system (Hoefer) for RyR2 proteins, or a semi-dry transfer system (Bio-Rad) for all other proteins. PVDF membranes were prepared by soaking in methanol for 1 minute and then in the appropriate transfer buffer for at least 30 minutes. The transfer apparatus was assembled according to the manufacturer's instructions. Transfer of RyR2 proteins by 'wet-blotting' was carried out for 1 hour at 400 mA, followed by 16 hours at 1.5 A at 10°C, whereas 'semi-dry' transfer of all other proteins was carried out 400 mA (limited to 25 V) for 1 hour at 4°C.

2.2.3.4. *Western blot analysis*

Once protein transfer was complete, the membrane was incubated with 5% (w/v) non-fat dried milk protein (Marvel) in TBS-T buffer (blocking buffer) for at least 1 hour at room temperature or overnight at 4°C. Primary antibodies were applied in the appropriate dilution (see Paragraph 2.1.9.) in blocking buffer for 1-2 hours at room temperature or overnight at 4°C. The membrane was then washed three times (for 10 minutes each time) with blocking buffer. A horseradish peroxidase-linked secondary antibody (raised against the species in which the primary antibody was produced) was then applied in a 1:10,000 dilution in blocking buffer for 1 hour at room temperature. The blot was then washed five times (10 minutes) with TBS-T buffer. Immunoreactive protein bands were visualised by enhanced chemiluminescence detection (ECL, Amersham-Pharmacia) according to manufacturer's instructions. The blot was exposed to X-ray film (Hyperfilm, GE Healthcare) for a suitable length of time which was determined by the level of the chemiluminescence signal.

2.2.4. *Cell biology techniques*

2.2.4.1. *Culture and calcium phosphate mediated transfection of Human Embryonic Kidney (HEK) 293 cells*

HEK cells were maintained in Dulbecco's Modified Eagle Medium (DMEM, Invitrogen) supplemented with foetal calf serum (10% v/v), glutamine (2 mM) and penicillin/streptomycin (100 μg/ml) (Invitrogen) in an incubator at 37°C, 5% CO_2 and

~80% humidity (Heraeus) using 150 ml flasks (Nunc). Cells (~1 x 10^6) at ~70% confluency were transfected with high purity (A_{260}/A_{280}>1.9) plasmid cDNA encoding GFP-hRyR2 (4-6 μg) using a calcium phosphate precipitation method (Chen and Okayama, 1987). Briefly, the plasmid DNA was mixed with sterile dH_20 and 18.5 μl of 2 M $CaCl_2$ to a total volume of 150 μl and vortexed vigorously. This mixture was then added dropwise (over a period of 30 seconds-1 minute) to 150 μl of warmed 2x HBS in a sterile 14 ml capacity polypropylene tube (Greiner) with continuous vigorous mixing to achieve a final $CaCl_2$ concentration of 125 mM and volume of 300 μl. Transfection complexes were then incubated for no longer than 30 minutes at room temperature in order for precipitates to start forming. These were then mixed by vortexing and added dropwise to the cells in 3 ml of complete DMEM before gentle mixing and incubation at 37°C, and 5% CO_2 for 16-18 hours. Precipitates were removed by washing twice with 0.9% w/v sterile saline solution, and cells were then incubated at 37°C, 5% CO_2 in complete DMEM for at least another 6 hours before harvesting by trypsinisation.

2.2.4.2. Immunofluorescence analysis of cell expressing GFP-hRyR2

Cells were collected by trypsinisation, pelleted and resuspended in complete DMEM before plating onto poly-lysine coated glass coverslips (22 mm x 22 mm, 0.08-0.12 mm thickness) at a density of ~1.5 x 10^5 cells/coverslip. These were left to adhere to the glass for 24 hours in the incubator before washing 3 times in 1x PBS and fixing in a 4% v/v paraformaldehyde/PBS solution for 10 minutes in the dark. Cells were then washed and re-hydrated in PBS for 1 hour at room temperature before washing in dH_2O and mounted on sides using Fluorsave™ (Calbiochem). Slides were then stored at 4°C in the dark until viewing. Detection of full length RyR2 in fixed cells was accomplished by the following method: re-hydrated fixed cells were permeabilised by incubation in a solution of 0.1% v/v Triton X-100 in PBS for 30 minutes at room temperature. This solution was then aspirated and the cells were washed (PBS). Non-specific immunoreactivity was blocked using foetal calf serum (10% v/v in PBS) prior to incubation in primary antibody (pAb-129, 1:100 in PBS, see Materials for epitope) for 90 minutes at room temperature, or overnight at 4°C. Coverslips were then washed and incubated with a fluorescent secondary antibody (1:250 Alexa Fluor® 546 conjugated goat anti-rabbit IgG, Molecular Probes) for 90 minutes at room temperature. After final washes, coverslips were mounted with Fluorsave as previously. Cells were visualised using an RS2 confocal microscope (Leica) with an

oil immersion, 40x objective lens (numerical aperture = 1.3). GFP fluorescence was excited with an Argon/Krypton laser (peak excitation 488 nm) and detected using a 515±30 nm band pass filter. Alexa-546 fluorescence was excited with a Helium/Neon laser (peak excitation 546 nm) and detected using a 572±30 nm band filter.

2.2.5. Intracellular Ca^{2+} imaging

Cells (1.5 x 10^5) on poly-lysine coated coverslips were loaded with Fluo-3 (10 μM in 20% w/v pluronic acid F-12) in DMEM containing glutamine (2 mM). The dye containing solution was added to each coverslip as a 200 μl meniscus and incubated at 37°C and 5% CO_2 for 90 minutes. Coverslips were then immersed in DMEM prior to Ca^{2+} imaging, for which they were washed and transferred to Krebs-Ringer HEPES buffer. For imaging, coverslips were sealed with vacuum grease (Beckman) to the underside of a specially made chamber so that the cells could be immersed in a set volume of KRH (see Figure 2.5.). Ca^{2+} dependent Fluo-3 fluorescence was visualised using a Leica RS2 confocal microscope with an oil immersion (numerical aperture = 1.3) 40x objective lens, using an Argon/Krypton laser. Excitation was at 488 nm, and the fluorescence was detected with a 515±30 nm band pass filter. Visual data was acquired every 2 seconds, in order to minimize the effects of photobleaching (1 frame = 2 seconds, with one experiment containing 40 frames) at 512 x 512 pixel resolution. Cells were imaged for 10 frames before the addition of caffeine (0.1 – 40 mM) in order that the average baseline fluorescence level could be collected. Cells on separate coverslips were used per application of caffeine to negate the effect of sequential caffeine application on intracellular Ca^{2+} handling in the same population of cells i.e. all Ca^{2+} release experiments were carried out against a background of comparable ER Ca^{2+} load status. Data were acquired from regions of interest (ROIs) representing global Ca^{2+} environments, typically of approximately 50 μm^2 in area (> 200 pixels). These were collected and analysed using Leica confocal software. Further analysis was carried out using Microsoft Excel, GraphPad Prism and Origin 7 software. Statistical analysis was performed using an unpaired Student's T-test and one-way ANOVA.

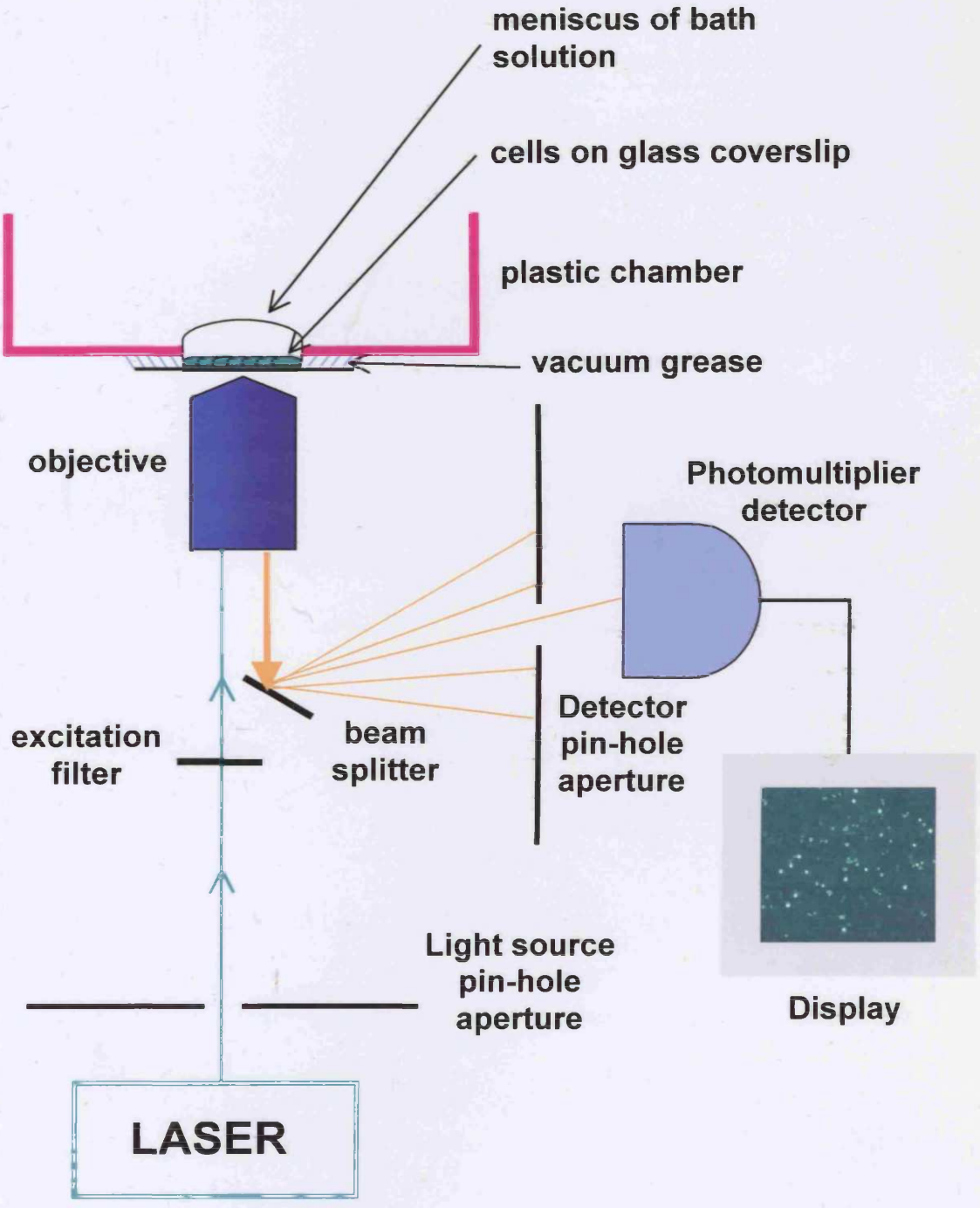

Figure 2.5. Schematic showing the experimental set-up for intracellular Ca^{2+} imaging. Coverslips were sealed with vacuum grease to the underside of a specially made chamber so that the cells could be immersed in a set volume of KRH and fluo-3 loaded cells were imaged by confocal microscopy, which captures emitted light from one focal plane at a time allowing 'optical sectioning'. This is achieved by a spatial filter in the form of a pin-hole or slit aperture that blocks emitted light from out-of-focus sections.

Chapter 3

Development of a recombinant expression system for functional characterisation of RyR2 mutants

3.1. Introduction

The mechanisms which underlie mutant RyR2 dysfunction in ARVD2 are currently unknown, and it is unclear whether the functional effects of these mutations are the same as those which result in CPVT (see section 1.5.2.2.). The ARVD2 mutants have not yet been characterised on a molecular level, and consequently there is a need to evaluate their functionality in appropriate experimental systems.
The use of recombinant expression systems has been central to the structural and functional characterisation of the RyR, especially in assigning specific functions to discrete domains of the polypeptide. Cloning of the cDNA sequences encoding the three RyR isoforms (Otsu et al., 1990; Nakai et al., 1990; Takeshima et al, 1989, 1993; Tunwell et al., 1996; Zorzato et al., 1990), enabled their manipulation by various molecular biological techniques in order to investigate specific aspects of protein characterisation in various cellular contexts. However, the vast size and complexity of RyR has somewhat hindered this process with regards to recombinant plasmid production and the generation of sufficient functional protein expression levels in mammalian cell lines, without the promotion of cellular toxicity (George et al., 2005). This chapter will describe the generation of ARVD2 mutants of RyR2, the optimisation of their expression as functional Ca^{2+} release channels in a non-excitable cell line, and an assessment of their expression levels and intracellular targeting.

3.1.1. The use of RyR deficient cell models as expression systems

Recombinant expression of RyR2 is problematic, and none of the available cell systems used for this purpose to date are optimal. Primary myocytes retain the native contractile phenotype and of course have the full complement of cardio-specific regulatory proteins, making them a highly suitable model for recombinant RyR characterisation. However, transfer of cDNA into these cells is notoriously difficult, and unsatisfactory levels of desired protein expression has been a problem (George et al., 2005; Censier et al., 1998). The development of immortalized cardiomyocytes (Claycomb et al., 1998) and myocytes derived from transgenic animals (Nakai et al., 1996, 1997; Takeshima et al., 1995) has overcome this problem. A particularly attractive expression system for recombinant RyR1 and RyR3 is that of the dyspedic skeletal myotube (1B5 – Moore et al., 1998). These cells are deficient in all three RyR isoforms, yet contain the full set of accessory proteins necessary for appropriate RyR regulation. Although the functionality of

RyR1 and RyR3 has been investigated in this system, characterisation of RyR2, which differs in its mode of regulation (Du et al., 1998; Nakai et al., 1997), may not be achievable in 1B5 cells. Unfortunately, there is not a similar dyspedic cell line that has been generated from a transgenic cardiomyocyte lineage. This means that the available cardiomyocyte cell lines contain endogenous RyR2 - which introduces additional complexity into the investigation of recombinant protein function due to the tetrameric nature of the channel. In other words, it is possible that the introduced recombinant RyR2 monomers will form heterotetramers of various stoichiometry with the endogenous proteins, an event which could complicate the interpretation of functional data.

The use of RyR-deficient cells permits functional characterisation of recombinant RyR2 channels, separated from these difficult aspects, while at the same time providing a physiologically relevant background for expression. It is for this reason that they are widely used in RyR2 studies and have provided valuable insights into the channel's domain functionality (see Figure 1.16., Chapter 1).

Although a disadvantage of RyR-null cell lines is the absence of cardiac-specific Ca^{2+} handling proteins that are proposed to regulate RyR function *in vivo*, valuable information regarding the functional characteristics of recombinant RyR2 has been generated from the study of purified channels, separated from their cellular environment. Indeed, the *in vitro* characterisation of channels derived from transfected null cells draws close parallels with those purified from cardiac tissue (Du et al., 1998; Bhat et al., 1999; Li & Chen, 2001; Xu & Meissner, 1998). However, this may be because the cardiac specific regulatory proteins bound to the RyR2 in cardiac tissue are dissociated during the purification strategies, or possibly because the functionality of the co-purified proteins is not retained outside of their native cellular environment. Alternatively, this may suggest the RyR2 tetramer alone undergoes some form of intrinsic regulation, which to some extent is not dependent on the still undefined macromolecular complex of cardiac accessory proteins.

Null cell models which have frequently been used in the structural and functional characterisation of RyR because of their ease of culture and transfection include Chinese Hamster Ovary (CHO, George et al., 2003b&c, 2004; Bhat et al., 1997a&c, 1999; Imagawa et al., 1992), African green monkey kidney (COS, Treves et al., 1994, 2002; Chen et al., 1993) and Human Embryonic Kidney cells (HEK, Du et al., 1998, 2001a, b & c; Tong et al., 1997, 1999b; Lynch et al., 1999; Brini et al., 2005; Rossi et al., 2002). However, the latter appears to be the RyR-deficient cell model most widely used in the characterisation of RyR2, in particular in the functional investigation of arrhythmia-linked RyR2 mutants (Wehrens et al., 2003; Lehnart et al.,

2004; Jiang et al., 2002b, 2004). Thus, HEK cells were used in this study in order that the results obtained may be compared directly with those from other groups characterising arrhythmia-linked RyR2 mutants in the same system. In addition, a human cell line was deemed a more appropriate system, for characterisation of the human RyR2 isoform.

However, there has been some controversy in the past regarding their RyR-null status, since Querfurth et al (1998) reported low level expression of an unspecified isoform of RyR in these cells, which was detectable only by highly sensitive immunoprecipitation of radiolabelled cells or by Western blotting of immunoprecipitates. More recently, others have reported endogenous expression of RyR1 in HEK293 cells, though levels of the protein were found to be extremely low and could only be detected at very low passage (<5) numbers (Luo et al., 2005), which were not used in this study. Nonetheless, these findings have been refuted by many groups who have been unable to detect any RyR protein in HEK cells by both Western blotting and Ca^{2+} imaging techniques (Tong et al., 1999b; Du et al., 1998, 2001b; Jiang et al., 2002b). As a result, HEK293 cells are generally accepted to be devoid of any functional RyR and have been routinely used as null cells in recombinant RyR studies.

3.1.2. Use of the eGFP fusion protein to identify recombinantly expressed RyR2 proteins

One of the main drawbacks of the use of heterologous expression systems for the study of RyR is that high efficiency transient transfection of this high molecular weight construct can be problematic. As such, the identification of cells expressing the recombinant protein for functional characterisation is of utmost importance. To this end, many protein expression tags have been developed, including the green fluorescent protein (isolated from *Aequoria Victoria*) which has been widely used as a reporter of gene expression (Prasher et al., 1992; Cubitt et al., 1995; Heim et al., 1995). The advantage of using GFP lies in the fact that additional co-factors, substrates or additional gene products are not required for its fluorescence. Moreover, GFP fluorescence is stable, species-independent, and can be monitored non-invasively in living cells using fluorescence microscopy or flow cytometry, while still being detectable by an anti-GFP antibody (Chalfie et al., 1994; Inouye &Tsuji, 1994).

Wild-type (WT) *Aequoria* GFP owes its visible absorbance (at 395 nm, with an emission maximum at 508 nm) and fluorescence to a p-

hydroxybenzylideneimidazolinone chromophore (Prasher et al., 1992) formed by cyclization of Ser65, Tyr66 and Gly67 of the 238 amino acid structure, followed by 1,2-dehydrogenation of the tyrosine. However, WT GFP has several undesirable properties including low fluorescent intensity, a lag in the development of fluorescence after protein synthesis and poor expression in mammalian cell types (Heim et al., 1995). Taking this into consideration, a variant of GFP (enhanced GFP or eGFP (CLONTECH)) was developed, which contains chromophore mutations ($S^{65}T$ and $F^{64}L$) which make the protein 35 times brighter than WT GFP (Zhang et al., 1996; Cormack et al., 1996). These amino acid replacements also result in a change in the spectral properties of the protein whereby the 395 nm absorption peak is shifted to longer wavelengths (488 nm excitation, 511 nm emission). Added advantages of this variant are that it has improved solubility and more efficient protein folding characteristics, as well as the fact that it has been codon-optimised by using the favoured codons of highly-expressed human proteins in place of the corresponding jellyfish codons for enhanced expression in mammalian cells (Zhang et al., 1996; Cormack et al., 1996). This makes eGFP an attractive means for direct measurement of transfection efficiency and protein expression levels in transient transfection assays.

Both the amino and carboxyl terminal end of eGFP have been successfully fused to a wide range of cytosolic and membrane bound proteins. However, it has been known that the use of these tags may not be completely benign on RyR function. Amino (N-) or carboxy- (C-) terminal fusion of RyR1 with eGFP profoundly altered the channel sensitivity to activation using RyR agonists, caffeine and 4-cmc, depending on the site of eGFP fusion (Treves et al., 2002). Despite this, the positive aspects of this epitope-tagging approach were emphasised after the demonstration that RyR1 tagged at its N-terminus with eGFP retained targeting to the SR and fully supported skeletal type EC coupling (Lorenzon et al., 2001) and that eGFP-RyR1 formed functional channels after its expression in RyR-deficient cells (Bhat et al., 1997c). However, the reason for these discrepant results with regard to the effect of GFP-tagging on RyR1 function is not known. Nevertheless, the conformational differences that exist between RyR isoforms (Serysheva et al., 1995; Sharma et al., 1998), and the disparity between RyR1 and RyR2 activation during EC coupling (physical coupling vs CICR) strongly indicate the aforementioned negative effects with RyR1 do not extrapolate to the other RyR isoforms (George et al., 2005). In agreement with this, N-terminal fusion of eGFP to RyR2 (George et al., 2003a) or glutathione S-transferase to RyR3 (Liu et al., 2001) did not discernibly affect the functionality of cellular localization of the recombinant channels. In addition, mapping of the N-

terminus on the three-dimensional structure of RyR2 reveals it to be in a relatively open and accessible location (see Figure 1.8.), which appears not to be constrained by folding of the protein. Nevertheless, demonstration that the extreme C-terminus is involved in channel oligomerization, and is highly sensitive to modification (Gao et al., 1997; Stewart et al., 2003), indicates that fusion of fluorescent tags to this end of the molecule would have a catastrophic effect on protein function.

3.2. Methods

3.2.1. Cloning and mutagenesis strategy

The mammalian expression vector containing the full length hRyR2 which was tagged at the N-terminus with eGFP (pcDNA3-eGFP-hRyR2) was obtained from Dr. Chris George (see Chapter 2, section 2.1.5.1.). The method of SDM employed in this study is limited to DNA sequences of ~6-8kb i.e. lengths of DNA which can be reliably amplified by thermal cycling using this polymerase. This meant that suitable mutagenesis cassettes of the RyR2 sequence had to be created as follows:
A *SpeI/SanDI* (-15bp to 5542bp) fragment was excised from hRyR2 and transferred to the intermediate vector pSL1180, (which had previously been modified to contain the *SanDI* restriction site -see Chapter 2, Figure 2.2.) to generate the $R^{176}Q$ and $L^{433}P$ mutations. Appropriate codons were changed (for $R^{176}Q$; CGA to CAA, for $L^{433}P$; CTT to CCT) using the mutagenesis protocol as detailed in section 2.2.1.10. using the primers shown in Appendix I. A similar strategy was used to construct $N^{2386}I$ (AAC to ATC) and $T^{2504}M$ (ACG to ATG) mutants using a *SanDI/KpnI* (5542bp to 7678bp) cassette from hRyR2 (see Figure 3.1.). Full length mutants were generated by the ligation of mutant cassettes into pcDNA3-eGFP-hRyR2 using *SpeI/SanDI* ($R^{176}Q$, $L^{433}P$) or *SanDI/KpnI* ($N^{2386}I$, $T^{2504}M$) strategies. The double mutant $R^{176}Q/T^{2504}M$ was constructed by ligation of the mutant $R^{176}Q$ fragment into the full length $T^{2504}M$ mutant. All constructs were verified at each cloning stage by restriction mapping, and automated sequencing was used to verify point mutations and 5' and 3' insertion boundaries.

3.2.2. Lipid mediated transfection of HEK 293 cells

HEK cells were maintained as described in section 2.2.4.1., and seeded (~1.5 x 10^6) at ~80-90 % confluency for transfection. This method of transfection uses cationic lipids to deliver DNA into the cells and was carried out according to the manufacturer's instructions (Invitrogen). Briefly, the plasmid DNA (4 μg, A_{260}/A_{280} >1.9) was mixed with minimal (i.e. not supplemented with foetal calf serum, since this decreases the efficiency of transfection) DMEM to a total volume of 200 μl. Lipofectamine2000 reagent (4 μl) was also mixed with minimal DMEM and incubated for 5 minutes at room temperature. DNA and lipid complexes were then combined before further incubation at room temperature for no more than 15 minutes. Cells

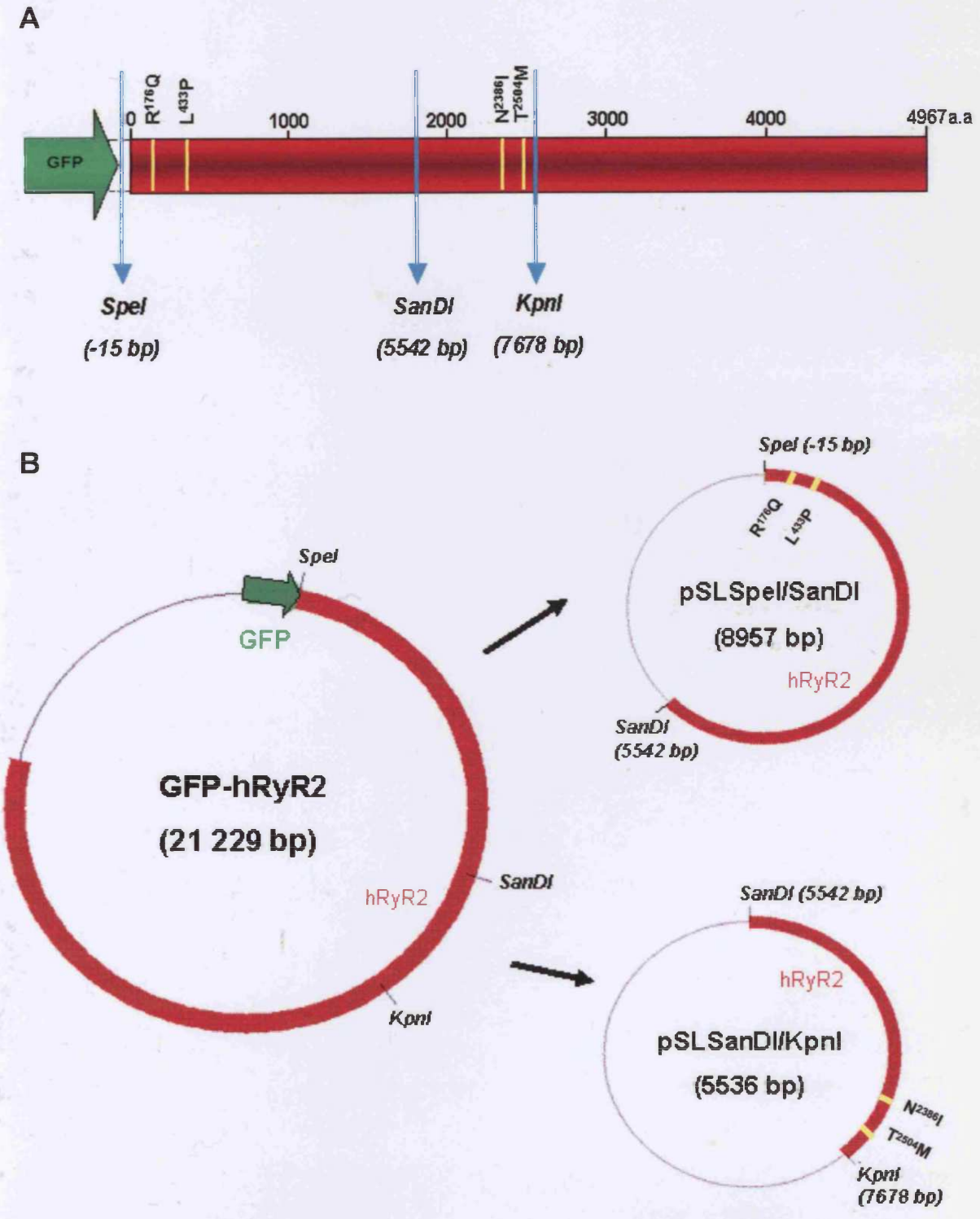

Figure 3.1. Cloning strategy. A) Schematic detailing the location of the ARVD2-linked mutations in human RyR2 relative to the restriction sites used to generate the mutagenesis cassettes. B) The plasmid containing the full-length sequence of human RyR2 was digested with SpeI/SanDI or SanDI/KpnI to generate mutagenesis cassettes suitable for SDM. Mutated cassettes were then re-ligated back into similarly digested plasmids. Restriction site co-ordinates seen here refer to the number of base pairs from the beginning of the clone and not from the start codon.

were washed with 0.9 % w/v saline solution before addition of the transfection complexes in 2 ml of minimal DMEM and incubation at 37°C, and 5% CO_2 for 16-18 hours. Transfection complexes were removed and cells were then incubated at 37°C, 5% CO_2 in complete DMEM for a further 6 hours before harvesting by trypsinisation.

3.2.3. Optimisation of GFP-hRyR2 expression using fluorescence activated cell sorting

Following lipid-mediated transfection, HEK cells underwent selection for the GFP-RyR2 plasmid using G418 (900 µg/ml, Rossi et al., 2002). Cells were cultured for 4 weeks before being collected by trypsinisation and adjusted to a density of 1.5 x 10^6 cells/ml in phosphate buffered saline (pH 7.4). Cell suspensions were subjected to fluorescence activated cell sorting (FACS, MoFlo, Dako Cytomation) using 488 nm Argon laser excitation and 530 ± 40 nm emission bandpass filter with sorting rates of <10, 000 cells/second to select for eGFP-RyR2 expression. Positively sorted cells characterised by > 10-fold fluorescence relative to non-expressing cells were selected and cultured in the presence of G418 to maintain selection of GFP-RyR2 expressing cells. Cells were re-sorted at ~4 week intervals to assess GFP-hRyR2 expression.

3.2.4. Determination of cellular proliferation

The proliferative capacity of sub-confluent untransfected HEK cells and FACS sorted GFP-hRyR2 HEK cells was determined on the same cell populations at 24 hour intervals for 96 hours. Cells were incubated with medium containing AlamarBlue (10% (v/v)) for 5 h prior to fluorometric analysis of aspirated medium (LS50B, PerkinElmer Life Sciences). Cellular metabolic activity reduces AlamarBlue from a nonfluorescent (blue) form into a fluorescent (red) form (Ex_{max}, 560 nm; Em_{max}, 590 nm). The oxidized and reduced forms of AlamarBlue are freely cell permeable and do not contribute to cellular toxicity (Matute-Bello et al., 1999). The seeding density of cells was adjusted to ensure that the cells were sub-confluent throughout these procedures (starting at 5 x 10^4 cells per well of a six well plate). The data obtained using alamarBlue cell viability assays was corroborated by haemocytometric estimation of cell number carried out in parallel experiments.

3.3. Results

3.3.1. Generation of ARVD2-linked RyR2 mutants

GFP tagged ARVD2–linked mutants ($L^{433}P$, $N^{2386}I$, $R^{176}Q$, $T^{2504}M$ and the 'double mutant' $R^{176}Q/T^{2504}M$) of hRyR2 were successfully generated by the cloning and mutagenesis strategy outlined above. Restriction mapping was used to confirm correct re-ligation of mutated fragments into full length pcDNA3-GFP-hRyR2, and ensure that the plasmid had not undergone any deletions or spontaneous recombination with the bacterial DNA. Digest of pcDNA-GFP-hRyR2 with the restriction enzymes shown in Figure 3.2. yields several fragments of different molecular weight which can be identified after agarose gel electrophoresis and act as a 'fingerprint' for the complete recombinant plasmid. This figure also shows restriction maps for the diagnostic digests used to identify pcDNA3-GFP-hRyR2, and the characteristic band patterns observed.
Base pair substitutions which resulted from SDM were verified by automated cycle sequencing (Figure 3.3.). Importantly, this technique also confirmed that no other mutations apart from those intended were introduced into the cDNA sequence.

3.3.2. Fluorescence activated sorting of HEK cells is not a viable strategy for optimal expression of GFP-hRyR2

A FACS–based strategy was used to select populations of cells exhibiting robust expression of eGFP-tagged RyR2 (see Figure 3.4.). Only cells which exhibited fluorescence that was > 10 fold that of untransfected HEKs were collected, and subsequently cultured in selective medium. FACS analysis of this population of cells after a period in culture (see table in Figure 3.4.B and Figure 3.5.A) revealed negligible retention of the GFP phenotype, with only 0.07 % of cells exhibiting fluorescence > 10^2. It was suspected either that a small number of untransfected HEK cells had been sorted with the GFP positive cells, and that these had 'out-grown' those expressing eGFP-hRyR2, due to their increased rate of proliferation (Figure 3.5.B), or that downregulation of eGFP-RyR2 protein expression had occurred. Thus, the population collected from this secondary sort were divided into 'high' (> 10^3 < 10^4) and 'low' (> 10^2 < 10^3) fluorescence groups, to investigate whether these different expression levels had any effect on the loss of phenotype observed. It was found that the 'high' sort population cells exhibited marked cell damage and did not survive in culture. However, the 'low' sort cells were viable, but

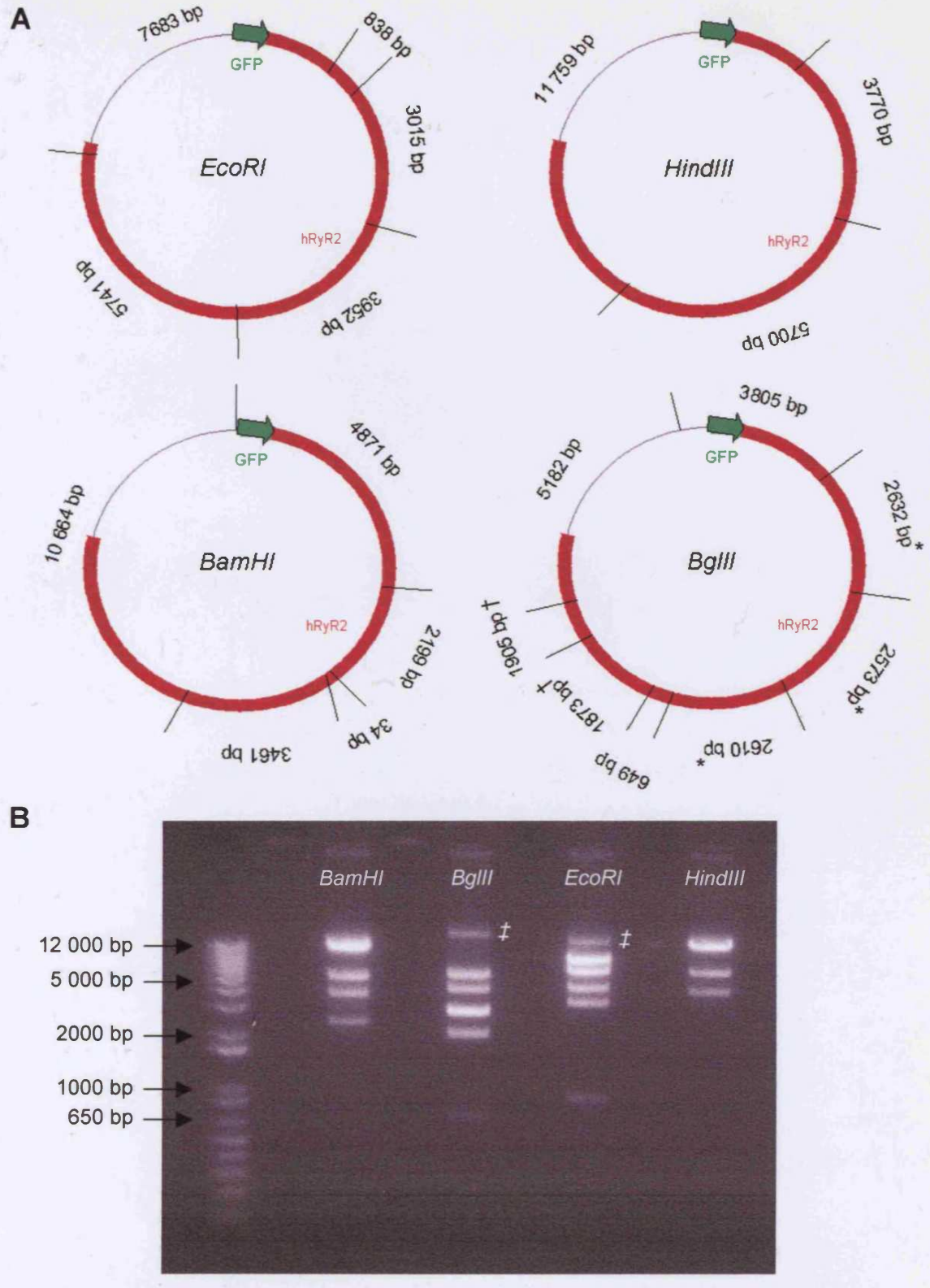

Figure 3.2. Identification of pcDNA3-GFP-hRyR2 by restriction mapping. A) Restriction maps of pcDNA3-GFP-hRyR2 digested with the enzymes shown, fragment sizes are displayed between restriction sites (represented by a line) * and † These fragments cannot be resolved and run as one band. B) Characteristic restriction patterns obtained when GFP-hRyR2 was cut with the enzymes shown above. It should be noted that the introduced mutations did not alter any restriction sites. ‡ These bands represent partially digested cDNA products.

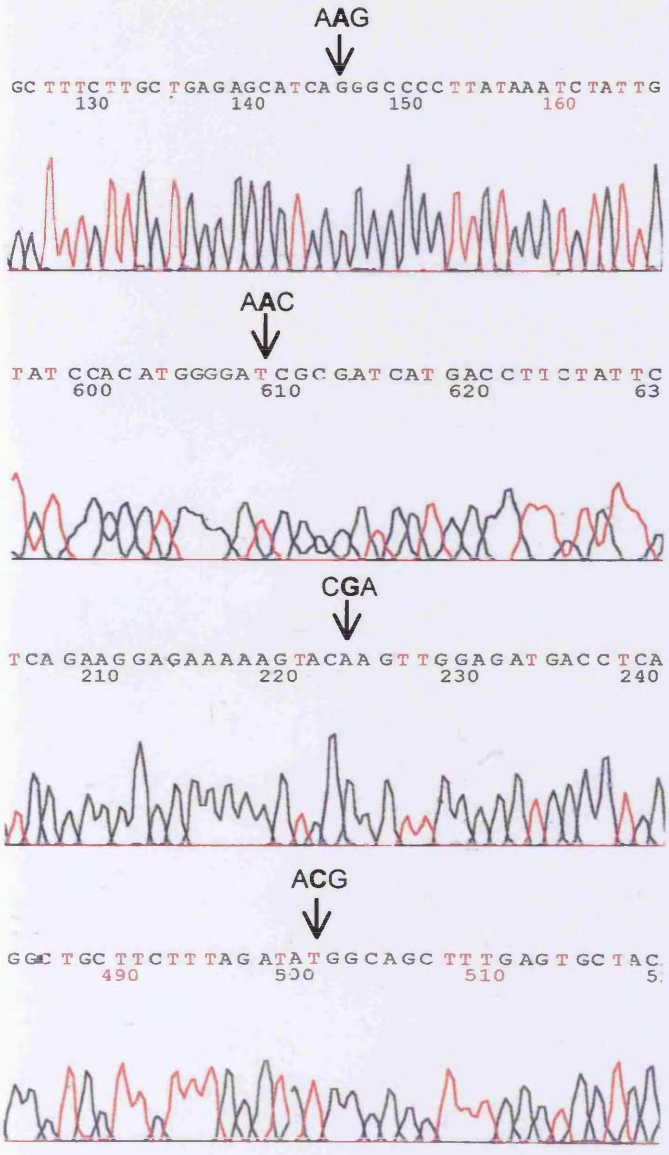

$L^{433}P$

Codon: GGC CNT GAT
Base change: T → C*
Amino acid: G [L → P] D

$N^{2386}I$

Codon: GGG ANC GCG
Base change: A → T
Amino acid: G [N → I] A

$R^{176}Q$

Codon: GTA CNA GTT
Base change: G → A
Amino acid: V [R → Q] V

$T^{2504}M$

Codon: GAT ANG GCA
Base change: C → T
Amino acid: D [T → M] A

Figure 3.3. Verification of mutations by sequencing. Electropherograms displaying point mutations created in the *hRyR2* sequence corresponding to those implicated in ARVD2. The resultant codon and amino acid changes are shown in the right-hand panel. *Base pair change of T→C was achieved, though is seen as A→G here because the sequencing primers used annealed to the complementary DNA strand i.e. sequencing was from the 3'→ 5' end. It must be noted that no other mutations, apart from those seen above were introduced into the sequence.

A

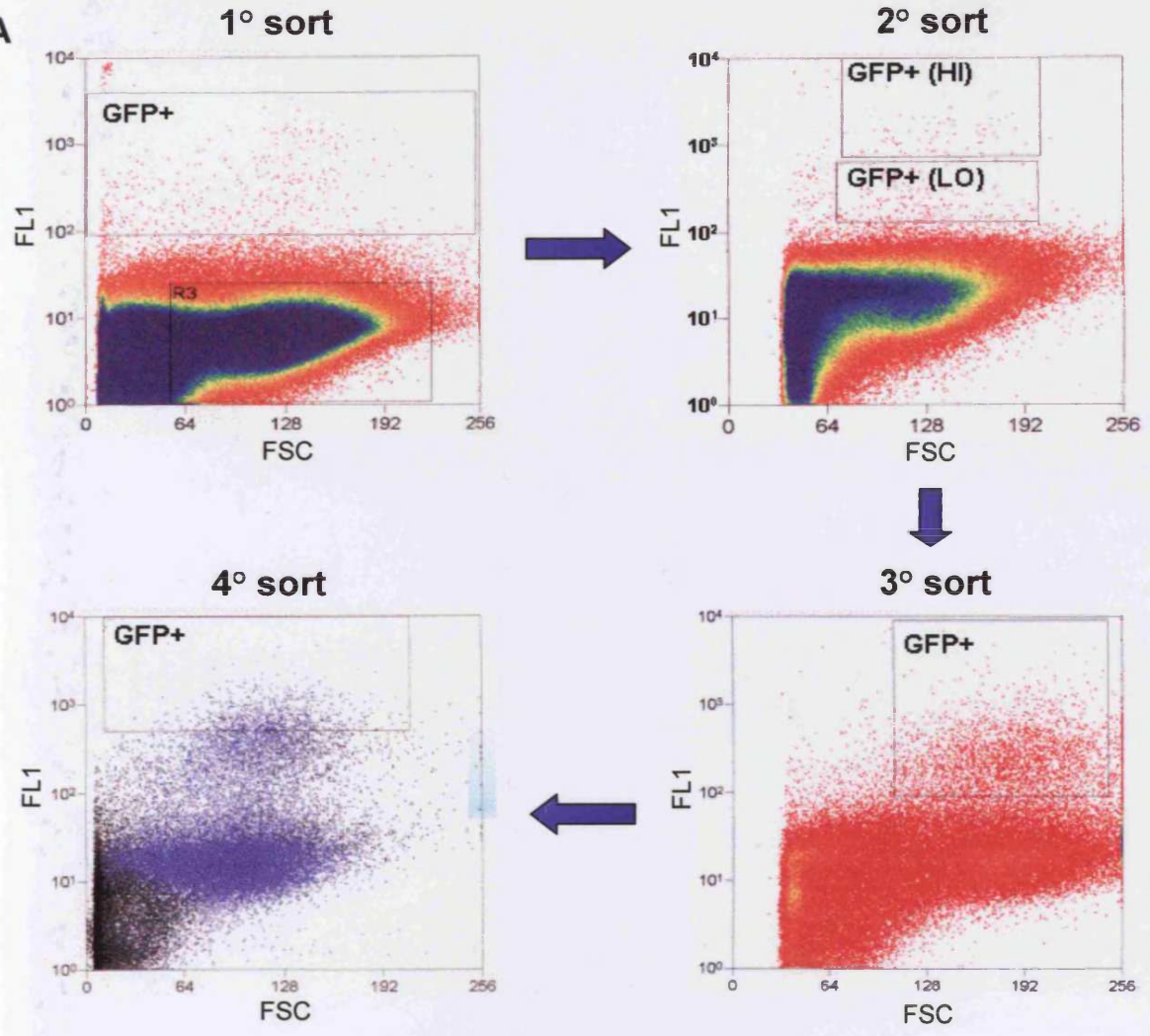

B

Sort	Time (days)*	Cell number	Number of positives	GFP+ (%)
1°	31	2.294×10^6	448	0.02
2°	44	485,965	LO: 243	0.05
			**HI: 79	0.02
3°	71	65,568	2966	4.52
4°	86	25,600	310	1.21

Figure 3.4. FACS analysis of GFP-hRyR2 expression. A) Non-clonal G418-resistant HEK cells stably expressing full-length GFP-hRyR2 were selected on the basis of GFP fluorescence (FL1, high angle scatter) intensity as shown. FSC denotes the low angle scatter and represents cell size. In all traces dots represent 'events'/cells and colour indicates relative cell number where red < orange < yellow < green <blue, except for the 4° sort where cell densities were not determined. Cells which exhibited > 10^2 fluorescence were collected (GFP+ boxes). B) Culture of FACS sorted cells resulted in loss of the GFP-positive phenotype. * This denotes the time in culture since transfection. ** Following the 2° sort, the 'HI' cells (i.e. cells expressing approximately >20 fold GFP-tagged hRyR2 relative to background (non-expressing) cells) exhibited pronounced cell damage and did not survive culture.

A

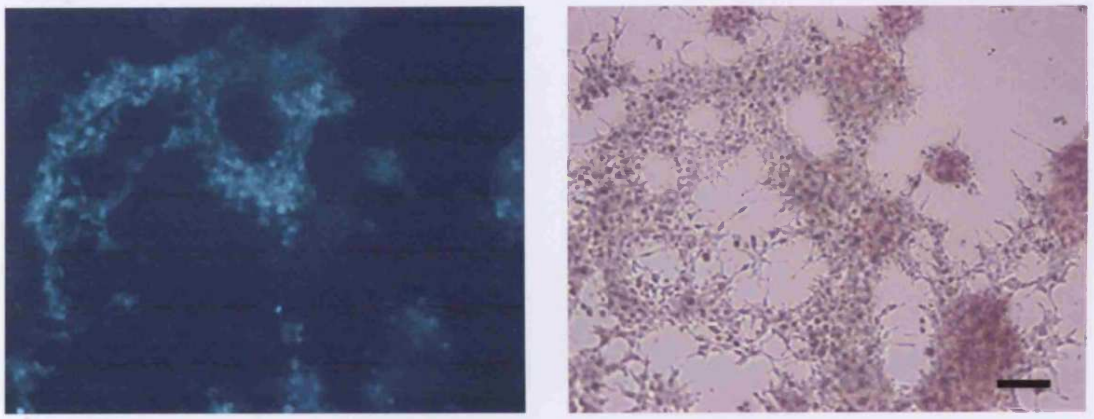

B

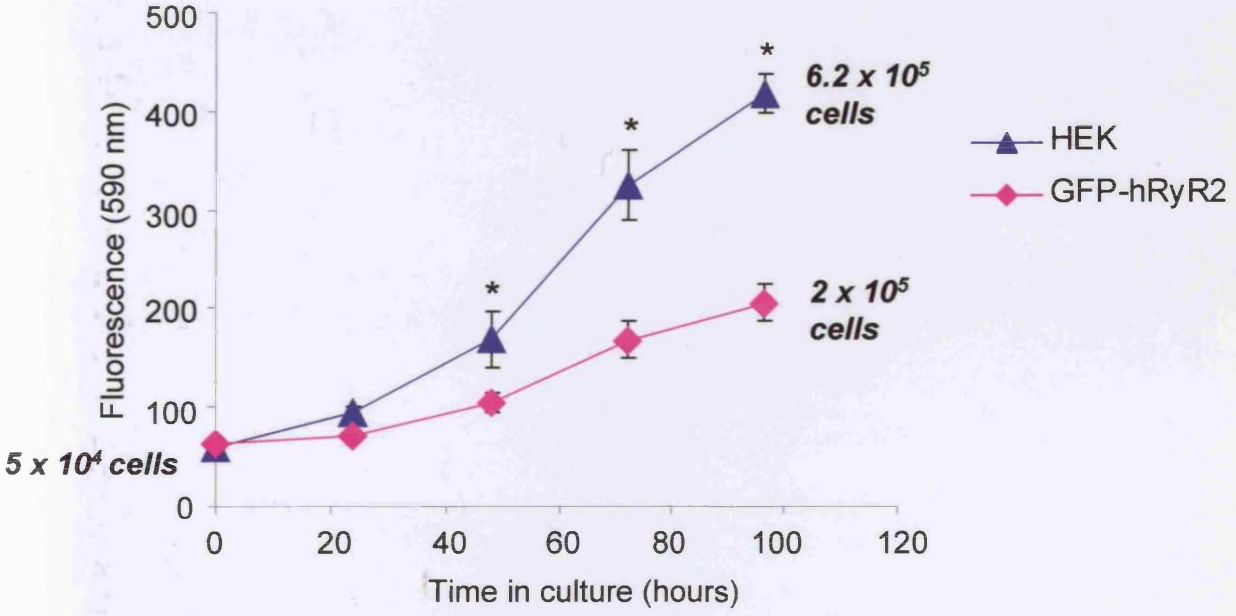

Figure 3.5. Deselection of GFP-hRyR2 expression occurs in culture and is associated with increased proliferation. A) An image of FACS sorted HEK cells taken after 4 days in culture (with selective antibiotic G418 (900 µg/ml)), showing that ~ 30 % of the cells have lost their GFP-positive phenotype. B) Cells expressing GFP-hRyR2 have a decreased rate of proliferation compared to untransfected HEK cells. Chemical reduction of the alamarBlue reagent resulting from cell growth causes an increase in its fluorescence at 590 nm. These results were confirmed by estimation of the cell number using a haemocytometer (labelled on the graph). Data are represented as mean ± S.E.M *p< 0.05.

still exhibited marked deselection after 27 days in culture with a ~95.5 % decrease in the percentage of GFP-positive cells (see Figure 3.4.B). Indeed, the levels of eGFP-hRyR2 protein expression were so low that they could not be demonstrated by immunoblotting. The proportion of GFP-positive cells after culture of those from the tertiary sort was further decreased, suggesting that due to the toxic effects of constitutive expression of this protein (George et al., 2003b), the levels of eGFP-hRyR2 stable expression required for this study could not be achieved by this method.

3.3.3. Transient expression of ARVD2-linked RyR2 mutants

Efficient transfection of HEK-293 cells was achieved using a calcium phosphate ($CaPO_4$) method (optimised for transfer of recombinant RyR2, see section 2.2.4.1.) and plasmid DNA of only the highest purity (A_{260}/A_{280}> 1.9). Figures 3.6.B and 3.7. demonstrate a transfection efficiency of ~20-30 % for WT and mutant constructs (as estimated by comparing the number of cells exhibiting eGFP fluorescence with the total number of cells present) which was routinely achieved using this technique, and was superior to lipofectamine-mediated transfer (see Figure 3.6.A). In addition, expression levels following $CaPO_4$ transfection were high enough to ensure easy detection of this toxic protein, without causing excessive cell death (see Figure 3.6.B). Importantly, the similar transfection efficiencies achieved also resulted in equivalent expression levels of WT and mutant RyR2 recombinant proteins as determined by densitometric analysis of immunoblots such as the one seen in Figure 3.8. Direct visualisation of the recombinant proteins using eGFP fluorescence (Figure 3.9., top panel), or following immunodetection using a high-titre anti-hRyR2 antibody (pAb1093) and Alexa^{546}-conjugated secondary antibody (middle panel) confirmed their correct targeting to the ER, as demonstrated by the characteristic lattice-like morphology of the staining. These images could be visualised simultaneously, since eGFP and Alexa^{546} are spectrally distinct (see section 2.2.4.2.), however it can be seen that the eGFP fluorescence is more intense than that of the Alexa^{546} antibody, indicating that it is the superior fluorophore. Pixel overlap analysis of at least six confocal images of these cells indicated the near total co-incidence between endogenous eGFP fluorescence and immunolocalisation via anti-RyR2 antibody labelling of recombinant protein (lower panel). This corroborated the immunoblotting analysis and strongly indicated the *in situ* expression of full-length recombinant WT and mutant RyR2. The size and morphology of cells expressing RyR2 mutants were indistinguishable from those expressing WT RyR2, which is

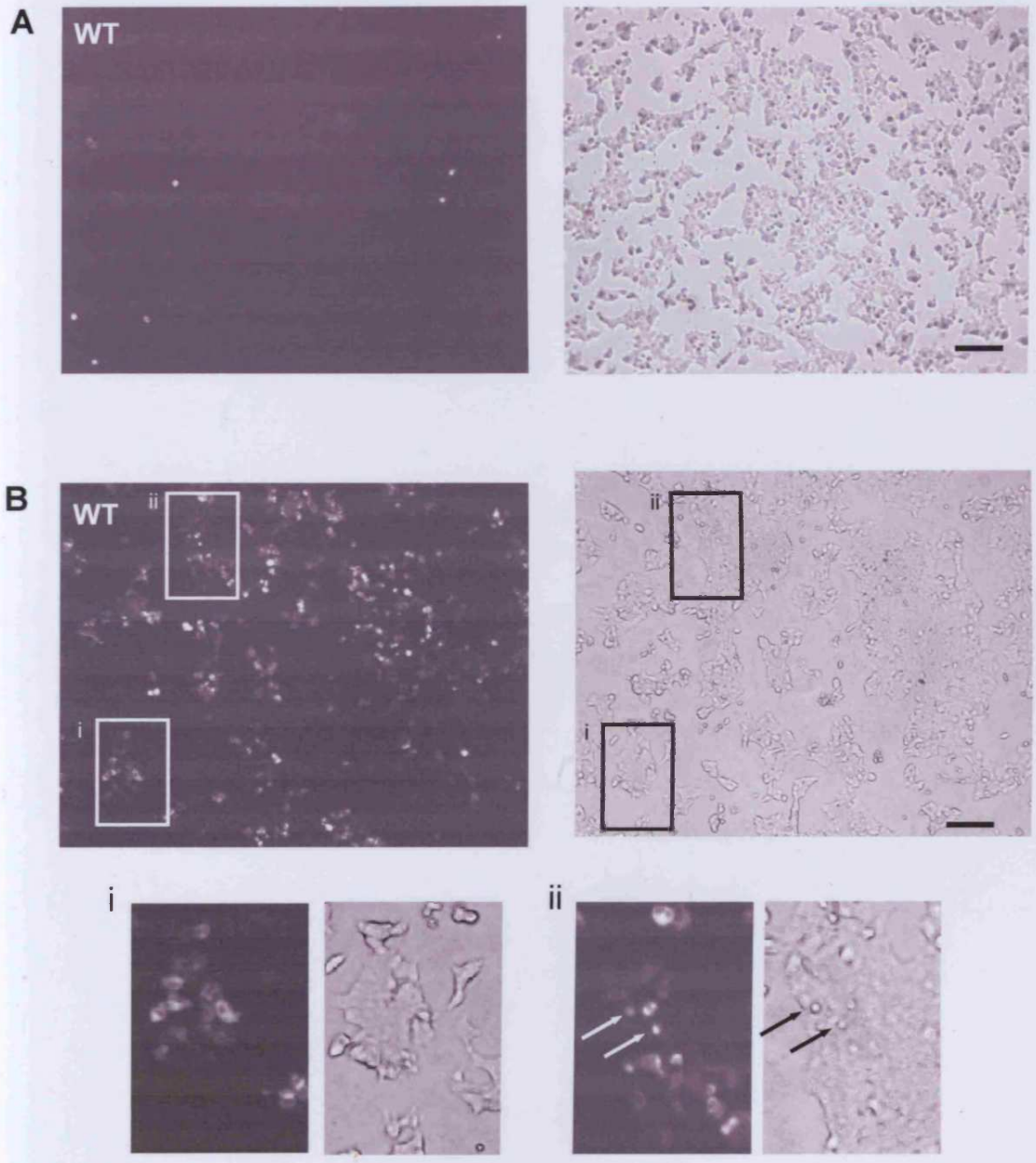

Figure 3.6. Expression of GFP-hRyR2 in HEK-293 cells following lipofectamine or calcium phosphate mediated transfection. The endogenous fluorescence of eGFP-tagged hRyR2 (left panel) was used to determine the efficiency of plasmid transfection by comparison with the total number of cells seen in the phase image (right panel). Transfection efficiencies of ~7-8% were achieved using lipofectamine (A), whereas efficiencies of 20-30% were routinely achieved using $CaPO_4$ (B) . Morphological assessment of transfected cells revealed that most were viable (as in region i), however high levels of RyR2 expression in some cells appeared to be cytotoxic (see region ii, non-viable cells are arrowed). Bar represents 150 µm.

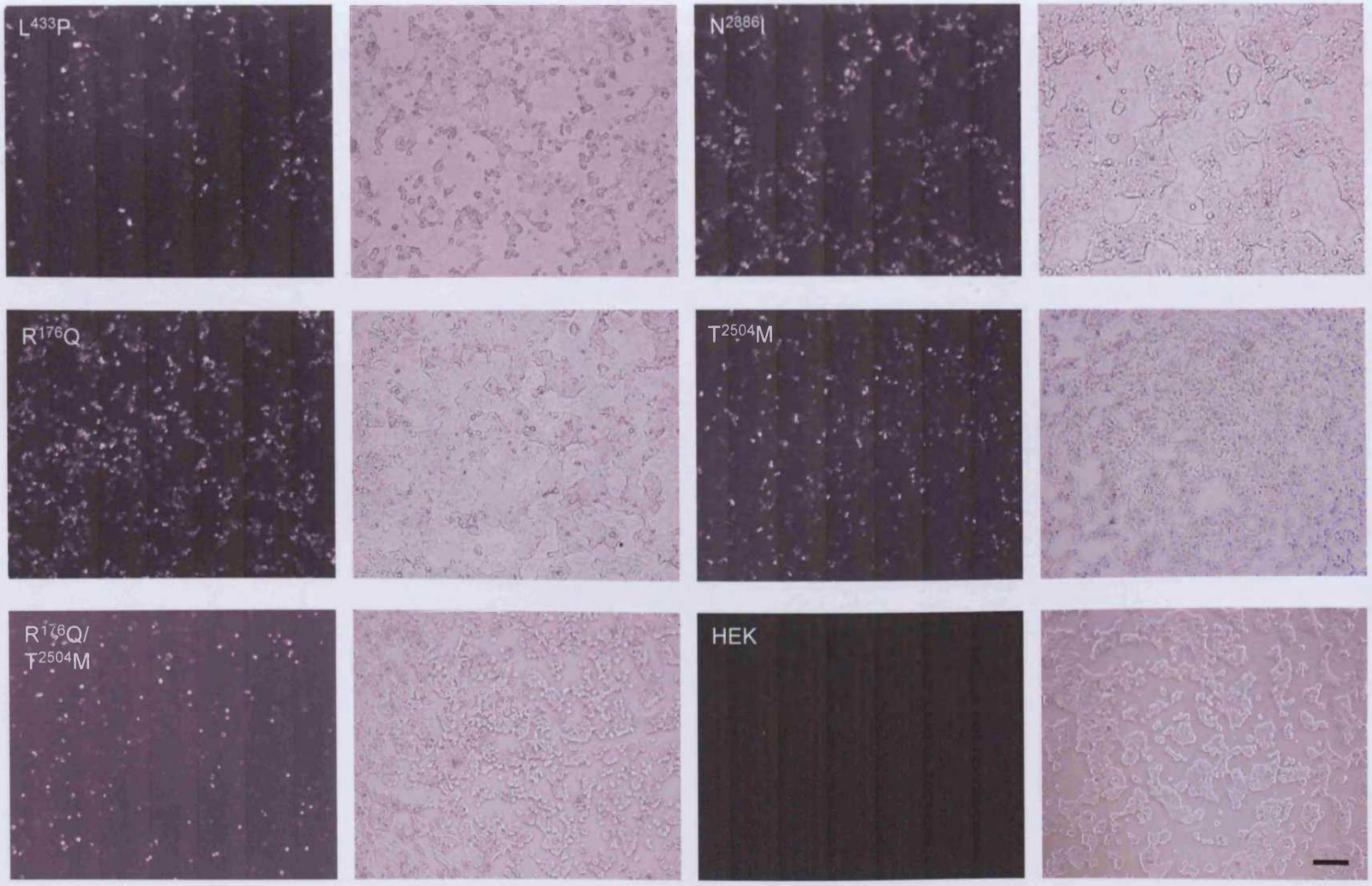

Figure 3.7. Expression of mutant GFP-hRyR2 in HEK cells following calcium phosphate mediated transfection. Similar transfection efficiencies (20-30 %) were achieved with mutant and WT GFP-hRyR2 constructs (see Figure 3.5.B). Transfection efficiencies were calculated as detailed in Figure 3.5. using fluorescence (left panels) and phase (right panels) images. Untransfected cells (HEK) did not exhibit intracellular GFP fluorescence. Bar represents 150 μm.

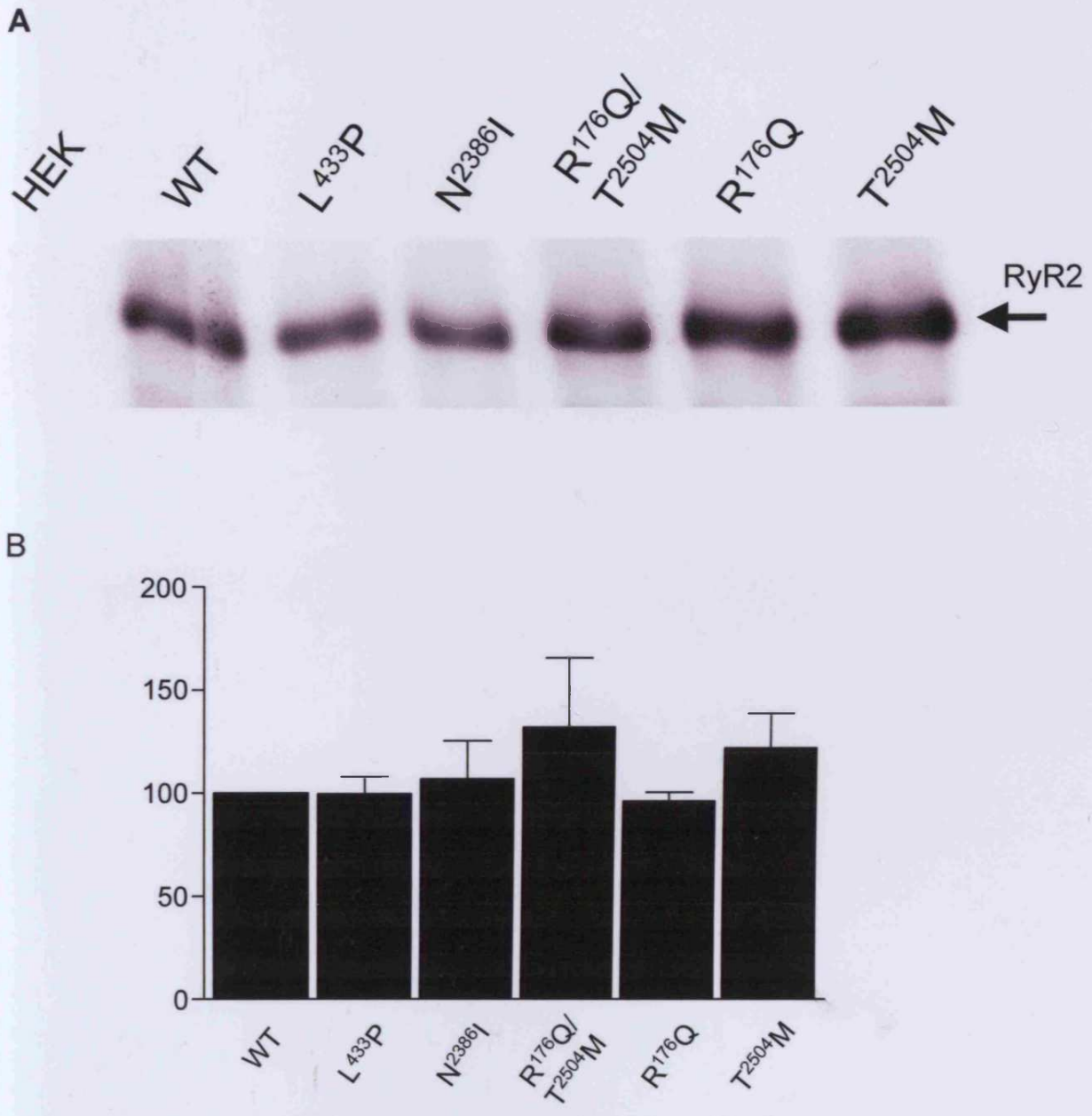

Figure 3.8. WT and mutant recombinant RyR2 proteins demonstrate equivalent expression levels. A) Post-nuclear supernatants (500 µg) from HEK cells transiently expressing WT and mutant RyR2 were immunoblotted using a mouse monoclonal anti-GFP antibody as described in section 2.2.3. A single band was detected for each construct above the 250kDa marker. B) Densitometric analysis of immunoblots was carried out on three separate experiments, results are expressed as a percentage of the signal for WT GFP-hRyR2 ± S.E.M.

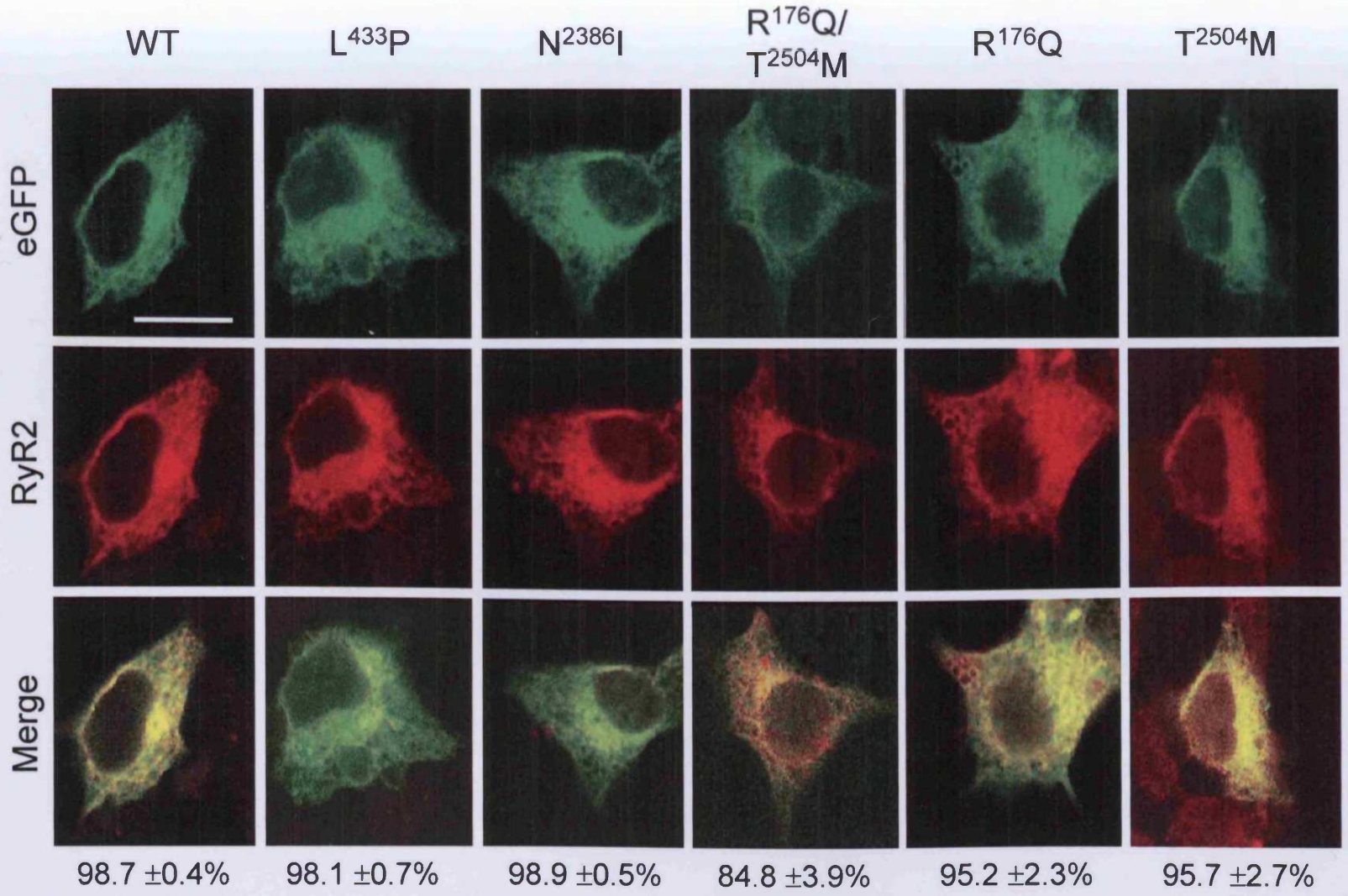

Figure 3.9. The intraceulluar localisation of recombinant WT and mutant RyR2. This was determined using endogenous eGFP fluorescence (top panels) or via immunofluorescent detection of recombinant protein using anti-RyR2 antisera (pAb1093) and an Alexa^{546} secondary antibody (middle panels). The direct overlay of eGFP- and immunoflurescence images obtained at high resolution was used to determine the extent of co-localisation of eGFP and antibody signals (calculated for each construct and expressed as the 'percentage overlap' (mean ± S.E.M.) underneath the appropriate image) as described previously (George et al., 2003) (lower panel; merge). Data (mean ± S.E.M.) were obtained from the analysis of at least 6 images in each instance. Bar represents 10 μm.

entirely consistent with previous studies showing that the resting cell phenotype is not perturbed following expression of SCD-linked RyR2 mutations (Wehrens et al., 2003; George et al., 2003a).

3.4. Discussion

3.4.1. Defined conditions are required for propagation of the eGFP-hRyR2 plasmid

eGFP tagged ARVD2–linked mutants ($L^{433}P$, $N^{2386}I$, $R^{176}Q$, $T^{2504}M$ and the 'double mutant' $R^{176}Q/T^{2504}M$) of hRyR2 were successfully constructed. However, propagation and isolation of these large, fragile plasmids was only possible by following the stringent procedures detailed in sections 2.2.1.3. and 2.2.1.5.-2.2.1.8., which were essential in order to avoid spontaneous rearrangements/deletion or degradation of the DNA, which can often occur under non-optimized conditions (George et al., 2005). These conditions included a low propagative temperature (typically 30°C), short durations in culture (≤18 hours), the use of a specific strain of bacteria adapted for viable transformation with large plasmids and resin-based DNA purification systems that do not shear the isolated plasmid (George et al., 2003c; Bhat et al., 1999). These precise procedures resulted in the production of high quality full-length plasmid DNA (Figure 3.2.B)

3.4.2. High levels of eGFP-hRyR2 could not be achieved through constitutive expression in HEK293 cells

HEK-293 cells were chosen for expression studies because they do not endogenously express RyR2, and consequently the channels formed from the recombinant proteins are homotetrameric, and not a mixture of wild-type/mutant homo- and heterotetramers of unknown stochiometry, which would complicate interpretation of results. In addition, these cells are the only widely used RyR2-deficient cells that are of human origin, indicating that they may be the most suitable null cell system for characterisation of the human protein.
Cellular expression of RyR has always been a challenge in terms of generating full-length recombinant protein and producing functional channels in sufficient quantity. Many techniques have been used for introducing RyR into cells including transfection (either by commercial lipid or calcium phosphate mediated techniques) microinjection, and virally mediated transfer. The latter two techniques are often

used when either lipid or chemical mediated transfection is not possible (i.e. for expression in primary cells) and are not always considered to be the optimal choice for use in cell lines for various reasons, depending on the nature of the study e.g. microinjection cannot practically be used for expression in large populations of cells, viral transfer is not applicable since the RyR2 cDNA is too large to be incorporated, furthermore this method can lead to artefactual results and cytotoxicity due to extreme overexpression. In addition, both techniques are expensive and technically difficult.

Non-clonal stable expression of eGFP-hRyR2 was attempted in this study in the hope of obviating the need for continuous rounds of transient transfection, however downregulation of expression, most likely due to the toxic nature of the protein precluded the use of these cells in this study. In addition, cells which demonstrated these 'tolerated' expression levels exhibited a decreased rate of proliferation, a phenomenon previously observed in RyR2 stable cell lines (George et al., 2003b), whereas very high levels of constitutive expression were cytotoxic. Thus, expression of the full-length functional protein likely causes disruption in intracellular Ca^{2+} handling, resulting in significant changes in the cellular phenotype. It could be argued that development of various clonal stable cell lines, with different eGFP-hRyR2 expression levels may have been beneficial, since one of the clones isolated may have expressed the protein at a level sufficient for study without being high enough to result in cell death. However, this is a time-consuming process and would need to be achieved for all six constructs expressed in this study, making it unfeasible within the time-scale of the project. Nevertheless, stable-expression of RyR using this strategy can also be problematic, possibly resulting in the production of full-length yet non-functional protein. This was apparent in a study by Rossi et al (2002), which demonstrated that there was little correlation between the levels of RyR1 and RyR3 expression in HEK-293 cells and the functionality of the resultant protein as measured by ^{3}[H]-ryanodine binding. Despite this, stable high-level expression of RyR1 and RyR3 have been achieved in null-cell systems with apparently very little deleterious effects on the cell phenotype (Manunta et al., 2000; Takeshima et al., 1989; Bhat et al., 1997c; Penner et al., 1989). However, successful stable expression of RyR2 in null cells has proved to be more difficult, perhaps because this isoform of the Ca^{2+} release channel is more sensitive to activation by ambient Ca^{2+} (Meissner et al. 1997; Chen et al., 1997a; Du et al., 1998, Li & Chen, 2001). Another reason for this could be the lack of endogenous RyR2 specific regulatory proteins: RyR1 and RyR3 are regulated by FKBP12, which is abundantly expressed in numerous tissues and cells (Marks, 1996; Shou et al.,

1998), while RyR2 is regulated by FKBP12.6, which has a more restricted tissue distribution and is not usually present at detectable levels in RyR-deficient cells such as HEKs (George et al., 2003c, Wehrens et al., 2003). Another potential disadvantage of stably expressing RyR2 is that there may be a greater likelihood of altering the expression profiles or activity of other proteins in the cell e.g. profound transcriptional alterations were seen in Chinese Hamster Ovary (CHO) cells overexpressing RyR2 (George et al., 2003b). This is particularly relevant since cardiac pathology is often associated with changes in Ca^{2+} handling proteins that contribute to the disease phenotype (Houser et al., 2000).
Recently, a HEK stable cell line inducibly expressing RyR2 was reported (Jiang et al., 2004). These induction systems allow precise control of RyR2 expression such that levels of the protein can upregulated to sufficient levels for study of the channel, but can also be maintained at relatively low levels in order to avoid disruption of cellular function. However, development of these systems for the number of mutations to be investigated was not possible within the tenure of this project.

3.4.3 Calcium phosphate mediated transfection of HEK cells yielded equivalent high levels of WT and mutant eGFP-hRyR2 expression

Since stable expression of eGFP-hRyR2 was not possible within the limit of this study, transient transfection strategies were attempted and optimised in order that sufficient levels of protein expression were achieved. Calcium phosphate mediated transfection is known to produce very high levels of RyR expression. This can be counterproductive in some cell lines (notably CHO cells), because of cytotoxic effects (George et al., 2003c; Bhat et al., 1997c). In these cases, lipid mediated transfection has been the superior method. In this study however the calcium phosphate method was most successful, achieving moderately high levels of expression without resulting in a large decrease in cell viablility. Indeed, the successful transfer of RyR2 cDNA into HEKs using $CaPO_4$ precipitation has also been previously demonstrated (Jiang et al., 2002b; Du et al., 2001a&b; Wehrens et al., 2003).
In addition, there was no evidence of the production of partial-length proteins (another unwanted artefact of RyR overexpression (Bhat et al., 1999; Rossi et al., 2002)) as shown by the detection of the full-length ~565 kDa protein by Western analysis in Figure 3.8., and by the fact that the anti-RyR2 pAb1093 antibody (which binds to C-terminal residues 4455-4474) was able to bind to its epitope.
Figure 3.9. shows that all recombinant proteins were localised to the ER. This is considered to be the correct localisation, since this is the corresponding organelle to

the SR in non-excitable cells, and suggests that fusion of the eGFP tag to the N-terminal of the RyR2 or the point-mutations introduced do not affect the proper intracellular localisation of these proteins.

Taken together, these results indicate that HEK-293 cells provide a viable expression system for the recombinantly constructed RyR2 mutants which can easily be detected by their endogenous eGFP fluorescence. However, a functional assay is needed to validate the activity of these recombinant proteins, and this will be addressed in the next chapter.

Chapter 4

Functional characterisation of WT and mutant hRyR2 in a living HEK cell system reveals functional heterogeneity

4.1. Introduction

The functional characterisation of RyR2 mutants is essential in order to delineate the molecular mechanisms by which genetic alteration of this SR Ca^{2+} release channel could result in an arrhythmogenic phenotype. However, only eight of the forty-three CPVT/ARVD2-linked mutants have thus far been characterised and the precise mode of RyR2 dysfunction in arrhythmia remains controversial (see section 1.5.2.2.2.), yet there seems to be a consensus that mutant channels are associated with abnormalities in the regulation of Ca^{2+} release from the SR lumen. It is thought that some of the reported discrepancies are the product of the different assays used to characterize RyRs, which can produce conflicting information that is difficult to interpret (George et al., 2005). Widely used techniques include:

1. Measurement of the electrophysiological current through the channel.
2. Assessment of the spatio-temporal characteristics of RyR-mediated Ca^{2+} release in cell systems.
3. Determination of the binding of a conformation-specific ligand to the protein.

Thus, these methods give an indication of the functional state of the channel under different conditions and from this we can infer how mutation could affect RyR2 ion channel activity.

Many *in vitro* techniques used to investigate RyR functionality involve removal of the channel from its cellular environment, enabling precise manipulation of the experimental conditions. However, because the channels are studied in isolation, the results obtained may not always necessarily be easily extrapolated to the physiological situation. It could be argued therefore, that RyR activity is more appropriately investigated in intact cell systems, which allows study of the channels in a more native context. A disadvantage of these systems is that they are more complex and it is difficult to identify underlying mechanisms from the experimental data. The main techniques used are summarised in the section below:

4.1.1. Single channel lipid bilayer analysis

Unlike channels located on the plasma membrane, macroscopic currents through populations of RyRs cannot be monitored using standard whole cell patch clamp recording techniques. Instead the channel must be incorporated into an artificial membrane system such as a planar phospholipid bilayer (Williams, 1995; Favre et

al., 1999). A solution of lipids in a hydrophobic solvent (usually n-decane) is smeared across a hole in a plastic septum to produce a lipid film (bilayer) separating two baths (see Figure 4.1.).

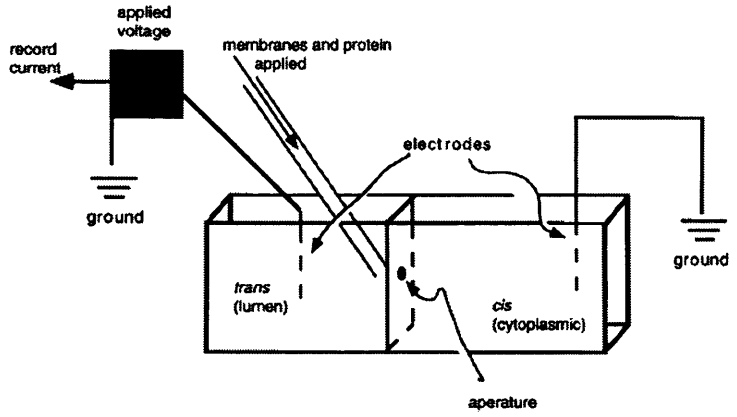

Figure 4.1. Planar lipid bilayer setup for recording single-channel currents (adapted from Marks, 1996). Membranes are formed across a hole in a partition between two chambers. After membrane formation, vesicles containing recombinant or native channels are added to the *cis* chamber. Channel insertion and subsequent experiments are monitored under voltage clamp conditions. Transmembrane voltage is controlled while ionic and pharmacological conditions of the chambers surrounding the membrane can be varied.

RyR from muscle homogenates are incorporated into bilayers either by direct vesicle (microsome) fusion or following purification of the channels from the SR by detergent-solubilisation. An advantage of using microsomes is that the RyR is present in its native membrane, increasing the likelihood that closely associated regulatory proteins may still be present (Marx et al., 2000). However, other types of channels may be present in the preparation, making it difficult to unambiguously measure current through RyRs, unless Ca^{2+} is used as the current carrier. Many single RyR channel studies however use a monovalent carrier to boost the signal-to noise ratio (see Table 1.3. section 1.3.4.), making it difficult to eliminate potential contaminating readings from other channels and so, for an unambiguous RyR current to be measured, the protein must be purified from the SR. Ion channel incorporations occur spontaneously with a fixed orientation (Sitsapesan & Williams, 1994; Williams et al., 2001) and can be detected by conductance changes in the bilayer membrane (Coronado et al., 1992). Once this happens, it is possible to determine the ionic conductance of a single channel and to monitor its gating by measuring the current through the membrane in response to an applied electrochemical gradient. The use of planar lipid bilayers enables control over the ionic composition of the solutions on both sides of the channel, and remains the only technique which permits detailed mechanistic information regarding channel conductance and gating to be obtained (Williams et al., 2001; Laver et al., 2001).

In particular, this is the only method by which channel subconductance states have been identified. These are events of intermediate current level, often interpreted as the result of channel dysfunction (see section 1.4.2.1.). However, there is much speculation as to whether these are actual channel events or are merely artefacts of RyR tetramer destabilisation following their isolation from the cell and detergent solubilisation (Bhat et al., 1999; George et al., 2005).

Solubilisation with the detergent CHAPS (3-[(3-cholamidopropyl)dimethylammonio]-1-propansulfonate) was also responsible for a loss of Ca^{2+} mediated RyR2 inhibition seen in a single channel study by Laver (2001) with no significant inhibition seen, even at 100 mM Ca^{2+}. These RyRs also showed a decreased sensitivity to inhibition by Mg^{2+} compared to native sheep cardiac channels. Similarly, RyR1 and RyR3 isoforms that have different Ca^{2+} sensitivities *in situ*, are found to have effectively the same Ca^{2+} sensitivity in detergent solubilised preparations (Chen et al., 1997a&b; Li & Chen, 2001). It is possible that these effects of solubilisation are due to the loss of accessory proteins (Wagenknecht et al., 1997; Du et al., 2001a; Carmody et al., 2001; George et al., 2005), suggesting that this kind of *in vitro* characterisation may not reflect the *in situ* modulation of the channel within the cell. Alternatively, some of the inconsistencies between *in situ* and bilayer work may be the result of the difference in oxygen tension in *ex vivo* conditions, since it has been demonstrated that this critically affects RyR channel regulation (Eu et al., 2000).

In addition, it is commonly found that the gating properties of ion channels differ to some extent from one channel to the next. This is a major problem of bilayer work, where recordings from one or at most a few channels are taken to represent a whole population.

Despite these drawbacks, the unique ability of single channel studies to investigate the biophysical characteristics of the RyR has made them an invaluable tool in the elucidation of channel regulatory mechanisms.

4.1.2. High affinity [^{3}H]ryanodine binding assays

One of the most important contributions to our ability to study the structure and function of the SR Ca^{2+} release channels was the discovery of the plant alkaloid ryanodine (see Figure 4.2.). Its discovery has contributed to the identification, purification and cloning of the Ca^{2+} release channel (Inui et al., 1987a; Imagawa et al., 1987; Lai et al., 1988b), and the identification of endogenous regulators, novel ligands and regulatory proteins. The production of radiolabelled ryanodine (Pessah

et al., 1985; Sutko et al., 1986) introduced a new approach in the study of RyR structure and function.

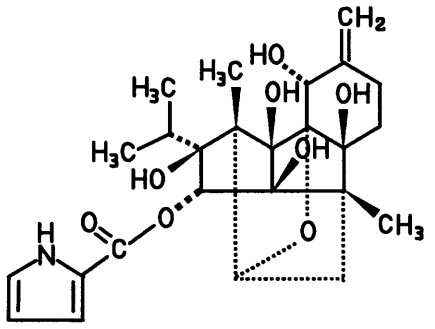

Figure 4.2. The chemical structure of ryanodine ($C_{25}H_{35}NO_9$).

Ryanodine binds with high affinity to the open conformation of RyR (Lai & Meissner, 1989), and changes in [^{3}H]ryanodine binding reflect changes in the functional state of the receptor (Chu et al., 1990; Meissner & El-Hashem, 1992). Thus it follows that [^{3}H]ryanodine binding is enhanced by activators of Ca^{2+} release and decreased by channel inhibitors.

The binding of [^{3}H]ryanodine to the Ca^{2+} release channel is however, quite complex. Equilibrium kinetic analyses of the binding of [^{3}H]ryanodine to skeletal and cardiac SR have demonstrated the existence of two classes of sites: a low affinity and high affinity site. There is only a single high affinity site for ryanodine per receptor tetramer (Lai et al., 1988b; McGrew et al., 1989), thought to be situated in the pore of the channel (residues 4820-4829 in RyR2 (Chen et al., 2002), residues 4475-5037 in RyR1 (Callaway et al., 1994; Witcher et al., 1994)). Various dissociation constant (K_d) values (2-200 nM) have been reported for this site – possibly due to [^{3}H]ryanodine binding to different, interconvertible states of the channel (Buck et al., 1992, Pessah & Zimanyi, 1991; Chu et al., 1990). The action of ryanodine on the channel is dependent on its concentration (see section 1.4.3.1.), with 5-40 nM causing channel activation, > 50 nM promoting substates and > 200 μM causing complete blockade (Bull et al., 1989; Buck et al., 1992). It has been suggested that binding to the high affinity site stabilizes the open state, while occlusion of the channel pore by ryanodine binding to the low affinity sites leads to decreased conductance (Lai et al., 1989). Alternatively, these phenomena could be due to conformational changes associated with the binding of ryanodine to allosteric regulatory sites (Fessenden et al., 2001). Whichever the mechanism, the fact that ryanodine itself can modify channel gating, producing ambiguous effects has

hampered its use in the dissection of the contribution of RyRs to intracellular Ca^{2+} signalling.

Another disadvantage of using ryanodine is its rate of association with the channel is too slow for experiments in intact cells (Pessah et al., 1987; Chu et al., 1990). To accelerate the onset of effect, micromolar, instead of nanomolar levels of ryanodine are used. During the initial phase of incubation, ryanodine may open RyRs and deplete the SR Ca^{2+} content, then at equilibrium, higher ryanodine concentrations may close RyRs. Therefore, although the effect of depleting the SR Ca^{2+} content or blocking its release may be macroscopically the same, the dual action of ryanodine makes it difficult to assess the availability of a releasable Ca^{2+} pool at any experimental point. In order to avoid these effects isolated SR vesicles or microsomes must be used, removing the channels from their native environment - an action which in itself could lead to changes in channel stability. For example, RyR2 pore mutants that were modulated by ryanodine in a cellular context did not demonstrate [^{3}H]ryanodine binding *in vitro* (Chen et al., 2002). Similarly, studies of RyR1 pore mutants reported discrepant results produced by cell-based and *in vitro* systems. Gao et al (2000) attributed this to the fact that the mutant channels were structurally unstable when removed from the cell or needed a 'cofactor', lost during isolation to maintain pharmacological regulation.

Similar discrepancies were seen in a study by Fessenden et al. (2004) where mutation of an EF hand-like region of RyR1 (scrambling of residues 4116-4127) did not affect functional responses to caffeine in intact myotubes, yet in *in vitro* [^{3}H]ryanodine binding experiments, both activation and inhibition by Ca^{2+} were altered significantly compared to WT RyR1.

Thus it is clear that some mutants cannot be assayed by ryanodine binding due to the fact that they cause disruption of the high affinity binding site, while others (especially those situated in the pore region) may be too unstable to be investigated outside of a stabilizing cellular environment. This suggests that this technique may be of limited use in the characterisation of the CPVT/ARVD2 mutants.

4.1.3. Ca^{2+} imaging in intact cells: Measurement of agonist induced Ca^{2+} release and Ca^{2+} sparks

While fundamental studies of RyR in controlled environments (i.e. in isolated microsomes, or in planar lipid bilayers) have made important contributions to our understanding of channel function, it is equally important to evaluate how the RyR is regulated in intact cells in the native physiological environment. This is clearly

important because the RyR channel appears to be affected by a vast array of endogenous factors. Indeed, rather subtle changes in gating properties could have a major impact on the physiological function of the SR Ca^{2+} release channel and the resultant cellular Ca^{2+} transient – a direct predictor of cardiac response.
This work complements and extends that from more isolated systems and is crucial in building a more comprehensive understanding of cardiac EC coupling and the regulation of SR Ca^{2+} release. However, it has the inherent disadvantage that it is harder to maintain control of all of the potentially relevant factors in the complex environment of the cell.
Most studies in intact cells involve the measurement of agonist-induced SR/ER Ca^{2+} release via RyR or Ca^{2+} sparks using fluorescent indicators. Ca^{2+} sparks are spontaneous localized Ca^{2+} release events, which were initially thought to be due to single channel openings (Cheng et al., 1993; Song et al. 1997). However, it seems more likely that Ca^{2+} sparks are due to a cluster of RyRs in an array, working synchronously as a single functional unit (Tsugorka et al., 1995; Lipp & Niggli, 1998). As well as occurring spontaneously, Ca^{2+} sparks can also be activated by Ca^{2+} entry via the L-type Ca^{2+} channel (Cannell et al., 1995; Lopez-Lopez et al., 1995). Indeed, spatio-temporal recruitment of Ca^{2+} sparks underlies the global Ca^{2+} signals that subsequently activate myocyte contraction, though individual sparks are generally not distinguishable during the normal twitch (Cannell & Soeller, 1998; Niggli, 1999) because they are synchronised by the activating influx of Ca^{2+}.
It has been suggested that spark probability may depend on binding of two Ca^{2+} ions to the RyR (Lopez-Lopez et al., 1995; Santana et al., 1996), and so, spark frequency and therefore Ca^{2+} release depend critically on the cytosolic Ca^{2+} concentration (Bers & Perez-Reyes, 1999). The frequency and amplitude of Ca^{2+} sparks also depends on SR Ca^{2+} load (Satoh et al., 1997) and this SR Ca^{2+} load effect may be related to increased open probability seen in bilayers when $[Ca^{2+}]$ is increased on the luminal side of the channel (Sitsapesan & Williams, 1995). Therefore, the microscopic effect on Ca^{2+} spark probability has exact parallels in terms of the global cellular Ca^{2+} transient, thus, spark frequency/amplitude measurements can be used as indicators or RyR activity. Since sparks are such small events, it has become customary to use the two-dimensional line scan mode of the confocal microscope to measure them with increased temporal resolution. This generally involves scanning a cell which is loaded with a Ca^{2+} indicator at a high frequency (e.g. every 2 miliseconds) along a line.
Ca^{2+} spark measurements tend only to be carried out in cardiac myocytes, since it would appear that RyRs expressed in a non-myocyte environment cannot undergo

this kind of basal spontaneous Ca^{2+} release (George et al., 2003a; Bhat et al., 1997c, 1999; Rossi et al., 2002; Du et al., 1998), though the reason for this remains to be defined. It is likely that a component of the cardiac-specific environment is necessary, for example, an accessory protein such as FKBP12.6, or that RyRs in the null cell environment cannot undergo inter-tetramer associations to form functional CRUs. In contrast, recombinant RyR3 does underlie Ca^{2+} sparks in null cell models (Rossi et al., 2002), however when expressed in transgenic myocytes, these sparks did not coalesce into waves and did not result in myocyte contraction (Takeshima et al., 1995).

Despite the fact that RyR2 channels expressed in non-excitable cell lines do not produce sparks, they still retain the ability to respond to Ca^{2+} and other agonists (Du & MacLennan, 1999; Chen et al., 1997; Li & Chen, 2001), demonstrating that these channels still undergo regulation within these cells. Measurement of the increase in intracellular [Ca^{2+}] in response to an agonist has been widely used to characterise recombinant RyRs (reviewed by George et al., 2005). The main agonists used in the activation of RyR1 and RyR2 include caffeine and 4-cmc, which are used mainly because of their specificity and potency of activation (Rousseau & Meissner, 1989; Ehrlich et al., 1994; Zorzato et al., 1993), and because they are membrane permeable. Caffeine, in particular, is useful since its action is quick and reversible, and has become the standard pharmacological tool for demonstrating activation of RyRs because it acts by sensitising the channel to ambient Ca^{2+} (Sitsapesan & Williams, 1990), providing a semi-physiological mechanism of activation.

Changes in intracellular Ca^{2+} concentration are measured non-invasively using fluorescent Ca^{2+} indicators - molecules whose optical properties change when they bind Ca^{2+}. A wide variety of Ca^{2+} indicators are currently available, with excitation and emission spectra ranging from UV to visible colours. Ca^{2+} sensitive fluorescent indicators can be broadly divided into single and dual (ratiometric) wavelength indicators on the basis of their spectral changes in response to Ca^{2+} elevation. Single-wavelength Ca^{2+} sensitive indicators (e.g. fluo-3) change their emission intensity upon binding Ca^{2+}. However, the intensity of emission is also proportional to the indicator concentration, so careful calibration is required. When Ca^{2+} binds to a dual wavelength indicator (e.g. fura-2), the excitation/emission spectrum changes, and by ratioing the emission of the indicator at these two wavelengths, a measure of Ca^{2+} can be made that is independent of the indicator concentration. However, these dual-wavelength indicators are only available with UV excitation, which can damage cells and result in enhanced autofluorescence. In addition, the exclusive requirement for UV excitation may be limited by hardware and experimental considerations.

Several different strategies can be employed to introduce indicators into the cytoplasm of cells (e.g. microinjection, infusion from whole cell patch pipettes, pinocytosis, transient plasma membrane permeabilization using osmotic shock or electroporation), however the most non-invasive method is passive loading using acetoxymethyl (AM) ester derivatives. Once the indicators are cytoplasmic, they undergo hydrolysis by endogenous esterases converting them to their Ca^{2+}-sensitive forms, the hydrophilic nature of which precludes their leakage from the cell. Calibration of the dye enables the actual [Ca^{2+}] present in the cell to be calculated (see Chapter 5).

The complexity in using such intact systems stems from the fact that the cell is in a dynamic state, and the actions of proteins other than the RyR have to be taken into account. For example, differences in the rate of decay of a Ca^{2+} transient is due to a combination of events: closure of the RyR channel, removal of Ca^{2+} from the cell via plasma membrane pumps and exchangers, and the activity of the SERCA pump -- yet the action of each component cannot be differentiated without a means of controlling each in turn (e.g. with inhibitors), which could subsequently alter other regulatory aspects of cellular Ca^{2+} signalling. However, despite the fact that interpretation of these experiments is complicated, they do provide a more integrated and comprehensive understanding of how SR Ca^{2+} release is regulated in physiological and pathophysiological contexts.

SCD-linked mutants of RyR2 have been investigated using all three of these techniques, sometimes with conflicting results (see section 1.5.2.2.2.). However, modulation of RyR2 function is complex with the channel integrating a diverse array of cellular inputs to effect the appropriate Ca^{2+} release. Consequently, it is possible that defects in diverse aspects of RyR2 regulation underlie cardiopathology, suggesting that analysis of the mutant channels should not be carried out in isolation, rather in systems which include as many of the physiological regulators of RyR2 as possible in a more native setting. In light of this, live cell Ca^{2+} imaging will be used in this study to assess the function of RyR2 mutants compared to that of the wild type channel.

4.2. Methods

4.2.1. Loading of HEK cells with Ca^{2+} orange AM

Cells (1 x 10^5) on poly-lysine coated coverslips were loaded with Ca^{2+} orange (10 μM in 20% w/v pluronic acid F-12) in DMEM containing glutamine (2 mM). The dye containing solution was added to each coverslip as a 200 μl meniscus and incubated at 37°C and 5% CO_2 for 45 minutes. Coverslips were then immersed in DMEM prior to Ca^{2+} imaging as described in section 2.2.5.

4.2.2. Measurement of the amplitude and temporal characteristics of Ca^{2+} transients

The following characteristics of the Ca^{2+} transients obtained were quantified:

1. The peak amplitude of Ca^{2+} release: This represents the magnitude of the change in fluorescence of the indicator following channel activation, and was expressed as F/F_0, where F is the maximum fluorescence observed, typically occurring ~5 seconds after agonist addition and F_0 is the indicator fluorescence determined in resting cells (see Figure 4.3.A). This is a general measure of channel activation.
2. The time to peak: this was taken as an estimation of how quickly the channel is activated. However, the time taken to reach maximum fluorescence will depend on the amplitude of the transient, meaning that only transients of equivalent amplitude may be compared (Figure 4.3.B).
3. Rate of Ca^{2+} release: This is represented by the change in fluorescence as a function of time. This parameter more accurately describes the rate of channel opening since the amplitude of the transient is considered (Figure 4.3.C).
4. The time taken to decay to half the maximal amplitude: This is an estimation of the rate of channel deactivation and of Ca^{2+} removal from the cytosol via sequestration into intracellular organelles (particularly the ER) or its extrusion from the cell through the plasma membrane localized pumps and exchangers. The half maximal amplitude value was chosen as an end point since some of the Ca^{2+} transients from the mutant channels did not return to the basal Ca^{2+} level. This parameter and the rate of Ca^{2+} release collectively represent a measure of the duration of the Ca^{2+} transient.

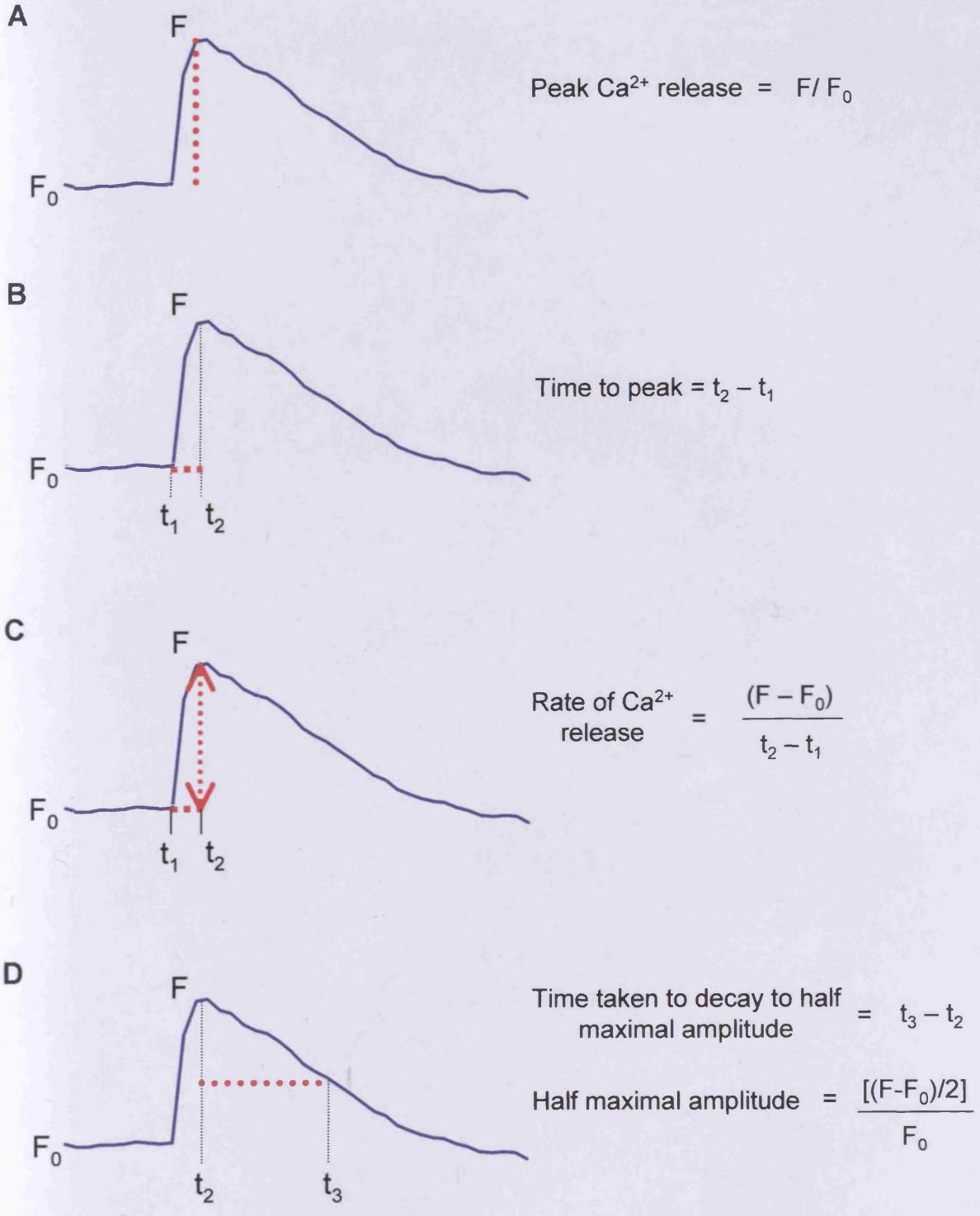

Figure 4.3. Schematics detailing how the amplitude and temporal aspects of Ca^{2+} release were measured. A to D represent Ca^{2+} transients where the parameters measured are shown as dotted red lines, equations for which can be seen alongside each schematic. F = maximum or peak fluorescence; F_0 = basal fluorescence; t_1 = time of agonist addition; t_2 = time at which maximum or peak fluorescence occurs; t_3 = time at which transient reaches half maximal amplitude.

It is anticipated that the separate evaluation of all these parameters will indicate which aspects of channel functionality are affected by mutation.

4.2.3. Measurement of ER Ca^{2+} load

ER Ca^{2+} load was estimated from peak Ca^{2+} release following the addition of thapsigargin (5 μM) to cells (George et al., 2003a). Thapsigargin (TG) is a selective and irreversible blocker of the sarco-endoplasmic reticulum Ca^{2+} ATPase which upon binding its target, causes passive depletion of the entire Ca^{2+} store (Thastrup et al., 1990). HEK cells expressing recombinant RyR exhibit a functionally compartmentalised ER Ca^{2+} store comprising a significant caffeine-insensitive component (Tong et al., 1999a), and thus TG was used instead of caffeine to estimate total ER Ca^{2+} load in HEK cells expressing WT and mutant RyR2. Fluo-3 loaded cells were prepared as in section 2.2.5. RyR2 expressing cells were first identified by the addition of 0.5 mM caffeine followed by several washes and complete extracellular solution exchange with fresh KRH buffer prior to TG application. Cells were imaged and data were acquired as described in section 2.2.5.

4.3. Results

4.3.1. The properties of Ca^{2+} orange render it unsuitable for use in HEK cells

Ca^{2+} orange was initially chosen for use in this study because it's spectral properties are distinct from those of eGFP (Ex 549 nm, Em 576 nm), permitting simultaneous imaging of their respective fluorescent signals. However, this dye consistently displayed intracellular compartmentalisation (Figure 4.4.A), thereby compromising its function as a cytosolic Ca^{2+} indicator. Furthermore, the fluorescence of this dye did not increase greatly even upon maximal Ca^{2+} release with 10 mM caffeine (Figure 4.4.B, compared with Fluo-3, Figure 4.6.), and transients of decreased amplitude could only be detected if the photo multiplier gain was increased, resulting in significantly increased background noise. This low signal–to-noise ratio, together with the significant comparmentalisation meant that a dose response to caffeine could not be measured using this dye, therefore making it unsuitable for use in this study.

4.3.2. Fluo-3 is a suitable Ca^{2+} indicator for use in cells expressing GFP-hRyR2

The Ca^{2+} indicator fluo-3 was used to accurately determine changes in intracellular [Ca^{2+}] in the transfected HEK cells. This particular indicator was used because of its large dynamic range, low compartmentalization tendency and appropriate apparent Ca^{2+} binding affinity (Thomas et al., 2000). Although these are desirable properties and are ideally suited for this study, fluo-3 has a nearly identical excitation/emission profile to eGFP and thus it is not possible to easily distinguish between their respective fluorescences. This posed two problems: 1) cells expressing the ER localised eGFP tagged hRyR2 recombinant proteins could not be identified by their fluorescence when loaded with fluo-3, 2) changes in the intensity of fluorescence emitted in the 515±30 nm region may not have been solely due to Ca^{2+} dependent changes in fluo-3 if the eGFP fluorescence was also altered by the agonist or Ca^{2+} itself.

However, cells expressing functional channels were easily identified by their characteristic caffeine response (see Figures 4.6. and 4.7.). Additionally, it was found that the intensity of the endogenous eGFP fluorescence of the recombinant proteins was unaltered following caffeine induced Ca^{2+} mobilization from intracellular stores (see Figure 4.5.A). This suggests that the fluorescence changes seen on caffeine addition to fluo-3 loaded HEK cells expressing GFP-hRyR2 are exclusively

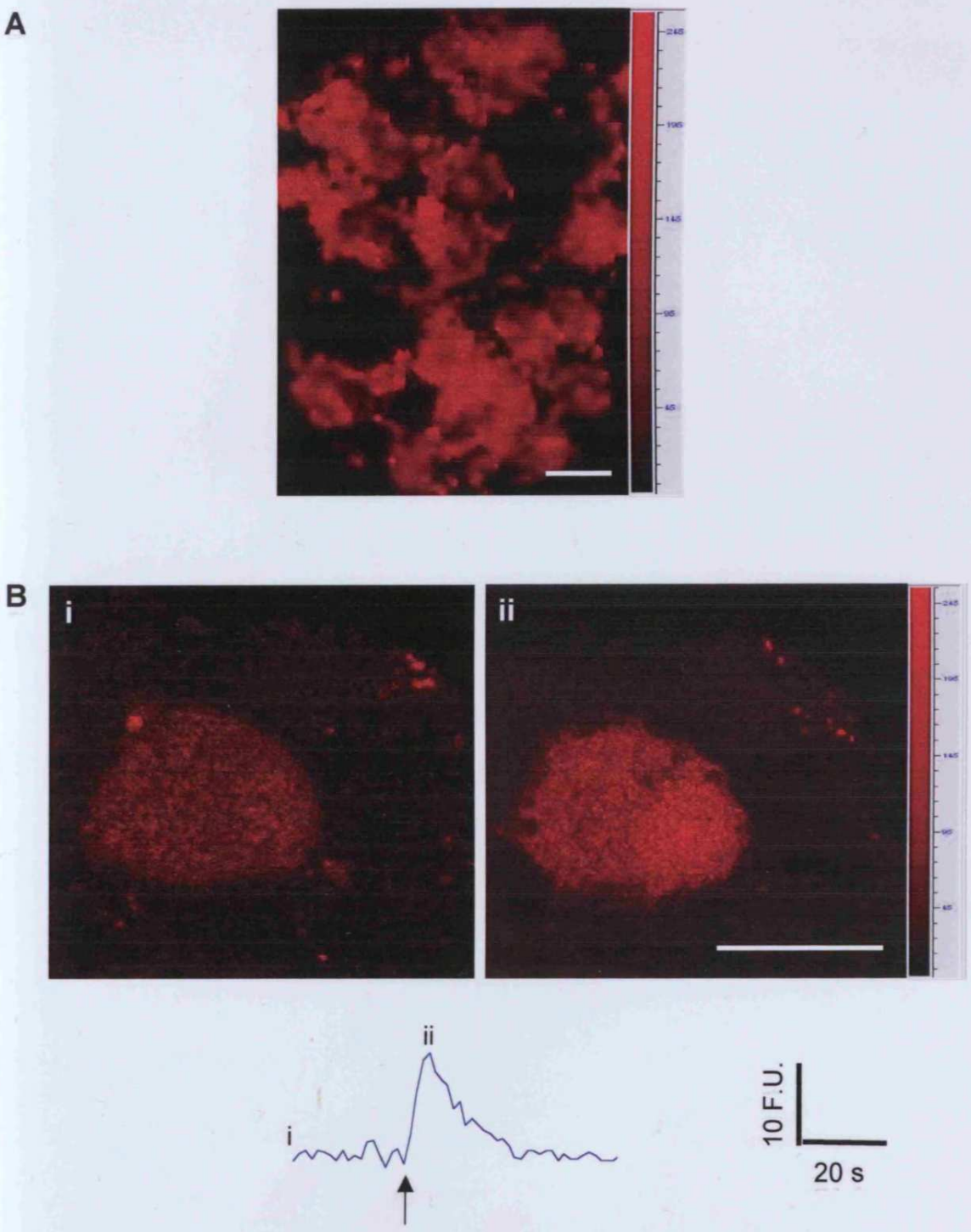

Figure 4.4. Properties of Ca^{2+} Orange which make it unsuitable for use in HEK cells. A) HEK cells loaded with Ca^{2+} Orange exhibit intracellular compartmentalisation of the dye. B) A transfected cell which appeared to have a uniform intracellular distribution of the indicator showed a small Ca^{2+} dependent increase in fluorescence on addition of 10 mM caffeine (arrowed), as shown by the transient. The images shown above were taken at the times denoted by i and ii.

the result of changes in the fluorescence of fluo-3. Furthermore, the typical eGFP fluorescence of the ER localised recombinant proteins was negligible when compared with the total cellular fluorescence following loading with fluo-3-AM (see Figure 4.5.B).

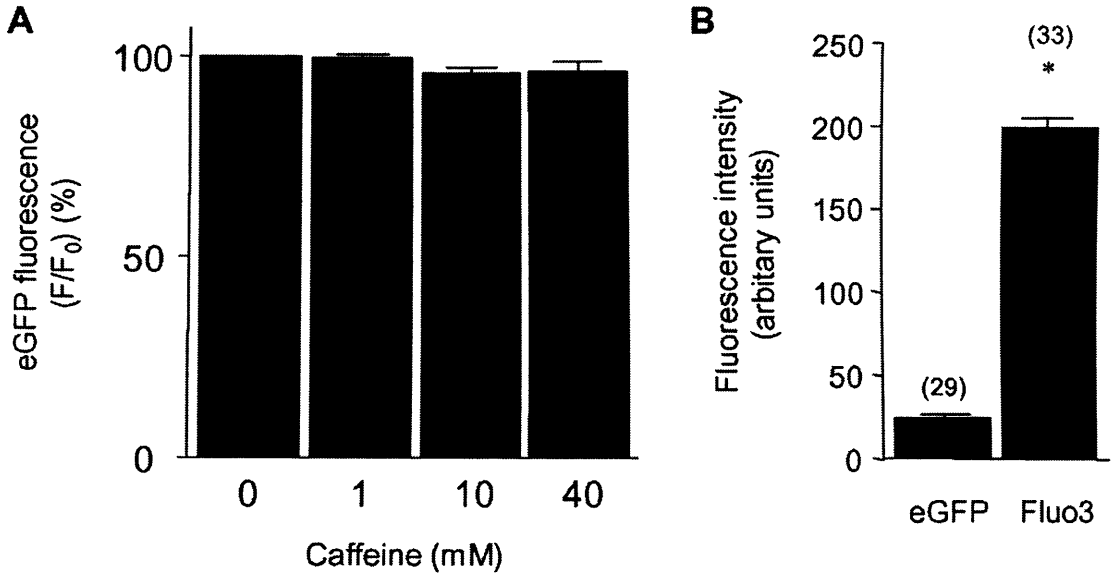

Figure 4.5. eGFP fluorescence is independent of caffeine-induced Ca^{2+} release. A) The peak change in eGFP fluorescence (F/F_0) is given as the maximum fluorescence determined following caffeine addition (F) expressed as a percentage of the eGFP fluorescence measured in resting cells (F_0; 100%) in cells expressing eGFP tagged WT RyR2. Data represent mean values ± S.E.M. (from n>4 coverslips, with >18 cells altogether in each instance). B) Typical eGFP fluorescence intensity following expression of eGFP-tagged RyR2 is normalized against fluo-3 fluorescence following loading of cells with the AM conjugated dye. Data were acquired from regions of interest representing single resting (non-stimulated) cells, typically of approximately 50 μm^2 in area (> 200 pixels). Data are plotted as mean values ± S.E.M., the number of cells analysed is shown in parentheses. *p <0.001.

4.3.3. Recombinant ARVD2-linked RyR2 mutants form functional Ca^{2+} release channels but exhibit heterogeneous caffeine-induced Ca^{2+} release

Cells expressing either WT or mutant GFP-RyR2 demonstrated ER Ca^{2+} release in response to caffeine (see Figures 4.6. and 4.7.), signifying that these recombinant proteins form functional homotetrameric ion channels within cells. It was also noticeable that, for both WT and mutant channels, the number of cells that exhibited a caffeine response per field of view corresponded almost exactly to the transfection efficiency. For example, in Figure 4.6, 5 out of the 16 cells in the field of view underwent caffeine-induced Ca^{2+} release, corresponding to the transfection efficiency obtained for WT eGFP-hRyR2 of ~ 30 % (see Chapter 3, Figures 3.6. and 3.7.). This correlation was also observed for the mutants, suggesting that expression was

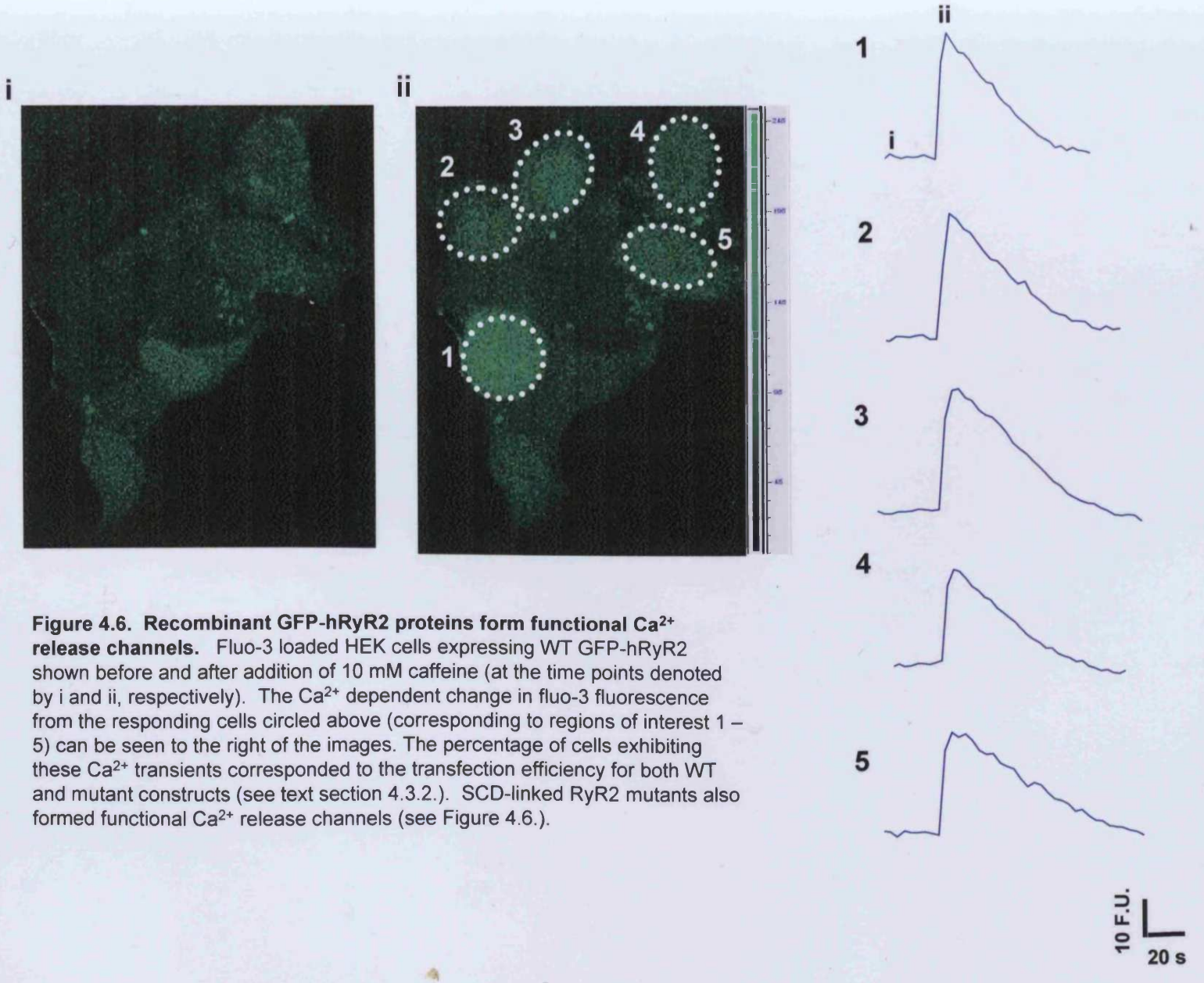

Figure 4.6. Recombinant GFP-hRyR2 proteins form functional Ca^{2+} release channels. Fluo-3 loaded HEK cells expressing WT GFP-hRyR2 shown before and after addition of 10 mM caffeine (at the time points denoted by i and ii, respectively). The Ca^{2+} dependent change in fluo-3 fluorescence from the responding cells circled above (corresponding to regions of interest 1 – 5) can be seen to the right of the images. The percentage of cells exhibiting these Ca^{2+} transients corresponded to the transfection efficiency for both WT and mutant constructs (see text section 4.3.2.). SCD-linked RyR2 mutants also formed functional Ca^{2+} release channels (see Figure 4.6.).

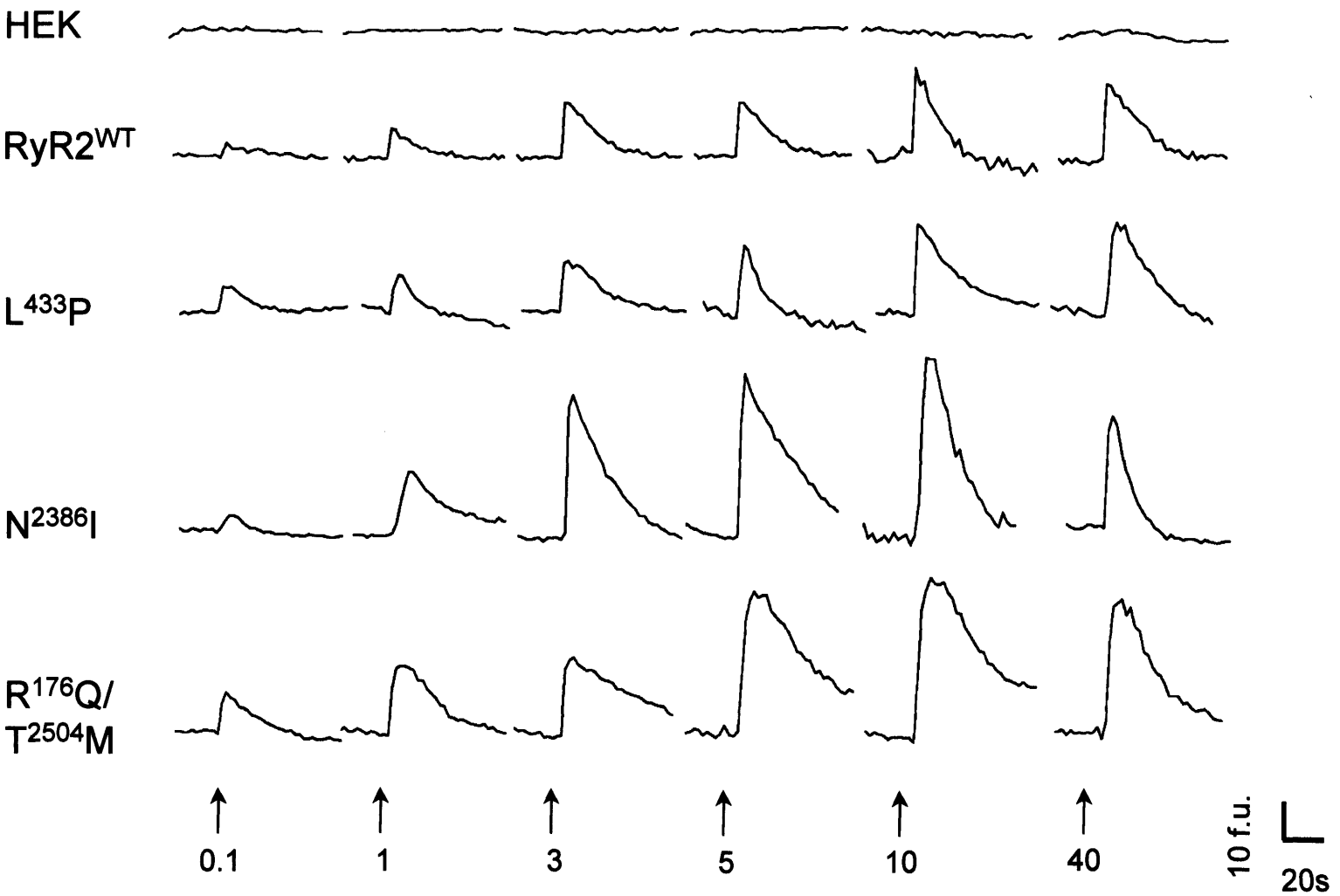

Figure 4.7. Representative Ca^{2+} transients evoked by caffeine addition to HEK cells expressing WT or ARVD2-linked mutants. Caffeine addition (mM) is arrowed. F.U. denotes arbitrary fluorescence units measured in defined regions of interest which correspond to whole single cells (typically approximately 50 μm^2 >200 pixels).

closely correlated with function in contrast with studies using stable expression of RyR1 and RyR3 (Rossi et al., 2002).

Figure 4.7. shows characteristic caffeine (0.1-40 mM) responses from single HEK cells expressing WT or mutant RyR2. This figure also demonstrates that untransfected HEK cells did not exhibit caffeine-induced Ca^{2+} release, confirming the lack of functional RyR in these cells. The amplitude characteristics of these and other similar transients were used to calculate the sigmoidal dose response curves shown in Figure 4.8. and 4.9. Under these experimental conditions WT GFP-hRyR2 has an EC_{50} of 1.56 ± 0.24 mM caffeine (i.e this is the concentration of caffeine which results in half-maximal activation of the channel), and a Hill constant (that in the context of these experiments is interpreted as the co-efficient representing the ease of transition of the channel from the closed to the open state) of 1.59 ± 0.13.

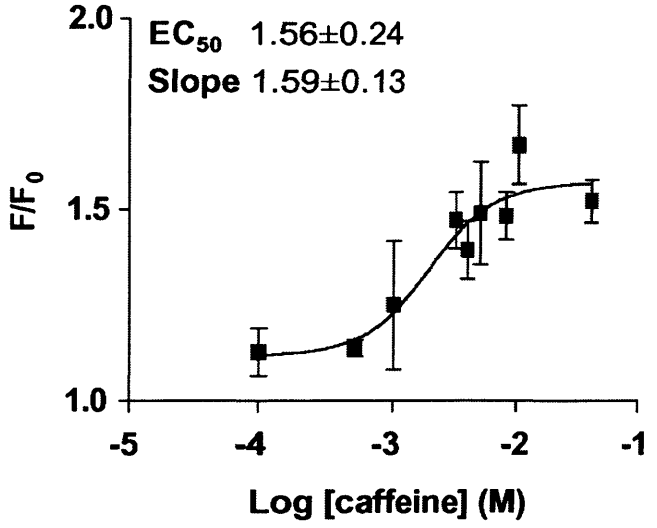

Figure 4.8. Caffeine dose response profile for WT GFP-hRyR2. The peak fluorescence change (F/F_0) following caffeine activation (0.1- 40 mM) is plotted as the maximum fluorescence (F) relative to the Ca^{2+}-dependent fluorescence of fluo-3 determined in resting cells (F_0) (see Figure 4.3.). EC_{50} and Hill coefficient values were calculated by non-linear regression analysis of the data using GraphPad Prism software. Data are mean ± S.E.M. and were derived from at least 3 experiments (> 6 cells per experiment).

Dose-response relationships constructed from caffeine-activated Ca^{2+} release in HEK cells expressing recombinant WT or mutant proteins revealed significant functional heterogeneity between the individual RyR2 mutants and when compared with WT RyR2. RyR2 mutants $N^{2386}I$ and $R^{176}Q/T^{2504}M$ exhibited enhanced sensitivity to caffeine activation (Figure 4.9.) as demonstrated by the fact that the dose-response curves are left-shifted resulting in significantly lower EC_{50} values. In addition, the

$N^{2386}I$ mutant also exhibited a significantly increased Hill coefficient, suggesting an enhanced transition from the closed to the open state. However, the Hill coefficient of $R^{176}Q/T^{2504}M$ was not significantly different from that of the WT, indicating that the kinetics of channel opening may be comparable.

Channels containing either the $R^{176}Q$ or $T^{2504}M$ mutation exhibited slightly left-shifted caffeine dose-response profiles (Figure 4.9.), however neither showed a significantly lower EC_{50} value, indicating that the effect of each mutation on its own is not as potent as that of the 'double' mutation. This would suggest that both mutations contribute to an altered Ca^{2+} release phenotype, but individually they may not cause sufficient channel dysfunction to result in arrhythmia, which would agree with the fact that they are found to co-segregate with the affected phenotype. However, the $T^{2504}M$ mutant exhibited an increased Hill slope value, which was not seen with the 'double' mutant, suggesting that the functional effects of the two mutants may not be directly additive.

In stark contrast to the above mutants, Ca^{2+} release through the $L^{433}P$ mutant was characterised by a significantly right-shifted dose response to caffeine indicating a decreased sensitivity to activation by this agonist. Upon activation, augmented Ca^{2+} release was not seen in cells expressing this mutant, however the significantly increased Hill coefficient of $L^{433}P$ suggests a mode of activation profoundly different to that of WT RyR2. This finding represents the first characterisation of an SCD-linked RyR2 mutant that exhibits markedly desensitised activation.

4.3.4. Analysis of the amplitude and temporal characteristics of Ca^{2+} release through RyR2 mutants

The peak Ca^{2+} release for WT and mutant GFP-hRyR2 proteins is shown in Figure 4.10. A. It can be seen that all mutants apart from $L^{433}P$ exhibit augmented Ca^{2+} release in response to 10 mM caffeine. In contrast, the peak release through $L^{433}P$ was not significantly different from that of the WT channel, but was significantly decreased when compared with that of the other ARVD2-linked mutants, reinforcing the view that this mutation affects RyR2 function in a significantly different manner.

The temporal profile of Ca^{2+} handling in cells expressing WT and mutant RyR2 was also investigated (Figure 4.10. B-D) in order to gain an insight into which aspects of Ca^{2+} release are affected by mutation (i.e. channel activation affecting rate of release, channel deactivation affecting the rate of transient decay). It is also important to note that these properties of Ca^{2+} release collectively determine the quantity of Ca^{2+} released, which could not be determined by integration of the Ca^{2+}

Figure 4.9. Dose-response profiles showing the caffeine activation of ARVD2-linked RyR2 mutants: N^{2386I} (open triangles), L^{433P} (closed triangles), R^{176Q} (closed circles), R^{176Q}/T^{2504M} (cross), and T^{2504M} (open squares). The dose response for WT GFP-hRyR2 (filled squares) is also shown in every graph for comparison (see Figure 4.8.). The peak fluorescence change (F/F_0), EC_{50}, and Hill coefficient values were determined as detailed in Figure 4.4. Data are given as mean ± S.E.M. and were derived from at least three experiments (> 6 cells per experiment). * and † represent $p<0.05$ and $p<0.005$ respectively, when compared to WT GFP-hRyR2.

transients in this study, since some of those originating from mutant channels (e.g. $R^{176}Q/T^{2504}M$, see Figure 4.7.) did not decay to resting Ca^{2+} levels (the significance of this will be discussed in Chapter 5), indicating that comparable analysis using the trapezoid rule could not be achieved.

There was no significant difference observed between the time to peak Ca^{2+} release following activation of WT and mutant RyR2 (Figure 4.10. B), but this parameter is dependent on the amplitude of Ca^{2+} release following caffeine addition which, as Figure 4.10.A demonstrated, was different between the mutant and WT channels. A parameter which takes this into account is the rate of Ca^{2+} release (Figure 4.10. C), which revealed significant heterogeneity between mutant and WT RyR2, with mutants $N^{2386}I$ and $L^{433}P$ having significantly increased rates.

Significant differences were also measured in the decay properties of the Ca^{2+} transients of individual RyR2 mutants when compared with WT RyR2 (Figure 4.10. D), with $R^{176}Q/T^{2504}M$ and $L^{433}P$ mutants having increased decay times. As discussed, the time taken for caffeine-induced Ca^{2+} transients to decay to half-peak amplitude represents an estimation of the rate of channel deactivation and of Ca^{2+} removal from the cytosol (though the relative contribution of these two processes is unknown).

An important finding from this work is that despite the marked amplitude and temporal heterogeneity that exists between the ARVD2-linked mutants, analysis of the precise mode of Ca^{2+} release through these channels (i.e. peak Ca^{2+} release versus rate of Ca^{2+} release versus rate of transient decay/sequestration or extrusion of released Ca^{2+}) predicted that the net effect of these RyR2 mutations would result in significantly augmented cytoplasmic Ca^{2+} following channel activation, a characteristic of VT (Priori et al., 2002). This can be clearly appreciated for $N^{2386}I$ and $R^{176}Q/T^{2504}M$ since both of these mutants display hyper-sensitised caffeine-induced Ca^{2+} release, and significantly augmented peak cytoplasmic Ca^{2+} levels when compared with WT RyR2 following cellular activation (Figure 4.9. and 4.10.A). Importantly, elevated cytoplasmic Ca^{2+} levels are also predicted to result from activation of the $L^{433}P$ channel. Although this mutant is less sensitive to activation, once activated, it exhibits a similar peak Ca^{2+} release to that determined in cells expressing WT RyR2 (Figure 4.10. A), the more rapid rise in cytoplasmic Ca^{2+} and the significantly prolonged transient (Figure 4.10. C and D) would result in a sustained elevation in cytoplasmic Ca^{2+} for considerably longer durations than would occur following activation of cells expressing WT RyR2.

Interestingly, the recombinant RyR2 channels containing either single mutations $R^{176}Q$ or $T^{2504}M$ showed increased peak Ca^{2+} release when compared with WT RyR2

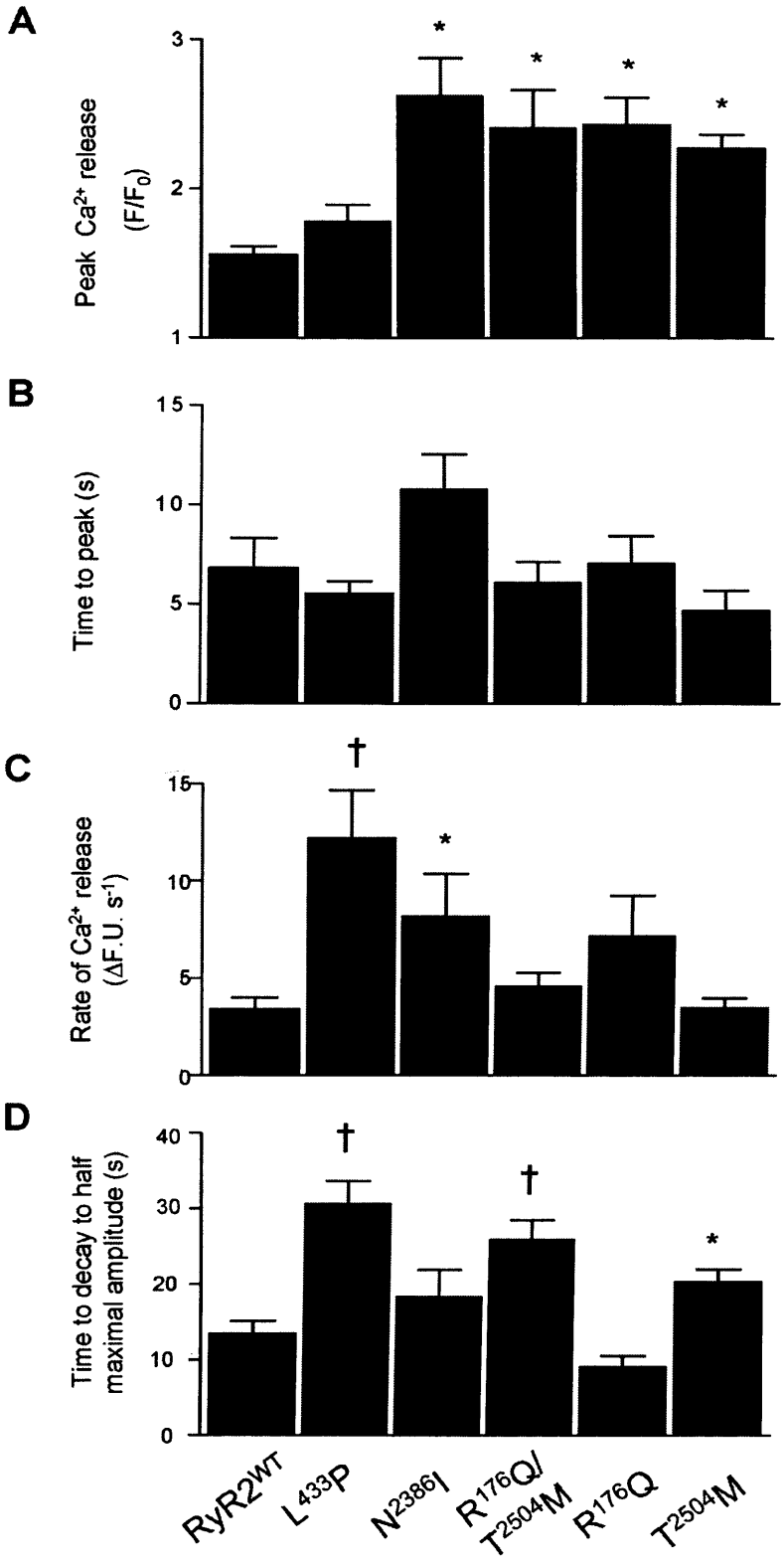

Figure 4.10. Profiling the caffeine-activated Ca^{2+} release through WT and mutant RyR2 channels. A) Peak Ca^{2+} release (F/F_0; see Figure 4.5. for definition). B) The time taken to peak Ca^{2+} release, C) the rate of Ca^{2+} release, plotted as the change in the Ca^{2+} dependent fluo-3 fluorescence per second and D) the time for half maximal decay of the Ca^{2+} transient were determined following analysis of Ca^{2+} transients triggered by addition of 10 mM caffeine in HEK cells expressing WT or mutant RyR2. Data are given as mean ± S.E.M. and was derived from analysis of at least 18 cells in each instance. * and † represent $p<0.05$ and $p<0.005$ respectively when compared with WT RyR2.

(Figure 4.10. A) but demonstrated significantly different Ca^{2+} release profiles when compared with the 'double' $R^{176}Q/T^{2504}M$ mutant, as well as with WT RyR2. Nevertheless, their functional characteristics are not as pronounced as those of the channels containing both mutations, yet their actions do not seem to be additive or complementary, emphasizing the complex nature of RyR2.

4.3.5. Cells expressing WT and mutant GFP-hRyR2 have equivalent ER Ca^{2+} loads

The amplitude and temporal characteristics of caffeine induced Ca^{2+} release determined above may be influenced by other cellular factors e.g. the relative activity of ER and plasma membrane Ca^{2+} pumps, cytoplasmic and ER Ca^{2+} buffers (Bers, 2002), the co-ordinated actions of which help shape cytoplasmic Ca^{2+} transients. Furthermore, the amplitude of Ca^{2+} release evoked by caffeine is critically dependent on the filling status of the ER Ca^{2+} store. Figure 4.11. shows the ER load of cells expressing WT and mutant GFP-hRyR2 as estimated by measuring the peak Ca^{2+} release following the addition of thapsigargin. These data demonstrate that the WT and mutant RyR2 cell populations appear to have comparable ER Ca^{2+} loads, suggesting that the channel dysfunction seen does not result from a more generalised dysfunction of cellular Ca^{2+} handling, though this cannot be completely ruled out without further work.

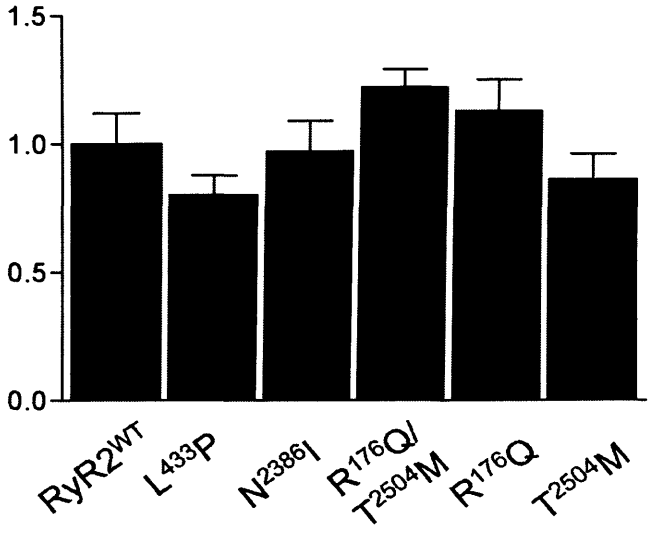

Figure 4.11. Comparable ER loads in 'resting' cells expressing WT and mutant RyR2. Data are expressed as a proportion of the peak Ca^{2+} release in HEK cells expressing WT RyR2 (1.00 ± 0.12) and are presented as mean ± S.E.M with n>25 cells in each instance. Data were not significantly different at $p<0.05$.

4.4. Discussion

4.4.1. The unavoidable use of Fluo-3 as a Ca^{2+} indicator

The use of a ratiometric Ca^{2+} indicator would have been favourable, since these are able to give a measure of Ca^{2+} which is independent of indicator concentration, thereby avoiding problems of uneven indicator distribution. However, such dual-wavelength indicators are only available with UV excitation, a spectral region which we were not able to excite with the lasers available on our confocal microscope. This limited us to the use of single-wavelength indicators, preferably one whose spectral properties were distinct from those of eGFP in order that loaded transfected cells may be identified before agonist addition. Measurement of Ca^{2+} release was attempted using Ca^{2+} Orange, which as its name suggests, is excited by longer wavelengths than eGFP. However, this dye underwent marked intracellular compartmentalisation and exhibited a low dynamic range, such that events of smaller amplitude could not be measured without increasing the photomultiplier gain and consequently the signal-to-noise ratio, therefore making it unsuitable for use in carrying out a caffeine dose-response. Ca^{2+} Orange has previously been successfully used in conjunction with eGFP (George et al., 2003a), however in this study it was used to measure global transients in myocytes where the magnitude of SR Ca^{2+} release would presumably be greater than in null cells. In addition, significant mitochondrial, ER and vesicular compartmentalisation has been previously demonstrated in HeLa cells loaded with Ca^{2+} Orange (Thomas et al., 2000). The only other spectrally distinct Ca^{2+} dye available to us was Ca^{2+} Crimson (Molecular Probes), however this is known to have similar properties to Ca^{2+} Orange (George et al., 2003a) and was therefore not considered.

In light of this, dyes with similar spectral properties to eGFP were considered, the best of which was considered to be fluo-3, having a large dynamic range (i.e. the change in intensity upon binding Ca^{2+} is large, giving a higher signal-to-noise ratio thus allowing the measurement of small changes in $[Ca^{2+}]$) and appropriate apparent Ca^{2+} binding affinity (Thomas et al., 2000). In addition, loading of HEK cells with fluo-3 resulted in uniform cytoplasmic fluorescence, with no visible mitochondrial/ER staining (see Figure 4.6.).

However, fluo-3 has an identical excitation/emission profile to eGFP and thus it was not possible to distinguish between their respective fluorescences. Nevertheless, it was conclusively shown that the eGFP fluorescence was independent of caffeine or the mobilized Ca^{2+}. Moreover, the intensity of fluo-3 signal was much greater than

that of eGFP (see Figure 4.4.) indicating that the determination of Ca^{2+} release in this study, which was calculated following the measurement of relative changes in intracellular fluorescence was entirely attributable to Ca^{2+} dependent changes in fluo-3 signals. These findings provide good evidence that fluo-3 could be used to accurately determine intracellular Ca^{2+} mobilization in the experimental system used.

4.4.2. ARVD2-linked RyR2 recombinant proteins form functional Ca^{2+} release channels

Dysfunctional Ca^{2+} release through SCD-linked RyR2 mutants is generally thought to occur following cellular stimulation (Wehrens et al., 2003; George et al., 2003a) and so the properties of caffeine- evoked Ca^{2+} transients in cell expressing WT or mutant RyR2s were characterised in this study. This drug was deemed the most suitable not only because it acts by sensitising the RyR2 to Ca^{2+}, but because it elicits SR Ca^{2+} release specifically via RyRs and not from IP_3Rs (the main ER Ca^{2+} release channels in HEK 293 cells (Luo et al., 2001)), of which it is an antagonist (Ehrlich et al., 1994). Consistent with previous reports of heterologous expression of recombinant RyR2 in null cell systems (George et al., 2003b & c; Du et al., 1998; Bhat et al., 1997c, 1999), Ca^{2+} sparks were not detected in these experiments. However, all recombinant channels demonstrated caffeine-induced Ca^{2+} release, suggesting that these proteins undergo appropriate regulation and can operate as Ca^{2+} release channels. This demonstrates that ARVD2-linked mutation of RyR2 does not result in a complete loss of protein function, often seen with other channelopathies (see Chapter 5, Table 5.1.), underlining the essential role of RyR2. Thus, neither ARVD2 or CPVT associated mutations result in non-functional homotetrameric channels, suggesting that the difference between these two conditions is more subtle than that between MH and CCD.

The caffeine dose-response curve for WT GFP-hRyR2 yielded an EC_{50} and Hill slope similar to those obtained for untagged rabbit RyR2 expressed in HEK cells (EC_{50} 1.1 $\pm$ 0.1 mM, Hill slope 1.29 $\pm$ 0.1) using similar Ca^{2+} release measurement techniques (Du et al., 1998). This indicates that these channels are similarly activated and that the N-terminal GFP tag does not interfere with RyR2 function, or alter channel sensitivity to caffeine as seen with RyR1 (Treves et al., 2002), which is in agreement with other RyR2 studies (George et al., 2003a). Moreover, the conformational and functional differences that exist between RyR1 and RyR2, especially with respect to channel activation (see sections 1.3.1., 1.4.2.5. and 1.4.3.2.), strongly suggested that N-terminal tagging of RyR2 would not alter function.

It can be seen that the amplitude of Ca^{2+} release (represented by F/F_0) increases with the caffeine dose up to 10 mM, with a pronounced quench in the signal seen at 40 mM (see Figures 4.7-4.9). It could be argued that inclusion of these measurements in the curve would produce artefactual results. However, calculation of the dose-response relationships without this point did not result in a marked change in the EC_{50} or Hill slope values.

4.4.3. $N^{2386}I$ and $R^{176}Q/T^{2504}M$ mutants demonstrate enhanced caffeine-induced Ca^{2+} release

$N^{2386}I$ and $R^{176}Q/T^{2504}M$ channels exhibited enhanced sensitivity to caffeine activation (Figure 4.8.) and augmented peak Ca^{2+} release (Figure 4.9.), suggesting that these mutants exhibit a 'gain-of-function' on activation. This is in accordance with a current model of RyR2 mutant hyper-sensitisation leading to augmented cytoplasmic Ca^{2+} levels which underpin the pathogenesis of SCD. However, even though the activation of these mutants leads to greater release, the temporal profile of their Ca^{2+} transients are different, with $N^{2386}I$ exhibiting an increased rate of release and Hill coefficient, and $R^{176}Q/T^{2504}M$ transients taking a longer time to decay to half maximal amplitude. This is reflected in Figure 4.6., which shows that the forms of the Ca^{2+} transients from these two mutants are clearly different. This suggests that different mutations may affect different aspects of Ca^{2+} release while nevertheless resulting in the same macroscopic effect.

However, the time to decay to half maximal amplitude does not directly represent channel deactivation and is more of an estimation of the rate of Ca^{2+} removal from the cytosol by pumps and exchangers. The expression levels and activity of these would critically affect the shape of the evoked Ca^{2+} transients and these parameters will be discussed in the next chapter.

It has been hypothesised that defective intra-RyR2 interaction may underpin the pathogenesis of SCD (Yamamoto & Ikemoto, 2002), and interestingly, the mutational loci of the $R^{176}Q$ and $T^{2504}M$ mutations (those that co-segregate with the affected phenotype) map to two regions of the RyR2 polypeptide proposed to mediate auto-regulation of channel activity (Yamamoto & Ikemoto, 2002). In light of this, it was investigated whether the presence of these two mutations in the same polypeptide potentiated their respective impact on RyR2 functionality. It was found that both single mutations resulted in channels which exhibited augmented Ca^{2+} release, suggesting that they both have an effect on channel function, and that neither of which is the result of a benign polymorphism. However, their caffeine sensitivity was

not significantly different to that of the WT, demonstrating that they do not exhibit such extreme functional characteristics alone as they do when in combination within the conformation of the protein. In spite of this, the characteristics of the 'double' mutant cannot simply be extrapolated from the functional effects of these single mutations, pointing to an additional level of complexity in the regulation of these channels. These mutations are situated at loci that are slightly removed from the proposed sites of N-terminal and central domain interaction (590-639 a.a. with 2460-2492 a.a., Yamamoto & Ikemoto, 2002), suggesting that the presence of one mutation may alter protein conformation in the vicinity of the interacting domain, but because it is not situated within the site itself, does not result in significant 'unzipping'. However, it could be speculated that the presence of both mutations cause sufficient disruption of the protein structure for 'unzipping' to occur, leading to hyper-activation. It is also possible that changes to the protein architecture caused only by the two mutations in combination may affect the binding of an accessory protein (such as that which occurs as a result of channel destabilisation on heart failure (Oda et al., 2005)), resulting in further channel dysregulation. Indeed, this may explain why the Ca^{2+} release properties of $R^{176}Q/T^{2504}M$ channels cannot be deduced from its constituent mutants.

4.4.4. *$L^{433}P$ exhibits desensitised caffeine-induced activation*

In contrast, the $L^{433}P$ mutant was less sensitive to activation by caffeine and exhibited a maximal release which was comparable to that of the WT channel. This characterisation of a desensitised RyR2 mutant fundamentally challenges the current perception that all SCD-linked RyR2 mutations represent straightforward 'gain-of-function' channelopathies. In this context, it should be noted that in cardiomyocytes, RyR2 inhibition dramatically perturbs intracellular Ca^{2+} fluxes resulting in subcellular alternans (Diaz et al., 2002), a phenomenon characterised by a beat-to-beat alteration of large and small amplitude Ca^{2+} transients which can lead to ventricular fibrillation (VF) and sudden cardiac death (Pastore et al., 1999). In cardiomyocytes, depressed RyR2 activity would result in a reduced amplitude Ca^{2+} transient, consequently less Ca^{2+} would be extruded by the NCX and more would be sequestered in the SR (Bers, 2002). This would make more Ca^{2+} available for the next beat, resulting in a large Ca^{2+} transient, which in turn would lead to increased extrusion and decreased sequestration, meaning that the next transient would have a reduced amplitude (Diaz et al., 2004; Eisner et al., 2000). However, evidence from work on atrial myocytes has indicated that the SR Ca^{2+} content is not different after

either the small or the large amplitude Ca^{2+} transient (Hüser et al., 2000), suggesting that alterations of SR Ca^{2+} release are more important than alterations of SR Ca^{2+} content, as is the case in this study (see Figure 4.10). In light of this, it has been suggested the reduced amplitude transients affect the next release because full Ca^{2+}-dependent inactivation of the channels has not been achieved, meaning that the RyRs are more readily activated at the next beat.

Interestingly, it has also been shown that Ca^{2+} transients which occur during alternans are notably prolonged (Kockskämper & Blatter, 2002; Diaz et al., 2002), and are similar to those seen from $L^{433}P$. Thus depression of RyR2 $L^{433}P$ channel function may represent an alternative mechanism in the pathogenesis of SCD.

Recently, it has been suggested that CPVT may underlie many swimming-triggered cardiac events, also thought to be caused by LQT1 which have occasionally been associated with T-wave alternans (Choi et al., 2004; Yoshinaga et al., 1999). In addition, swimming is an activity which would be more likely to predispose an individual to EADs (rather than DADs, which are assumed to precipitate CPVT/ARVD2) owing to the lower heart rate caused by the voluntary apnoea and cold water immersion. Intriguingly, it has been shown that reduced RyR2 Ca^{2+} transients can also lead to delayed inactivation of I_{Ca}, resulting in AP prolongation providing a substrate for EADs (Gomez & Richard, 2004). However, it remains to be seen as to whether this could be a possible mechanism of arrhythmia for swimming-triggered CPVT.

It should be noted that although this is the first report of a desensitised RyR2 mutant, channelopathies arising from 'reduction-of function' or even 'loss-of-function' mutations in other channels have long been known to associate with cardiac pathology and sudden death (for reviews see Keating & Sanguinetti, 2001; Towbin, 2001; Marban, 2002). In particular, mutations in the β subunits of both the slow and rapidly activating delayed rectifier K^+ channels (*mink* and *MiRP1*) cause reductions in function by shifting the voltage dependence of activation or diminishing the K^+ current respectively, resulting in long QT syndromes (LQT) type 5 and 6. Indeed, different mutations in the cardiac Na^+ channel (*SCN5A*) can result in gain-, reduction-,or loss-of-function effects on channel function, which all lead to slightly different forms of cardiac arrhythmia (LQT3 (Sanguinetti, 1999; Priori et al., 2003), idiopathic ventricular fibrillation (Chen et al., 1998; Krishnan & Antzelevitch, 1991) and Brugada syndrome (Brugada & Brugada, 1992) – see Table 1.4.).

However, more detailed investigation of the amplitude and temporal aspects of Ca^{2+} release through $L^{433}P$ suggests that its desensitised caffeine-activation may have affected the dynamic of the Ca^{2+} transients themselves such that a more sustained

release of the same peak amplitude resulted. Indeed, it can be seen from Figures 4.6. and 4.8. that transients through $L^{433}P$ rise faster and decay more slowly compared to those through the WT. This would presumably prolong the time for which the intracellular [Ca^{2+}] is elevated and may result in a greater amount of Ca^{2+} being released. Therefore, although the action of this mutation can initially be viewed as a 'reduction-of–function' due to its desensitised activation, once activated the mode of Ca^{2+} release is enhanced, not by an increase in peak amplitude as with the 'gain-of-function' mutants characterised, but by an increase in the duration of release. Thus, it is important to stress that despite significant functional heterogeneity, the finding that caffeine activation of all RyR2 mutants characterised in this study resulted in augmented cytoplasmic Ca^{2+} levels following cellular stimulation, is in compliance with the occurrence of cytoplasmic Ca^{2+} overload underlying VT (see Figure 4.12.). In this context, this data draw close parallels with the observed functional heterogeneity of RyR1 mutations associated with MH and CCD, where profound functional differences between RyR1 mutants underpin similar disease phenotypes (McCarthy et al., 2000 and see section 1.5.1.1.).

At first the decreased sensitivity of $L^{433}P$ could be interpreted as a result of reduced amplitude transients which are a consequence of a decreased ER load, as has been observed with 'leaky' CCD mutations, present in an analogous region of RyR1 (e.g. $T^{523}S$). Such mutants are thought to be inherently 'leaky', leading to an increase in the resting Ca^{2+} level in the absence of channel activation by halothane, accordingly these patients suffer from hypotonia and muscle weakness from infancy (Tong et al., 1999b; Lynch et al., 1999; Avila & Dirksen, 2001). In this study, measurement of the ER loads of cells expressing mutant or WT RyR2 showed that they were comparable, indicating that the observed functionality of $L^{433}P$ is not likely to be the result of the actions of this mutant channel on the status of the ER prior to activation. However this issue is complex, and may involve upregulation of other Ca^{2+} handing proteins in an attempt to re-establish Ca^{2+} homeostasis, a matter which will be addressed in the next chapter.

In addition, while a mode of channel dysfunction characterised by enhanced basal activity adequately explains the muscle weakness seen in CCD patients, it is not compatible with the clinical presentation of CPVT/ARVD2, since most of the affected individuals exhibit a normal resting phenotype with no sign of cardiopathology and with arrhythmia being precipitated mainly under conditions of physical/emotional stress.

Alternatively, elements of the functionality of $L^{433}P$ are closer to those of the 'EC uncoupled' MH/CCD mutants which can still undergo CICR and, when expressed as

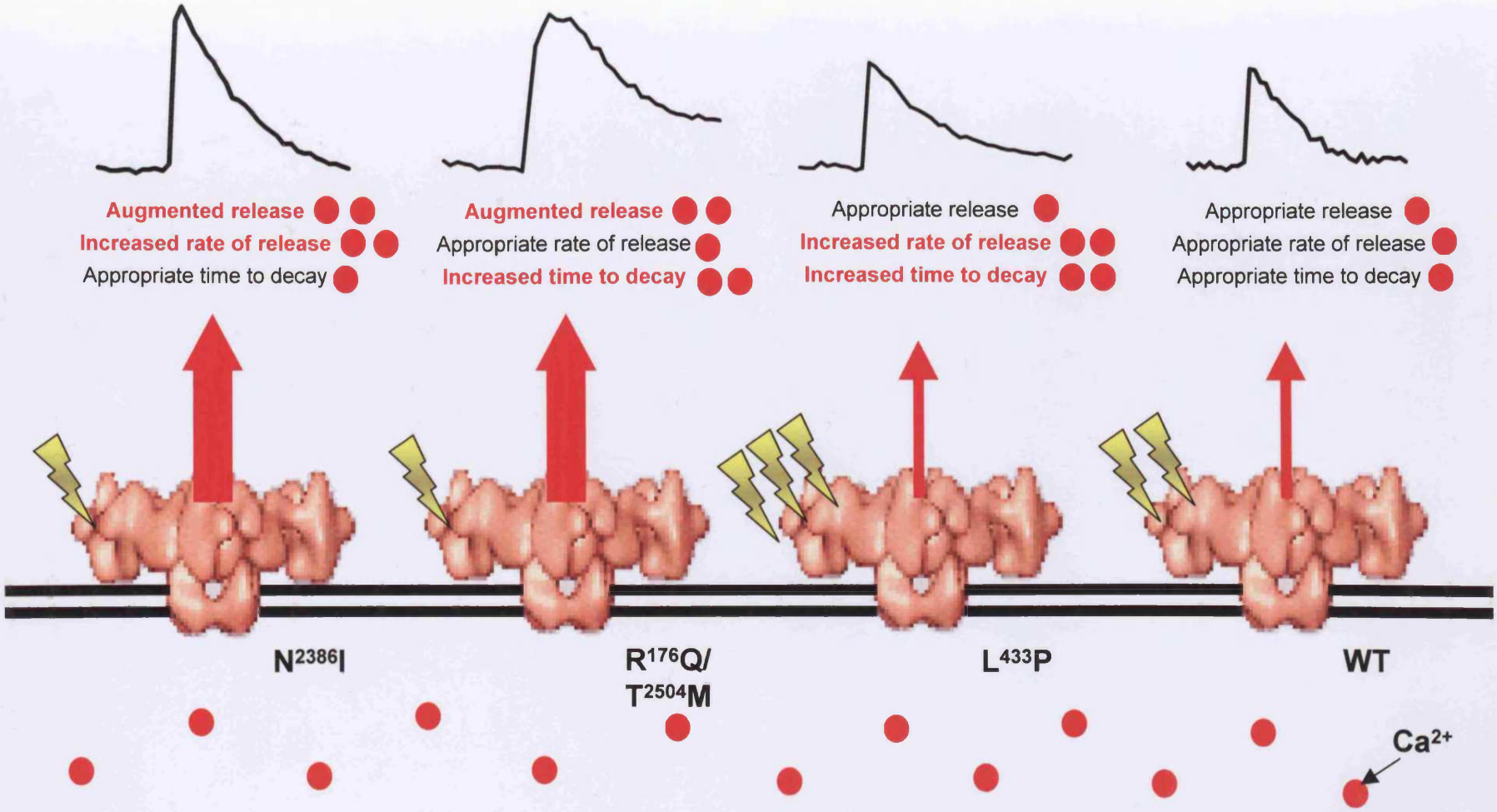

Figure 4.12. Functional heterogeneity of ARVD2-linked mutants is still predicted to result in elevated cytoplasmic Ca^{2+} following maximal caffeine-induced channel activation. The number of thunderbolts represents the dose of caffeine required to produce comparable activation of the channels and the thickness of the red arrow represents the magnitude to Ca^{2+}release. Consideration of both amplitude and temporal characteristics of the transients revealed that although they do not all exhibit augmented peak Ca^{2+} release, elevated cytoplasmic Ca^{2+} levels (represented by the red circles) may result due to sustained release.

heterotetramers with WT RyR1, exhibit a decreased amplitude of Ca^{2+} in the presence of a full Ca^{2+} store (Brini et al., 2005). However, these mutants are exclusively found in the C-terminal of the channel and are thought to disrupt the permeation of Ca^{2+} through the pore (Avila et al., 2003).

Mutations in MH domain 2 of RyR1 have also been characterised as having a decreased sensitivity to activation by caffeine and 4-cmc (Du et al., 2001a), effects which lead the authors to speculate that this region constitutes the caffeine and 4-cmc binding sites, though this is unlikely since other mutations in this region actually enhance the caffeine response (Tong et al., 1997), and the binding site for 4-cmc has since been found to be in the C-terminus (Fessenden et al., 2004). This work clearly demonstrates however, that mutation of RyR1 can result in a 'reduction-in-function' which is not the product of a decrease in ER load (Du et al., 2001a), suggesting that this could also be possible for mutants of RyR2. Furthermore, this work shows that two different mutations within the same domain of the RyR can have heterogeneous effects on function.

Interestingly, it has been speculated that the interaction between caffeine and RyR2 may be mediated by a portion of the N-terminal domain (amino acids 305-2150), which encompasses the $L^{433}P$ locus (Masumiya et al., 2003). This suggestion was made on the basis that deletion of this region abolishes the caffeine response. However, while it is likely that the caffeine binding domain of RyR2 is in the N-terminus of the protein (George et al., 2004), the extent of this deletion (comprising ~37% of the entire protein) means that the exact site of caffeine interaction may still be removed from the mutated locus, therefore although additional work is required it is unlikely that the $L^{433}P$ locus is the caffeine interaction site since this mutant exhibits peak caffeine-induced Ca^{2+} release comparable to that of the WT.

In summary, this data provides the first evidence that ARVD2-linked RyR2 mutants may be functionally heterogeneous. This is in contrast to other reports which have characterised mutants which are functionally similar (George et al., 2003a; Wehrens et al., 2003; Jiang et al., 2004). Importantly, the work presented here implies that there may not be a unifying mechanism underpinning RyR2 dysfunction, and thus the molecular basis of aberrant Ca^{2+} release in stress-induced VT and SCD appears to be more complex than previously anticipated. Subsequently, this may have profound consequences for the therapeutic modulation of RyR2 in the pathogenesis of VT, where stabilisation of the closed state is currently favoured (Wehrens et al., 2004b). Furthermore, these data clearly point to the requirement for comprehensive functional characterisation of newly identified RyR2 mutations on an individual basis.

Chapter 5

In situ characterisation of the Ca^{2+} sensitivity of ARVD2-linked RyR2 mutants

5.1. Introduction

5.1.1. Ca^{2+} regulation of RyR2

As discussed in Chapter 1, section 1.4.1.1., cytosolic Ca^{2+} has both excitatory and inhibitory effects on RyR2. The bimodal Ca^{2+} dependence of RyR2 is controlled by high-affinity Ca^{2+} activation and low-affinity Ca^{2+}-inactivation sites accessible from the cytosolic side of the channel (Meissner & Henderson, 1987; Chu et al., 1993; Laver et al., 1995; Xu et al., 1996). Many putative Ca^{2+} binding sites throughout the RyR1 sequence have been proposed from the use of site-directed antibodies (Chen et al., 1993), Ca^{2+} overlay assays (Chen and MacLennan, 1994) and RyR1/ RyR2 chimeras (Du & MacLennan, 1999; Nakai et al., 1999; Fessenden at al., 2004 – see Chapter 1, Figure 1.16.).

Although inactivation of this isoform by cytosolic Ca^{2+} could not be demonstrated in many single channel or ryanodine binding studies (Rousseau et al., 1986; Chu et al., 1993; Du & MacLennan, 1999), others showed variable inhibition at 0.5-10 mM (Laver et al., 1995; Copello et al., 1997; Marengo et al., 1998; Györke & Györke, 1998; Li & Chen, 2001). Inactivation by 10 μM-1 mM Ca^{2+} has been observed in Ca^{2+} release studies with cardiac SR vesicles (Chamberlain et al., 1984; Zimanyi & Pessah, 1991; Chu et al., 1993) and permeabilized cells (Fabiato, 1985), which more closely mimic the membrane environment of the channel *in situ* than do the conditions of lipid bilayer experiments, suggesting that Ca^{2+}-dependent inactivation of RyR2 may be an important channel regulatory mechanism *in vivo*. The variability in the extent of inhibition at high cytosolic [Ca^{2+}] among various studies has been attributed to the fragility of the inactivation mechanism, which can be disrupted by high Cs^{+} concentrations and solubilisation in CHAPS detergent (Györke & Györke, 1998; Laver et al., 1995).

A single amino acid of RyR1 (E^{4032}) has been proposed to act as a 'Ca^{2+} sensor' since mutation of this conserved glutamate to alanine abolished caffeine response and ryanodine binding, though this may be simply due to disruption of the high affinity ryanodine binding site (Du & MacLennan, 1998). However, the corresponding mutant of RyR2 ($E^{3987}A$) displayed a 1000 fold reduction in Ca^{2+} sensitivity, without a change in the affinity of [^{3}H] ryanodine binding or single-channel conductance (Li & Chen, 2001), suggesting that the Ca^{2+} activation site is located in the C-terminus of the protein.

Importantly, the way in which RyR2 responds to cytoplasmic Ca^{2+} is also critically dependent on lumenal Ca^{2+}. In particular, high lumenal [Ca^{2+}] has been shown to

enhance the sensitivity of the cytosolic Ca^{2+} activation mechanism, and essentially reversed Ca^{2+} mediated inhibition (Györke & Györke, 1998). The inter-dependent nature of cytosolic and lumenal Ca^{2+} means their respective roles cannot easily be separated, thereby complicating the interpretation of experiments in which they are altered.

5.1.2. Mechanisms of RyR2 dysfunction in SCD

Recently, it was demonstrated that arrhythmia-linked mutants of RyR2 had an increased sensitivity to lumenal Ca^{2+} activation (Jiang et al., 2004), resulting in a lower ER Ca^{2+} threshold for spontaneous release (a process the authors refer to as store-overload-induced Ca^{2+} release (SOICR)). This work would suggest that disruption of lumenal Ca^{2+} sensing is a pathological process, and since the mutants investigated were all situated either in the channel pore ($N^{4895}D$) or in close proximity ($N^{4104}K$, $R^{4497}C$) it may be that they may cause disruption or alteration of lumenal Ca^{2+} binding sites. This raises the question of whether mutations in the N-terminus and central domain of the protein result in a similar lumenal sensitisation by inducing long-range structural changes, and this remains to be determined. However, it is probable that the complex nature of RyR structure-function, the number of reported mutations in different domains, together with the phenotypic heterogeneity would preclude a common mechanism of mutant RyR2 dysfunction in arrhythmia.
Other proposed mechanisms that have been investigated to date include the idea that mutant RyR2 channels ($S^{2246}L$, $R^{2474}S$, $R^{4497}C$) may be hyperphosphorylated, leading to the dissociation of FKBP12.6 (Wehrens et al., 2003). However mutants ($S^{2246}L$, $N^{4104}K$, $R^{4497}C$) were also found to show sensitised Ca^{2+} release by an FKBP12.6-independent mechanism (George et al., 2003a), and one was revealed as disrupting intra-RyR interactions ($R^{2474}S$; Yamamoto & Ikemoto, 2002). Some mutants have also been shown to exhibit a loss of Mg^{2+} inhibition ($P^{2328}S$, $Q^{4201}R$, $V^{4653}F$; Lehnart et al., 2004). This is of particular interest since it is known that Mg^{2+} and Ca^{2+} share a common inhibitory mechanism (Laver et al., 1997), and it has been proposed that channel inhibition by Mg^{2+}, rather than by Ca^{2+} is the physiologically relevant mechanism (Lamb et al., 1993). This theory would provide an alternate explanation for why RyR2 only shows inhibition by mM Ca^{2+} in bilayer studies, when $[Ca^{2+}]$ never reaches this level in cardiac muscle, even though channel inhibition at lower Ca^{2+} levels has been seen in more native systems (see section 5.1.1.).
There is therefore no consensus mechanism, which is applicable to all mutations. Noticeably, the mutations characterised so far are located in the central domain and

C-terminus of the protein, however there seems to be no correlation between mechanism and mutational locus, or between mechanism and the amino acid change.

Table 5.1. details the nature of the each CPVT/ARVD2-linked RyR2 amino acid substitution, which are summarised with respect to mutational locus in Figure 5.1. It can be seen that hydrophobicity and conformation dependent changes dominate in the N-terminus, and while these are still quite common in the central domain, more conservative changes are also observed here. These are also quite prevalent in the C-terminus, especially in the part of the channel which forms the conductance pathway (~4800-4900 a.a., see Table 5.1.). Such conservative amino acid changes are also found in the pore region of RyR1, and are normally associated with 'EC uncoupled' CCD channels (Brini et al., 2004). Substitution of a similar residue would imply that these regions of the protein structure may be especially sensitive to alteration, and that they are essential for channel function. A change in the size of amino acid at loci in the C-terminus is also associated with CPVT/ARVD2, suggesting that the channel architecture is particularly constrained in this region. There is also a greater variety in the type of substitution seen in the C-terminus of the protein, though this may merely be due to the fact that this locus contains the greatest proportion of mutations.

5.1.3. RyR2 dysfunction as a result of defective Ca^{2+} sensing

The results in Chapter 4 show that ARVD2-linked mutants of RyR2 exhibited markedly altered caffeine sensitivity compared to WT. As caffeine is thought to act as an RyR2 agonist by sensitising the channel to ambient Ca^{2+} (Rousseau & Meissner, 1989), it could be inferred that a shift in the caffeine sensitivity of the channel might correspond to a shift in the Ca^{2+} sensitivity (Gomez & Richard, 2004). However, this cannot always be inferred since caffeine is known to have two modes of action, with higher doses (significantly 40 mM, see section 5.4.2.) having a Ca^{2+}-independent effect (Sitsapesan & Williams, 1990).

It has been proposed that altered sensitivity of mutant RyR2 to cytoplasmic [Ca^{2+}] ($[Ca^{2+}]_c$) may underlie SCD in arrhythmia-susceptible individuals (Choi et al., 2004), and even though lumenal Ca^{2+} sensing has been implicated in channel dysfunction, the sensitivity of RyR2 mutants to cytosolic Ca^{2+} has not yet been investigated. In light of this, the work presented in this chapter was carried out to investigate the sensitivity of the functionally heterogeneous ARVD2-linked N-terminal and central domain mutants to $[Ca^{2+}]_c$, in a permeabilised, living cell context. This represents a

$P^{164}S$	P	important in determining conformation	$N^{4097}S$	N	larger amino acid, otherwise similar
	S	H-bonding, possible phosphorylation		S	smaller amino acid, otherwise similar
$R^{176}Q$	**R**	**positive charge**	$N^{4104}K$	N	no charge, H-bonding
	Q	**no charge, H-bonding**		K	positive charge
$R^{414}L$	R	positive charge, hydrophilic	$E^{4146}K$	E	acidic, negative charge
	L	no charge, hydrophobic		K	basic, positive charge
$R^{414}C$	R	positive charge	$T^{4158}P$	T	H-bonding
	C	forms disulphide bonds		P	possible alteration in conformation
$I^{419}F$	I	similar amino acids	$Q^{4201}R$	Q	no charge, H-bonding
	F			R	positive charge
$R^{420}W$	R	positive charge, hydrophilic	$R^{4497}C$	R	positive charge
	W	no charge, hydrophobic		C	forms disulphide bonds
$L^{433}P$	**L**	**hydrophobic**	$F^{4499}C$	F	hydrophobic
	P	**possible alteration in conformation**		C	forms disulphide bonds
$S^{2246}L$	S	hydrophilic, H-bonding, possible phosphorylation	$M^{4504}I$	M	similar amino acids
	L	hydrophobic		I	
$V^{2306}I$	V	similar amino acids	$A^{4510}T$	A	hydrophobic
	I			T	hydrophilic, H-bonding
$E^{2311}D$	E	similar amino acids	$A^{4607}P$	A	hydrophobic
	D			P	possible alteration in conformation
$P^{2328}S$	P	important in determining conformation	$V^{4653}F$	V	aliphatic small amino acid
	S	H-bonding, possible phosphorylation		F	aromatic small amino acid
$N^{2386}I$	**N**	**hydrophilic, H-bonding**	$G^{4671}R$	G	acidic, no charge, weakly hydrophobic, small amino acid
	I	**hydrophobic**		R	basic, positive charge, hydrophilic, large amino acid
$A^{2387}P$	A	hydrophobic	$V^{4771}F$	V	aliphatic small amino acid
	P	possible alteration in conformation		F	aromatic small amino acid
$Y^{2392}C$	Y	H-bonding	$I^{4848}V$	I	similar amino acids
	C	forms disulphide bonds		V	
$R^{2401}H$	R	similar amino acids	$A^{4860}G$	A	similar amino acids
	H			G	
$A^{2403}T$	A	hydrophobic	$I^{4867}M$	I	similar amino acids
	T	hydrophilic, H-bonding		M	
$R^{2474}S$	R	positive charge	$V^{4880}A$	V	similar amino acids
	S	no charge, H-bonding		A	
$V^{2475}F$	V	aliphatic small amino acid	$N^{4895}D$	N	no charge
	F	aromatic small amino acid		D	negative charge
$T^{2504}M$	**T**	**hydrophilic, H-bonding**	$P^{4902}L$	P	important in determining conformation
	M	**Hydrophobic**		L	Hydrophobic
$L^{2534}V$	L	similar amino acids	$E^{4950}K$	E	acidic, negative charge
	V			K	basic, positive charge
$L^{3778}F$	L	aliphatic	$R^{4959}Q$	R	positively charge
	F	aromatic		Q	no charge, H-bonding
$G^{3946}S$	G	weakly hydrophobic			
	S	hydrophilic, H-bonding			

Table 5.1. The nature of CPVT/ARVD2-linked RyR2 amino acid substitutions. Mutations shown in bold represent the ones characterised in this study, and those in shaded boxes represent those characterised by others (see text for details). Figure 5.1. summarizes the relationship between the mutational locus and the nature of amino acid change, in particular it should be noted that mutations located in the conduction pathway of the channel (~4800-4900 a.a.) result from conservative amino acid substitutions, suggesting that non-conservative substitutions in this part of the protein are lethal. Despite the progress that has been made in determining the molecular basis of mutant RyR2 dysfunction, there is no link between mechanism, disease severity, mutational locus, or the nature of the amino acid change.

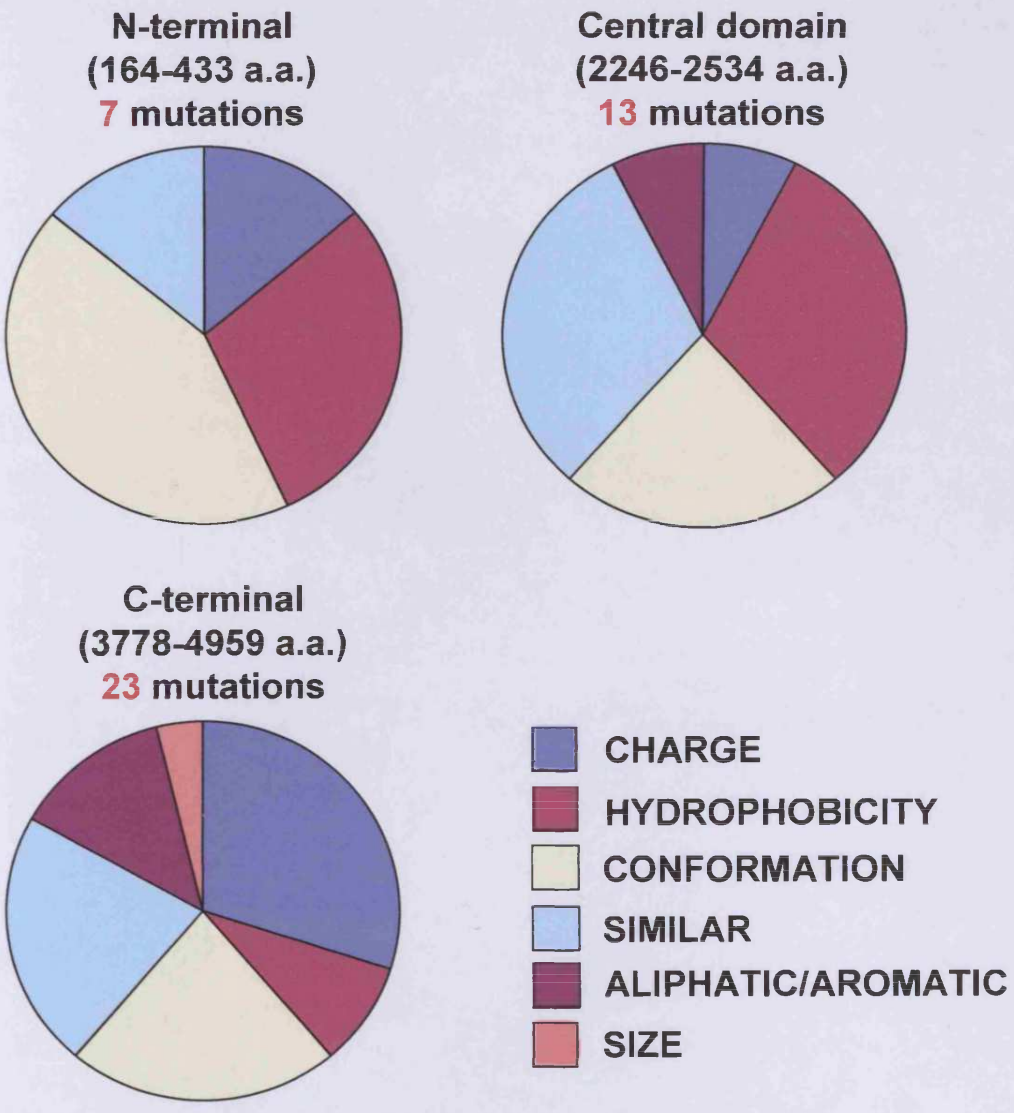

Figure 5.1. Summary of the relationship between CPVT/ARVD2 mutational locus and the type of amino acid change. Conformation and hydrophobicity based substitutions seem to dominate in the N-terminus, while more conservative and charge based changes are prevalent in the central domain and C-terminus. It should be noted however, that the apparent nature of each substitution type may be skewed by the number of mutations occurring in each domain. Thus, the large number of conservative changes in the conduction pathway (4800-4900 a.a.) of the channel appear under represented in this chart (see text and Table 5.1.). In instances where the substitution induced multiple changes (e.g. $L^{433}P$ changes both size and conformation), the one considered to cause most disruption to the protein structure was tallied (taken in the order: charge >conformation >hydrophobicity > size > aliphatic/aromatic).

novel approach to studying the Ca^{2+} sensitivity of RyR, which should reflect the activity of the channel under more physiological conditions, in contrast with other techniques which require removal of the channel from its cellular environment. As discussed above and in Chapter 4, section 4.1.1., isolation of the channel may cause problems with its stability, suggesting that the results obtained may not directly extrapolate to the physiological situation. In addition, isolation of the channels would expose them to *in vitro* oxygen tensions, which would critically affect RyR function (Sun et al., 2003; Eu et al., 2000) and so, not only do these cell based experiments represent the investigation of WT and mutant RyR2 channels in a more native membrane environment, but also their characterisation under more under physiological redox conditions.

5.2. Methods

5.2.1. *Cellular permeabilisation using streptolysin-O and manipulation of $[Ca^{2+}]_c$*

Cells were loaded with fluo-3 AM as described in section 2.2.5. prior to permeabilisation in KRH buffer containing fluo-3 AM (10 μM) and streptolysin-O (SLO) (George et al., 2003b). SLO is a prototype of the cholesterol-binding family of bacterial exotoxins, which forms large pores in the plasma membrane of mammalian cells and has been widely used to investigate cellular processes on a short time scale (George et al., 2003b; Li et al., 2002; Walev et al., 2001; Fawcett et al., 1998; Bhakdi et al., 1993). Upon membrane binding, toxin monomers oligomerize to form aggregates that represent large transmembrane pores whose diameters can reach 35 nm (Bhakdi et al., 1996). SLO permeabilisation conditions were titrated as recommended by Walev et al. (2001). Optimal plasma membrane-specific permeabilisation of ~80 % of the cell population was achieved using a SLO concentration of 100 U (~50 μg protein)/200 μl/1.5 x 10^5 cells/ 22 mm^2 for 30 minutes. Deviation from these parameters either resulted in insufficient permeabilisation (e.g. if the cells were seeded at a higher density (> 2 x 10^5), or if the time of incubation was decreased (< 25 minutes)), or cell death (e.g. if the incubation time was increased (> 35 minutes), or if the SLO concentration was increased (> 125 U)), possibly due to organellar damage, though the exact cause remains to be determined. Cells were considered to be sufficiently permeabilised if the addition of 2 mM $CaCl_2$ caused an increase in intracellular fluorescence that did not decrease with time (i.e. if cells failed to initiate an outward Ca^{2+} flux due to loss of plasma membrane pumps and exchangers – see Figure 5.2.). Cells retained viability and fluo-3 fluorescence after permeabilisation as assessed by ER Ca^{2+} release.

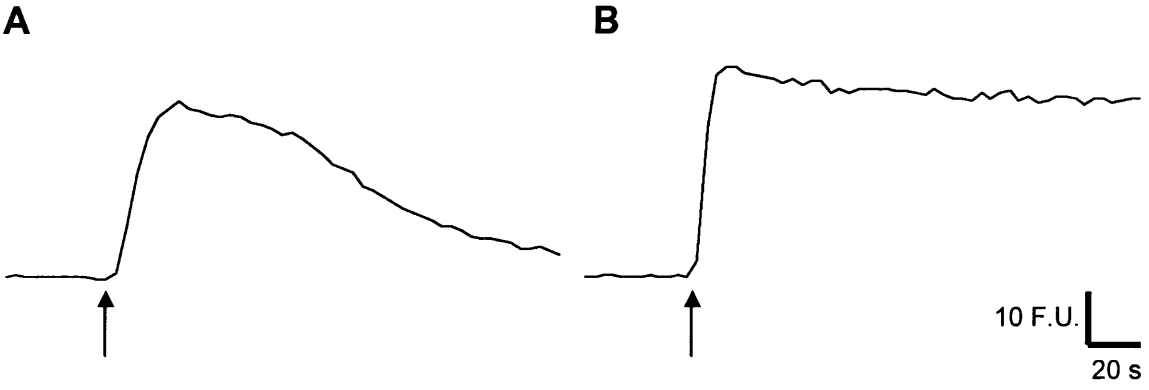

Figure 5.2. Ca^{2+} flux in intact and permeabilised HEK cells. The addition of 2 mM $CaCl_2$ (arrowed) increased the intracellular Ca^{2+}-dependent fluo-3 fluorescence in both intact (A) and permeabilised (B) cells. The Ca^{2+} decreases with time in intact cells as it is pumped out via plasma membrane pumps and exchangers, which are lost in permeabilised cells and so the elevated fluorescence intensity persists.

Following SLO permeabilisation, cells were immediately washed in solution (100 mM KCl, 20 mm HEPES, and 1 mM $MgCl_2$, pH 7.4), before incubation for 5 minutes in this solution containing known free $[Ca^{2+}]$ (0.1 nM - 61 μM) to clamp $[Ca^{2+}]_c$. Known $[Ca^{2+}]$ in these solutions was obtained using different ratios of 10mM EGTA and 10mM CaEGTA (see section 2.1.8.) calculated using REACT II software (Cybersolutions; http://www.cyber-sol.co.uk), shown in Table 5.2. It should be noted that although these solutions differed in the amount of free Ca^{2+}, the concentration of Mg^{2+} was kept constant. A schematic showing the entire permeabilisation/ equilibration procedure can be seen in Figure 5.3.

Solution (EGTA:CaEGTA ratio)	Free $[Ca^{2+}]$	Log $[Ca^{2+}]$
10E	0.1 nM	-10.00
14E:1CaE	25 nM	-7.60
10E:1CaE	42 nM	-7.38
4E:1CaE	83 nM	-7.08
3E:1CaE	126 nM	-6.90
1E:1CaE	380 nM	-6.42
1E:3CaE	1.14 μM	-5.94
1E:10CaE	3.43 μM	-5.46
10CaE	61.68 μM	-4.21

Table 5.2. Calibration solutions and their corresponding free $[Ca^{2+}]$. Ratios were calculated using REACT II software (Duncan et al., 1999). $[Mg^{2+}]$ was constant in each solution (1 mM).

Cells were equilibrated in these solutions for no more than 5 minutes in order to maintain ER Ca^{2+} load status and prevent resealing of SLO pores in high $[Ca^{2+}]$. In order to determine the apparent Ca^{2+} binding affinity of fluo-3 in HEK cells the cellular fluorescence at each clamped $[Ca^{2+}]_c$ was averaged over 20 seconds at 0.5 Hz, and the relationship between the known intracellular $[Ca^{2+}]$ and fluo-3 fluorescence was analysed by non-linear regression using GraphPad Prism software to yield an apparent K_d ($K_{d,\ app}$) of 733±143 nM (from n = 10 cells) (see Figure 5.4.).

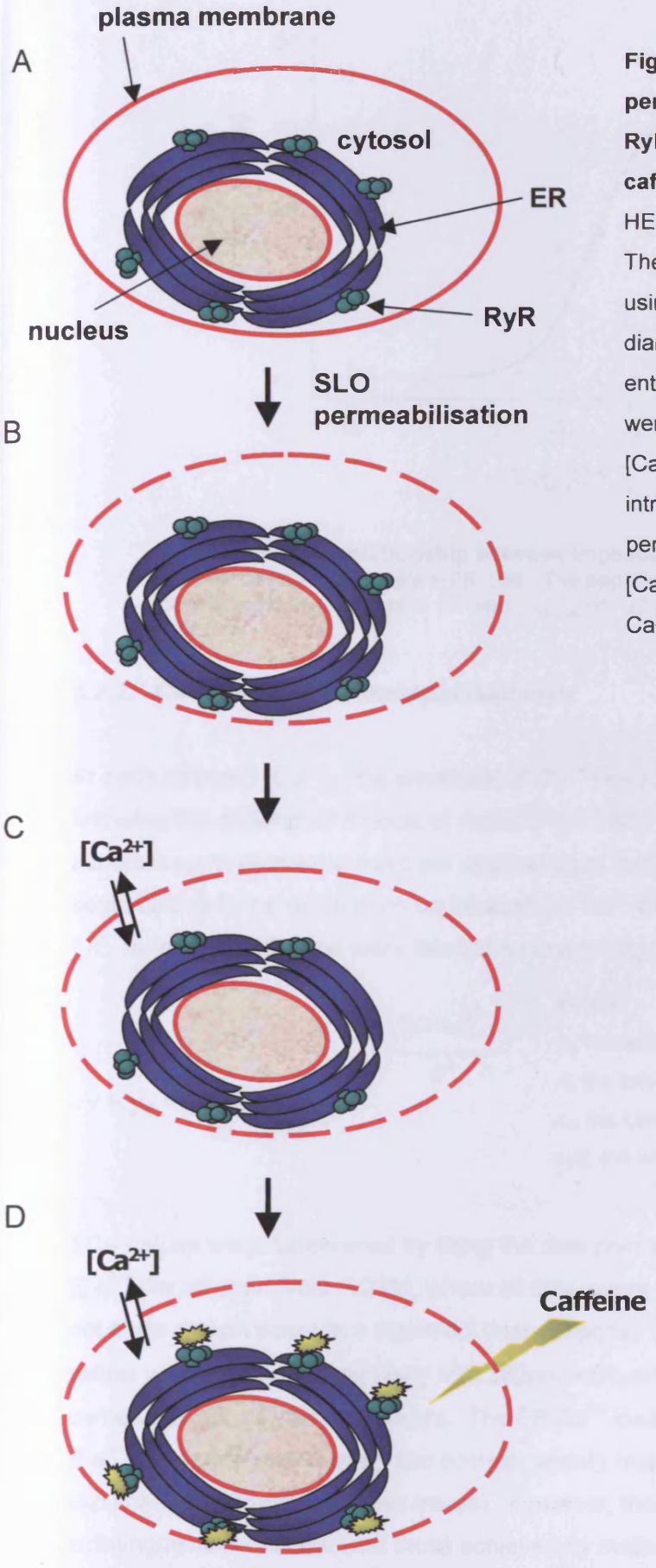

Figure 5.3. Schematic detailing SLO permeabilisation of HEK cells expressing RyR2, manipulation of $[Ca^{2+}]_c$ and caffeine-induced Ca^{2+} release. A) shows a HEK cell with various features labelled. B) The plasma membrane was permeabilised using SLO, creating pores < 35 nm in diameter so that only small molecules can enter/leave the cell. C) Permeabilised cells were immersed in solutions of known free $[Ca^{2+}]$. The free exchange of extra- and intracellular solutions due to permeabilisation allowed manipulation of the $[Ca^{2+}]_c$. D) Caffeine was used to trigger Ca^{2+} release at a range of imposed $[Ca^{2+}]_c$.

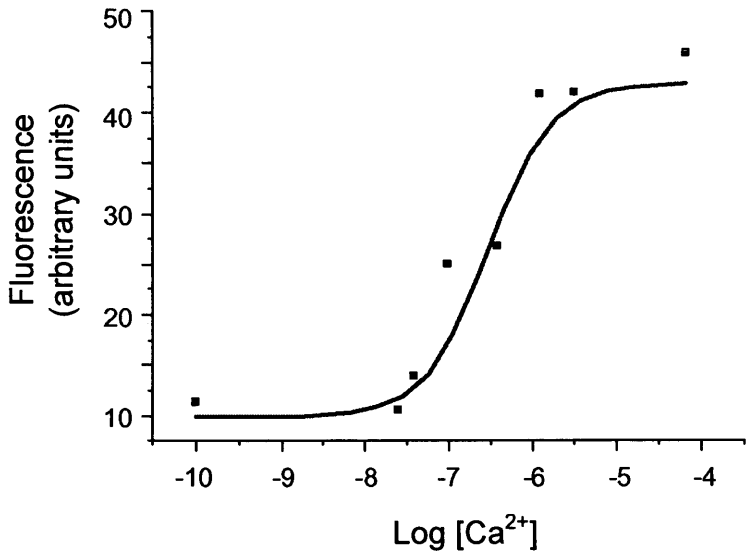

Figure 5.4. The relationship between imposed $[Ca^{2+}]_c$ and fluo-3 fluorescence in a single HEK cell. The apparent K_d was calculated from average measurements in 10 cells, $K_{d,\,app}$ of 733 ± 143 nM.

5.2.2. Ca^{2+} imaging of permeabilised cells

At each clamped $[Ca^{2+}]_c$, the amplitude of Ca^{2+} release via RyR2 was triggered following the addition of a bolus of caffeine (10 mM). In each instance, cells on separate coverslips were used per application of caffeine to negate the effect of sequential caffeine application on intracellular Ca^{2+} handling. Data were plotted as F/F_0 for each $[Ca^{2+}]_c$ and were fitted to a curve using a Gaussian equation.

$$y = y_0 + \frac{A}{w.\sqrt{\pi}/2} e^{-\frac{2(x-x_0)^2}{w^2}}$$

Where:

y_0, represents the baseline offset

A, the total area under the curve from baseline

x_0, the centre of the peak

$w/2$, the width of the peak at half height

EC_{50} values were determined by fitting the data points obtained with 0.1 – 380 nM $[Ca^{2+}]$ (for all apart from RQTM, where all data points were used since the curve does not show deactivation) to a sigmoidal dose response curve with variable slope. IC_{50} values were determined similarly with 380nm – 61 μM values. All analyses were carried out using Origin 7 software. The ER Ca^{2+} load in permeabilised cells at fixed $[Ca^{2+}]_c$ was determined using two complementary methods (see Figure 5.5. for explanation and representative traces). However, these methods yielded indistinguishable results, and those achieved by method B are shown in this thesis.

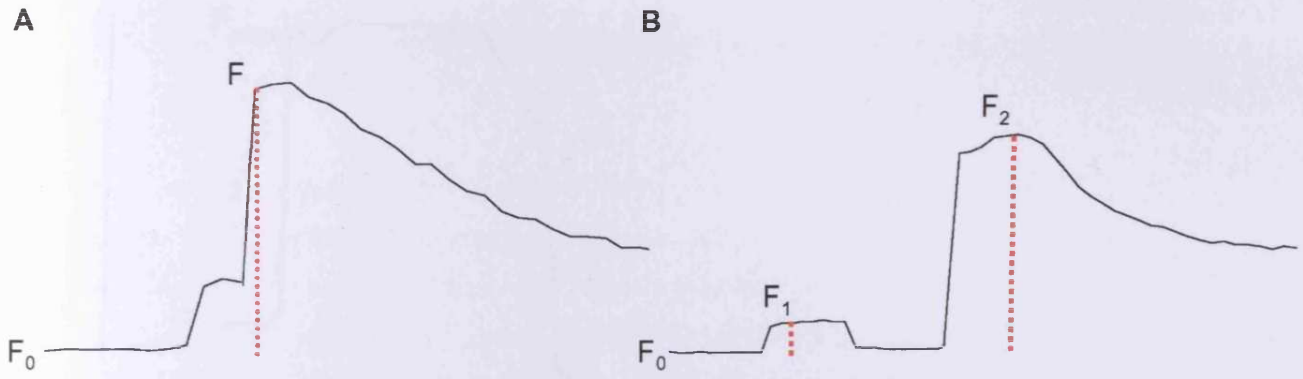

Figure 5.5. Estimation of the ER Ca^{2+} load in permeabilised cells using TG (5 µM). Representative transients which describe the two different methods used, which yielded indistinguishable results. Caffeine (0.5 mM) was added to identify cells expressing RyR2. A) shows the Ca^{2+} flux seen on addition of caffeine (0.5 mM) immediately followed by TG to a HEK cell expressing WT RyR2. B) shows the Ca^{2+} release in response to the caffeine dose (F_1), followed by a wash out with the appropriate known [Ca^{2+}] solution before addition of TG. The amplitude denoted by the red dashed line was measured as the total peak release (F, in method A, the sum of F_1+ F_2 in method B), which was expressed as a proportion of the basal fluorescence (F_0).

5.2.3. Measurement of basal Ca^{2+} levels in intact cells

Basal Ca^{2+} levels in cells expressing WT or mutant RyR2 were calculated from fluorescence data using the equation:

$$[Ca^{2+}] = K_{d,\,app}\,(F - F_{min})/(F_{max} - F)$$

(Grynkiewicz et al., 1985)

where F_{min} and F_{max} represent the minimum and maximum fluorescent signals determined following the addition of EGTA (20 mM) or ionomycin (2 µM) respectively, and F represents the initial fluorescence (see Figure 5.6.). Cells expressing recombinant WT or mutant RyR2 were identified by the addition of 0.5 mM caffeine, followed by wash-out and complete solution exchange.

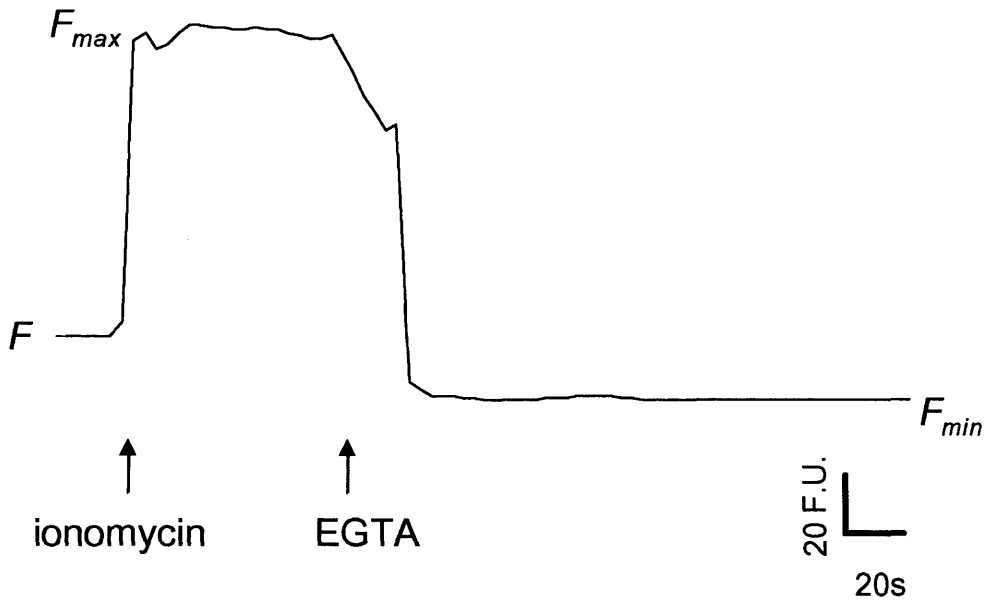

Figure 5.6. Determination of maximal (F_{max}) and minimal (F_{min}) Ca^{2+} dependent intracellular fluo-3 fluorescence. F_{max} and F_{min} were determined by the addition of the ionophore ionomycin (2 μM), and the Ca^{2+} chelator EGTA (20 mM) respectively. These values, in conjunction with the initial fluorescence (F), were used to calculate the resting cytosolic Ca^{2+} concentration.

5.3. Results

5.3.1. *The* in situ *Ca^{2+} dependence of caffeine triggered Ca^{2+} release of WT and mutant RyR2*

As demonstrated in Chapter 4, profound heterogeneity exists between the ARVD2 mutants characterised in this study, including a mutant which displayed a 'reduction-of-function'. The present work attempted to investigate the molecular basis of this functional heterogeneity, with respect to the Ca^{2+} sensitivity of mutant RyR2 channels, which was evaluated by the Ca^{2+}-dependence of caffeine triggered Ca^{2+} release in living HEK cells.

Recombinant WT RyR2 exhibited a bi-phasic curve with maximal caffeine activation occurring at $[Ca^{2+}]_c$ of 380 nM (see Figure 5.7.). As $[Ca^{2+}]_c$ increased > 380 nM, caffeine activation of RyR2 was progressively inhibited, returning to almost complete inhibition at $[Ca^{2+}]_c \sim 10$ μM. This shows that WT RyR2 channels exhibit Ca^{2+} dependent activation and inactivation in the cell, a phenomenon which is not generally seen in bilayer experiments, but has been observed in other experimental systems, as discussed in section 5.1.1.

The values of $[Ca^{2+}]_c$ for half-maximal channel activation (EC_{50}) and inhibition (IC_{50}) are given in Table 5.3.

RyR2	EC_{50} (nM)	IC_{50} (μM)
WT	42 ± 2	3.3 ± 0.6
$N^{2386}I$	45 ± 26	1.3 ± 1.3
$L^{433}P$	39 ± 9	24 ± 6.6*
$R^{176}Q/T^{2504}M$	146 ± 117	ND

Table 5.3. Ca^{2+} dependence of caffeine activation of ARVD2-linked RyR2 mutants. $[Ca^{2+}]_c$ required for half-maximal activation and inhibition (EC_{50} and IC_{50}, respectively) of WT and mutant RyR2 in response to caffeine (10 mM) was calculated following non-linear regression analysis of data shown in Figure 5.3. as described in the text. Data are given as mean ± SE (> 60 cells). ND represents not determined. *$p < 0.01$

The caffeine activation of human RyR2 in this permeabilised HEK cell system is in close agreement with the characterisation of caffeine activation of recombinant mouse RyR2 in planar lipid bilayers (EC_{50} 42 nM (cells) vs 93 nM (bilayers), Li & Chen, 2001), demonstrating that RyR2 remains fully functional following cellular permeabilisation. The $N^{2386}I$ mutation also exhibited a bi-phasic activation/inhibition

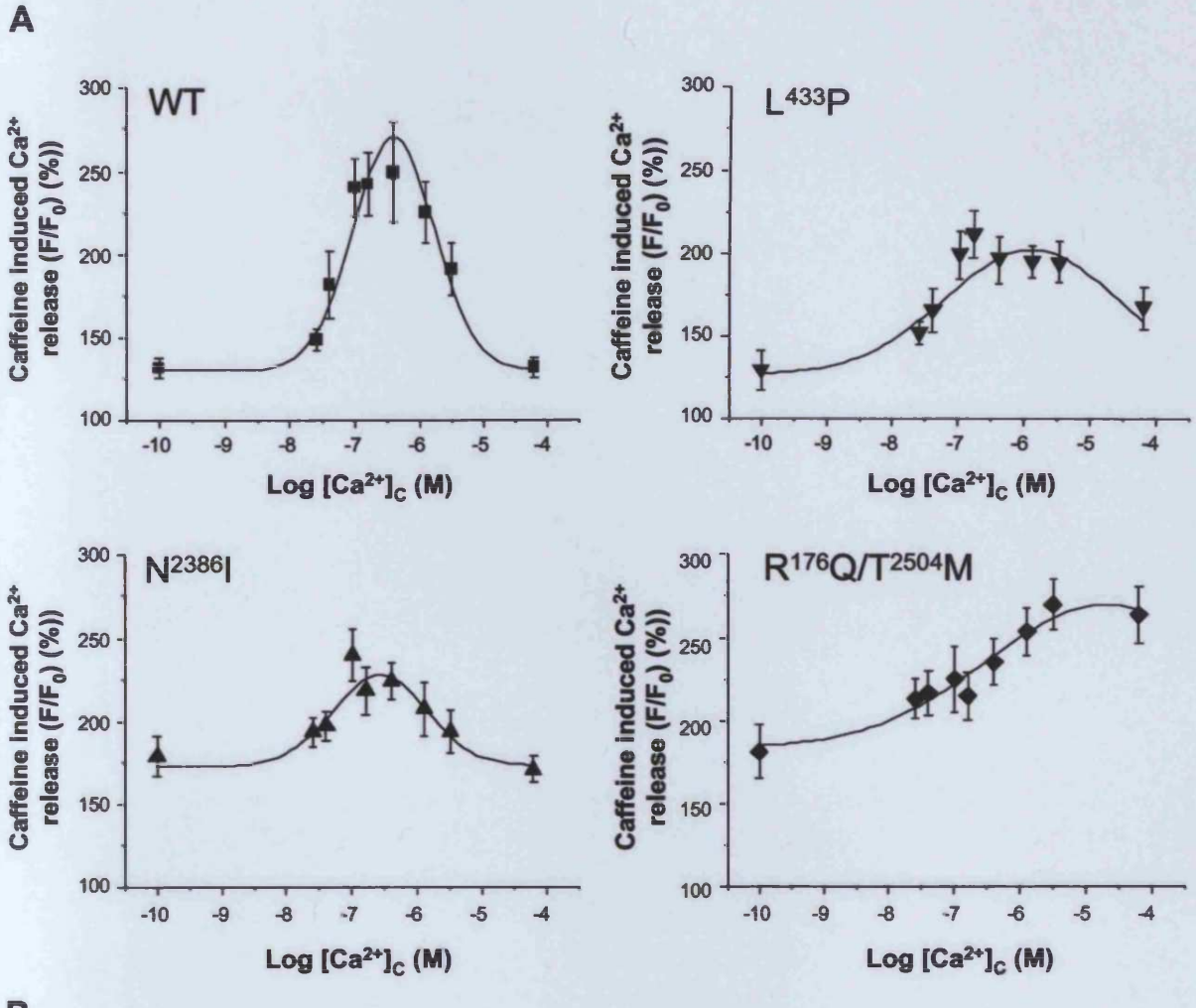

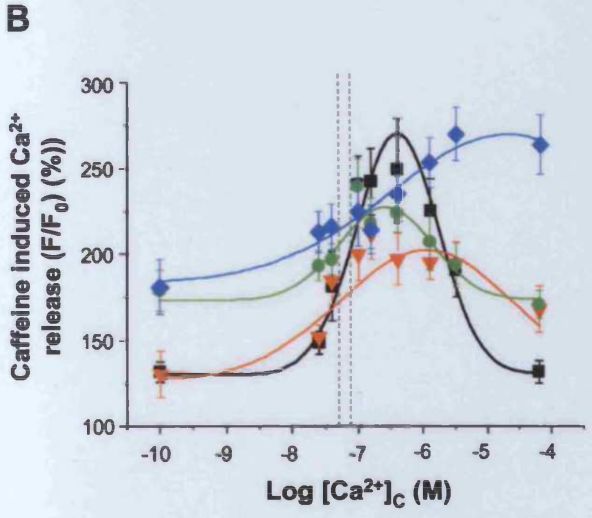

Figure 5.7. The Ca^{2+} dependence of caffeine activation of RyR2 mutants in living HEK cells. A) The activation of WT and mutant RyR2 following the addition of caffeine (10 mM) to SLO-permeabilised cells at clamped $[Ca^{2+}]_c$ was determined. B) WT (black), $L^{433}P$ (red), $N^{2386}I$ (green) and $R^{176}Q/T^{2504}M$ (blue) graphs overlaid. Vertical dashed bars indicate the range of resting $[Ca^{2+}]_c$ (~50-90 nM, i.e. $\log[Ca^{2+}]_c$ ~ -7.1 to –7.3) determined in intact (non-permeabilised) cells. Caffeine-induced Ca^{2+} release was determined as the peak change in fluorescence following caffeine addition (F) relative to resting fluorescent signals (F_0) and is expressed as a percentage. Data are given as means ± SE (n = 4 experiments, >15 cells analysed per experiment).

profile (Figure 5.7.) characterised by equivalent EC_{50} and IC_{50} values to those obtained for WT RyR2 (see Table 5.3.). However, these values mask the finding that this mutation profoundly perturbed the Ca^{2+} sensitivity of the channel. Strikingly, the $N^{2386}I$ channel exhibited marked caffeine activation (> 160% activation when compared with non-stimulated cells, ~ 30% higher than that of the WT) at 0.1 nM and 61 μM $[Ca^{2+}]_c$, indicating that this mutation resulted in a partial loss of Ca^{2+} dependent regulation.

$L^{433}P$, a mutant which in Chapter 4 showed desensitised caffeine-induced Ca^{2+} release, exhibited a similar Ca^{2+} dependent activation profile to WT RyR2, but showed a decreased sensitivity to Ca^{2+} inhibition when compared with WT RyR2 (see Table 5.3. for IC_{50} values). Like, $N^{2386}I$, the 'double' mutant $R^{176}Q/T^{2504}M$ was characterised by a similar EC_{50} to WT RyR2 that masked a significant Ca^{2+}-independence of caffeine activation of the channel. However, unlike $N^{2386}I$, the $R^{176}Q/T^{2504}M$ mutation resulted in a complete loss of Ca^{2+}-dependent inhibition of Ca^{2+} release following caffeine stimulation, and so IC_{50} values could not be calculated (Figure 5.7. and Table 5.3.).

5.3.2. Resting $[Ca^{2+}]_c$ levels in cells expressing WT or ARVD2-linked mutants of RyR2

Despite the apparent lack of Ca^{2+}-dependent channel modulation following caffeine stimulation, expression of the mutant channels does not condition resting, non-stimulated, intact cells to elevated $[Ca^{2+}]_c$ as shown in Figure 5.8. This suggests that mutant RyRs are appropriately regulated at rest, and would agree with the model of RyR2 Ca^{2+} release dysfunction triggered by cellular stimulation, in keeping with the normal phenotype of SCD-susceptible individuals at rest.

The range of experimentally determined resting $[Ca^{2+}]_c$ in intact cells is in the range of 50-90 nM (log $[Ca^{2+}]$ ~ -7.1-7.3) and is indicated by vertical dashed lines in Figure 5.9. Calculation of the magnitude of Ca^{2+} release following caffeine application to permeabilised cells 'clamped' at the measured resting $[Ca^{2+}]_c$ of non-permeabilised cells (using the formula in section 5.2.2.) predicted that $N^{2386}I$ and $R^{176}Q/T^{2504}M$ exhibited hyper-activated Ca^{2+} release (216 % and 228 %, respectively), when compared to WT RyR2 (186 %). In contrast, $L^{433}P$ was predicted to exhibit equivalent Ca^{2+} release (173 %) in response to caffeine addition. These values predicted from data obtained in permeabilised cells corroborate the data shown in Chapter 4 which assigns $N^{2386}I$ and $R^{176}Q/T^{2504}M$, but importantly not $L^{433}P$ as 'gain-of-function' channelopathies.

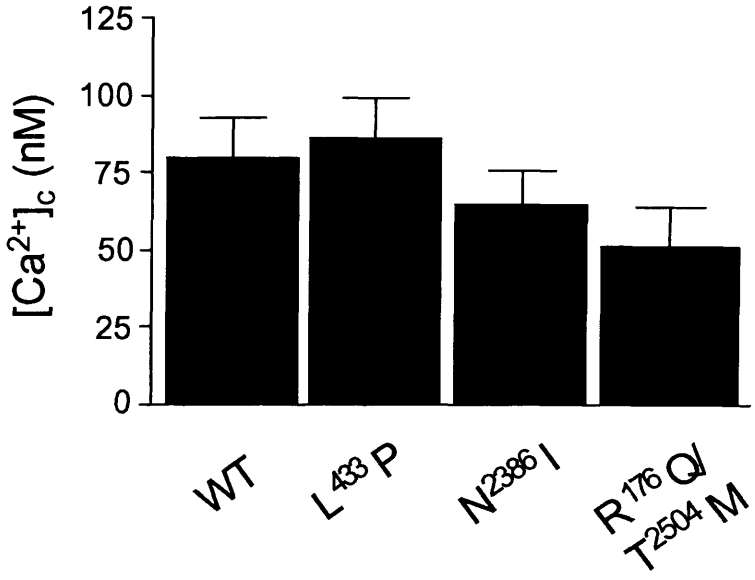

Figure 5.8. Resting Ca^{2+} levels in HEK cells expressing WT and mutant GFP-RyR2. These were measured by the method detailed in section 5.2.3. Data are given as mean ± SEM (n = 5, >12 cells per experiment) and are not significantly different at $p< 0.05$.

5.3.3. Investigation of the ER Ca^{2+} load of permeabilised cells expressing WT or mutant RyR2 at different $[Ca^{2+}]_c$

The amplitude of Ca^{2+} release through RyR is critically dependent on the status of the ER Ca^{2+} store. In light of this, the filling status of the ER Ca^{2+} store of cells expressing mutant or WT RyR2 was determined at each imposed $[Ca^{2+}]_c$. This would determine whether the different Ca^{2+} sensitivities of the SCD-linked mutants were due, in part, to accompanying changes in ER Ca^{2+} storage. Furthermore, it was important to ensure that the loss of Ca^{2+}-dependent inhibition was not due to changes in the ER following cellular permeabilisation/ $[Ca^{2+}]_c$ manipulation, since it has been shown that increasing $[Ca^{2+}]_c$ can lead to an increased store content in permeabilised cells (Orchard et al., 1998). Figure 5.9. shows comparable ER filling status in all cells at a range of imposed $[Ca^{2+}]_c$, indicating that the permeabilisation protocol did not significantly perturb the ER Ca^{2+} loading status. The relatively constant ER loads in these cells suggests specific SLO permeabilisation of the plasma membrane and not of the ER, indicating that the cytoplasm and the intracellular Ca^{2+} store remain physically and functionally compartmentalised. In addition, ER load values predicted by the trend lines at log $[Ca^{2+}]$ –7.1 to –7.3 (shown as dashed vertical lines) were not significantly different to those obtained in intact cells (see Table 5.4.). However, the predicted values from the permeabilised cells

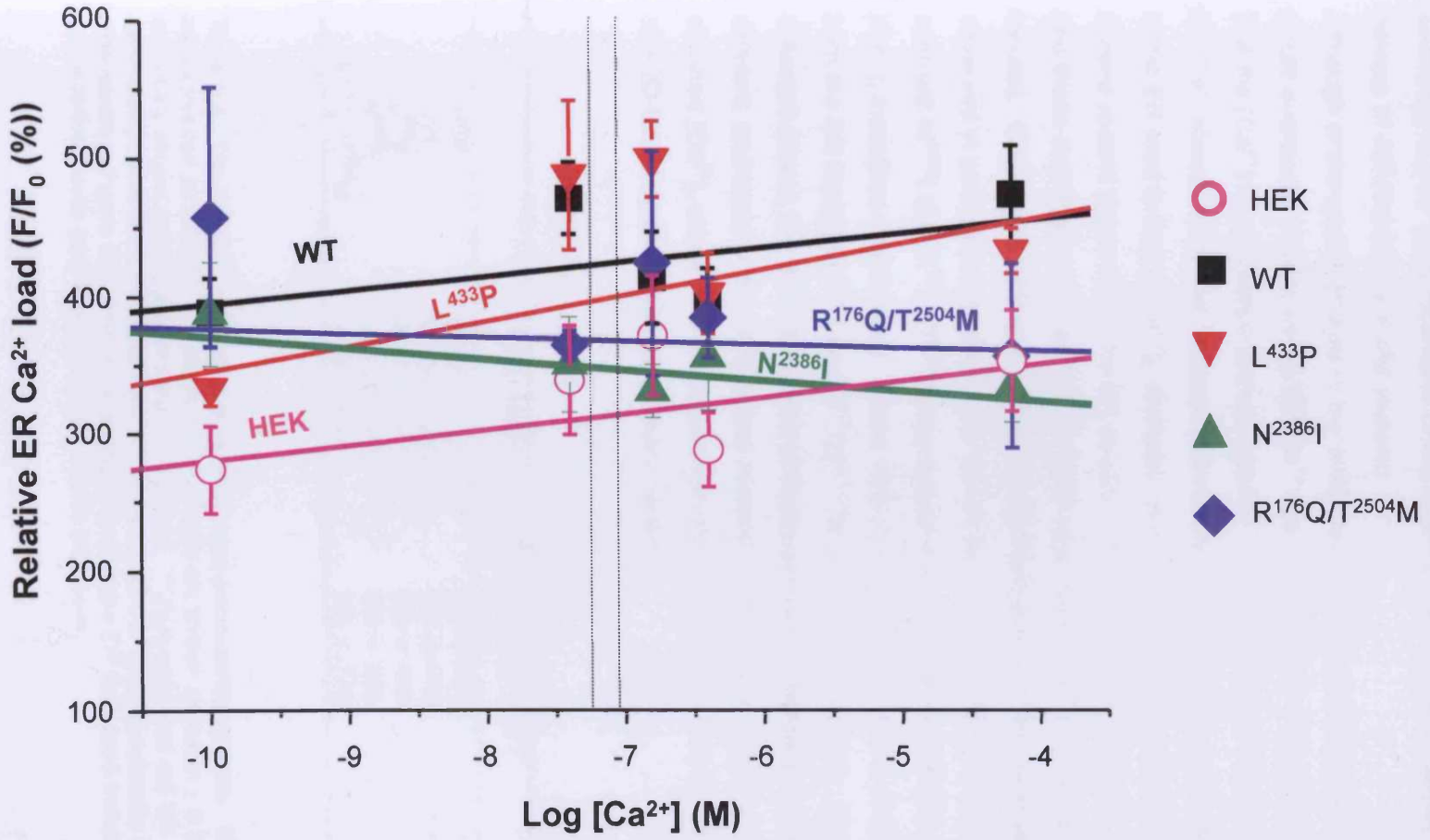

Figure 5.9. The ER Ca^{2+} store status remains unaffected following manipulation of $[Ca^{2+}]_c$. This was estimated in SLO-permeabilised cells at fixed $[Ca^{2+}]_c$ by determining peak release following the addition of caffeine (0.5 mM) and TG (5 μM) (see Figure 5.4.). Data represent the peak change in fluo-3 fluorescence (F) relative to the resting fluorescent signal (F_0) expressed as a percentage and are given as means ± SEM (n = 3 experiments, > 15 cells analysed per experiment). The vertical dashed lines indicate the estimated ER Ca^{2+} load at the $[Ca^{2+}]_c$ measured in non-permeabilised cells, which is in the range of ~50-90 nM (log $[Ca^{2+}]$ -7.1 to –7.3, see Figure 5.8). These values are in agreement with the range of experimentally determined ER Ca^{2+} loads of intact cells expressing these mutants (see Table 5.4.). The relative ER Ca^{2+} loads of cells expressing WT or mutant GFP-hRyR2 at each of the $[Ca^{2+}]_c$ imposed were not significantly different ($p>0.05$). The ER Ca^{2+} load values for cells expressing $L^{433}P$ at log $[Ca^{2+}]$ -7.38 and -6.90 are significantly different from that at -10.00, however this does not affect the trend of the line, which is not significantly different from WT at $p<0.05$.

are somewhat lower than those obtained with intact cells, indicating that the Ca^{2+} buffering capacity of the bathing solution may have affected the transient amplitude in permeabilised cells. Nevertheless, this data suggests that alterations in channel sensitivity to $[Ca^{2+}]_c$, independent of the lumenal Ca^{2+} store, underpin the functional defects of ARVD2-linked RyR2 mutants.

Although prolonged exposure to the extremes of $[Ca^{2+}]_c$ used in these experiments would eventually impact on the ER Ca^{2+} status, the data in Figure 5.9. demonstrates that the $[Ca^{2+}]$ manipulation protocol used (i.e. 5 minutes equilibration) maintained ER Ca^{2+} status. However, despite there being no statistically significant differences in the ER load in these $[Ca^{2+}]_c$ 'clamped' cells, two trends are apparent. First, there is a trend toward hyper-filling the ER as $[Ca^{2+}]_c$ is increased in untransfected HEK cells, and those expressing WT and $L^{433}P$ RyR2 (see Table 5.4. for relative gradient values). Since HEK cells are endogenously RyR deficient, the relative hyper-filling observed in untransfected cells here cannot be due to RyR-dependent processes. In contrast, $N^{2386}I$ and $R^{176}Q/T^{2504}M$ expression was associated with ER depletion as $[Ca^{2+}]_c$ increases (Table 5.4.). These data may be indicative of a small Ca^{2+} leak from the ER through $N^{2386}I$ and $R^{176}Q/T^{2504}M$ as $[Ca^{2+}]_c$ increases. However, as indicated above, the ER Ca^{2+} stores in these permeabilised cells are not significantly different, and none of the SCD-linked mutants studied here condition the cell to elevated $[Ca^{2+}]_c$ under non-stimulated conditions, indicating that at rest, the presence of SCD-linked mutations is functionally benign.

	Intact cells*	Permeabilised cells**	Gradient
HEK	352.56 ± 19.73	322 to 326	+ 0.607 ± 0.06
WT	463.58 ± 43.68	427 to 430	+ 0.505 ± 0.18
$L^{433}P$	409.77 ± 30.13	396 to 403	+ 0.782 ± 0.04
$N^{2386}I$	431.22 ± 4.3	354 to 358	- 0.727 ± 0.20
$R^{176}Q/T^{2504}M$	490 ± 38.01	368 to 370	- 0.122 ± 0.14

Table 5.4. The ER Ca^{2+} store status in intact and permeabilised cells. ER load values are expressed as F/F_0 (%). * Values for intact cells are shown as mean ± S.E.M. and were previously shown as normalised data in Chapter 4. ** Permeabilised cell ER load values were extrapolated from the trend lines in Figure 5.9. at the 'resting' cytosolic Ca^{2+} levels determined in Figure 5.8. The relative gradients of these ER Ca^{2+} load trend lines from permeabilised cells (see Figure 5.9.) are shown alongside.

5.3.4. *Expression of ARVD2-linked RyR2 mutants does not disrupt the expression profiles of endogenously expressed Ca^{2+} handling proteins*

It was important to determine the expression profile of key Ca^{2+} handling proteins within the ER, as the ER Ca^{2+} load determined could be influenced by altered expression of lumenal Ca^{2+} binding/modulating proteins following expression of mutant RyR2 channels. For example, the expression of WT and mutant CCD-linked RyR1 in HEK cells was found to result in the upregulation of SERCA2b expression, as a compensatory mechanism against enhanced store depletion (Tong et al., 1999b). However, equivalent levels of expression of WT or mutant RyR2 did not significantly perturb the endogenous levels of SERCA and calreticulin (CRT) proteins which are intimately involved in intracellular Ca^{2+} handling (Figure 5.10.). Although no detectable levels of CSQ were found in HEK cells, high levels of this protein were found in rabbit cardiac muscle, suggesting that this is an SR specific protein which is not expressed in non-muscle cells.

It should also be noted that the changes in the expression profile of CaM were also sought, however this was not possible because this protein was not able to be detected even in rabbit cardiac muscle homogenate with the antibody employed.

Thus, the comparable ER Ca^{2+} stores determined in Figure 5.9. were underpinned by similar expression profiles, suggesting that any disruption of Ca^{2+} handling which resulted from the expression of the mutant channels did not lead to any compensatory changes in the levels of proteins which maintain or regulate the ER status. This is in agreement with the idea that it is post-activation RyR2 channel dysfunction which results in arrhythmia.

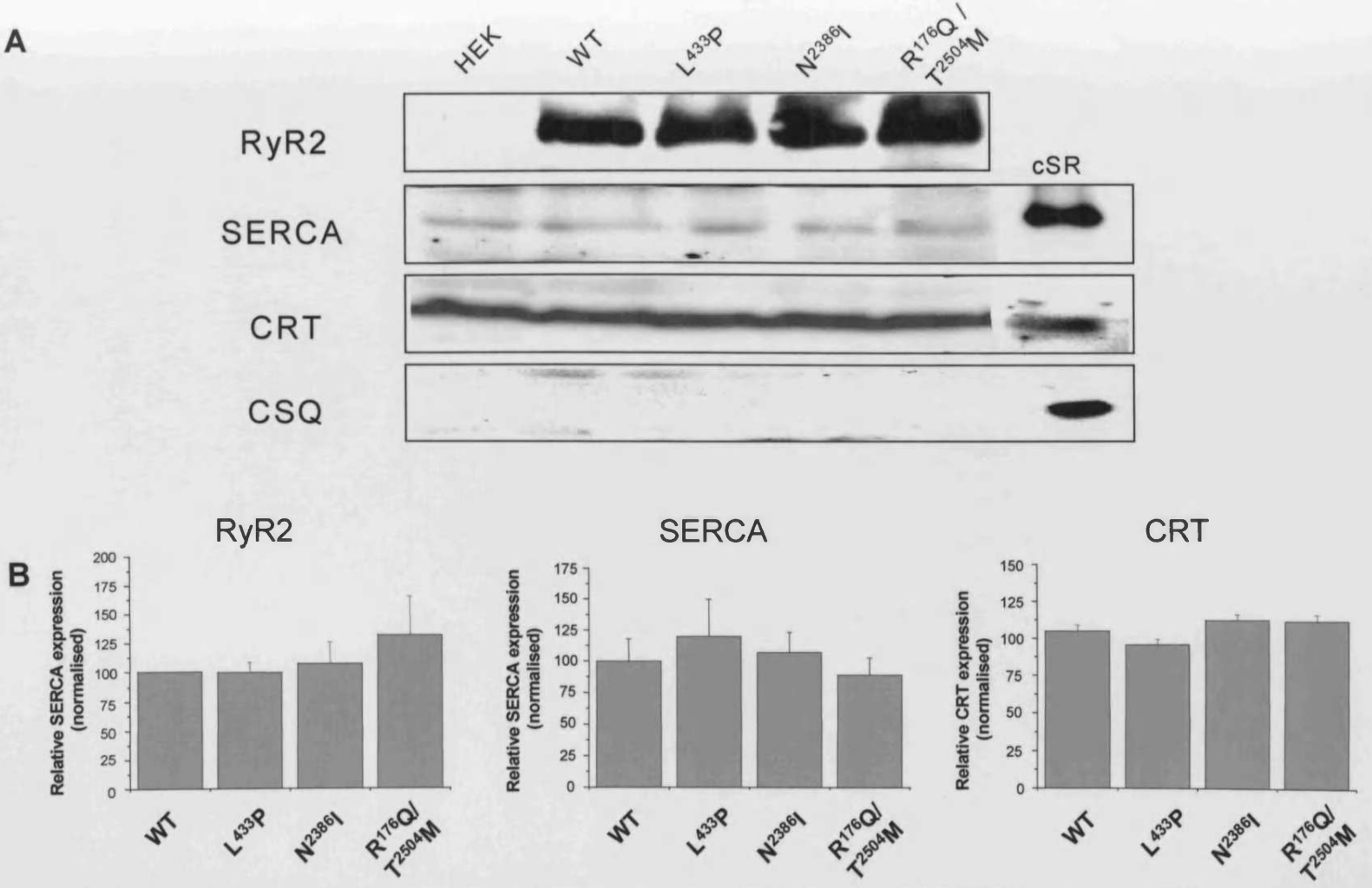

Figure 5.10. Endogenous levels of SERCA and CRT were not significantly altered following expression of WT or mutant RyR2. A) Levels of SERCA (~ 110 kDa), CRT (~ 47 kDa, but migrates at ~ 65 kDa due to endogenous glycosylation) and CSQ (~ 45 kDa) were determined following immunoblot analysis of post-nuclear supernatants (SERCA and CRT, 100 µg; CSQ, 250 µg) obtained from untransfected HEK cells or from cells expressing WT or mutant RyR2. Levels of CaM could not be detected due to the inefficiency of the antibody employed. Rabbit cardiac homogenates (50 µg, prepared by Dr. D Reynolds) were used as controls. B) Densitometric analysis of recombinant mutant RyR2 expression was normalised to the expression levels of the WT, and SERCA and CRT levels in cells expressing recombinant WT or mutant RyR2 were normalised to the levels of SERCA and CRT determined in untransfected HEK cells. Data are plotted as means ± SEM and are derived from analysis of at least 4 separate blots.

5.4. Discussion

5.4.1. Investigation of the Ca^{2+}-dependence of WT and mutant RyR2 Ca^{2+} release in permeabilised living cells

This study represents the first determination of the Ca^{2+}-dependence of mutant RyR2 channel activation and inhibition in living cells. ARVD2-linked mutations $L^{433}P$, $N^{2386}I$ and $R^{176}Q/T^{2504}M$ resulted in channels which exhibited significantly altered Ca^{2+} sensitivity of caffeine triggered Ca^{2+} release. The inhibition profiles of these mutants differed markedly from those of the WT channel which exhibited a biphasic Ca^{2+} release profile with the channel being inhibited at low (<10 nM) and high (> 10 μM) $[Ca^{2+}]_c$. The results presented here show that, in a cell-based assay, the activation and inhibition of WT RyR2 is tightly regulated by $[Ca^{2+}]_c$, in contrast to reports that WT RyR2 displays pronounced insensitivity to Ca^{2+}-dependent inhibition *in vitro* (Du & MacLennan, 1999). However, as discussed in section 5.1.1. and 4.1.1., these discrepant results can be attributed to the fragility of the inactivation mechanism and often arise from the use of particular assays to determine channel functionality (^{3}[H] ryanodine binding versus single channel studies used to determine the channel's 'open' status) (Li & Chen, 2001; Du & MacLennan, 1999; Fessenden et al., 2004). Thus, evaluation of channel inactivation in a cell system would be more likely to maintain the regulatory mechanisms present *in vivo*. Despite this, the values of Ca^{2+} dependent activation obtained in permeabilised cells expressing WT RyR2 in this study are in close agreement with the *in vitro* characterisation of the Ca^{2+} dependence of caffeine-stimulated Ca^{2+} release through WT RyR2 in planar lipid bilayers (see section 5.3.1., Li & Chen, 2001). This data also confirm sensitised Ca^{2+}-dependent channel activation in the presence of caffeine (EC_{50} of 42 nM versus 260 nM in the absence of caffeine (Li & Chen, 2001)). Caffeine also appears to dramatically sensitise RyR2 to Ca^{2+}-dependent inhibition by a factor of ~ 600 fold (IC_{50} 3.3 μM (this study) versus 2.1 mM in the absence of caffeine using bilayer studies (Li & Chen, 2001)), although this discrepancy could be due to the use of a different assay system.

5.4.2. Using caffeine-induced release to study the Ca^{2+} sensitivity of RyR2

The use of caffeine to investigate Ca^{2+} sensitivity in these experiments makes interpretation of the data complex, since we cannot assume that the effects seen are

the consequence of Ca^{2+} acting alone. Even though caffeine acts as an agonist by sensitising the channel to Ca^{2+}, we assumed that WT and mutant RyR2 have an equal affinity for caffeine. For example, $N^{2386}I$ and $R^{176}Q/T^{2504}M$ display considerable caffeine activation at 0.1 nM [Ca^{2+}], - this is taken to indicate that these mutants are not inhibited by low $[Ca^{2+}]_c$, or that they can be activated by caffeine at low [Ca^{2+}], however it is possible that this mutant has a greater affinity for caffeine itself and that this augmented activation could be due to the direct action of caffeine on the channel (i.e. in a Ca^{2+} independent manner). Such effects are known to occur with high caffeine doses (Sitsapesan and Williams, 1989), however they have only been shown to be significant at 40 mM, with only very infrequent openings seen with 5-10 mM caffeine at 80 pM [Ca^{2+}]. This suggests that the Ca^{2+} independent effect of caffeine in this study would have been minimal.

Another concern is that caffeine is not an endogenously occurring activating ligand of RyR2. However, the use of a non-myocytic cell line means that β-adrenergic agonists cannot be used, limiting us to pharmacological agonists of RyR2, of which caffeine is the most suitable since the effects are reversible and it has been extensively used to investigate RyR function in biochemical and cell-based assays. Nonetheless, the advantages of HEK cells as an RyR-deficient expression system have already been discussed (see section 3.1.1.), in particular the use of these cells means that the data obtained can be more easily compared with that from other studies of mutant RyR2 characterisation, since this cell line is most widely used for this purpose.

5.4.3. Altered Ca^{2+} sensitivity as a candidate mechanism of RyR2 dysfunction in SCD

Despite attractive candidate mechanisms for Ca^{2+} release abnormalities through mutant RyR (see Chapter 1, section 1.5.2.2.2.), the precise mechanistic basis of RyR2 dysfunction in arrhythmia remains poorly defined. Recently, functional characterisation of three C-terminal CPVT-linked mutants revealed that lumenal Ca^{2+} sensitisation underpinned RyR2 dysfunction, rather than RyR2 dysfunction induced by changes in ER Ca^{2+} storage *per se* (Jiang et al., 2004). These latter findings are in agreement with those found in this chapter and are in accord with the hypothesis of Choi et al. (2004), who proposed that arrhythmic phenotype may not be absolutely dependent on altered SR Ca^{2+} store status. Consequently, it is entirely feasible that in some instances, arrhythmogenic susceptibility may arise from an altered response to $[Ca^{2+}]_c$. However, it is also important to remember that changes in cytoplasmic

Ca^{2+} will affect lumenal Ca^{2+} storage and *vice versa*, indicating that these Ca^{2+} pools cannot be functionally separated within the cells, and could both contribute to the effects seen.

Results shown in chapter 4 suggested that channel activation would be predicted to result in prolonged $[Ca^{2+}]_c$ elevation. Work presented in this chapter confirms and extends this concept by providing evidence that, in the same mutants, the failure to completely terminate Ca^{2+} release following channel stimulation may arise as a consequence of a loss of Ca^{2+} dependent inactivation (~8-10 fold) that would prolong the $[Ca^{2+}]_c$ elevation, and directly increase the likelihood of DAD and arrhythmia in susceptible individuals. In particular, the desensitisation to inactivation seen with $L^{433}P$ and $R^{176}Q/T^{2504}M$ mutants reflects the fact that Ca^{2+} transients from these channels exhibited a sustained decay period (as seen in Chapter 4, Figure 4.7). However, it is important to note that this study does not shed any light on the precise mechanism underlying the abnormal RyR2 Ca^{2+} release termination observed (e.g. defective inactivation, adaptation etc), and a detailed investigation of the pathophysiological role of Ca^{2+}-dependent inactivation in terminating ER/SR Ca^{2+} release provides scope for future study.

The molecular determinants of RyR Ca^{2+}-dependent inactivation have been proposed to lie in the C-terminus (Du & MacLennan, 1999; Fessenden et al., 2004), at loci entirely separate from those of the mutants investigated in this study. However, these loci were initially determined for RyR1, which is thought to be more sensitive to Ca^{2+} dependent inactivation and so may depend on different Ca^{2+} regulatory binding sites. However, it is important to note that a mutation in the N-terminus of RyR1 which results in porcine MH was found to undergo decreased Ca^{2+} dependent inactivation as determined by [^{3}H]ryanodine binding experiments (Fill et al., 1990), suggesting not only that desensitisation to Ca^{2+}-dependent inactivation may be a mechanism of RyR1 dysfunction in MH, but also that this may be achieved by mutation at a locus removed from that thought to mediate inactivation. Nevertheless, when considering the complex conformational architecture of structural domains within the folded RyR2 tetramer, the data presented in this chapter strongly supports a role for the N-terminal and central domains in Ca^{2+}-dependent inactivation, and may point to SCD-linked mutational 'hot-spots' occurring at sites of key intra-RyR conformational interaction. This is fully consistent with the determinants of RyR Ca^{2+} sensitivity being dependent on the proper, folded conformation of the intact channel. In light of this, the mutational loci may be important in determining the precise mechanistic basis of RyR2 dysfunction in SCD,

in keeping with the suggestion that similar pathological phenotypes could arise from markedly distinct mechanistic bases (Allen, 2003).

Although the data presented in this chapter suggests that these mutations result in a loss of cytosolic Ca^{2+}-dependent inhibition, it does not however preclude the possibility that they exhibit hypersensitivity to the ER Ca^{2+} store, such as those characterised by Jiang et al. (2004). Lumenal Ca^{2+} sensitivity was not investigated in this study, and since the effects of lumenal Ca^{2+} can manifest themselves as changes in cytosolic Ca^{2+} sensitivity (Györke & Györke, 1998), it is possible that our results may reflect altered lumenal sensitivity.

Although sensitivity to Mg^{2+} inhibition was not investigated in this study (and each experimental buffer contained a fixed [Mg^{2+}] of 1 mM), our experiments do not exclude desensitisation to Mg^{2+} inhibition as a potential mechanism of channel dysfunction in ARVD2. However, it is clear that mutant channel dysfunction in this study is entirely independent of FKBP12.6 since HEK cells are devoid of its expression.

5.4.4. Potential limitations of the experimental system

The experimental system used here has some limitations; in particular it should be noted that it is possible that the decrease in fluo-3 signal seen at 61 μM $[Ca^{2+}]_c$ for WT RyR2 could have been due to saturation of the indicator, since this [Ca^{2+}] is ~80x the $K_{d\ (app)}$ determined in this study. However, a corresponding decrease in signal was not observed at this $[Ca^{2+}]_c$ in permeabilised cells expressing RyR2 mutants, especially those expressing $R^{176}Q/T^{2504}M$. Moreover, Ca^{2+} release was observed at this high $[Ca^{2+}]_c$, including dissipation of Ca^{2+} from the ER on addition of TG, suggesting that saturation of the dye did not occur, or was not complete at 61μM. This is confirmed by the shape of the calibration curve seen in Figure 5.4. which shows that complete saturation of the dye does not occur at this [Ca^{2+}]. However, the [Ca^{2+}] at which complete saturation did occur was not investigated in this study.

5.4.5. Limitations of the method used to evaluate ER Ca^{2+} status

Determination of the ER Ca^{2+} load in this study was carried out by calculating the peak TG- and caffeine-mediated release. While this approach is widely used and is believed to be a good method of determining ER status, it is an indirect measure taken at a single time point and therefore cannot be used to monitor dynamic

changes in ER Ca^{2+}. This suggests that although we found that expression of RyR2 mutants did not lead to persistent changes in the ER store, the way in which these measurements were made could mean that important transient changes in ER [Ca^{2+}] were not detected. This is important since variation in the ER load would complicate interpretation of the data obtained. For example, the relatively constant nature of the ER in permeabilised cells measured at high $[Ca^{2+}]_c$ meant that the decrease in release seen through WT RyR2 at this Ca^{2+} level was interpreted as channel inactivation and not as a decrease in the availability of releasable ER Ca^{2+}. Nevertheless, dynamic changes in ER Ca^{2+} can only be assessed using techniques that measure the free ER [Ca^{2+}] e.g. low Ca^{2+} affinity dyes, or a targeted aequorin bioluminescent probe. These techniques are not without their limitations: low affinity Ca^{2+} dyes may face potential interference from other metals (e.g. Mg^{2+}, Zn^{2+}) which have a high affinity for these indicators, and they may load into cellular compartments other than the ER (e.g. Golgi, mitochondria, lysosomes). While ER targeted aequorin would overcome these difficulties, use of these probes is notoriously difficult and numerous discrepancies have been reported (Montero et al., 1995; Meldolesi & Pozzan, 1998). Furthermore, the design, expression and bioluminescence measurement of such a probe was outside the scope of this project.
However, gross changes in the ER Ca^{2+} storage capacity were expected on expression of the WT and mutant channels in line with previous work (Jiang et al., 2004; George et al., 2003a), and therefore measurement of the total ER Ca^{2+} load was thought to be more suitable. In this respect, TG was used in favour of caffeine release, since HEK cells exhibit a functionally compartmentalised store which comprises a significant caffeine insensitive component (Tong et al., 1999a).

5.4.6. Compensatory changes in the expression of ER Ca^{2+} handling proteins in RyR2 transfected cells

The expression levels of proteins thought to be intimately involved in regulating the ER load, and thus RyR-mediated Ca^{2+} release were found to be comparable in cells expressing mutant or WT channels. This would suggest that the equivalent ER loads determined in Chapter 4 were not achieved by compensatory changes in the expression levels of SERCA or CRT. CSQ was detected in rabbit cardiac tissue but not in HEK cells, suggesting that this is an SR specific protein, and it is for this reason that the levels of CRT were investigated since, like CSQ, it is an intra-lumenal protein which binds Ca^{2+} with low affinity and may have a putative role in Ca^{2+} storage (Michalak et al., 1999). However, unlike CSQ, CRT has a wider tissue and

intracellular distribution and a role for this protein in direct RyR regulation has not been established.
It should also be noted that, while FKBP12 is expressed in HEK cells, FKBP12.6 is not detectable at the protein level (Wehrens et al., 2003; S. Zissimopoulos, personal communication) and so expression of this regulator was not evaluated.
Levels of SERCA expression (isoform SERCA2b in HEK cells (Tong et al., 1999b)) were unchanged on expression of mutant RyR2, suggesting that changes to the ER caused by augmented Ca^{2+} release through these channels was not compensated for by enhanced synthesis of this protein. This is in contrast to work on MH/CCD mutants of RyR1, expression of which in HEK cells led to increased expression of this Ca^{2+} ATPase (Tong et al., 1999b). However, it is important to note that the activity of this pump was not investigated in this study, and so maintenance of the ER Ca^{2+} store on expression of RyR2 mutants may have been mediated in this way.

5.4.7. How does the characterisation of these mutants fit with the clinical phenotype of SCD susceptible patients?

The RyR2 mutants characterised in this study exhibit abnormal regulation by $[Ca^{2+}]_c$ following channel activation in living cells. This represents an important finding since it is known that perturbation of Ca^{2+} release underlies arrhythmogenesis (Bers, 2001), yet we do not know the pathological mechanisms that manipulate $[Ca^{2+}]_c$ in such a way as to induce the profound Ca^{2+} release dysfunction associated with the onset of VT. This is important since the large $[Ca^{2+}]_c$ changes that underpin every cardiac cycle do not, under normal circumstances, trigger arrhythmia in susceptible SCD-susceptible individuals. Results presented here would agree with the observation that affected mutation carriers present a normal resting phenotype i.e. resting $[Ca^{2+}]_c$ levels were not perturbed on expression of the mutant channels, and ER $[Ca^{2+}]$ and Ca^{2+} handling protein expression levels were comparable to WT. This phenotypically normal resting state together with the stress/exercise requirement for the development of arrhythmia suggests that, in addition to mutation, gross RyR2 dysfunction requires an additional 'trigger'. Thus, a systematic evaluation of stress/exercise induced 'factors' that exacerbate RyR2 dysfunction, e.g. other components of the cellular Ca^{2+} handling machinery that contribute to RyR2 channel abnormalities in stressful circumstances, represents an important path of investigation.

Chapter 6

Investigating WT and mutant RyR2 protein-protein interactions

6.1. Introduction

6.1.1. Accessory proteins and RyR2 regulation

As discussed in Chapter 1, section 1.4.2. RyR2 undergoes regulation by numerous accessory proteins which bind to both cytoplasmic and lumenal sides of the protein. The function of many of these proteins, which form a 'macromolecular complex' with RyR, normally involves stabilization (e.g. FKBP12.6) or inhibition of the channel (e.g. sorcin, CaM), thereby ensuring appropriate Ca^{2+} release. Since these accessory proteins play such a pivotal role, it is therefore feasible that failure to associate with the RyR, either because of defects in these proteins themselves or defects in the channel, would result in channel dysfunction and Ca^{2+} dysregulation. Indeed it has been suggested that lack of direct RyR2 regulation by CSQ mutants (in addition to the loss of its Ca^{2+} buffering capability) is responsible for the autosomal recessive form of CPVT (Terentyev et al., 2003; Viatchenko-Karpinski et al., 2004). In addition, a decreased affinity of mutant RyR2 channels for FKBP12.6 has been proposed to be responsible for the autosomal dominant form of this disease (Wehrens et al., 2003), though results presented in this thesis suggest an FKBP12.6-independent mechanism is more likely (see section 5.4.3.).

Many approaches have been employed to determine the interaction of proteins with the RyR, but most require the interaction to take place *in vitro* and cannot easily discriminate between more than one candidate protein at a time (e.g. immunoprecipitation, cross-linking, GST-pulldown assays) because they rely on the use of specific antibodies to recognise the interacting protein. There are few approaches by which a set of unknown proteins can be screened for interaction with a known protein; some are very complex (e.g. Surface Plasmon Resonance analysis) and require that the interacting proteins be identified by mass spectrometry, which is both time consuming and expensive. More straight-forward methods developed involve two-hybrid techniques. The most well characterised of these is yeast two-hybrid (Y2H), which uses a transcriptional based assay to evaluate protein-protein interactions (Fields & Song, 1989). This introduces an extra advantage over the previously mentioned *in vitro* methods, since in this system protein-protein interactions occur *in vivo*, and so the proteins are more likely to adopt their native conformation. Variations on this approach (designed to circumvent problems in the conventional Y2H system with proteins which are themselves transcription factors) involve reconstitution of an essential signalling pathway by interacting proteins anchored at the plasma membrane (Ras recruitment system, Broder et al., 1998)

which enables colony growth, or reconstitution of enzyme function (split-ubiquitin system, Johnsson & Varshavsky, 1994). The latter system has an inherent advantage in that the reaction takes place in the cytoplasm and is not constrained by consideration of intracellular localization. However, these newer techniques are not as well characterized as the conventional Y2H system.

Another *in vivo* technique used to screen for interacting proteins is phage display, in which proteins encoded by cDNA libraries cloned into the viral DNA are displayed on the surface of the phage as a fusion with one of the coat proteins. Phage displaying a protein that specifically binds to a target protein can be isolated and identified following bacterial infection.

However, the Y2H system seems to be favourable when using mammalian cDNA libraries since yeast are eukaryotes and so codon usage and translation is likely to be closer to that occurring in mammalian cells than when recombinant proteins are expressed in bacteria. In addition, the Y2H system has a high degree of sensitivity because the protein-protein interaction is amplified many-fold through a transcriptional process.

Y2H has also been used with considerable success to demonstrate many of the intra- and inter-molecular interactions of the inositol 1,4,5- trisphophate receptor (reviewed in Patterson et al., 2004), including that with FKBP12 (Cameron et al., 1995) and Ca^{2+} binding proteins (CaBP, Zeng et al., 2003), suggesting that this technique is applicable to Ca^{2+} release channels.

CPVT/ARVD2 mutations are thought to be located at sites of potential inter-domain contact within the channel, suggesting that their presence may cause disruption of this interaction, however we must also consider the possibility that that some of the mutational loci could be sites of accessory protein interaction. For example, the three proposed FKBP12.6 binding sites (see Chapter 1, Figure 1.16.) in the N-terminal, central and C-terminal domains of the protein contain 5, 7 and 22 mutations respectively (~79% of the total number of mutations), though these represent vast putative sites of interaction.

In light of this, the work presented in this chapter aims to address whether the altered Ca^{2+} release functionality of the mutant channels established in chapters 4 and 5 was associated with defective protein-protein interaction. Differences in intermolecular interactions between the mutation susceptible regions of RyR2 and accessory proteins, were investigated using Y2H genetic screens of a human cardiac library using short mutant and WT fragments of RyR2.

6.1.2. *Yeast two-hybrid*

Yeast two-hybrid is an *in vivo* transcription based assay used to identify protein-protein interactions. The system used was the MatchMaker GAL4 system (Clontech – see Chapter 2, section 2.2.2.). The Y2H assay is based on the fact that GAL4, a eukaryotic transcription factor, is composed of two physically separable, functionally independent domains. GAL4 contains a DNA binding domain (BD, corresponding to amino acids 1-147 of the GAL4 protein) that binds to a specific enhancer sequence upstream of the promoter and gene to be transcribed, and a transcription activation domain (AD, corresponding to amino acids 768-881 of the GAL4 protein) that directs the RNA polymerase II complex to initiate transcription. When co-expressed in yeast, the separated DNA-BD and AD recombinant peptides do not directly interact with each other and thus cannot activate transcription. However, if the DNA-BD and AD are brought into close proximity in the promoter region, then transcriptional activation will be restored (see Figure 6.1.).

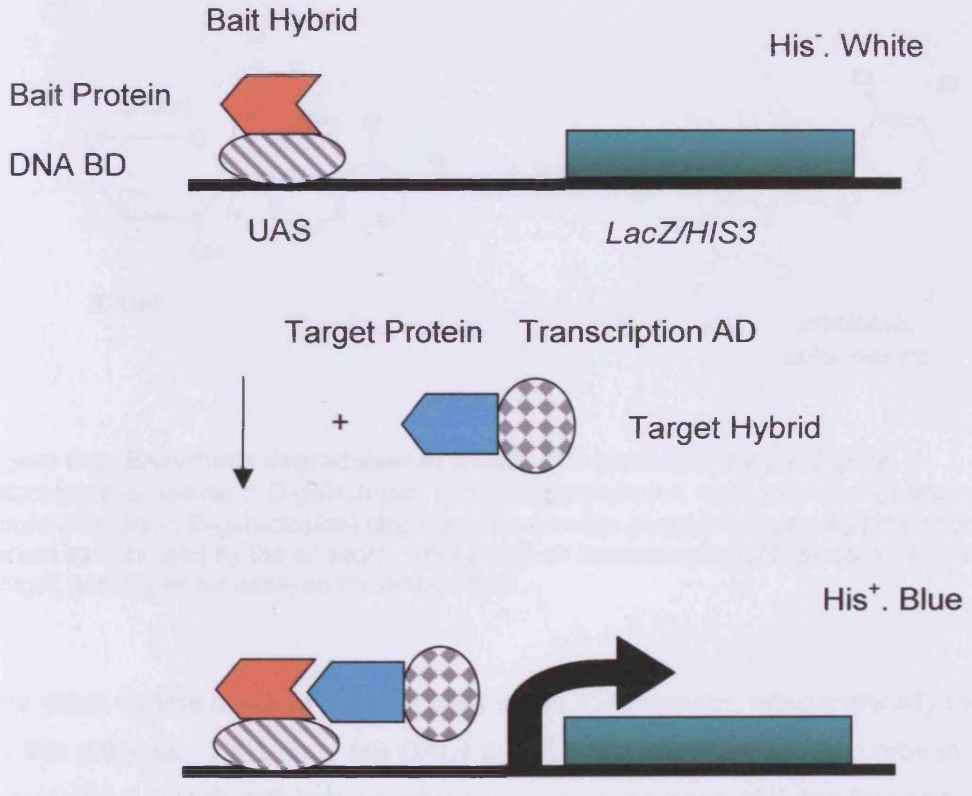

Figure 6.1. The yeast two-hybrid system. Required components are a transcriptional activation domain (AD) fused target protein, a DNA binding domain (BD) fused bait protein, which binds to an upstream activating sequence (UAS), directing expression of reporter/selection genes. Interaction between bait and target proteins leads to transcriptional activation of *LacZ* and *HIS3* reporters, reflected as blue colour following exposure to X-Gal, and growth on selective medium lacking in the amino acid histidine.

Two different cloning vectors are used to generate fusions of DNA-BD or AD domains (bait and target vector respectively, see Figure 2.3.) with proteins, which potentially interact with each other. The recombinant proteins are co-expressed in yeast and are targeted to the yeast nucleus. An interaction between a bait protein and a target protein creates a novel transcriptional activator which initiates transcription of reporter genes, thereby making the protein-protein interaction phenotypically detectable. If the two hybrid proteins do not interact with each other, the reporter genes will not be transcribed. The system utilises two reporter genes (*HIS3* and *LacZ*) under the control of two different GAL4-responsive promoters. The *HIS3* nutritional reporter gene provides an elegant and sensitive growth selection for positive interactions, which can be further verified by an assay for β-galactosidase activity (encoded by the *LacZ* reporter gene). Activity of this enzyme in yeast colonies was evaluated using a colony filter lift assay, whereby the lysed yeast cells on filter paper are exposed to X-Gal (5-bromo-4-cholro-3-indolyl-β-D-galactoside), a synthetic enzyme substrate which upon cleavage and oxidation produces the insoluble blue dye, 5-bromo-4-chloro-indigo (see Figure 6.2.)

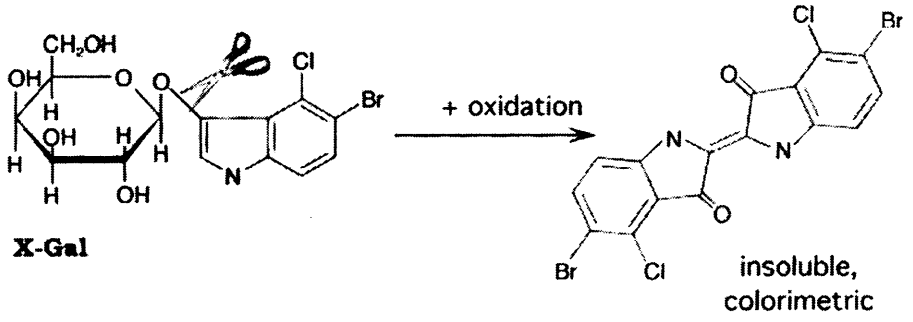

Figure 6.2. Enzymatic degradation of X-Gal. The product of the *LacZ* gene, β-galactosidase cleaves β-D-galactoside containing substrates, such as X-Gal (5-bromo-4-chloro-3-indolyl-β-D-galactoside) targeting between the glycosyl oxygen and the anomeric carbon as indicated by the scissors. This yields an insoluble product (5-bromo-4-chloro-indigo), which can be assayed colorimetrically.

The yeast strains used as the host cells in the Y2H system, are genetically modified for this purpose. Thus, they are *GAL4* and *GAL80* (which encodes a protein repressor of *GAL4*) deficient, in order to avoid interference of these two endogenous proteins with the assay. In addition, they are *TRP1* and *LEU2* deficient i.e. yeast strains are auxotrophic for tryptophan and leucine, unless they are transformed with the bait (which carries the *TRP1* gene) or target (which carries the *LEU2* gene)

plasmids. Thus, these plasmids provide nutritional selection markers when yeast are cultured in medium lacking tryptophan and/or leucine. The yeast strains used are also deficient for histidine, since the enhancer-promoter sequences of the *HIS3* gene have been substituted by DNA sequences recognised by the *GAL4* transcription factor, thereby creating a GAL4-responsive, *HIS3* reporter gene. In fact, low level expression of the HIS3 gene still occurs, driven by a weak constitutive promoter. However, this background growth is suppressed by a competitive inhibitor of the HIS3 protein (3-amino-1,2,3-triazole) which is included in the histidine-deficient selective growth medium. The Y2H system can be used to screen a collection of random unknown library clones for potentially interacting partners of a bait protein. The library clones are always fused to the *GAL4* AD, therefore the target plasmid is also known as the library plasmid. An overview of the experimental design for a Y2H library screen is given in Figure 6.3.

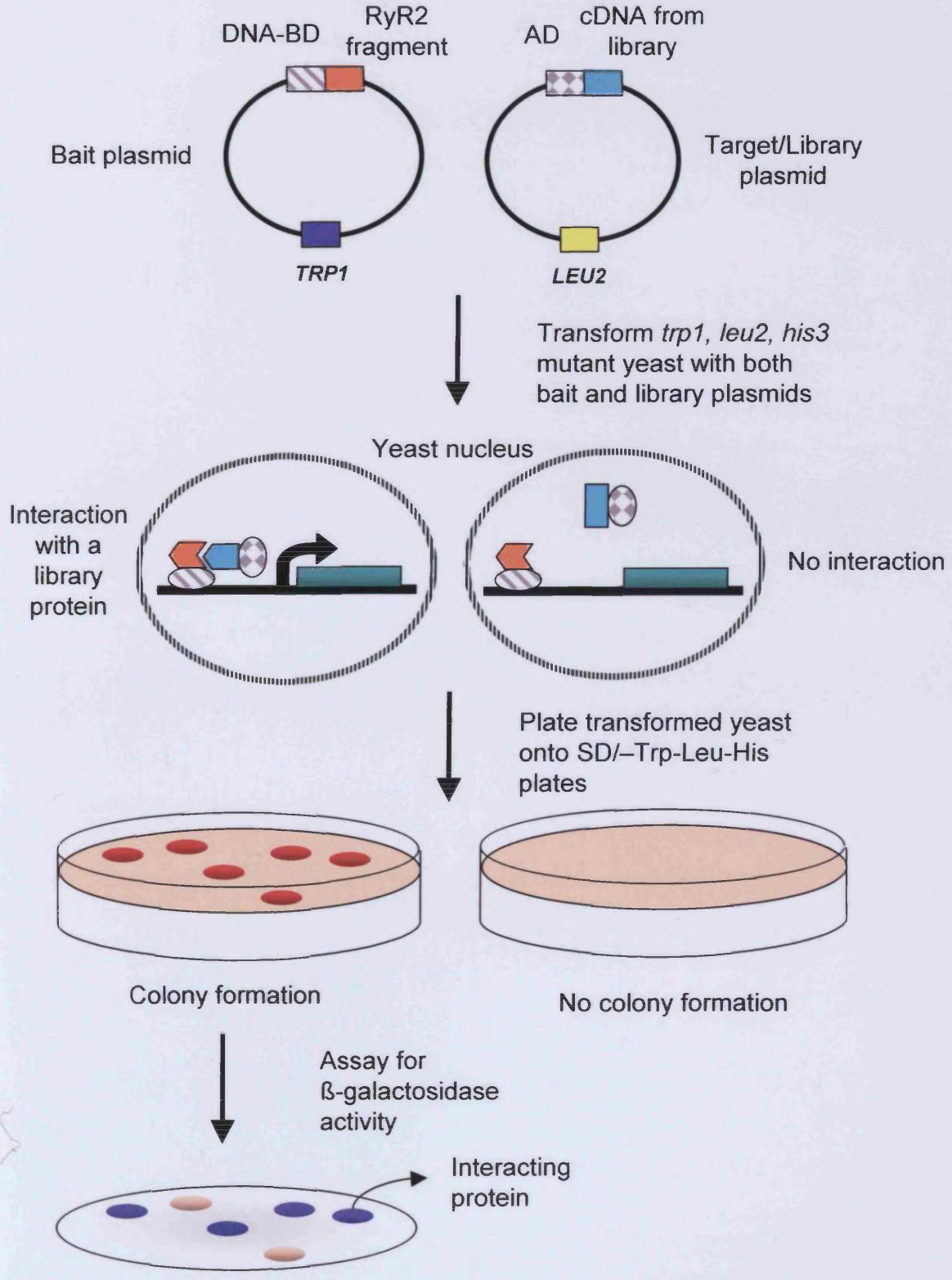

Figure 6.3. Detection of interacting proteins using Y2H. The bait and library plasmids (containing RyR2 fragments and human cardiac library clones respectively) is introduced by sequential transformation. Yeast is plated onto selective drop-out (SD) agar plates lacking tryptophan and leucine to select colonies transformed with both bait and library constructs. The medium also lacks histidine to select for colonies containing interacting proteins, which would activate transcription of the *HIS3* gene. $HIS3^+$ colonies are then assayed for ß-galactosidase activity.

6.2. Methods

6.2.1. Cloning strategy

Fragments of mutant and wild type hRyR2 (RQ/WTRQ, 530-720 bp; LP/WTLP, 1320-1540 bp; NI/WTNI, 7080-7340 bp; TM/WTTM, 7560-7750 bp, see Figure 6.4. for corresponding amino acids) were amplified by PCR (see Chapter 2, section 2.2.1.11.) using *Pfu* polymerase and primers containing suitable restriction sites (*EcoRI* and *SalI* - see Appendix I) in frame with the T7 promoter of the pGBKT7 vector, which resulted in fusion products with an N-terminal GAL4 DNA Binding Domain and c-myc tag.

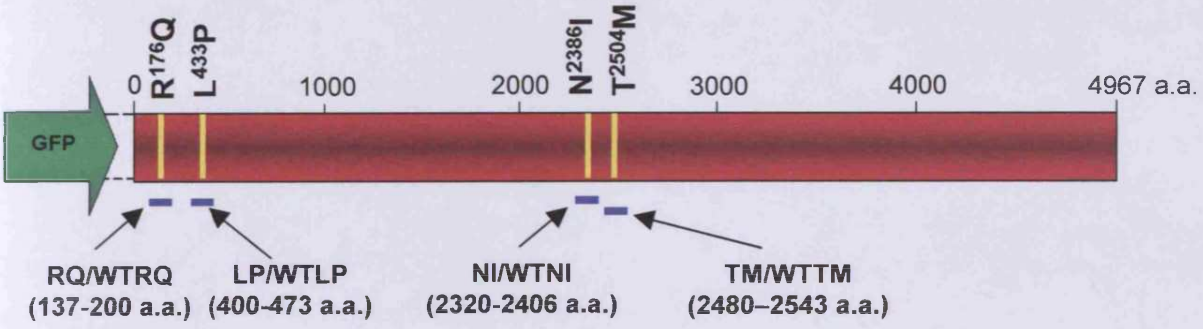

Figure 6.4. Schematic showing the co-ordinates of the Y2H constructs. Fragments were amplified from the full length wild type and mutant hRyR2 constructs (engineered in Chapter 3) and cloned into the bait (pGBKT7) vector. These fragments were short (~ 75 a.a.) in order to avoid aberrant protein folding which could result in artefactual interactive events.

6.2.2. Amplification of human cardiac cDNA library

A human cardiac library containing 3.5 x 10^6 independent clones (cloned into the yeast–two hybrid pACT2 vector using *EcoRI-XhoI* sites -Clontech) was obtained from Dr. S Zissimopoulos as a frozen bacterial culture (in LB 25% v/v glycerol).
The library was amplified according to the manufacturer's instructions as follows:
The 1 ml aliquot of bacterial culture was thawed on ice, resuspended in 40 ml of LB broth, and incubated at 37°C with shaking at 225 rpm for 30 minutes to ensure complete resuspension. The resulting bacterial culture was then plated onto 100, 200 mm diameter LB agar plates (containing 100 µg/ml ampicillin), with 400 µl of cell suspension per plate, and incubated at 37°C for 18 hours. The density of bacterial growth from this was extremely high, and the lawn of bacteria from each plate was

containing 25% v/v glycerol). The resulting bacterial culture was then incubated at 30°C with shaking for 1 hour, before separating to 20 x 50 ml aliquots and harvesting by centrifugation (3000 *x*g for 1 hour, Allegra 6R, Beckman). Bacterial pellets were then stored at -80°C until DNA could be extracted by the Wizard® PureFection system (Promega), which employs DNA-binding magnetic beads for purification (see section 2.2.1.8). Each 50 ml aliquot (equivalent to ~ 400 ml of a standard overnight culture) yielded ~ 240 µg/ml plasmid DNA, with ~ 4.8 mg of DNA being obtained in total. All plasmid preparations were pooled and divided into 500 µl aliquots and stored at -20˚C.

6.3. Results

6.3.1. Characterisation of bait proteins

Efficient transfer of bait constructs into yeast strains was achieved by the standard lithium acetate method (see section 2.2.2.2.), and all recombinant proteins were expressed at their correct molecular weight in this system, without degradation as shown in Figure 6.5. Expression levels were not homogeneous, and interestingly WT N-terminal fragments were expressed at a somewhat higher level than the corresponding mutant fragments, whereas WT fragments in the central domain had a much lower expression level compared to their corresponding mutant fragments. This pattern of expression was preserved in both yeast strains and the reason for this heterogeneity in protein levels remains to be resolved.

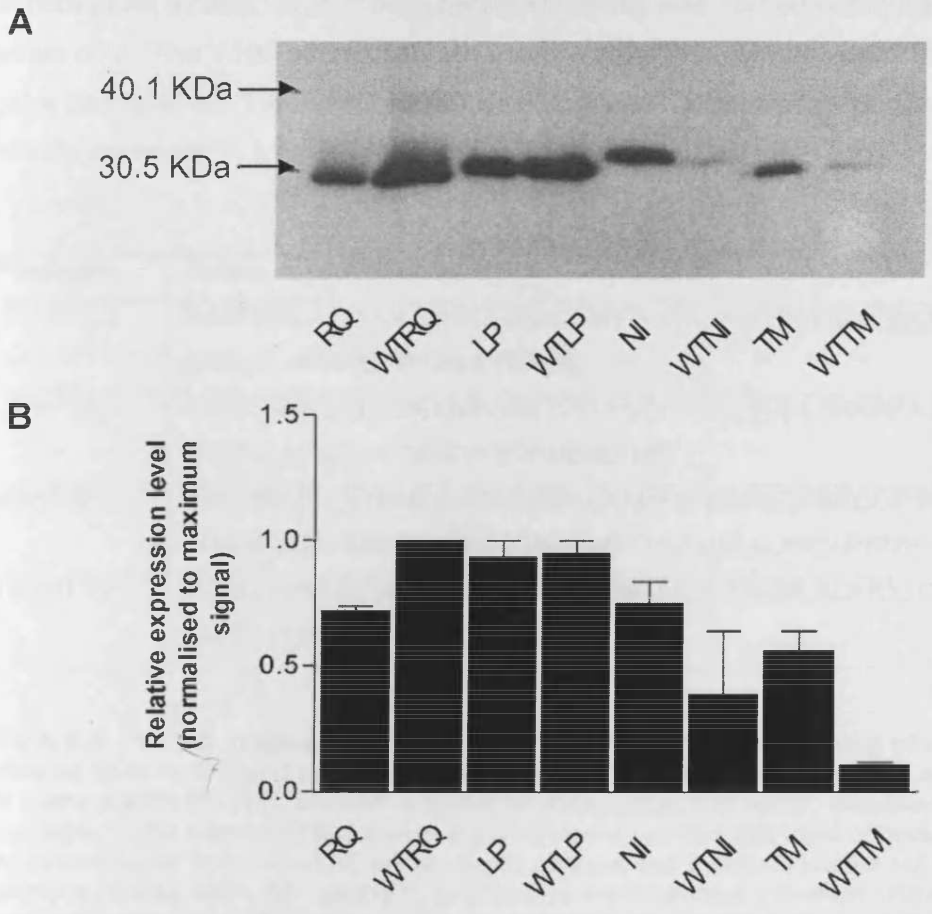

Figure 6.5. Expression of bait RyR2 fragments in yeast strain CG1945. A) Protein extracts (50 μg) from transformed yeast were immunoblotted with an antibody against the c-myc epitope tag, demonstrating that all recombinant proteins were detected at their expected molecular weight (RQ/WTRQ, ~27kD; LP/WTLP, ~28kD; NI/WTNI, ~30kD; TM/WTTM, ~27kD). B) Densitometric analysis confirmed that expression levels were heterogeneous, though the reason for this variability in expression levels is unknown and a similar pattern of expression was found in the Y190 yeast strain.

None of the hRyR2 fragments either alone, or in the presence of the empty target/library vector showed autonomous activation in either yeast strain, as assessed by the β-galactosidase assay (not shown). This is an aberrant interaction of the bait with the AD which activates transcription of the reporter genes, and is normally associated with acidic proteins, since acidic residues are thought to be associated with activating regions of transcription factors (Ma & Ptashne, 1987; Ruden, 1992; Ruden et al., 1991). In agreement with this, Table 6.1. shows that most of the peptides used were not acidic in nature or highly charged and were therefore unlikely to result in autonomous activation. However, NI/WTNI constructs were found to be acidic, but this did not condition them to auto-activation and consequently they were deemed suitable for use in this Y2H system. This lack of autonomous activation is essential since spurious interaction with the library vector would yield false positive results. Constructs were tested for autonomous activation in both yeast strains, even though library screening was carried out in the CG1945 strain only. The Y190 strain is known to show enhanced expression of the *LacZ* gene (Bartel et al., 1993) and so any weak autonomous activation would be more readily observed.

Fragment	Amino acid sequence	pI
RQ/WTRQ	RSSTDKLAFDVGLQEDTTGEACWWTIHPASKQRSEGEKV**R/Q**V GDDLILVSVSSERYLHLSYGNGS	5.14/ 4.85
LP/WTLP	DGISLSRSQHEESRTARVIRSTVFLFNRFIRG**L/P**DALSKKAKAST VDLPIESVSLSLQDLIGYFHPPDEHLEHE	6.07/ 6.07
NI/WTNI	VRLLIRRPECFGPALRGEGGNGLLAAMEEAIKIAEDPSRDGPSPN SGSSKTLDTEEEEDDTIHMG**N/I**AIMTFYSALIDLLGRCAPEMH	4.54/ 4.54
TM/WTTM	VQDFLLHLLEVGFLPDLRAAASLD**T/M**AALSATDMALALNRYLCT AVLPLLTRCAPLFAGTEHHAS	5.28/ 5.28

Table 6.1. Peptide fragments of hRyR2 used for Y2H genetic screening of a human cardiac library. Mutated amino acids are underlined and are shown in bold. Calculation of pI (using the PROTCALC function available on www.justbio.com which calculates the pI according to the method of Bjelquist et al (1993)) demonstrates that most of these peptide fragments (apart from NI/WTNI) are not highly charged and therefore should not lead to spurious binding of the AD leading to autonomous transcriptional activation. However, it was later shown that NI/WTNI fragments did not undergo auto-activation and were therefore suitable for Y2H library screening.

6.3.2. Genetic screens of a human cardiac DNA library using WT and mutant RyR2 fragments

Because of the complexity inherent in assays taking place within a subcellular compartment of a living organism, a key issue for the effective use of yeast two-hybrid is the elimination of false positive results. It is for this reason that CG1945 was used as the host for genetic screening of the cardiac library, since this strain exhibits more stringent control of expression of the *LacZ/HIS3* genes (due to promoter differences) than Y190, making the detection of weak or transient false interactions less likely.

Pre-transformed CG1945 yeast containing the human cardiac library in the pACT2 vector were subsequently transformed with each bait construct and colonies containing interacting proteins were selected by growth on SD/-Leu-Trp-His medium. The efficiency of transformation and number of clones screened per transformation can be seen in Table 6.2. The cDNA library employed contains 3.5×10^6 independent clones, suggesting that at the average transformation efficiency achieved ($\sim 4 \times 10^5$), ~9 separate library transformations would be required to screen the whole library. This figure is also dependent on a completely different set of clones being analysed with every library transformation, which is of course highly unlikely since some clones may be more highly represented than others. This suggests that, for each construct a maximum of $\sim 1.2 \times 10^6$ independent clones were analysed (~ 1/3 of the total number), indicating that not every clone may have been investigated. However, the time required to ensure analysis of all library clones (calculated as ~170 weeks) would have exceeded the time available for this project and so this was not feasible. However, the number of clones screened by each fragment was comparable, and so should not have any bearing on the number of interactions detected with WT compared with mutant fragments.

Construct	Number of library screens/ transformations	Transformation efficiency (colonies/μg DNA)*	Number of clones screened**	Total number of HIS$^+$ colonies	Number positive for β-galactosidase assay
RQ	3	2342	4.1×10^5	1	0
WTRQ	3	2114	3.7×10^5	0	0
LP	3	2000	3.6×10^5	0	0
WTLP	3	2500	4.3×10^5	0	0
NI	3	2858	4.9×10^5	1	0
WTNI	3	2514	4.4×10^5	12	9
TM	3	2516	4.4×10^5	8	0
WTTM	3	1829	3.2×10^5	15	0

Table 6.2. Summary of Y2H screens. * Represents the average transformation efficiency per screen/transformation for each construct. ** Represents the number of clones screened per transformation. Colonies containing interacting proteins were selected by their HIS$^+$ phenotype, however transcription of the *LacZ* gene was not activated in all of these colonies.

Nevertheless, Table 6.2. demonstrates that these screens identified many HIS$^+$ colonies predicted to contain interacting proteins. The WTTM and WTNI fragments appeared to show most interaction, initially suggesting that the mutation susceptible central domain of the RyR2 interacts with more accessory proteins than the N-terminal, and that mutation in this region abolished some of these interactions. Results at this stage also suggested that the $R^{176}Q$ mutation produced a novel interaction not detected with the corresponding region of WT RyR2. However, the majority of the HIS$^+$ colonies (~76 %) did not test positively for β-galactosidase expression, suggesting that they did not represent true interactions. The colony growth seen was most likely the result of background *HIS3* expression, even though the inhibitor 3-AT was added to the growth medium. Surprisingly, none of the many HIS$^+$ colonies arising from screens with the TM and WTTM constructs exhibited β-galactosidase expression, though the relevance of this is unknown since all library transformations were carried out with the same levels of stringency.

These findings emphasise the importance of the use of two reporter genes regulated by separate promoters in eliminating false positive interactions.

Conversely, 75% of HIS$^+$ colonies from the WTNI screens exhibited β-galactosidase expression, confirming interaction of a library expression product with the bait fragment. This data suggests that the lower expression level of WTNI compared to that of the NI fragment (see Figure 6.5.) does not seem to have any bearing on the detection of interactions. The identity of the interacting proteins from these colonies was then investigated.

6.3.3. Identification of the interacting proteins

The main advantage of using Y2H in screening an expression library is the availability of the cloned gene for the interacting protein. In this study DNA was isolated from the colonies which exhibited β-galactosidase expression and further selected by transformation into *E.coli* (as described in section 2.2.2.7.). Isolated plasmids were analysed by restriction digest to obtain the approximate length of the interacting sequence, summarised in Table 6.3.

Interacting sequence	Approximate length (bp)
# 1	550
# 2	2000
# 3	2000
# 4	1250
# 5	1050
# 6	350
# 7	1200
# 8	750
# 9	850

Table 6.3. Approximate length of WTNI interacting sequences. Lengths were determined by agarose gel electrophoresis after restriction digest with *HindIII*, which cuts either side of pACT2 multiple cloning site with an excess of 750 bp (see Chapter 2, Figure 2.3.).

cDNA sequences obtained were compared against all known nucleotide sequences using the BLAST software program available at the NCBI website in order to find their identity. These sequences were also translated into peptides from all six open reading frames (using the SIXPACK option on the JEMBOSS software, available at http://www.hgmp.mrc.ac.uk), since as well as being transcribed from the ADH1 promoter, it is possible that the insert may also be transcribed in the reverse orientation from a cryptic promoter within the ADH1 terminator (Chien et al., 1991). Peptides obtained were also aligned with database sequences using the BLAST software. The 'highest scoring matches' from these database searches can be seen in Table 6.4. and alignment of the translated peptides to their matches can be found in Appendix II.

Since sequences # 8 and #9 represented the same protein, it was considered whether all of the clones isolated from this library screen shared a common motif or exhibited high homology with each other. Figure 6.6. demonstrates this not to be the case, (apart from # 8 and # 9) since multiple alignment revealed no significant similarity between these sequences. Thus, interaction of these peptides with the WTNI fragment was not due to a common binding sequence.

Interacting sequence	cDNA homology	Accession number	% Identity (base pairs)	Peptide homology	Accession number	% Identity (amino acids)
# 1	*Homo sapiens* haplotype U7 mitochondrion, complete coding sequence.	AF382011	98 % identity over 9255-9608 of 16568	*Macaca mulatta* cytochrome oxidase subunit III	AAB02131	68 % identity over 7-57 of 77
# 2	*Homo sapiens* phosphoprotein enriched in astrocytes 15 (PEA 15)	NM_003768 NM_013287	99 % identity over 147-673 of 2486	*Homo sapiens* PEA15	NM_003768 NM_013287	98% identity over 20-120 of 130
	Homo sapiens protein enriched in diabetes (PED)	Y13736	99% identity over 133-660 of 2352	*Homo sapiens* PED	Y13736	98% identity over 20-120 of 130
# 3	*Homo sapiens* eukaryotic translation initiation factor (eIEF) 3, subunit 6 interacting protein	AF077207 NM_016091	99 % identity over 18-478 of 1901	*Homo sapiens* eIEF associated protein HSPC021	AAD27002.1	87% identity over 1-113 of 564
# 4	*Homo sapiens* enoyl Coenzyme A hydratase domain	BC044574.1	98 % identity over 42-531 of 1212	*Homo sapiens* enoyl Coenzyme A hydratase domain containing 2 (ECHDC2)	AAH44574.1	89 % identity over 28-167 of 292
# 5	*Homo sapiens* 3 BAC RP11-689C17, human genome project sequencing clone	AC104638	97 % identity over 14685-14257 of 34051	*Alu* subfamily SB2 sequence (contamination warning entry)	N/A	60% identity over 1-84 and 186-199 of 603
# 6	*Homo sapiens* cardiac ankyrin repeat protein (CARP)	NM_014391.1	95 % identity over 227-528 of 1901	*Homo sapiens* CARP	AAH18667.1	98 % identity over 1-93 of 319
	Homo sapiens cytokine inducible nuclear protein	X83703	95 % identity over 227-528 of 1901	*Homo sapiens* cytokine inducible nuclear protein	A57291	98 % identity over 1-93 of 319
# 7	*Homo sapiens* chromosome 18, clone RP11-749G1	AC091103.4	80 % identity over 10129-10180 of 204340	*Rattus norvegicus* hypothetical protein XP_240835	XP_240835.1	28 % identity over 52-153 of 188
# 8	*Homo sapiens* cardiac troponin I	NM_000363.3	99% identity over 50-730 of 787	*Homo sapiens* cardiac troponin I	NP_000354	100 % identity over 1-184 of 210
# 9	*Homo sapiens* cardiac troponin I	NM_000363.3	99 % identity over 76-677 of 787	*Homo sapiens* cardiac troponin I	NP_000354	100 % identity over 1-57 of 210

Table 6.4. Homology of sequences found to interact with WTNI hRyR2 fragment. cDNA and translated peptide sequences isolated from a human cardiac library were compared to all known sequences using the BLAST software at NCBI, only the closest matches are shown here. PEA15 and PED were equally homologous to sequence # 2, and are in fact identical proteins (see Figure 6.6.). CARP and cytokine inducible nuclear protein were also found to be identical proteins as well as exhibiting equal homology to sequence # 6. See Appendix II for aligments of the sequences isolated with the corresponding peptides.

```
SEQUENCE_8      --------------PWDPEGHPGGPLTDPPNAPVLALPPAIPGLSLSMADGSSDAAREPR
SEQUENCE_9      AAASTSSSPEETDGPWDPEGHPGGPLTDPPNAPVLALPPAIPGLSLSMADGSSDAAREPR
SEQUENCE_7      ---------------WRPRGSEFAAASTNGNVAFLG------GFLLLLFCNYQTQVRYWY
SEQEUNCE_2      -------QLKSACKEDIPSEKSEEITTGSAWFSFLESHNKLDKDNLSYIEHIFEISRRPD
SEQUENCE_4      -------------GPRRPRFCASCSTLEAPSGPRLRFRRGGRGASEIQVRALAGSDQGIT
SEQUENCE_5      ---------------SVHLNPVKNLVLQILIHCSLKKRLGQAPWLTLAIPAPLEAEAGRS
SEQUENCE_6      -------------------KPYKTPSANMMVLKVEELVTGKKNGNGEAGEFLPEDFRDGE
SEQUENCE_1      --------------PNRGPLSPPNDLRPSHVISLPLHNAPHTRPTNQHTNHIPMMARCNT
SEQUENCE_3      -------------ASEAAMSYPADDYESGAAYDPYAYPSDYDMHTGDPKQDLAYERQYEQ

SEQUENCE_8      PAPAPIRRRSSNYRAYATEPHAKKKSKISASRKLQLKTLLLQ----IAKQELEREAEERR
SEQUENCE_9      PAPAPIRRRSSNYRAYATEPHAKKKSKISASRKLQLKTLLLQ----IAKHSWSERRRSGA
SEQUENCE_7      PALDFQMKFS---RRQLRLKYYTKISKGSILRYLYDDT----------------------
SEQEUNCE_2      LLTMVVDYRTRVLKISEEDELDTKLTRIPSAKKYKDIIRQPSEEEIINWLPHRRRPEQGG
SEQUENCE_4      EILMNRPSARNALGNVFVSELLETLAQLREDRQVRVLLFRSGVKGVFCAGADLKEREQMS
SEQUENCE_5      QGQEIETILANTAKFSLHQKYKKSAGRGGGRLQSQPLRRPRQENGVDPGGRGCSEPRSHH
SEQUENCE_6      YEAAVTLEKQEDLKTLLAHPVTLGEQQWKSEKQREAELKKKKLEQRSKLENLEDLEIIIQ
SEQUENCE_1      RKHIPRPPHTTCPKRPSIRDNPIYYLRSFFLRRIFLSLLPLQPSPYPPIRRALAPNRHHP
SEQUENCE_3      QTYQVIPEVIKNFIQYFHKTVSDLIDQKVYELQASRVSSDVIDQKVYEIQDIYENSWTKL
                                          :

SEQUENCE_8      GEKGRALSTRCQPLELAGLGFAELQDLCRQLHARVDKVDEERYDIEAKVTKNITEIADLT
SEQUENCE_9      ERRGAL-------------------------------------------------------
SEQUENCE_7      -------------------------------------------------------------
SEQEUNCE_2      GRGGRLDLHQTTPFPHPPGEGARATHHLPTY-----------------------------
SEQUENCE_4      EAEVGVFVQRLRGLMNDIAAFPAPTIAAMDGFALGGGLELALACDLRVAASSAVMGLIET
SEQUENCE_5      CTPAWATERDSVSKKKRKH------------------------------------------
SEQUENCE_6      LKKKKKKTREIYES----------------------------------------------
SEQUENCE_1      AKSPRSPTPKHX------------------------------------------------
SEQUENCE_3      TERFFKNTPWPRG-----------------------------------------------

SEQUENCE_8      QKIFDLRGKFKRPTLRRVRISADAMMQALLGARAKESLDLRAHLKQVKKEDTEKE
SEQUENCE_9      ---------------------------------------------------------
SEQUENCE_7      ---------------------------------------------------------
SEQEUNCE_2      ---------------------------------------------------------
SEQUENCE_4      TRGL------------------------------------------------------
SEQUENCE_5      ---------------------------------------------------------
SEQUENCE_6      ---------------------------------------------------------
SEQUENCE_1      ---------------------------------------------------------
SEQUENCE_3      ---------------------------------------------------------
```

Figure 6.6. Multiple alignment of isolated sequences reveals significant similarity between identical proteins # 8 and # 9 only. Shading denotes identical amino acids, alignment was carried out using CLUSTALW v1.8 software available on http://clustalw.genome.jp.

While many novel associations predicted by two-hybrid library screens reflect the actual biological association of two proteins *in vivo*, at times the apparent interaction between the two proteins may not be functionally or physiologically relevant or possible. This seems to apply to many of the interacting sequences isolated in the present study, which represent some of the most commonly found Y2H false-positives e.g. heat shock proteins, mitochondrial (sequence # 1and # 4) and ribosomal (sequence # 3) proteins (Sebriiskii & Golemis, 2001; Golemis et al., 1999). Sequence # 6 seemed to be a relevant candidate for interaction as cardiac ankyrin repeat protein (CARP) since it is known that ankyrins affect the intracellular targeting

of ion channels and mutations in these proteins have been found to result in arrhythmia (LQTs type 4, see Table 1.4., Mohler et al., 2003). However, this protein is localized in the nucleus and is also known as cytokine inducible nuclear protein, a modulator of transcription (Zolk et al., 2002), suggesting that this may be a non-physiological interaction (Sebriiskii & Golemis, 2001). The precise reason for the aberrant interaction of these proteins is not known, however it is suspected to be the consequence of the reaction taking place in the nucleus, a cellular compartment in which many of the bait and library proteins would not normally be expressed.
Other sequences selected by the WTNI bait appear to represent 'peptides' derived from DNA which would normally be non-coding e.g. *Alu* repeats (sequence # 5) which result in hypothetical proteins (sequence # 7) and may be due to a cloning artefact which arose during preparation of the cDNA library.

Elimination of these false positives leaves sequences # 2, # 8 and # 9 as possible candidates for interaction. Sequences # 8 and # 9 both represent troponin I (TnI), the inhibitory component of the troponin complex (also consisting of a Ca^{2+} binding and a tropomyosin binding subunit) which effects and regulates muscle contraction. TnI is known to bind actin, though the physiological significance of its interaction with RyR2 is unknown and it may be that this represents an artefactual interaction which is a product of the mis-localisation of these proteins to the nucleus. However, it is possible that these two proteins could come into contact with one another *in vivo*, since troponin I is localised in the cytoplasm. Thus, we cannot completely rule out this interaction, especially since this clone was isolated by two independent library screens (see Table 6.4.). Sequence # 8 represents 88 % of the coding sequence of TnI, while sequence # 9 represents the N-terminal 28 %, suggesting that it is this N-terminal portion which is responsible for binding since it is present in both interacting sequences (see Figure 6.7.A).
Sequence # 2 shows high homology with Phosphoprotein enriched in astrocytes 15 also known as Phosphoportein enriched in diabetes (PEA15/PED) which are identical to each other (see Figure 6.7.B). The sequence isolated from the library represents the C-terminal 81 % of the coding sequence of this protein, suggesting that the very N-terminus of this protein was not required for RyR2 interaction.

A Troponin I/Sequence 8

MADGSSDAAREPRPAPAPIRRRSSNYRAYATEPHAKKKSKISASRKLQLKTLLLQIAKQELEREAE
ERRGEKGRALSTRCQPLELAGLGFAELQDLCRQLHARVDKVDEERYDIEAKVTKNITEIADLTQKI
FDLRGKFKRPTLRRVRISADAMMQALLGARAKESLDLRAHLKQVKKEDTEKENREVGDWRKNIDAL
SGMEGRKKKFES

Troponin I/Sequence 9

MADGSSDAAREPRPAPAPIRRRSSNYRAYATEPHAKKKSKISASRKLQLKTLLLQIAKQELEREAE
ERRGEKGRALSTRCQPLELAGLGFAELQDLCRQLHARVDKVDEERYDIEAKVTKNITEIADLTQKI
FDLRGKFKRPTLRRVRISADAMMQALLGARAKESLDLRAHLKQVKKEDTEKENREVGDWRKNIDAL
SGMEGRKKKFES

B

```
PEA15   MAEYGTLLQDLTNNITLEDLEQLKSACKEDIPSEKSEEITTGSAWFSFLESHNKLDKD
PED     MAEYGTLLQDLTNNITLEDLEQLKSACKEDIPSEKSEEITTGSAWFSFLESHNKLDKD
        ************************************************************

PEA15   NLSYIEHIFEISRRPDLLTMVVDYRTRVLKISEEDELDTKLTRIPSAKKYKDIIRQPS
PED     NLSYIEHIFEISRRPDLLTMVVDYRTRVLKISEEDELDTKLTRIPSAKKYKDIIRQPS
        ************************************************************

PEA15   EEEIIKLAPPPKKA
PED     EEEIIKLAPPPKKA
        **************
```

Figure 6.7. Proportion of Troponin I and PEA15/PED proteins encoded by the library sequences isolated. A) Sequence # 8 and # 9 represent 88 % and 28 % of the coding sequence of TnI respectively as denoted by the shaded regions. B) PEA15 and PED are identical proteins. Alignment of the peptide sequences using the CLUSTALW v1.8 software available from http://clustalw.genome.jp shows that the sequences are 100 % homologous. The sequence isolated from the library vector (sequence # 2) represents 81 % of the total protein as denoted by the shaded region.

Since the WT but not the mutated RyR2 fragment was able to isolate these clones from the human cardiac cDNA library, it would suggest that the $N^{2386}I$ mutation abolishes interaction of RyR2 with these proteins. However, because library screening was not as extensive as desired, it is possible that the interaction of these proteins with the NI Y2H fragment may not have been detected. For this reason, the interaction of the PEA15/PED and TnI library proteins with the NI Y2H fragment was directly investigated by β-galactosidase assay following co-transformation of the constructs into the Y190 strain of yeast.

Results of this experiment showed that the $N^{2386}I$ mutation genuinely eliminated interaction of PEA15/PED with this region of the RyR2, as demonstrated by the lack of β-galactosidase activity in yeast co-expressing these two proteins (see Figure 6.8.). This was also found to be true for both TnI fragments, suggesting that whether

or not the interaction of this protein with RyR2 occurs *in vivo*, the presence a single point mutation is sufficient to cause its disruption.

These results also suggest that transcription of the reporter genes in colonies co-expressing the WTNI Y2H fragment and PEA15/PED or either of the TnI fragments is the result of *bona fide* protein-protein interaction and is not the consequence of auto-activation by the library proteins. This data suggests SCD-linked mutation of RyR2 is capable of disrupting protein-protein interactions, and that this could be associated with disease pathogenesis. However the significance of the interaction of these proteins with RyR2 is not known and will be discussed in the next section.

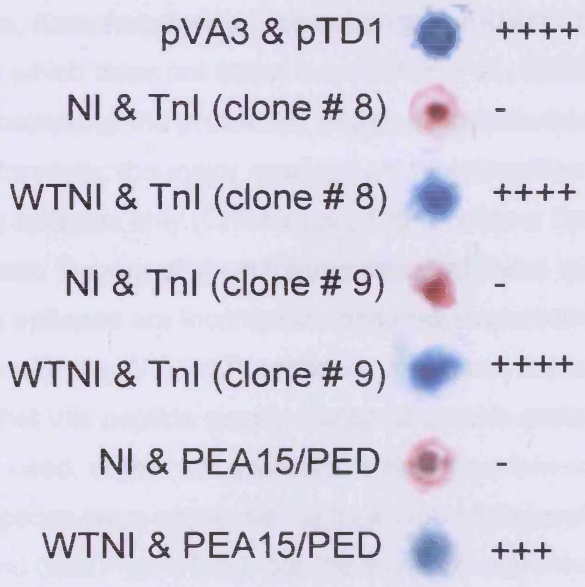

Figure 6.8. $N^{2386}I$ mutation abolishes interaction of TnI and PEA15/PED with RyR2. A colony lift β-galactosidase assay was used to evaluate protein-protein interaction, activity of the enzyme in the lysed colonies was detected by the breakdown of X-Gal to give a blue colour. ++++ and +++ indicates rapid and moderate rate of chromogenic development in this assay in comparison to the interaction of hybrid proteins encoded for by the positive control vectors pVA3 and pTD1.

6.4. Discussion

6.4.1. *Bait hybrid protein characteristics and their effects on the stringency of Y2H library screening*

Y2H genetic screens of a human cardiac cDNA expression library were carried out using short (~ 70 a.a.) fragments of WT and mutant RyR2. It could be argued that protein-protein interactions may be difficult to find due to the small nature of these peptides. However, the use of larger fragments of RyR2 corresponding to discrete domains is not favoured since they may not adopt native protein conformation in the yeast system and thus produce aberrant interactive events. For example, a recent Y2H study using a larger fragment of RyR1 (135 a.a.) encompassing the FKBP12 binding site, demonstrated an interaction with FKBP12.6 (Tiso et al., 2002), an interaction which does not occur *in vivo* (Xin et al., 2002). Thus, using smaller peptides decreases the probability of detecting false interactions because of aberrant folding. Moreover, the major requirement for interaction is the presence of the interacting epitopes only (Chien et al., 1991), without the surrounding sequence. Nevertheless, the use of short fragments could mean that in some instances the interacting epitopes are incomplete, and may explain the lack of any apparent interaction with the WTLP/LP peptides. However, this is unlikely and it is more probable that this peptide simply shows no protein-protein interaction under the conditions used, or that the appropriate library protein was not encountered.
All bait peptides were expressed at their correct molecular weights in both yeast strains used (see Figure 6.5.), but the levels of expression were heterogeneous with WTNI and WTTM fusion proteins exhibiting particularly low levels of expression compared to their corresponding mutant hybrids. It was anticipated that this difference in expression levels would lead to difficulties with the library screening since the likelihood of isolating an AD/library protein of interest may depend upon the expression characteristics of the bait hybrid. However, it transpired that library screens using these recombinant proteins identified more HIS^+ colonies than any of the other RyR2 constructs, indicating that (especially in the case of WTNI, which demonstrated *bona fide* interaction with proteins from the library) this difference in protein expression level did not appear to influence the stringency of Y2H library screening.
The somewhat acidic pI of the WTNI/NI recombinant proteins was initially thought to render them unsuitable for use in this Y2H system since they may have been able to mimic the activating regions of transcription factors, which are commonly acidic in

nature. Nevertheless, these constructs did not autonomously activate transcription of the reporter genes, demonstrating that they could be used in this two-hybrid approach.

6.4.2. Elimination of false-positives

The transformation efficiency achieved, and therefore the number of Y2H screens needed to be carried out for each construct meant that it was not possible to investigate interaction of the RyR2 fragments with every clone in the library within the time scale of this project. It is therefore probable that interaction with many of the less abundant cardiac proteins was overlooked since the probability of isolating a particular library protein depends upon the corresponding mRNA abundance in the source tissue. Nevertheless, many apparent (i.e. HIS^+) interactions were observed using some of the bait proteins (see Table 6.2.), however the majority of these were eliminated by virtue of the fact that β-galactosidase activity could not be demonstrated in these colonies. Thus, only colonies which exhibited the activity of both reporter gene products were investigated further, demonstrating that the required level of stringency was used in the selection of positive colonies. Despite this, four of the nine interacting clones isolated were mitochondrial or nuclear proteins involved in transcription and translation, which represent commonly found Y2H false positives (Golemis et al., 1999; Sebriiskii & Golemis, 2001). These misleading results are thought to occur as a result of the requirement for expression and interaction to take place in the nucleus, and this lack of comparmentalisation represents a disadvantage of the Y2H system.

Other false positives may be the result of cloning errors which occurred during preparation of the library (e.g. sequence # 5) or were not pursued further because they did not show significant homology to any published sequence (e.g. sequence # 7). It must also be noted that these clones showed very limited homology to each other on the peptide level (see Figure 6.6), signifying that their interaction with the WTNI fragment of RyR2 was not dependent on a common binding motif.

Although Table 6.4. displays the identity of the most homologous sequences found, it should be noted that less homologous cDNA sequences/proteins (i.e. the second, third closest matches etc) were also examined. Most of these represented different isoforms of the highest scoring protein from different species, and thus not likely to be physiologically relevant. Others were not considered because of their low homology to the isolated clone.

The region surrounding the $N^{2386}I$ mutation has been proposed to be the FKBP12.6 binding site (2361-2496; Marx et al., 2000), which was originally identified using Y2H. However, we were unable to isolate FKBP12.6 from the human cardiac library using our WTNI Y2H fragment. This may be because the fragment used did not encompass the entire proposed FKBP12.6 binding site. However, binding of FKBP12.6 to this site is controversial and it has recently been proposed that this short portion of the central domain is not sufficient to support the interaction with FKBP12.6, and that the true site of interaction is in the C-terminus of RyR2 (Zissimopoulos & Lai, 2005). It has also been suggested that the interaction with FKBP12.6 is conformation dependent (George et al., 2004; Oda et al., 2005), with several loci contributing to the binding site; this would suggest that the interaction would not be identified using short peptides in a Y2H system and the use of longer fragments may result in aberrant protein folding (see section 6.4.1.).

6.4.3. Significance of the interaction of Troponin I and PEA15/PED with a WT but not mutant fragment of RyR2

Disruption of accessory protein interaction has been suggested to be involved in the pathogenesis of SCD (Wehrens et al., 2003; Terentyev et al., 2003; Viatchenko-Karpinski et al., 2004). Thus, the aim of the work presented in this chapter was to determine whether the functional abnormalities of the ARVD2 mutants investigated were associated with abnormal accessory protein interaction. This was attempted by screening mutant and WT fragments of RyR2 for interaction with a Y2H library of proteins derived from cardiac tissue. Residues 2320-2406 of RyR2 were found to interact with two different proteins: Troponin I and PEA15/PED, however these interactions were abolished by the $N^{2386}I$ mutation, suggesting that this mutation causes disruption of a protein binding site. However, the significance of this with respect to SCD is not known.

Troponin I is the inhibitory subunit of troponin, the thin filament regulatory complex which confers Ca^{2+} sensitivity to muscle actomyosin ATPase activity. TnI binds to actin, and when complexed with Troponin T and tropomyosin acts to inhibit the interaction of actin and myosin in the absence of Ca^{2+} bound Troponin C. Twenty mutations in TnI are associated with familial hypertrophic cardiomyopathy, a condition which has various clinical manifestations ranging from asymptomatic to severe heart failure and sudden cardiac death (Gomes & Potter, 2004), and mutation is thought to increase the Ca^{2+} sensitivity of contraction. However, the relevance of RyR2-TnI interaction remains to be investigated and indeed the interaction itself

needs to be confirmed by other experimental techniques before further speculation can be made. Nevertheless, TnI is known to bind to polycystin-2 (Li et al., 2003a) and polycystin-L (Li et al., 2003b), members of another Ca^{2+} release channel family, and is thought to regulate these channels by inhibiting Ca^{2+} induced activation. TnI has also been found to interact with RyR1 (Varsanyi et al., 2002), however in contrast to this study the proposed binding site was situated in the C-terminus of the channel (residues 4580-4640 and 4859-4917). This interaction was also found to inhibit channel activity in bilayer studies when the peptide was added to the luminal chamber.

PEA15/PED is a 15 kDa cytoskeletal associated phosphoprotein which is a substrate of PKC (Condorelli et al., 1998). Levels of this protein have been found to be elevated in the muscle and adipose tissue of type II diabetics, and in its phosphorylated state is believed to control the level of the Glut1 plasma membrane glucose transporter and translocation of the Glut 4 transporter, leading to impaired insulin-stimulated glucose transport, a major cause of insulin resistance. Although RyR2 function is thought to be compromised in type II diabetes (Bidasee et al., 2003), it remains to be determined how direct interaction of this protein with RyR2 influences channel function and consequently how disruption of this interaction could lead to arrhythmia.

Nevertheless, recent work on the dysfunction of RyR2 in HF has indicated that dissociation of FKBP12.6 occurs as the result of defective inter-domain interactions (Oda et al., 2005), suggesting that disruption of this accessory protein interaction was a consequence, rather than a cause of channel instability. This work suggests that, even though the interaction of the central domain of RyR2 with TnI and PEA15/PED may not be significant with regard to the regulation of Ca^{2+} release, the fact that the $N^{2386}I$ mutation disrupts these interactions indicates that amino acid substitution at this residue could have a profound effect on the protein structure resulting in domain 'unzipping'. Thus, disruption of protein interaction by mutation could be the consequence of more fundamental defects. This indicates that in some instances, the dissociation of accessory proteins may be misinterpreted as the cause of channel dysfunction, and that further investigation of the channel would be necessary to confirm this. This would also signify that the disruption of protein-protein interactions could act as an indicator of major changes within the protein structure.

Chapter 7

Summary of findings and conclusions

7.1. ARVD2-linked RyR2 mutants localise to the ER and form functional homotetrameric channels when transiently expressed in HEK cells

eGFP-tagged ARVD2-linked mutants of hRyR2 ($L^{433}P$, $N^{2386}I$, $R^{176}Q$, $T^{2504}M$ and the 'double mutant' $R^{176}Q/T^{2504}M$) were successfully constructed by *in vitro* site-directed mutagenesis. Their expression was optimised in HEK cells, a cell line widely used for the characterisation of RyR2 mutants due to the fact that it is RyR-deficient, thus ensuring the formation of homotetrameric WT or mutant channels.

Stable expression of eGFP-hRyR2 was unsuccessful, since the toxic nature of the channel precluded the sustained production of sufficient recombinant protein levels for investigation. However, transient expression using a calcium phosphate method of transfection resulted in the production of full-length WT and mutant RyR2 proteins, which were correctly targeted to the ER in HEK cells, indicating that tagging with eGFP did not affect channel localisation. WT and mutant constructs demonstrated similar transfection efficiencies and were expressed at equivalent levels as determined by immunoblotting.

These recombinant proteins formed functional Ca^{2+} release channels as demonstrated by caffeine-induced Ca^{2+} release. This is in contrast to some CCD-linked RyR1 mutants, which do not exhibit Ca^{2+} release when expressed as homotetramers (Lynch et al., 1999), suggesting that the functional defects caused by RyR2 mutation are not as extreme. Indeed, RyR2 mutations identified to date represent the lower end of the spectrum of phenotypic severity, since mutations resulting in a complete lack of RyR2 function would not be compatible with long term survival (Takeshima et al., 1998).

Moreover, the WT GFP-hRyR2 channel exhibited a similar caffeine-activation profile to that previously published for untagged rabbit RyR2 (Du et al., 1998, 1999), signifying that the N-terminal tag present in this study did not alter RyR2 function with respect to its caffeine-sensitivity.

7.2. Functional heterogeneity of ARVD2-linked mutants still predicts Ca^{2+} overload

Functional characterisation of the ARVD2 mutants was necessary in order to discover the nature of dysfunctional Ca^{2+} release proposed to result in disease pathology. Since it is known that aberrant Ca^{2+} release through mutant channels is manifested following cellular stimulation, the temporal and amplitude properties of caffeine-evoked transients from cells expressing WT or mutant RyR2 were

evaluated. Caffeine was used to trigger Ca^{2+} release in this non-myocytic system because it sensitises RyR Ca^{2+} activation and thereby represents a pharmacological tool to mimic Ca^{2+} regulation occurring *in vivo*.

Ca^{2+} release was measured in living cells using confocal laser scanning microscopy and a fluorescent Ca^{2+} indicator. Hardware limitations precluded the use of ratiometric UV excitable dyes, and experimental evaluation of Ca^{2+} orange found that its significant intracellular compartmentalisation compromised its function as a cytoplasmic Ca^{2+} indicator, rendering it unsuitable for this study. However, the eGFP fluorescence of the recombinant proteins was found to be Ca^{2+} independent, and thus the spectrally similar dye, fluo-3, was successfully used to measure Ca^{2+} changes in these cells. $N^{2386}I$ and $R^{176}Q/T^{2504}M$ mutants exhibited augmented and sensitised caffeine-induced Ca^{2+} release, in agreement with the current hypothesis that RyR2 mutants exhibit a 'gain-of-function' upon activation, leading to Ca^{2+} overload under conditions of emotional/physical stress.

Contrastingly, the $L^{433}P$ mutant exhibited desensitised caffeine activation, suggesting that mutations may affect different aspects of Ca^{2+} release and that there is unlikely to be a unifying mechanism of channel dysfunction in SCD. This is in line with other ion channelopathies, where different forms of dysfunction can result in the same macroscopic effect (see Chapter 5, Table 5.1.).

Nevertheless, comprehensive examination of Ca^{2+} release profiles revealed that $L^{433}P$ exhibits a more sustained Ca^{2+} transient (rising faster, and decaying more slowly), which would most likely prolong the period of elevated Ca^{2+}, possibly leading to an increase of cytoplasmic Ca^{2+} following cellular stimulation. Consequently, this result demonstrates that $L^{433}P$ does not represent a true 'reduction-of-function' mutant and that despite significant functional heterogeneity, maximal activation of all ARVD2-linked mutants is still predicted to result in Ca^{2+} overload.

7.3. 'Double' mutant characteristics cannot be extrapolated from those of the $R^{176}Q$ and $T^{2504}M$ channels - an additional level of complexity ?

The mutations which constitute $R^{176}Q/T^{2504}M$ were also separately investigated, and both single mutants exhibited enhanced Ca^{2+} release, though their caffeine sensitivity was not significantly different to that of the WT. This demonstrates that the single mutants do not exhibit the same extent of channel dysfunction alone as they do when in combination within the conformation of the protein, and it may be that the presence of both mutations is a pre-requisite for arrhythmogenesis. Though it should be noted that the presence of mutations is not necessarily a predictor of arrhythmia (Bauce et

al., 2002). Nevertheless, the Ca^{2+} release properties of the 'double' mutant cannot be inferred from those of its component mutations, underlining the complexity of the RyR2 structure-function relationship. Thus it was inferred that changes to the channel caused only by the presence of both mutations resulted in an additional disruptive event (e.g. $R^{176}Q/T^{2504}M$ channels may exhibit gross structural changes which result in the dissociation of a regulatory accessory protein), thereby explaining this observation. However, further investigation is necessary to confirm this.

7.4. ARVD2-linked RyR2 mutations exhibit altered Ca^{2+}-dependent regulation

In this study, the Ca^{2+} sensitivity of WT and mutant channel activation and inactivation was investigated in a cellular context. This novel approach, using permeabilised cells was undertaken in an effort to examine channel function under conditions where the regulatory mechanisms more closely approximate to those present *in vivo*, since the techniques normally used to evaluate RyR Ca^{2+} sensitivity involve isolation of the channel from its native environment. In this environment, the activation and inhibition of WT RyR2 appears to be tightly regulated by $[Ca^{2+}]_c$, in contrast to *in vitro* findings of others (Du & MacLennan, 1999; Li & Chen, 2001). The $N^{2386}I$ mutant also exhibited a bi-phasic activation/inactivation profile, however this was accompanied by marked caffeine-induced channel activation at both low (0.1 nM) and high (61 μM) $[Ca^{2+}]_c$, effects not seen with WT channels. $L^{433}P$ and $R^{176}Q/T^{2504}M$ mutants showed a significant and complete loss of Ca^{2+}-dependent inhibition respectively – results which are in accordance with the prolonged Ca^{2+} transients via these channels, resulting from slower decay to half maximal amplitude. Thus, altered $[Ca^{2+}]_c$ sensitivity manifesting as decreased Ca^{2+}-dependent inhibition represents a feasible mechanism of channel dysfunction in SCD, since it may result in incomplete termination of Ca^{2+} release, prolonging $[Ca^{2+}]_c$ elevation and increasing the likelihood of DADs. Importantly however, this work does not exclude other likely mechanisms of RyR2 dysregulation. Notably, the inter-dependent nature of cytoplasmic and lumenal Ca^{2+} pools, and the observation that lumenal effects can manifest as changes in $[Ca^{2+}]_c$ sensitivity (Gyorke & Gyorke, 2001) could signify that the ARVD2 mutants investigated are also differentially sensitive to activating ER $[Ca^{2+}]$ such as those characterised by Jiang et al. (2004).

7.5. Reconciling defective Ca^{2+} handling phenotype with clinical presentation

The results presented agree with the observation that affected mutation carriers exhibit a normal resting phenotype. Resting cytoplasmic and ER Ca^{2+} environments were not significantly perturbed by the expression of mutant RyR2 channels. Furthermore, this was not achieved by compensatory changes in the expression profiles of the ER proteins SERCA and CRT, demonstrating that the functional effects of the RyR2 mutants did not alter cellular levels of these Ca^{2+} handling proteins. Despite this, we cannot exclude the possibility that the activity of these proteins, in particular that of the SERCA pump was altered, since this was not evaluated in this study. This phenotypically normal resting state could suggest that RyR2 dysregulation as a result of mutation alone does not lead to arrhythmogenesis, as evidenced by the asymptomatic nature of a number of RyR2 mutation carriers (Bauce et al., 2002). Furthermore, since normal cardiac cycling does not induce VT it points to the role of an accessory 'trigger' present during emotional or physical stress in the gross disruption of RyR2 function (notably, in these experiments Ca^{2+} release dysfunction was triggered pharmacologically by caffeine) and consequently Ca^{2+} handling during EC coupling.

7.6. $N^{2386}I$ mutation of RyR2 disrupts putative accessory protein interactions: a possible role for protein-protein interaction in VT pathogenesis

Y2H genetic screens using mutant associated fragments of RyR2 revealed an interaction between residues 2320-2406 of the channel with two cardiac proteins: Troponin I and PEA15/PED. However, these proteins did not bind to the corresponding mutant fragment, indicating that the $N^{2386}I$ mutation causes disruption of these interactions.

Troponin I is thought to bind to and inhibit other ion channels (e.g. polycystin-2, and RyR1), suggesting that it could have an inhibitory effect on RyR2, though this has not previously been reported and further studies are required to conclusively demonstrate a functional role of TnI on RyR2 regulation. The significance of the RyR2-PEA15/PED interaction is also unclear and so the effects of disrupting this interaction cannot be predicted at this stage. Furthermore, the validity of these interactions must be tested using other experimental methods to evaluate their relevance to RyR2 dysfunction in arrhythmogenesis. Nevertheless, these data provide preliminary evidence that certain RyR2 mutations result in disruption of

protein-protein interactions. It should be noted that since yeast cells were not stimulated with any RyR2 agonists, it was presumed that the abolition of these interactions by the $N^{2386}I$ mutation occurred under resting conditions, and that these data do not provide evidence for a stress-induced change in protein-protein interactions, and investigation of this was not possible using this system. Nevertheless, it could be speculated that lack of interaction with these proteins could increase the inherent propensity for arrhythmia following activation of the channel.

Appendix I – Oligonucleotide primer details

Site directed mutagenesis primers

Name	sequence	length (bp)	GC content	T_m (°C)	Restriction site	Notes
PSLSanDIF	GGATCCATATATAGGG**A**CCCGGGTTATAAT	30	43%	78.4°C	N/A	Forward primer used for insertion of a SanDI restriction site into pSL1180
PSLSanDIR	ATTATAACCCGGG**T**CCCTATATATGGATCC	30	43%	78.4°C	N/A	Reverse primer used for insertion of a SanDI restriction site into pSL1181
hRYR2 R176QF	GAAGGAGAAAAAGTA**CAA**GTTGGAGATGACCT	32	41%	69.9°C	N/A	Forward primer for mutagenesis of hRyR2 (R176Q)
hRyR2 R176QR	AGGTCATCTCCAAC**TTG**TACTTTTTCTCCTTC	32	41%	69.9°C	N/A	Reverse primer for mutagenesis of hRyR2 (R176Q)
hRyR2 L433PF	GATTTATAAGGGGC**CCT**GATGCTCTCAGCAAG	32	50%	76.1°C	N/A	Forward primer for mutagenesis of hRyR2 (L433P)
hRyR2 L433PR	CTTGCTGAGAGCATC**AGG**GCCCCTTATAAATC	32	50%	76.1°C	N/A	Reverse primer for mutagenesis of hRyR2 (L433P)
hRyR2 N2386IF	CTATCCACATGGGG**ATC**GCGATCATGACCTT	31	52%	77.8°C	N/A	Forward primer for mutagenesis of hRyR2 (N2386I)
hRyR2 N2386IR	AAGGTCATGATCGC**GAT**CCCCATGTGGATAG	31	52%	77.8°C	N/A	Reverse primer for mutagenesis of hRyR2 (N2386I)
hRyR2 T2504MF	CTGCTTCTTTAGAT**ATG**GCAGCTTTGAGTGCT	32	44%	73.4°C	N/A	Forward primer for mutagenesis of hRyR2 (T2504M)
hRyR2 T2504MR	AGCACTCAAAGCTGC**CAT**ATCTAAAGAAGCAG	32	44%	73.4 °C	N/A	Reverse primer for mutagenesis of hRyR2 (T2504M)

Appendix I – Oligonucleotide primer details (continued)

Yeast two hybrid construct primers

Name	sequence	length (bp)	GC content	T_m (°C)	Restriction site	Notes
RQ FOR	CCGCAGGAATTCCGGTCTTCAACTGATAAG	30	50%	76.7°C	EcoRI	Used to generate Y2H constructs
RQ REV	CCCATCGTCGACTCAGTTGCCATAAGACAAGTG	33	52%	79.4°C	SalI	Used to generate Y2H constructs
LP FOR	CCGCAGGAATTCGGCATAAGTTTGTCGAGATCC	33	52%	80.9 °C	EcoRI	Used to generate Y2H constructs
LP REV	CCCATCGTCGACTCAGTCTTCATGCTCTAAATG	33	48%	77.4 °C	SalI	Used to generate Y2H constructs
NI FOR	CCGCAGGAATTCGTGAGATTGCTCATTCGG	30	53%	80.5°C	EcoRI	Used to generate Y2H constructs
NI REV	CCCATCGTCGACTCACAAATGCATCTCAGGAGC	33	55%	82.5°C	SalI	Used to generate Y2H constructs
TM FOR	CCGCAGGAATTCGAGGTTCAAGACTTCCTC	30	53%	78 °C	EcoRI	Used to generate Y2H constructs
TM REV	CCCATCGTCGACTCAGAGTCAATGAGAGAAGCG	33	55%	80.8 °C	SalI	Used to generate Y2H constructs

Sequencing primers

V2-	ATACCCAGGTGGAGGAAG	18	56%	65°C	N/A	Verification of the *SpeI* restriction site boundary
B23F1	CTCGAATAAGTGAACGCC	18	50%	58°C	N/A	Verification of the *SanDI* restriction site boundary
V13+	GGAGTCCACTTCCAATTC	18	50%	57°C	N/A	Verification of the RQ mutation
V7-	GAGTGCATAGACCGTTTG	18	50%	55°C	N/A	Verification of the LP mutation
SPFOR 7160-80	GTCGCATATGGAAGAAGCCATCAAAATC	28	43%	75°C	N/A	Verification of the NI mutation
CF12	GGGAATGGGCTTCTTGCA	18	56%	66°C	N/A	Verification of the TM mutation and *KpnI* restriction site boundary
T7	TAATACGACTCACTATAGGG	20	40%	51°C	N/A	Verification of all Y2H bait constructs

Appendix I – Oligonucleotide primer details (continued)

Sequencing primers (continued)

Name	sequence	length (bp)	GC content	Tm (°C)	Restriction site	Notes
pACT2F	CTATTCGATGATGGAGATACCCCACCAAAC	30	47%	73°C	N/A	Verification of interacting Y2H library clones
pACT2R	TGTAACTTGCGGGGTTTTTCAGTATATACGAT	32	38%	71°C	N/A	Verification of interacting Y2H library clones

Base pairs/codons changed by mutagenesis are shaded.

Restriction sites within primers are underlined.

Appendix II - Alignments of pACT2 sequences isolated by Y2H with their corresponding proteins

Sequence 1

68 % identity over 7-57 of 77 a.a.

```
cytochrome_oxidase_subunit_III      ----------------------SSVSLLNNIWLSHVISLLLHHPTNTRP
SEQUENCE_1                          SLGGHMAMEAPGIRIRGRVDPNRGPLSPPNDLRPSHVISLPLHNAPHTRP
                                                        ..:*  *::  ****** **:..:***

cytochrome_oxidase_subunit_III      TNQYTNLIPMMTRHCTRKHIPRPPHNTRPK--NLRYGITLFISEAFFFVG
SEQUENCE_1                          TNQHTNHIPMMARCNTRKHIPRPPHTTCPKRPSIRDNPIYYLRSFFLRRI
                                    ***:** ****:*  **********.* **  .:* .   :: . *:

cytochrome_oxidase_subunit_III      FF-----------------------------------
SEQUENCE_1                          FLSLLPLQPSPYPPIRRALAPNRHHPAKSPRSPTPKHX
                                    *:
```

Sequence 2

98% identity over 20-120 of 130 a.a.

```
PEA15/PED           MAEYGTLLQDLTNNITLEDLEQLKSACKEDIPSEKSEEITTGSAWFSFLESHNKLDKDNL
SEQUENCE_2          ASLGCHMAMDAPGIRIRGRVDQLKSACKEDIPSEKSEEITTGSAWFSFLESHNKLDKDNL
                     :    :  * ..      ::**************************************

PEA15/PED           SYIEHIFEISRRPDLLTMVVDYRTRVLKISEEDELDTKLTRIPSAKKYKDIIRQPSEEEI
SEQUENCE_2          SYIEHIFEISRRPDLLTMVVDYRTRVLKISEEDELDTKLTRIPSAKKYKDIIRQPSEEEI
                    ************************************************************

PEA15/PED           IKLAPPPKKA-----------------------------------
SEQUENCE_2          INWLPHRRRPEQGGGRGGRLDLHQTTPFPHPPGEGARATHHLPTY
                    *:  *  ::.
```

Sequence 3

87% identity over 1-113 of 564 a.a.

```
eukaryotic_translation_initia       --------------------------------MSYPADDYESEAAYDPYA
SEQUECNE_3                          YDVPDYASLGGHMAMEAPGIRIRGRVDASEAAMSYPADDYESGAAYDPYA
                                                                    ********** *******

eukaryotic_translation_initia       YPSDYDMHTGDPKQDLAYERQYEQQTYQVIPEVIKNFIQYFHKTVSDLID
SEQUENCE_3                          YPSDYDMHTGDPKQDLAYERQYEQQTYQVIPEVIKNFIQYFHKTVSDLID
                                    ************************************************

eukaryotic_translation_initia       QKVYELQASRVSSDVIDQKVYEIQDIYENSWTKLTERFFKNTPWPEAEAI
SEQUENCE_3                          QKVYELQASRVSSDVIDQKVYEIQDIYENSWTKLTERFFKNTPWPRG---
                                    *******************************************..

eukaryotic_translation_initia       APQVGNDAVFLILYKELYYRHIYAKVSGGPSLEQRFESYYNYCNLFNYIL
SEQUENCE_3                          --------------------------------------------------

eukaryotic_translation_initia       NADGPAPLELPNQWLWDIIDEFIYQFQSFSQYRCKTAKKSEEEIDFLRSN
SEQUENCE_3                          --------------------------------------------------

eukaryotic_translation_initia       PKIWNVHSVLNVLHSLVDKSNINRQLEVYTSGGDPESVAGEYGRHSLYKM
SEQUENCE_3                          --------------------------------------------------

eukaryotic_translation_initia       LGYFSLVGLLRLHSLLGDYYQAIKVLENIELNKKSMYSRVPECQVTTYYY
SEQUENCE_3                          --------------------------------------------------
```

```
eukaryotic_translation_initia      VGFAYLMMRRYQDAIRVFANILLYIQRTKSMFQRTTYKYEMINKQNEQMH
SEQUENCE_3                         --------------------------------------------------

eukaryotic_translation_initia      ALLAIALTMYPMRIDESIHLQLREKYGDKMLRMQKGDPQVYEELFSYSCP
SEQUENCE_3                         --------------------------------------------------

eukaryotic_translation_initia      KFLSPVVPNYDNVHPNYHKEPFLQQLKVFSDEVQQQAQLSTIRSFLKLYT
SEQUENCE_3                         --------------------------------------------------

eukaryotic_translation_initia      TMPVAKLAGFLDLTEQEFRIQLLVFKHKMKNLVWTSGISALDGEFQSASE
SEQUENCE_3                         --------------------------------------------------

eukaryotic_translation_initia      VDFYIDKDMIHIADTKVARRYGDFFIRQIHKFEELNRTLKKMGQRP
SEQUENCE_3                         -----------------------------------------------
```

Sequence 4

89 % identity over 28-167 of 292 a.a.

```
ECHDC2          --------MLRVLCLLRPWRPLRARGCASDGAAGG-----------SEIQVRALAGPDQ
SEQUENCE_4      LGWSLWPWTAPGIRIRGPRRPRFCASCSTLEAPSGPRLRFRRGGRGASEIQVRALAGSDQ
                          : :  * **  . .*::  *..*            **********.**

ECHDC2          GITEILMNRPSARNALGNVFVSELLETLAQLREDRQVRVLLFRSGVKGVFCAGADLKERE
SEQUENCE_4      GITEILMNRPSARNALGNVFVSELLETLAQLREDRQVRVLLFRSGVKGVFCAGADLKERE
                ************************************************************

ECHDC2          QMSEAEVGVFVQRLRGLMDDIAAFPAPTIAAMDGFALGGGLELALACDLRVAASSAVMGL
SEQUENCE_4      QMSEAEVGVFVQRLRGLMNDIAAFPAPTIAAMDGFALGGGLELALACDLRVAASSAVMGL
                ******************:*****************************************

ECHDC2          IETTRGLLPGAGGTQRLPRCLGVALAKELIFTGRRLSGTEAHVLGLVNHAVAQNEEGDAA
SEQUENCE_4      IETTRGL-------------------------------------------------------
                *******

ECHDC2          YQRARALAQEILPQAPIAVRLGKVAIDRGTEVDIASGMAIEGMCYAQNIPTRDRLEGMAA
SEQUENCE_4      ------------------------------------------------------------

ECHDC2          FREKRTPKFVGK
SEQUENCE_4      ------------
```

Sequence 5

60% identity over 1-84 and 186-199 of 603 a.a.

```
Alu_subfamily_SB2_sequence      ------------------------GRARWLTPVIPALWEAEAGGS-GQEI
SEQUENCE_5                      SVHLNPVKNLVLQILIHCSLKKRLGQAPWLTLAIPAPLEAEAGRSQGQEI
                                                        *:* *** .***  ***** * ****

Alu_subfamily_SB2_sequence      ETILANKVKP-RLYKYKKLAGRGGGRLS-QLLGRLRQENGVNPGSGACSE
SEQUENCE_5                      ETILANTAKFSLHQKYKKSAGRGGGRLQSQPLRRPRQENGVDPGGRGCSE
                                ******..*     **** ********. * * * ******:**. .***

Alu_subfamily_SB2_sequence      PRLRHCSPQSGLGDRARLRLKKAGRGGSRLSQHFGRPRRVDHEVRRSRPS
SEQUENCE_5                      PRSHHCTP------------------------------------------
                                ** :**:*

Alu_subfamily_SB2_sequence      WLTRNPVSTKNTKNPGAVAGACSPSYWGGGRRMATREAELAVSRDCATAV
SEQUENCE_5                      --------------------------------------------------

Alu_subfamily_SB2_sequence      RSPAWATERDSVSKKPGAVAHACNPSTLGGRGGWIMRSGDRDHPGQGETP
SEQUENCE_5                      ---AWATERDSVSKKKRKH-----------------------------
                                   ************
```

```
Alu_subfamily_SB2_sequence      SLLKIQKISRARWRAPVVPATGEAEAGEWREPGKRSLQAEIAPLQSAVRP
SEQUENCE_5                      --------------------------------------------------

Alu_subfamily_SB2_sequence      GRQSETPSQKKFFLRRSLALSPRPDCGLQWRNLGSLQAPLPGFTPFSCLS
SEQUENCE_5                      --------------------------------------------------

Alu_subfamily_SB2_sequence      LPSSWDYRRPPPRPANFLYFRRGFTLLARMVSISPHDPPASASQSAGITG
SEQUENCE_5                      --------------------------------------------------

Alu_subfamily_SB2_sequence      VSHRARFFDGVSLCRPGRTADCSGAISAHCKLRFPGSRHSPASASPVAGT
SEQUENCE_5                      --------------------------------------------------

Alu_subfamily_SB2_sequence      TGARHRARLIFCIFSRDGVSPCPGWSRSPDLMIHPPRPPKVLGLQAATAP
SEQUENCE_5                      --------------------------------------------------

Alu_subfamily_SB2_sequence      GFFETESRSVAQAGLRTAVAQSRLTASSASRVHAILLPQPPQLGLQAPAT
SEQUENCE_5                      --------------------------------------------------

Alu_subfamily_SB2_sequence      APGFFVFLVETGFHLVSQDGLDLLTSSTRLGLPKCWDYRREPPRPA
SEQUENCE_5                      ----------------------------------------------
```

Sequence 6

98 % identity over 1-93 of 319 a.a.

```
cardiac_ankyrin_repeat_protein      ----------------------MMVLKVEELVTGKKNGNGEAGEFLPEDFR
SEQUENCE_6                          EAPGIRIRGRVDKPYKTPSANMMVLKVEELVTGKKNGNGEAGEFLPEDFR
                                                          ******************************

cardiac_ankyrin_repeat_protein      DGEYEAAVTLEKQEDLKTLLAHPVTLGEQQWKSEKQREAELKKKKLEQRS
SEQUENCE_6                          DGEYEAAVTLEKQEDLKTLLAHPVTLGEQQWKSEKQREAELKKKKLEQRS
                                    **************************************************

cardiac_ankyrin_repeat_protein      KLENLEDLEIIIQLKKRKKYRKTKVPVVKEPEPEIITEPVDVPTFLKAAL
SEQUENCE_6                          KLENLEDLEIIIQLKKKKKKTREIYES-----------------------
                                    ****************:**  :

cardiac_ankyrin_repeat_protein      ENKLPVVEKFLSDKNNPDVCDEYKRTALHRACLEGHLAIVEKLMEAGAQI
SEQUENCE_6                          --------------------------------------------------

cardiac_ankyrin_repeat_protein      EFRDMLESTAIHWASRGGNLDVLKLLLNKGAKISARDKLLSTALHVAVRT
SEQUENCE_6                          --------------------------------------------------

cardiac_ankyrin_repeat_protein      GHYECAEHLIACEADLNAKDREGDTPLHDAVRLNRYKMIRLLIMYGADLN
SEQUENCE_6                          --------------------------------------------------

cardiac_ankyrin_repeat_protein      IKNCAGKTPMDLVLHWQNGTKAIFDSLRENSYKTSRIATF
SEQUENCE_6                          ----------------------------------------
```

Sequence 7

28 % identity over 52-153 of 188 a.a.

```
hypothetical_protein_XP_240835      MYRFRIGLRDSDFESNLERLIHLHIRVINNSAELGICPSRSCYPFVFCVA
SEQUENCE_7                          --------------------------------------------------

hypothetical_protein_XP_240835      ARNTNAFTTVSSPSGKSSCPSELCPHFAGGNLLLLSCENYCSIVICPRVLC
SEQUENCE_7                          WRPRGSEFAAASTNGN--------VAFLGGFLLLLFCNYQ----------
                                     *  .:  :.:*..*:          * ** ***   **
```

```
hypothetical_protein_XP_240835      THVKFVVQLLLVNKKQCTRAGLGRMVLRTTEALKITQFRQVLCHSLSSSL
SEQUENCE_7                          TQVRYWYPALDFQMKFSRRQ-----------LRLKYYTKISKGSILRYL
                                    *:*::    * .: * . *            *::. : ::   *:   *

hypothetical_protein_XP_240835      PRQEVRIAVCITFTDTERRDFLERGASTVDSKDSSGRS
SEQUENCE_7                          YDDT--------------------------------
                                      :
```

Sequence 8

100 % identity over 1-184 of 210 a.a.

```
Troponin_I          ------------------------------------------MADGSSDAAREPRPA
SEQUENCE_8          EAPGIRIRGRVDPWDPEGHPGGPLTDPPNAPVLALPPAIPGLSLSMADGSSDAAREPRPA
                                                             ***************

Troponin_I          PAPIRRRSSNYRAYATEPHAKKKSKISASRKLQLKTLLLQIAKQELEREAEERRGEKGRA
SEQUENCE_8          PAPIRRRSSNYRAYATEPHAKKKSKISASRKLQLKTLLLQIAKQELEREAEERRGEKGRA
                    ************************************************************

Troponin_I          LSTRCQPLELAGLGFAELQDLCRQLHARVDKVDEERYDIEAKVTKNITEIADLTQKIFDL
SEQUENCE_8          LSTRCQPLELAGLGFAELQDLCRQLHARVDKVDEERYDIEAKVTKNITEIADLTQKIFDL
                    ************************************************************

Troponin_I          RGKFKRPTLRRVRISADAMMQALLGARAKESLDLRAHLKQVKKEDTEKENREVGDWRKNI
SEQUENCE_8          RGKFKRPTLRRVRISADAMMQALLGARAKESLDLRAHLKQVKKEDTEKE-----------
                    ********************************************

Troponin_I          DALSGMEGRKKKFES
SEQUENCE_8          ---------------
```

Sequence 9

100 % identity over 1-57 of 210 a.a.

```
Troponin_I          ----------------------------------------------------MADG
SEQUENCE_9          AMEAPGIRIAAASTSSSPEETDGPWDPEGHPGGPLTDPPNAPVLALPPAIPGLSLSMADG
                                                                       ****

Troponin_I          SSDAAREPRPAPAPIRRRSSNYRAYATEPHAKKKSKISASRKLQLKTLLLQIAKQELERE
SEQUENCE_9          SSDAAREPRPAPAPIRRRSSNYRAYATEPHAKKKSKISASRKLQLKTLLLQIAKHSWSER
                    ************************************************:. ...

Troponin_I          AEERRGEKGRALSTRCQPLELAGLGFAELQDLCRQLHARVDKVDEERYDIEAKVTKNITE
SEQUENCE_9          RRSGAERRGAL-------------------------------------------------
                     ..   .:*

Troponin_I          IADLTQKIFDLRGKFKRPTLRRVRISADAMMQALLGARAKESLDLRAHLKQVKKEDTEKE
SEQUENCE_9          ------------------------------------------------------------


Troponin_I          NREVGDWRKNIDALSGMEGRKKKFES
SEQUENCE_9          --------------------------
```

Appendix III - Abbreviations

A	ampere(s)	**$Ca_v1.2$**	L-type voltage gated Ca^{2+} channel/dihydropyridine receptor
A_{260}	absorbance at 260 nm	**CCD**	central core disease
a.a.	amino acid	**cDNA**	complementary DNA
AC	adenylyl cyclase	**cfu**	colony forming units
AM	acetoxymethyl ester	**CHAPS**	3-[(3Cholamidopropyl) dimethylammonio]-1-propanesulfonate
AP	action potential	**CICR**	Ca^{2+}-induced-Ca^{2+}-release
ARVD2	arrhythmogenic right ventricular dysplasia type 2	**4-cmc**	4-chloro-m-cresol
3-AT	3-amino-1,2,4-triazole	**CMV**	cytomegalovirus
ATP	adenosine trisphosphate	**COSHH**	control of substances hazardous to health
BCA	bicinchoninic acid	**CPVT**	catecholaminergic polymorphic ventricular tachycardia
β-AR	β-adrenergic receptor	**CRU**	Ca^{2+} release unit
β-gal	β-galactosidase	**CSQ**	calsequestrin
BSA	bovine serum albumen	**DAD**	delayed afterdepolarisation
bp	base pair(s)	**DMEM**	Dulbecco's modified eagle medium
°C	degrees Celsius	**DMF**	N,N-dimethylfprmamide
Ca^{2+}	ionized calcium	**DMSO**	dimethyl sulphoxide
cADPr	cyclic adenosine diphosphate ribose	**DNA**	deoxyribonucleic acid
CaMKII	calmodulin dependent kinase II	**dNTP**	2'-deoxyribonucleotide 5'-triphosphate
cAMP	cyclic adenosine monophosphate	**DO**	drop-out yeast medium

dpi	dots per inch	**HF**	heart failure
DR	divergent region	**-His**	yeast drop-out medium lacking histidine
EAD	early afterdepolarisation	**HOCM**	hypertrophic obstructive cardiomyopathy
EC	excitation-contraction	**HPLC**	high-pressure liquid chromatography
EC_{50}	The molar concentration of an agonist, which produces 50% of the maximum possible response for that agonist	**IC_{50}**	the molar concentration of an antagonist, which produces 50% of the maximum possible inhibition for that antagonist
ECG	electrocardiograph	**I_{Ca}**	inward Ca^{2+} current
ECL	enhanced chemiluminescence	**ICD**	implantable cardioverter defibrillator
EDTA	ethylene-diamine-tetraacetic acid	**ID**	intercalated disc
EGTA	ethylene glycol-bis (β-aminoethylether)-N,N,N',N'-tetraacetic acid	**IgG**	immunoglobulin G
EM	electron microscopy	**IP_3R**	inositol inositol-1,4,5-trisphosphate receptor
ER	Endoplasmic reticulum	**IVF**	idiopathic ventricular fibrillation
F	Farrad(s)	**JLNS**	Jervell and Lange-Nielsen syndrome
FCS	Foetal calf serum	**K^+**	ionized potassium
FKBP12	FK506 binding protein 12	**kb**	kilobase(s)
FKBP12.6	FK506 binding protein 12.6	**K_d**	dissociation constant
g	gram(s)	**kDa**	kiloDalton(s)
g	the acceleration due to gravity	**KDS**	potassium dodecyl sulphate
HEK	human embryonic kidney cells	**KRH**	Krebs-Ringer Hepes buffer
HEPES	N-2-hydroxyethylpiperazine-N'-2-ethanesulphonic acid	**L**	litre

LB	Luria Bertani medium	**nM**	nanomoles/nanomolar
-Leu	yeast drop-out medium lacking leucine	**nm**	nanometre
LiAc	lithium acetate	**NO**	nitric oxide
LQTS	long QT syndrome	**ng**	nanogram(s)
M	molar	**NZY**	nutrient Z amineA and yeast extract medium
MCS	multiple cloning site	**Ω**	ohm(s)
MH	malignant hyperthermia	**ORF**	open reading frame
Mg^{2+}	ionised magnesium	**pAb**	polyclonal antibody
mg	milligram(s)	**PAGE**	polyacrylamide gel elecrophoresis
ml	millilitre(s)	**PBS**	phosphate buffered saline
mM	millimoles/molar	**PCR**	polymerase chain reaction
mm	millimetre	**PEG**	polyethylene glycol
µg	microgram(s)	**PKA**	protein kinase A
µl	microlitre	**PLN**	phospholamban
µM	micromoles/molar	**PMCA**	plasma membrane Ca^{2+} ATPase
µm	micrometer	**PMT**	photomultiplier tube
Mito	mitochondria	**PP1**	protein phosphatase 1
Na^{+}	ionized sodium	**PP2A**	protein phosphatase 2A
NCX	Na^{+}/Ca^{2+} exchanger	**ppm**	parts per million

PVDF	polyvinylidene fluoride	**TG**	thapsigargin
ROI	region of interest	**T_m**	melting temperature
RNA	ribonucleic acid	**Tn C**	the Ca^{2+} binding component of troponin
rpm	revolutions per minute	**Tn I**	the inhibitory, actin binding component of troponin
RyR	ryanodine receptor	**Tn T**	the tropomyosin binding component of troponin
SCD	sudden cardiac death	**Tris**	tris(hydroxymethyl)aminomethane
SD	synthetic drop-out yeast medium	**-Trp**	yeast drop-out medium lacking tryptophan
SDS	sodium dodecyl sulphate	**TT**	t-tubule(s)
SERCA	sarco(endo)plasmic reticulum Ca^{2+} ATPase	**UTR**	untranslated region
SL	sarcolemma	**UV**	ultraviolet
SLO	streptolysin-O	**V**	volt(s)
sorcin	**so**luble drug **r**esistance related **c**alcium binding prote**in**	**VGCC**	voltage-gated calcium channel
SR	sarcoplasmic reticulum	**VT**	ventricular tachycardia
SUNDS	sudden and unexpected nocturnal death syndrome	**v/v**	volume/volume
TAE	tris-acetate-EDTA buffer	**w/v**	weight/volume
TBS	tris buffered saline	**X-gal**	5-bromo-4-chloro-3-indoyl-β-D-galactopyranoside
TBS-T	TBS-Tween20	**Y2H**	yeast-two hybrid
TE	tris-EDTA buffer	**YNB**	yeast nitrogen base
TEMED	N,N,N',N'-tetramethylethylenediamine	**YPD**	yeast peptone dextrose medium

Bibliography

Abbott, G.W., Sesti, F., Splawski, I., Buck, M.E., Lehmann, M.H., Timothy, K.W., Keating, M.T., and Goldstein, S.A. (1999) MiRP1 forms IKr potassium channels with HERG and is associated with cardiac arrhythmia. *Cell* **97(2)**; 175-87

Ahern, G.P., Junankar, P.R. and Dulhunty, A.F. (1994) Single channel activity of the ryanodine receptor calcium release channel is modulated by FK-506. *Federation of European Biochemical Societies Letters* **352(3)**; 369-74

Ahern, G.P., Junankar, P.P. and Dulhunty, A.F. (1997) Subconductance states in single-channel activity of skeletal muscle ryanodine receptors after removal of FKBP12. *Biophysical Journal* **72(1)**; 146-62

Ahmad, F., Li, D., Karibe, A., Gonzalez, O., Tapscott, T., Hill, R., Weilbaecher, D., Blackie, P., Furey, M., Gardner, M., Bachinski, L.L. and Roberts, R. (1998) Localization of a gene responsible for arrhythmogenic right ventricular dysplasia to chromosome 3p23. *Circulation* **98(25)**; 2791-5

Allen, G.C., Fletcher, J.E., Huggins, F.J., Conti, P.A. and Rosenberg, H. (1990) Caffeine and halothane contracture testing in swine using the recommendations of the North American Malignant Hyperthermia Group. *Anesthesiology* **72(1)**; 71-6

Allen, P.D. (2003) Not all sudden death is the same. *Circulation Research* **93**; 484-486

Allouis, M., Probst, V., Jaafar, P., Schott, J. and Le Marec, H. (2005) Unusual clinical presentation in a family with catecholaminergic polymorphic ventricular tachycardia due to a G14876A ryanodine receptor gene mutation. *American Journal of Cardiology* **95**; 700-702

Altschul, S.F., Madden, T.L., Schaffer, A.A., Zhang, J., Zhang, Z., Miller, W. and Lipman, D.J. Gapped BLAST and PSI-BLAST: a new generation of protein database search programs. *Nucleic Acids Research* **25(17)**; 3389-402

Ausubel, F., Brent, R., Kingston, R.E., Moore, D.D., Seidman, J.G., Smith, J.A. and Struhl, K. (1997) Short protocols in molecular biology. Third Edition. John Wiley & sons Incorporated, NY, USA

Avila, G. and Dirksen, R.T. (2001) Functional effects of central core disease mutations in the cytoplasmic region of the skeletal muscle ryanodine receptor. *Journal of General Physiology* **118(3)**; 277-90

Avila, G., O'Connell, K.M. and Dirksen, R.T. (2003) The pore region of the skeletal muscle ryanodine receptor is a primary locus for excitation-contraction uncoupling in central core disease. *Journal of General Physiology* **121(4)**; 277-86

Baker, M.L., Serysheva, I.I., Sencer, S., Wu Y., Ludtke, S.J., Jiang, W., Hamilton, S.L. and Chiu, W. (2002) The skeletal muscle Ca^{2+} release channel has an oxidoreductase-like domain. *Proceedings of the National Academy of Sciences of the United States of America* **99**; 12155-12160

Balshaw, D.M., Xu, L., Yamaguchi, N., Pasek, D.A. and Meissner, G.M. (2001) Calmodulin binding and inhibition of cardiac muscle calcium release channel (ryanodine receptor). *Journal of Biological Chemistry* **276**; 20144-20153

Barg, S., Copello, J.A. and Fleischer, S. (1997) Different interactions of cardiac and skeletal muscle ryanodine receptors with FK-506 binding protein isoforms. *American Journal of Physiology* **272(5 Pt 1)**; C1726-33

Bartel, P., Chien, C., Stenglanz, R. and Fields, S. (1993) Elimination of false positives that arise using the two-hybrid system. *BioTechniques* **14**; 920-924

Bassani, R.A., Bassani, J.W. and Bers, D.M. (1994a) Relaxation in ferret ventricular myocytes: unusual interplay among calcium transport systems. Journal of Physiology **476(2)**; 295-308

Bassani, J.W., Bassani, R.A. and Bers, D.M. (1994b) Relaxation in rabbit and rat cardiac cells: species-dependent differences in cellular mechanisms. *Journal of Physiology* **476(2)**; 279-93

Bauce, B., Rampazzo, A., Basso, C., Bagattin, A., Daliento, L., Tiso, N., Turrini, P., Thiene, G., Danieli, G.A. and Nava, A. (2002) Screening for ryanodine receptor type 2 mutations in families with effort-induced polymorphic ventricular arrhythmias and sudden death. *Journal of the American College of Cardiology* **40**; 341-349

Bayer, K.U., Harbers, K. and Schulman, H. alphaKAP is an anchoring protein for a novel CaM kinase II isoform in skeletal muscle. *European Molecular Biology Organisation Journal* **17(19)**; 5598-605

Beard, N.A., Sakowska, M.M., Dulhunty, A.F. and Laver, D.R. (2002) Calsequestrin is an inhibitor of skeletal muscle ryanodine receptor calcium release channels. *Biophysical Journal* **82**; 310-320

Benkusky, N.A., Farrell, E.F. and Valdivia, H.H. (2004) Ryanodine receptor channelopathies. *Biochemical and Biophysical Research Communications* **322**; 1280-1285

Berlin, J.R., Bassani, J.W. and Bers, D.M. (1994) Intrinsic cytosolic calcium buffering properties of single rat cardiac myocytes. *Biophysical Journal* **67**; 1775-87

Berne, R.M. and Levy M.N. (1993) Cardiovascular physiology (third edition). St Louis: C.V. Mosby

Berridge, M.J. (1997) Elementary and global aspects of calcium signalling. *Journal of Experimental Biology* **200**; 315-319

Berridge, M.J., Bootman, M.D. and Roderick, H.L. (2003) Calcium signalling: dynamics, homeostasis and remodelling. *Nature Reviews - Molecular Cell Biology* **4**; 517-529

Berridge, M.J., Lipp, P. and Bootman, M.D. (2000) The versatility and universality of calcium signalling. *Nature Reviews - Molecular cell biology* **1**; 11-21

Bers, D.M. (2001) Excitation-contraction coupling and cardiac contractile force (second edition). Dodrecht (Netherlands): Kluwer academic publishers.

Bers, D.M. (2002) Cardiac excitation-contraction coupling. *Nature* **415**; 198-204

Bers, D.M. (2004) Macromolecular complexes regulating cardiac ryanodine receptor function. *Journal of Molecular and Cellular Cardiology,* **37**; 417-429

Bers, D.M. and Peres-Reyes, E. (1999) Ca^{2+} channels in cardiac myocytes: structure and function in Ca^{2+} influx and intracellular Ca^{2+} release. *Cardiovascular Research* **42**; 339-360

Bers, D.M. and Stiffel, V.M. (1993) Ratio of ryanodine to dihydropyridine receptors in cardiac and skeletal muscle and implications for E-C coupling. *American Journal of Physiology* **264(6 Pt 1)**; C1587-93

Bhakdi, S., Bayley, H., Valeva, A., Walev, I., Walker, B., Kehoe, M., Palmer, M..Fawcett, J.M., Harrison, S.M., and Orchard, C.H. (1998) A method for reversible permeabilization of isolated rat ventricular myocytes. *Experimental Physiology* **83(3)**; 293-303

Bhakdi, S., Weller, U., Walev, I., Martin, E., Jonas, D. and Palmer, M. (1993) A guide to the use of pore-forming toxins for controlled permeabilization of cell membranes. *Medical Microbiology and Immunology* **182(4)**; 167-75

Bhat, M.B., Hayek, S.M., Zhao, J., Zang, W., Takeshima, H., Wier, W.G. and Ma, J. (1999) Expression and functional characterization of the cardiac muscle ryanodine receptor Ca($^{2+}$) release channel in Chinese hamster ovary cells. *Biophysical Journal* **77(2)**; 808-16

Bhat, M.B., Zhao, J., Hayek, S., Freeman, E.C., Takeshima, H. and Ma, J. (1997a) Deletion of amino acids 1641-2437 from the foot region of skeletal muscle ryanodine receptor alters the conduction properites of the Ca release channel. *Biophysical Journal* **73**; 1320-1328

Bhat, M.B., Zhao, J., Takeshima, H. and Ma, J. (1997b) Functional calcium release channel formed by the carboxyl-terminal portion of the ryanodine receptor. *Biophysical Journal* **73**; 1329-1336

Bhat, M.B., Zhao, J., Zang, W., Balke, C.W., Takeshima, H., Wier, W.G. and Ma, J. (1997c) Caffeine-induced release of intracellular Ca^{2+} from Chinese hamster ovary cells expressing skeletal muscle ryanodine receptor. *Journal of General Physiology* **110**; 749-762

Bidasee, K.R., Besch, H.R. Jr, Gerzon, K. and Humerickhouse, R.A. (1995) Activation and deactivation of sarcoplasmic reticulum calcium release channels: molecular dissection of mechanisms via novel semi-synthetic ryanoids. *Molecular and Cellular Biochemistry* **149-150**; 145-60

Bidasee, K.R., Nallani, K., Yu, Y., Cocklin, R.R., Zhang, Y., Wang, M., Dincer, U.D. and Besch, H.R. (2003) Chronic diabetes increases advanced glycation end products on cardiac ryanodine receptors/calcium release channels. *Diabetes* **52**; 1825-1836

Bjellqvist, B., Hughes, G.J., Pasquali, C.H., Paquet, N., Ravier, F., Sanchez, J.C., Frutiger, S. and Hochstrasser, D.F. (1993) The focusing positions of polypeptides in immobilised pH gradients can be predicted from their amino acid sequences. *Electrophoresis* **14**; 1023-1031

Block, B.A., Imagawa, T., Campbell, K.P. and Franzini-Armstrong, C. (1988) Structural evidence for direct interaction between the molecular components of the transverse tubule/sarcoplasmic reticulum junction in skeletal muscle. Journal of Cell Biology **107(6 Pt 2)**; 2587-600

Bootman, M., Niggli, E., Berridge, M. and Lipp, P. (1997) Imaging the hierarchical Ca^{2+} signalling system in HeLa cells. *Journal of Physiology* **499**; 307-14

Bosanac, I., Alattia, J.R., Mal, T.K., Chan, J., Talarico, S., Tong, F.K., Tong, K.I., Yoshikawa, F., Furuichi, T., Iwai, M., Michikawa, T., Mikoshiba, K. and Ikura, M. (2002) Structure of the inositol 1,4,5-trisphosphate receptor binding core in complex with its ligand. *Nature* **420(6916)**; 696-700

Brandt, N.R., Caswell, A.H., Brandt, T., Brew, K., and Mellgren, R.L. (1992) Mapping the calpain proteolysis products of the junctional foot protein of the skeletal muscle triad junction. *Journal of Membrane Biology* **127(1)**; 35-47

Brillantes, A.B., Ondrias, K., Scott, A., Kobrinsky, E., Ondriasova, E., Moschella, M.C., Jayaraman, T., Landers, M., Ehrlich, B.E. and Marks, A.R. (1994) Stabilization of calcium release channel (ryanodine receptor) function by FK506-binding protein. *Cell* **77(4)**; 513-23

Brini, M. (2004) Ryanodine receptor defects in muscle genetic diseases. *Biochemical and Biophysical Research Communications* **322(4)**; 1245-55

Brini, M., Manni, S., Pierobon, N., Du, G.G., Sharma, P., MacLennan, D.H. and Carafoli, E. (2005) Ca^{2+} signaling in HEK-293 and skeletal muscle cells expressing recombinant

ryanodine receptors harboring malignant hyperthermia and central core disease mutations. *Journal of Biological Chemistry* **280(15)**; 15380-9

Broder, Y.C., Katz, S. and Aronheim A. (1998) The ras recruitment system, a novel approach to the study of protein-protein interactions. *Current Biology* **8(20)**; 1121-4

Brugada, P. and Brugada, J. (1992) Right bundle branch block, persistent ST segment elevation and sudden cardiac death: a distinct clinical and electrocardiographic syndrome. A multicenter report. *Journal of American College of Cardiology* **20(6)**; 1391-6

Buck, E., Zimanyi, I., Abramson, J.J. and Pessah, I.N. (1992) Ryanodine stabilizes multiple conformational states of the skeletal muscle calcium release channel. *Journal of Biological Chemistry* **267(33)**; 23560-7

Bull, R., Marengo, J.J., Suarez-Isla, B.A., Donoso, P., Sutko, J.L. and Hidalgo, C. (1989) Activation of calcium channels in sarcoplasmic reticulum from frog muscle by nanomolar concentrations of ryanodine. *Biophysical Journal* **56(4)**; 749-56

Bultynck, G., Rossi, D., Callewaert, G., Missiaen, L., Sorrentino, V., Parys, J.B. and De Smedt, H. (2001) The conserved sites for the FK506-binding proteins in ryanodine receptors and inositol 1,4,5-trisphosphate receptors are structurally and functionally different. *Journal of Biological Chemistry* **276**; 477158-447724

Cadwell, J.J. and Caswell, A.H. (1982) Identification of a constituent of the junctional feet linking terminal cisternae to transverse tubules in skeletal muscle. *Journal of Cell Biology* **93(3)**; 543-50

Callaway, C., Seryshev, A., Wang, J.P., Slavik, K.J., Needleman, D.H., Cantu, C. 3rd, Wu, Y., Jayaraman, T., Marks, A.R. and Hamilton, S.L. (1994) Localization of the high and low affinity [^{3}H]ryanodine binding sites on the skeletal muscle Ca^{2+} release channel. *Journal of Biological Chemistry* **269(22)**; 15876-84

Cameron, A.M., Nucifora, F.C. Jr, Fung, E.T., Livingston, D.J., Aldape, R.A., Ross, C.A. and Snyder, S.H. (1997) FKBP12 binds the inositol 1,4,5-trisphosphate receptor at leucine-proline (1400-1401) and anchors calcineurin to this FK506-like domain. *Journal of Biological Chemistry* **272(44)**; 27582-8

Cameron, A.M., Steiner, J.P., Sabatini, D.M., Kaplin, A.I., Walensky, L.D. and Snyder, S.H. (1995) Immunophilin FK506 binding protein associated with inositol 1,4,5-trisphosphate receptor modulates calcium flux. *Proceedings of the National Academy of Sciences of the United States of America* **92(5)**; 1784-8

Cannell, M.B., Cheng, H. and Lederer, W.J. (1995) The control of calcium release in heart muscle. *Science* **268(5213)**; 1045-9

Cannell, M.B. and Soeller, C. (1999) Mechanisms underlying calcium sparks in cardiac muscle. *Journal of General Physiology* **113(3)**; 373-6

Carmody, M., Mackrill, J.J., Sorrentino, V. and O'Neill, C. (2001) FKBP12 associates tightly with the skeletal muscle type 1 ryanodine receptor, but not with other intracellular calcium release channels. *Federation of European Biochemical Societies Letters* **505**; 97-102

Caswell, A.H., Brandt, N.R., Brunschwig, J.P. and Purkerson, S. (1991) Localization and partial characterization of the oligomeric disulfide-linked molecular weight 95,000 protein (triadin) which binds the ryanodine and dihydropyridine receptors in skeletal muscle triadic vesicles. *Biochemistry* **30(30)**; 7507-13

Censier, K., Urwyler, A., Zorzato, F. and Treves, S. (1998) Intracellular calcium homeostasis in human primary muscle cells from malignant hyperthermia-susceptible and normal individuals. *Journal of Clinical Investigation* **101**; 1233-1242

Cerrone, M., Colombi, B., Santoro, M., di Barletta, M.R., Scelsi, M., Villani, L., Napolitano, C., and Priori, S.G. (2005) Bidirectional ventricular tachycardia and fibrillation elicited in a knock-in mouse model carrier of a mutation in the cardiac ryanodine receptor. *Circulation Research* **96(10)**; 77-82

Chalfie, M., Tu, Y., Euskirchen, G., Ward, W.W. and Prasher, D.C. (1994) Green fluorescent protein as a marker for gene expression. *Science* **263(5148)**; 802-5

Chamberlain, B.K., Volpe, P. and Fleischer, S. (1984) Inhibition of calcium-induced calcium release from purified cardiac sarcoplasmic reticulum vesicles. *Journal of Biological Chemistry* **259(12)**; 7547-53

Chen, S.R.W., Ebisawa, K., Li, X. and Zhang, L. (1998) Molecular identification of the ryanodine receptor Ca^{2+} sensor. *Journal of Biological Chemistry* **273**; 14675-14678

Chen, S.R., Leong, P., Imredy, J.P., Barlett, C., Zhang, L. and MacLennan, D.H. (1997) Single-channel properties of the recombinant skeletal muscle Ca^{2+} release channel (ryanodine receptor). *Biophysical Journal* **73(4)**; 1904-12

Chen, S.R.W., Li, X., Ebisawa, K. and Zhang, L. (1997) Functional characterisation of the recombinant type 3 Ca^{2+} release channel (ryanodine receptor) expressed in HEK293 cells. *Journal of Biological Chemistry* **272**; 24234-24246

Chen, S.R.W., Li, P., Zhao, M., Li, X. and Zhang, L. (2002) Role of the proposed pore-forming segment of the Ca^{2+} release channel (ryanodine receptor) in ryanodine interaction. *Biophysical Journal* **82**; 2436-2447

Chen, S.R.W. and MacLennan, D.H. (1994) Identification of calmodulin, Ca^{2+}, and ruthenium red binding domains in the Ca^{2+} release channel (ryanodine receptor) of rabbit skeletal muscle sarcoplasmic reticulum. *Journal of Biological Chemistry* **269**; 22698-22704

Chen, C. and Okayama, H. (1987) High efficiency transformation of mammalian cells by plasmid DNA. *Molecular and Cellular Biology* **7**; 2745–52

Chen, S.R.W., Zhang, L. and MacLennan, D.H. (1993) Antibodies as probes for Ca^{2+} activation sites in the Ca^{2+} release channel (ryanodine receptor) of rabbit skeletal muscle sarcoplasmic reticulum. *Journal of Biological Chemistry* **268**; 13414-13421

Cheng, H., Lederer, W.J. and Cannell, M.B. (1993) Calcium sparks: elementary events underlying excitation-contraction coupling in heart muscle. *Science* **262**; 740-4

Cherednichenko, G., Hurne, A.M., Fessenden, J.D., Lee, E.H., Allen, P.D., Beam, K.G. and Pessah, I.N. (2004) Conformational activation of Ca^{2+} entry by depolarization of skeletal myotubes. *Proceedings of the National Academy of Sciences of the United States of America* **101**; 15793-15798

Chien, C.T., Bartel, P.L., Sternglanz, R. and Fields, S. (1991) The two-hybrid system: a method to identify and clone genes for proteins that interact with a protein of interest. Proceedings of the National Academy of Sciences of the United States of America 88(21); 9578-82

Chien, K.R., Ross, J. Jr, and Hoshijima, M. (2003) Calcium and heart failure: the cycle game. *Nature Medicine* **9(5)**; 508-9

Ching, L.L., Williams, A.J. and Sitsapesan, R. (2000) Evidence for Ca^{2+} activation and inactivation sites on the luminal side of the cardiac ryanodine receptor complex. *Circulation Research* **87**; 201-206

Choi, G., Kopplin, L.J., Tester, D.J., Will, M.L., Haglund, C.M. and Ackerman, M.J. (2004) Spectrum and frequency of cardiac channel defects in swimming-triggered arrhythmia syndromes. *Circulation* **110**; 2119-2124

Chu, A., Diaz-Munoz, M., Hawkes, M.J., Brush, K. and Hamilton, S.L. (1990) Ryanodine as a probe for the functional state of the skeletal muscle sarcoplasmic reticulum calcium release channel. *Molecular Pharmacology* **37(5)**; 735-41

Chu, A., Fill, M., Stefani, E and Entman, M.L. (1993) Cytoplasmic Ca^{2+} does not inhibit the cardiac muscle sarcoplasmic reticulum ryanodine receptor Ca^{2+} channel, although $Ca(^{2+})$-induced Ca^{2+} inactivation of Ca^{2+} release is observed in native vesicles. *Journal of Membrane Biology* **135**; 49-59

Clapham, D.E. (1995) Calcium signalling. *Cell* **80**; 259-268.

Claycomb, W.C., Lanson, N.A. Jr, Stallworth, B.S., Egeland, D.B., Delcarpio, J.B., Bahinski, A. and Izzo, N.J. Jr. (1998) HL-1 cells: a cardiac muscle cell line that contracts and retains phenotypic characteristics of the adult cardiomyocyte. *Proceedings of the National Academy of Sciences of the United States of America* **95(6)**; 2979-84

Cohn, J.N. (1995) Plasma norepinephrine and mortality. *Clinical Cardiology* **18(3 Suppl I)**; I9-12

Cohn, J.N., Levine, T.B., Olivari, M.T., Garberg, V., Lura, D., Francis, G.S., Simon, A.B. and Rector, T. (1984) Plasma norepinephrine as a guide to prognosis in patients with chronic congestive heart failure. *New England Journal of Medicine* **311(13)**; 819-23

Condorelli, G., Vigliotta, G., Iavarone, C., Caruso, M., Tocchetti, C.G., Andreozzi, F., Cafieri, A., Tecce, M.F., Formisano, P., Beguinot, L. and Beguinot, F. (1998) PED/PEA-15 gene controls glucose transport and is overexpressed in type 2 diabetes mellitus. *European Molecular Biology Organisation Journal* **17(14)**; 3858-66

Copello, J.A., Barg, S., Onoue, H. and Fleischer, S. (1997) Heterogeneity of Ca^{2+} gating of skeletal muscle and cardiac ryanodine receptors. *Biophysical Journal* **73(1)**; 141-56

Copello, J.A., Barg, S., Sonnleitner, A., Porta, M., Diaz-Sylvester, P., Fill, M., Schindler, H. and Fleischer, S. (2002) Differential activation by Ca^{2+}, ATP and caffeine of cardiac and skeletal muscle ryanodine receptors after block by Mg^{2+}. *Journal of Membrane Biology* **187**; 51-64

Cormack, B.P., Valdivia, R.H. and Falkow, S. (1996) FACS-optimized mutants of the green fluorescent protein (GFP). *Gene* **173(1 Spec No)**; 33-8

Coronado, R., Kawano, S., Lee, C.J., Valdivia, C. and Valdivia, H.H. (1992) Planar bilayer recording of ryanodine receptors of sarcoplasmic reticulum. *Methods in Enzymology* **207**; 699-707

Coronado, R, Morrissette, J., Sukhareva, M and Vaughan, DM. (1994) Structure and function of ryanodine receptors. *American Journal of Physiology* **266**; 1485-1504

Cranefield, P.F. and Wit, A.L. (1979) Cardiac arrhythmias. *Annual Review of Physiology* **41**; 459-72

Cubitt, A.B., Heim, R., Adams, S.R., Boyd, A.E., Gross, L.A. and Tsien, R.Y. (1995) Understanding, improving and using green fluorescent proteins. *Trends in Biochemical Science* **20(11)**; 448-55

Diaz, M.E., Eisner, D.A. and O'Neill, S.C. (2002) Depressed ryanodine receptor activity increases variability and duration of the systolic Ca^{2+} transient in rat ventricular myocytes. *Circulation Research* **91**; 585-593

Diaz, M.E., O'Neill, S.C. and Eisner, D.A. (2004) Sarcoplasic reticulum calcium content fluctuation is the key to cardiac alternans. *Circulation Research* **94**; 650-656

Doi, M., Yano, M., Kobayashi, S., Kohno, M., Tokuhisa, T., Okuda, S., Suetsugu, M., Hisamatsu, Y., Ohkusa, T., Kohno, M. and Matsuzaki, M. (2002) Propanolol prevents the development of heart failure by restoring FKBP12.6-mediated stabilization of ryanodine receptor. *Circulation* **105**; 1374-1379

Dolmetsch, R.E., Xu, K. and Lewis, R.S. (1998) Calcium oscillations increase the efficiency and specificity of gene expression. *Nature* **392**; 933-6

Dower, W.J., Miller, J.F. and Ragsdale, C.W. (1988) High efficiency transformation of E. coli by high voltage electroporation. *Nucleic Acids Research* **16(13)** 6127-45

Doyle, D.A., Cabral, J.M., Pfuetzner, R.A., Kuo, A., Gulbis, J.M., Cohen, S.L., Chait, B.T. and MacKinnon, R. (1998) The structure of the potassium channel: Molecular basis of K^+ conduction and selectivity. *Science* **280**; 69-77

Du, G.G., Imredy, J.P. and MacLennan, D.H. (1998) Characterization of recombinant rabbit cardiac and skeletal muscle Ca^{2+} release channels (ryanodine receptors) with a novel [^{3}H] ryanodine binding assay. *Journal of Biological Chemistry* **273**; 33259-33266

Du, G.G., Khanna, V.K. and MacLennan, D.H. (2000) Mutation of divergent region 1 alters caffeine and Ca^{2+} sensitivity of the skeletal muscle Ca^{2+} release channel (ryanodine receptor). *Journal of Biological Chemistry* **275(16)**; 11778-83

Du, G.G. and MacLennan, D.H. (1998) Functional consequences of mutations of conserved, polar amino acids in transmembrane sequences of the Ca^{2+} release channel (ryanodine receptor) of rabbit skeletal muscle sarcoplasmic reticulum. *Journal of Biological Chemistry* **273(48)**; 31867-72

Du, G.G. and MacLennan, D.H. (1999) Ca^{2+}-inactivation sites are located in the COOH-terminal quarter of recombinant rabbit skeletal muscle Ca^{2+} release channels (ryanodine receptors). *Journal of Biological Chemistry* **274**; 26120-26126

Du, G.G., Oyamada, H., Khanna, V.K. and MacLennan, D.H. (2001a) Mutations to Gly^{2370}, Gly^{2373} or Gly^{2375} in malignant hyperthermia domain 2 decrease caffeine and cresol sensitivity of the rabbit skeletal-muscle Ca^{2+}-release channel (ryanodine receptor isoform 1). *Biochemical Journal* **360**; 97-105

Du, G.G., Sandhu, B., Khanna, V.K., Guo, X.H. and MacLennan, D.H. (2002) Topology of the Ca^{2+} release channel of skeletal muscle sarcoplasmic reticulum (RyR1). *Proceedings of the National Academy of Sciences of the United States of America* **99**; 16725-16730

Du, G.G., Xinghua, G., Khanna, V.K. and MacLennan, D.H. (2001b) Functional characterisation of mutants in the predicted pore region of the rabbit cardiac muscle Ca^{2+} release channel (ryanodine receptor isoform 2). *Journal of Biological Chemistry* **276**; 31760-31771

Du, G.G., Xinghua, G., Khanna, V.J. and MacLennan, D.H. (2001c) Ryanodine sensitizes the cardiac Ca^{2+} release channel (ryanodine receptor isoform 2) to Ca^{2+} activation and dissociates as the channel is closed by Ca^{2+} depletion. *Proceedings of the National Academy of Sciences of the United States of America* **98**; 13625-13630

Duggal, P., Vesely, M.R., Wattanasirichaigoon, D., Villafane, J., Kaushik, V. and Beggs, A.H. (1998) Mutation of the gene for IsK associated with both Jervell and Lange-Nielsen and Romano-Ward forms of Long-QT syndrome. *Circulation* **97(2)**; 142-6

Duke, A.M., Hopkins, P.M. and Steele, D.S. (2002) Effects of Mg^{2+} and sarcoplasmic reticulum luminal Ca^{2+} on caffeine-induced Ca^{2+} release in skeletal muscle from humans susceptible to malignant hyperthermia. *Journal of Physiology* **544.1**; 85-95

Dulhunty, A.F. and Pouliquin, P. (2003) What we don't know about the structure of ryanodine receptor calcium release channels. *Clinical and Experimental Pharmacology and Physiology* **30(10)**; 713-23

Dumaine, R., Towbin, J.A., Brugada, P., Vatta, M., Nesterenko, D.V., Nesterenko, V.V., Brugada, J., Brugada, R. and Antzelevitch, C. (1999) Ionic mechanisms responsible for the electrocardiographic phenotype of the Brugada syndrome are temperature dependent. *Circulation Research* **85(9)**; 803-9

Dumaine, R., Wang, Q., Keating, M.T., Hartmann, H.A., Schwartz, P.J., Brown, A.M. and Kirsch, G.E. (1996) Multiple mechanisms of Na^{+} channel-linked long-QT syndrome. *Circulation Research* **78(5)**; 916-24

Duncan, L., Burton, F.L., and Smith, G. L. (1999) REACT: Calculation of free metal and ligand concentrations using a Windows-based computer program. *Journal of Physiology* **517.P**; 2P

Ehrlich, B.E., Kaftan, E., Bezprozvannaya, S. and Bezprozvanny, I. (1994) The pharmacology of intracellular Ca^{2+}-release channels. *Trends in Pharmacological Science* **15(5)**; 145-9

Eisner, D.A, Choi, H.S., Diaz, M.E., O'Neill, S.C. and Trafford, A.W. (2000) Integrative analysis of calcium cycling in cardiac muscle. *Circulation Research* **87**; 1087-1094

Eisner, D.A., Isenberg, G. and Sipido, K.R. (2003) Normal and pathological excitation-contraction coupling in the heart - an overview. *Journal of Physiology* **1**; 3-4

Eisner, D.A. and Trafford, A.W. (2000) No role for the ryanodine receptor in regulation cardiac contraction? *News in Physiological Sciences* **15**; 275-279

Eisner, D.A., Trafford, A.W., Diaz, M.E., Overend, C.L. and O'Neill, S.C. (1998) The control of Ca release from the cardiac sarcoplasmic reticulum: regulation versus autoregulation. *Cardiovascular Research* **38(3)**; 589-604

El-Hayek, R., Saiki, Y., Yamamoto, T. and Ikemoto, N. (1999) A postulated role of the near amino-terminal domain of the ryanodine receptor in the regulation of the sarcoplasmic reticulum Ca^{2+} channel. *Journal of Biological Chemistry* **274**; 33341-33347

Ellis, F.R. and Harriman, D.G. (1973) A new screening test for susceptibility to malignant hyperpyrexia. *British Journal of Anaesthesiology* **45(6)**; 638

Eu, J.P., Sun, J., Xu, L., Stamler, J.S. and Meissner G. (2000) The skeletal muscle calcium release channel: coupled O_2 sensor and NO signaling functions. *Cell* **102(4)**; 499-509

Eu, J.P., Xu, L., Stamler, J.S. and Meissner, G. (1999) Regulation of ryanodine receptor by reactive nitrogen species. *Biochemical Pharmacology* **57**; 1079-1084

Fabiato, A. (1983) Calcium-induced release of calcium from the cardiac sarcoplasmic reticulum. *American Journal of Physiology* **245**; 1-14

Fabiato, A. (1985) Time and calcium dependence of activation and inactivation of calcium-induced release of calcium from the sarcoplasmic reticulum of a skinned canine cardiac Purkinje cell. *Journal of General Physiology* **85(2)**; 247-89

Fabiato, A. (1989) Appraisal of the physiological relevance of two hypotheses for the mechanism of calcium release from the mammalian SR: CICR vs. charge-coupled release. *Molecular and Cellular Biochemistry* **89(2)**; 135-40

Fabiato, A. and Fabiato, F., (1979) Calcium and cardiac excitation-contraction coupling. *Annual Reviews of Physiology* **41**; 473-84

Farrell, E.F., Antaramian, A., Rueda, A., Gomez, A.M. and Valdivia, H. (2003) Sorcin inhibits calcium release and modulates excitation-contraction coupling in the heart. *Journal of Biological Chemistry* **278**; 34660-34666

Farrell, E.F., Lokuta, A.A., Valdivia, H.H. (2005) A phosphomimetic analog of sorcin with impaired regulation of cardiac ryanodine receptors. *Biophysical Journal (Annual Meeting Abstracts)* **88 (1)**; 534-534A

Fawcett, J.M., Harrison, S.M. and Orchard, C.H. (1998) A method for reversible permeabilization of isolated rat ventricular myocytes. *Experimental Physiology* **83(3)**; 293-303

Favre, I., Sun, Y.M. and Moczydlowski, E. (1999) Reconstitution of native and cloned channels into planar bilayers. *Methods in Enzymology* **294**; 287-304

Fedida, D., Noble, D., Rankin, A.C. and Spindler, A.J. (1987) The arrhythmogenic transient inward current iTI and related contraction in isolated guinea-pig ventricular myocytes. *Journal of Physiology* **392**; 523-42

Fessenden, J.D., Chen, L., Wang, Y., Paolini, C., Franzini-Armstrong, C., Allen, P.D. and Pessah, I.N. (2001) Ryanodine receptor point mutant $E^{4032}A$ reveals an allosteric interaction with ryanodine. *Proceedings of the National Academy of Sciences of the United States of America* **98(5)**; 2865-70

Fessenden, J.D., Feng, W., Pessah, I.N. and Allen, P.D. (2004) Mutational analysis of putative calcium binding motifs within the skeletal ryanodine receptor isoform, RyR1. *Journal of Biological Chemistry* **279(51)**; 53028-35

Fessenden, J.D., Perez, C.F., Goth, S., Pessah, I.N. and Allen, P.D. (2003) Identification of a key determinant of ryanodine receptor type 1 required for activation by 4-chloro-m-cresol. *Journal of Biological Chemistry* **278**; 28727-28735

Fessenden, J.D., Wang, Y., Moore, R.A., Chen, S.R., Allen, P.D. and Pessah, I.N. (2000) Divergent functional properties of ryanodine receptor types 1 and 3 expressed in a myogenic cell line. *Biophysical Journal* **79(5)**; 2509-25

Fields, S. and Song, O. (1989) A novel genetic system to detect protein-protein interactions. *Nature* **340(6230)**; 245-6

Fill, M. and Copello, J.A. (2002) Ryanodine receptor calcium release channels. *Physiological Reviews* **82**; 893-922

Fill, M., Coronado, R., Mickelson, J.R., Vilven, J., Ma, J.J., Jacobson, B.A. and Louis, C.F. (1990) Abnormal ryanodine receptor channels in malignant hyperthermia. *Biophysical Journal* **57(3)**; 471-5

Flucher, B.E. and Franzini-Armstrong, C. (1996) Formulation of junctions involved in excitation-contraction coupling in skeletal and cardiac muscle. *Proceedings of the National Academy of Sciences of the United States of America* **93(15)**; 8101-6

Franzini-Armstrong, C. (1970) Studies of the triad: 1. Structure of the junction in frog twitch fibres. *Journal of Cell Biology* **47**; 488-499

Franzini-Armstrong, C. and Kish, J.W. (1995) Alternate disposition of tetrads in peripheral couplings of skeletal muscle. *Journal of Muscle Research and Cell Motility* **16(3)**; 319-24

Franzini-Armstrong, C. and Protasi, F. (1997) Ryanodine receptors of striated muscles: a complex channel capable of multiple interactions. *Physiological Reviews* **77(3)**; 699-729

Franzini-Armstrong, C., Protasi, F., and Ramesh, V. (1999) Shape, size, and distribution of Ca^{2+} release units and couplons in skeletal and cardiac muscles. *Biophysical Journal* **77**; 1528-1539

Fruen, B.R., Bardy, J.M., Byrem, T.M., Strasburg, G.M. and Louis, C.F. (2000) Differential Ca^{2+} sensitivity of skeletal and cardiac muscle ryanodine receptors in the presence of calmodulin. *American Journal of Physiology - Cell Physiology* **279(3)**; C724-33

Fuentes, O., Valdivia, C., Vaughan, D., Coronado, R. and Valdivia, H.H. (1994) Calcium-dependent block of ryanodine receptor channel of swine skeletal muscle by direct binding of calmodulin. *Cell Calcium* **15(4)**; 305-16

Futatsugi, A., Kato, K., Ogura, H., Li, S.-T., Nagata, E., Kuwajima, G., Tanaka, K., Itohara, S. and Mikoshiba, K. (1999) Facilitation of NMDAR-independent LTP and spatial learning in mutant mice lacking ryanodine receptor type 3. *Neuron* **24**; 701-713

Gaburjakova, M., Gaburjakova, J., Reiken, S., Huang, F., Marx, S.O., Rosemblit, N. and Marks, A.R. (2001) FKBP12 binding modulates ryanodine receptor channel gating. *Journal of Biological Chemistry* **276**; 16931-16935

Galione, A. (1993) Cyclic ADP-ribose: a new way to control calcium. *Science* **259**; 325-6

Galione, A., Lee, H.C. and Busa, W.B. (1991) Ca^{2+}-induced Ca^{2+} release in sea urchin egg homogenates: modulation by cyclic ADP-ribose. *Science* **253(5024)**; 1143-6

Gao, L., Balshaw, D., Xu, L., Tripathy, A., Xin, C. and Meissner, G. (2000) Evidence for a role of the lumenal M3-M4 loop in skeletal muscle Ca^{2+} release channel (ryanodine receptor) activity and conductance. *Biophysical Journal* **79(2)**; 828-40

Gao, L., Tripathy, A., Lu, X. and Meissner, G. (1997) Evidence for a role of C-terminal amino acid residues in skeletal muscle Ca^{2+} release channel (ryanodine receptor) function. *Federation of European Biochemical Societies Letters* **412(1)**; 223-6

Gemayel, C., Pelliccia, A. and Thompson, P.D. (2001) Arrhythmogenic right ventricular cardiomyopathy. *Journal of the American College of Cardiology* **38(7)**;1773-81

George, C.H., Higgs, G.V. and Lai, F.A. (2003a) Ryanodine receptor mutations associated with stress-induced ventricular tachycardia mediate increased calcium release in stimulated cardiomyocytes. *Circulation Research* **93**; 531-540

George, C.H., Higgs, G.V., Mackrill, J.J., Lai, F.A. (2003b) Dysregulated ryanodine receptors mediate cellular toxicity: restoration of normal phenotype by FKBP12.6. *Journal of Biological Chemistry* **278**; 28856-28864

George, C.H., Jundi, H., Thomas, N.L., Scoote, M., Walters, N., Williams, A.J. and Lai, F.A. (2004) Ryanodine receptor regulation by intramolecular interaction between cytoplasmic and transmembrane domains. *Molecular Biology of the Cell* **15(6)**; 2627-38

George, C.H., Sorathia, R., Bertrand, B.M.A. and Lai, F.A. (2003c) *In situ* modulation of the human cardiac ryanodine receptor (hRyR2) by FKBP12.6. *Biochemical Journal* **370**; 579-589

George, C.H., Yin, C.C. and Lai, F.A. (2005) Toward a molecular understanding of the structure-function of ryanodine receptor Ca^{2+} release channels: perspectives from recombinant expression systems. *Cell Biochemistry and Biophysics* **42**; 197-222

Gillard, E.F., Otsu, K., Fujii, J., Khanna, V.K., de Leon, S., Derdemezi, J., Britt, B.A., Duff, C.L., Worton, R.G. and MacLennan D.H. (1991) A substitution of cysteine for arginine 614 in the ryanodine receptor is potentially causative of human malignant hyperthermia. *Genomics* **11(3)**; 751-5

Golemis, E.A., Serebriiskii, I. and Law, S.F. (1999) The yeast two-hybrid system: criteria for detecting physiologically significant protein-protein interactions. *Current Issues in Molecular Biology* **1(1-2)**; 31-45

Gomes, A.V. and Potter, J.D. (2004) Cellular and molecular aspects of familial hypertrophic cardiomyopathy caused by mutations in the cardiac troponin I gene. *Molecular and Cellular Biochemistry* **263(1-2)**; 99-114

Gomez, A.M. and Richard, S. (2004) Mutant cardiac ryanodine receptors and ventricular arrhythmias: as 'gain-of-function' obligatory? *Cardiovascular Research* **64**; 3-5

Graham, F.L., Smiley, J., Russell, W.C. and Nairn, R. (1977) Characteristics of a human cell line transformed by DNA from human adenovirus type 5. *Journal of General Virology* **36(1)**; 59-74

Grynkiewicz, G., Poenie, M. and Tsien, R.Y. (1985) A new generation of Ca^{2+} indicators with greatly improved fluorescence properties. *Journal of Biological Chemistry* **260**; 3440-50

Guo, X., Laflamme, M.A. and Becker, P.L. (1996) Cyclic ADP-ribose does not regulate sarcoplasmic reticulum Ca^{2+} release in intact cardiac myocytes. *Circulation Research* **79(1)**; 147-51

Györke, S. and Fill, M. (1993) Ryanodine receptor adaptation: control mechanism of $Ca(^{2+})$-induced Ca^{2+} release in heart. *Science* **260(5109)**; 807-9

Györke, I. and Györke, S. (1998) Regulation of the cardiac ryanodine receptor channel by luminal Ca^{2+} involves luminal sensing sites. *Biophysical Journal* **75**; 2801-2810

Györke, I., Hester, N., Jones, L.R. and Györke, S. (2004) The role of calsequestrin, triadin, and junctin in conferring cardiac ryanodine receptor responsiveness to luminal calcium. *Biophysical Journal* **86**; 2121-2128

Haghighi, K., Gregory, K.N. and Kranias, E.G. (2004) Sarcoplasmic reticulum Ca-ATPase-phospholamban interactions and dilated cardiomyopathy. *Biochemical and Biophysical Research Communications* **322(4)**; 1214-22

Haghighi, K., Kolokathis, F., Pater, L., Lynch, R.A., Asahi, M., Gramolini, A.O., Fan, G.C., Tsiapras, D., Hahn, H.S., Adamopoulos, S., Liggett, S.B., Dorn, G.W. 2nd, MacLennan, D.H., Kremastinos, D.T. and Kranias, E.G. (2003) Human phospholamban null results in lethal dilated cardiomyopathy revealing a critical difference between mouse and human. *Journal of Clinical Investigation* **111(6)**; 869-76

Hain, J., Onoue, H., Mayrleitner, M., Fleischer, S. and Schindler, H. (1995) Phosphorylation modulates the function of the calcium release channel of sarcoplasmic reticulum from cardiac muscle. *Journal of Biological Chemistry* **270**; 2074-2081

Hakamata, Y., Nakai, J., Takeshima, H. and Imoto, K. (1992) Primary structure and distribution of a novel ryanodine receptor/calcium release channel from rabbit brain. *Federation of European Biochemical Societies Letters* **312**; 229-35

Hanahan, D. (1983) Studies on transformation of Escherichia coli with plasmids. *Journal of Molecular Biology* **166(4)**; 557-80

Hasenfuss, G. (1998) Alterations of calcium-regulatory proteins in heart failure. *Cardiovascular Research* **37(2)**; 279-89

Hasenfuss, G., Reinecke, H., Studer, R., Meyer, M., Pieske, B., Holtz, J., Holubarsch, C., Posival, H., Just, H. and Drexler, H. (1994) Relation between myocardial function and expression of sarcoplasmic reticulum Ca^{2+}-ATPase in failing and nonfailing human myocardium. *Circulation Research* **75(3)**; 434-42

Hauptman, P.J. and Kelly, R.A. (1999) Digitalis. *Circulation* **99(9)**; 1265-70

Hayek, S.M., Zhu, X., Bhat, M.B., Zhao, J., Takeshima, H. and Valdivia, H.H., Ma, J. (2000) Characterization of a calcium-regulation domain of the skeletal-muscle ryanodine receptor. *Biochemical Journal* **351(1)**; 57-65

Heim, R., Cubitt, A.B. and Tsien, R.Y. (1995) Improved green fluorescence. *Nature* **373(6516)**; 663-4

Hermann-Frank, A., Richter, M., Sarkozi, S., Mohr, U. and Lehrmann-Horn, F. (1996) 4-chloro-m-cresol, a potent and specific activator of the skeletal muscle ryanodine receptor. *Biochimica et Biophysica Acta* **1289**; 31-40

Hernandez-Cruz, A., Diaz-Munoz, M., Gomez-Chavarin, M., Canedo-Merino, R., Protti, D.A., Escobar, A.L., Sierralta, J. and Suarez-Isla, B.A. (1995) Properties of the ryanodine-sensitive release channels that underlie caffeine-induced Ca^{2+} mobilization from intracellular stores in mammalian sympathetic neurons. *European Journal of Neuroscience* **7(8)**; 1684-99

Hobai, I.A. and O'Rourke, B. (2001) Decreased sarcoplasmic reticulum calcium content is responsible for defective excitation-contraction coupling in canine heart failure. *Circulation* **103(11)**; 1577-84

Holmberg, S.R. and Williams, A.J. (1990) The cardiac sarcoplasmic reticulum calcium-release channel: modulation of ryanodine binding and single-channel activity. *Biochimica et Biophysica Acta* **1022(2)**; 187-93

Hoppe, U.C., Marban, E., Johns, D.C. (2001) Distinct gene-specific mechanisms of arrhythmia revealed by cardiac gene transfer of two long QT disease genes, HERG and KCNE1. *Proceedings of the National Academy of Sciences of the United States of America* **98(9)**; 5335-40

Houser, S.R., Piacentino, I. V. and Weisser, J. (2000) Abnormalities of calcium cycling in the hypertrophised and failing heart. *Journal of Molecular and Cellular Cardiology* **32**; 1595-1607

Hüser, J., Wang, Y.G., Sheehan, K.A., Cifuentes, F., Lipsius, S.L. and Blatter, L.A. (2000) Functional coupling between glycolysis and excitation-contraction coupling underlies alternans in cat heart cells. *Journal of Physiology* **524(3)**; 795-806

Hymel, L., Inui, M., Fleischer, S. and Schindler, H. (1988) Purified ryanodine receptor of skeletal muscle sarcoplasmic reticulum forms Ca^{2+}-activated oligomeric channels in planar bilayers. *Proceedings of the National Academy of Sciences of the United States of America* **85**; 441-445

Ikemoto, N., Antoniu, B., Kang, J.J., Meszaros, L.G. and Ronjat, M. (1991) Intravesicular calcium transient during calcium release from sarcoplasmic reticulum. *Biochemistry* **30(21)**; 5230-7

Ikemoto, N. and Yamamoto, T. (2000) Postulated role of inter-domain interaction within the ryanodine receptor in Ca^{2+} channel regulation. *Trends in Cardiovascular Medicine* **10(7)**; 310-6

Imagawa, T., Nakai, J., Takeshima, H., Nakasaki, Y. and Shigekawa, M. (1992) Expression of Ca^{2+}-induced Ca^{2+} release channel activity from cardiac ryanodine receptor cDNA in Chinese hamster ovary cells. *Journal of Biochemistry (Tokyo)* **112(4)**; 508-13

Imagawa, T., Smith, J.S., Coronado, R. and Campbell, K.P. (1987) Purified ryanodine receptor from skeletal muscle sarcoplasmic reticulum is the Ca^{2+}-permeable pore of the calcium release channel. Journal of Biological Chemistry **262(34)**; 16636-43

Inouye, S. and Tsuji, F.I. (1994) Aequorea green fluorescent protein. Expression of the gene and fluorescence characteristics of the recombinant protein. *Federation of European Biochemical Societies Letters* **341(2-3)**; 277-80

Inui, M., Saito, A. and Fleischer, S. (1987a) Purification of the ryanodine receptor and identity with feet structures of junctional terminal cisternae of sarcoplasmic reticulum from fast skeletal muscle. *Journal of Biological Chemistry* **262**; 1740-7

Inui, M., Saito, A. and Fleischer, S. (1987b) Isolation of the ryanodine receptor from cardiac sarcoplasmic reticulum and identity with the feet structures. *Journal of Biological Chemistry* **262**; 15637-15642

Janse, M.J. (2004) Electrophysiological changes in heart failure and their relationship to arrhythmogenesis. *Cardiovascular Research* **61(2)**; 208-17

Jayaraman, T., Brillantes, A., Timerman, A.P., Fleischer, S., Erdjument-Bromage, H., Tempst, P. and Marks, A.R. (1992) FK506 binding protein associated with the calcium release channel (ryanodine receptor). *Journal of Biological Chemistry* **267**; 9474-9477

Jenden, D.J. and Fairhurst, A.S. (1969) The pharmacology of ryanodine. *Pharmacological Reviews* **21**; 1-25

Jervell, A., Lange-Nielsen, F. (1957) Congenital deaf-mutism, functional heart disease with prolongation of the Q-T interval and sudden death. *American Heart Journal* **54(1)**; 59-68

Jeyakumar, L.H., Copello, J.A., O'Malley, A.M., Wu, G., Grassucci, R., Wagenknecht, T. and Fleischer, S. (1998) Purifiaction and characterization of ryanodine receptor 3 from mammalian tissue. *Journal of Biological Chemistry* **273**; 16011-16020

Jiang, M.T., Lokuta, A.J., Farrell, E.F., Wolff, M.R., Haworth, R.A. and Valdivia, H.H. (2002a) Abnormal Ca^{2+} release, but normal ryanodine receptors, in canine and human heart failure. *Circulation Research* **91(11)**; 1015-22

Jiang, D., Xiao, B., Li, X. and Chen, S.R.W. (2003) Smooth muscle tissues express a major dominant negative splice variant of the type 3 Ca^{2+} release channel (ryanodine receptor). *Journal of Biological Chemistry* **278**; 4763-4769

Jiang, D., Xiao, B., Yang, D., Wang, R., Zhang, L., Cheng, H. and Chen, S.R.W. (2004) RyR2 mutations linked to ventricular tachycardia and sudden death reduce the threshold for stor-overload-induced Ca^{2+} release (SOICR). *Proceedings of the National Academy of Sciences of the United States of America* **101**; 13062-13067

Jiang, D., Xiao, B., Zhang, L. and Chen, S.R.W. (2002b) Enhanced basal activity of a cardiac Ca^{2+} release channel (ryanodine receptor) mutant associated with ventricular tachycardia and sudden death. *Circulation Research* **91**; 4763-9

Johnsson, N. and Varshavsky, A. (1994) Split ubiquitin as a sensor of protein interactions in vivo. *Proceedings of the National Academy of Sciences of the United States of America* **91(22)**; 10340-4

Jones, L.R., Suzuki, Y.J., Wang, W., Konayashi, Y.M., Ramesh, V. and Franzini-Armstrong, C. (1998) Regulation of Ca^{2+} signalling in transgenic mouse cardiac myocytes overexpressing calsequestrin. *Journal of Clinical Investigation* **101**; 1385-1393

Jones, L.R., Zhang, L., Sanborn, K., Jorgensen, A.O. and Kelley, J. (1995) Purification, primary structure, and immunological characterization of the 26-kDa calsequestrin binding protein (junctin) from cardiac junctional sarcoplasmic reticulum. *Journal of Biological Chemistry* **270(51)**; 30787-96

Kaftan, E., Marks, A.R. and Ehrlich, B.E. (1996) Effects of rapamycin on ryanodine receptor/Ca($^{2+}$)-release channels from cardiac muscle. *Circulation Research* **78(6)**; 990-7

Kapiloff, M.S. (2002) Contributions of protein kinase A anchoring proteins to compartmentation of cAMP signalling in the heart. *Molecular Pharmacology* **62;** 193-199

Kay, J.E. (1996) Structure function relationships in the FK506-binding protein (FKBP) family of peptidylprolyl cis-trans isomerases. *Biochemical Journal* **314**; 361-85

Keating, M.T. and Sanguinetti, M.C. (2001) Molecular and cellular mechanisms of cardiac arrhythmias. *Cell* **104**; 569-580

Kelly, R.A., Balligand, J.L. and Smith, T.W. (1996) Nitric oxide and cardiac function. *Circulation Research* **79(3)**; 363-80

Kirchhefer, U., Neumann, J., Bers, D.M., Buchwalow, I.B., Fabritz, L., Hanske, G., Justus, I., Riemann, B., Schmitz, W. and Jones, L.R. (2003) Impaired relaxation in transgenic mice overexpressing junctin. *Cardiovascular Research* **59(2)**; 369-79

Knollmann, B.C., Kirchhof, P., Sirenko, S.G., Degen, H., Greene, A.E., Schober, T., Mackow, J.C., Fabritz, L., Potter, J.D. and Morad, M. (2003) Familial hypertrophic cardiomyopathy-linked mutant troponin T causes stress-induced ventricular tachycardia and Ca^{2+}-dependent action potential remodeling. *Circulation Research* **92(4)**; 428-36

Kobayashi, S., Yamamoto, T., Parness, J. and Ikemoto, N. (2004) Antibody probe study of Ca^{2+} channel regulation by interdomain interaction within the ryanodine receptor. *Biochemical Journal* **380**; 561-569

Koch, W.J., Lefkowitz, R.J. and Rockman, H. A. (2000) Functional consequences of altering myocardial adrenergic receptor signalling. *Annual Reviews of Physiology* **62**; 237-60

Kockskämper, J. and Blatter, L.A. (2002) Subcellular Ca^{2+} alternans represents a novel mechanism for generation of arrhythmogenic Ca^{2+} waves in cat atrial myocytes. *Journal of Physiology* **545**; 65-79

Kohno, M., Yano, M., Kobayashi, S., Doi, M., Oda, T., Tokuhisa, T., Okuda, S., Kohno, M. and Matsuzaki, M. (2003) A new cardioprotective agent, JTV519, improves defective channel gating of ryanodine receptor in heart failure. *American Journal of Physiology. Heart and Circulatory Physiology* **284**; 1035-1042

Krishnan, S.C. and Antzelevitch, C. (1991) Sodium channel block produces opposite electrophysiological effects in canine ventricular epicardium and endocardium. *Circulation Research* **69(2)**; 277-91

Lahat, H., Pras, E., Olender, T., Avidan, N., Ben-Asher, E., Man, O., Levy-Nissenbaum, E., Khoury, A., Lorber, A., Goldman, B., Lancet, D. and Eldar, M. (2001) A missense mutation in a highly conserved region of CASQ2 is associated with autosomal recessive catecholamine-induced polymorphic ventricular tachycardia in Bedouin families from Israel. *American Journal of Human Genetics* **69**; 1378-1384

Lai, F.A., Anderson, K., Rousseau, E., Liu, Q.Y. and Miessner, G. (1988a) Evidence for a Ca^{2+} channel within the ryanodine receptor complex from cardiac sarcoplasmic reticulum. *Biochemical and Biophysical Research Communications* **151**; 441-9

Lai, F.A., Erickson, H., Block, B.A. and Meissner, G. (1987) Evidence for a junctional feet-ryanodine receptor complex from sarcoplasmic reticulum. *Biochemical and Biophysical Research Communications* **143**; 704-9

Lai, F.A., Erickson, H., Rousseau, E., Liu, Q.Y. and Meissner, G. (1988b) Purification and reconstitution of the calcium release channel from skeletal muscle. *Nature* **331**; 315-9

Lai, F.A. and Meissner, G. (1989) The muscle ryanodine receptor and its intrinsic Ca2+ channel activity. Journal of Bioenergetics and Biomembranes 21(2); 227-46

Lai, F.A., Misra, M., Xu, L., Smith, H.A. and Meissner, G. (1989) The ryanodine receptor Ca^{2+} release channel complex of skeletal muscle sarcoplasmic reticulum. Evidence for a cooperatively coupled, negatively charged homotetramer. *Journal of Biological Chemistry* **264**; 16776-85

Laitinen, P.J., Brown, K.M., Piippo, K., Swan, H., Devaney, J.M., Brahmbhatt, B., Donarum, E.A., Marino, M., Tiso, N., Viitasalo, M., Toivonen, L., Stephan, D.A. and Kontula, K. (2001) Mutations of the cardiac ryanodine receptor (RyR2) gene in familial polymorphic ventricular tachycardia. *Circulation* **103(4)**; 485-90

Lamb, G.D. (1993) Ca^{2+} inactivation, Mg^{2+} inhibition and malignant hyperthermia. *Journal of Muscle Research and Cell Motility* **14(6)**; 554-6

Lamb, G.D. and Stephenson, D.G. (1996) Effects of FK506 and rapamycin on excitation–contraction coupling in skeletal muscle fibres of the rat. *Journal of Physiology* **494**; 569–76

Larach, M.G. (1989) Standardization of the caffeine halothane muscle contracture test. North American Malignant Hyperthermia Group. *Anaesthesia and Analgesia* **69(4)**; 511-5

Launikonis, B.S., Zhou, J., Royer, L., Shannon, T.R., Brum, G. and Rios, E. (2005) Confocal imaging of $[Ca^{2+}]$ in cellular organelles by SEER, Shifted Excitation and Emission Ratioing of fluorescence. *Journal of Physiology* Jun 9; [Epub ahead of print]

Laver, D.R. (2005) Coupled calcium release channels and their regulation by luminal and cytosolic ions. *European Biophysical Journal* **34(5)**; 359-68

Laver, D. (2001) The power of single channel recording and analysis: its application to ryanodine receptors in lipid bilayers. *Clinical and Experimental Pharmacology and Physiology* **28(8)**; 675-86

Laver, D.R., Baynes, T.M. and Dulhunty, A.F. (1997) Magnesium inhibition of ryanodine receptor calcium channels: Evidence for two independent mechanisms. *Journal of Membrane Biology* **156**; 213-229

Laver, D.R., Roden, L.D., Ahern, G.P., Eager, K.R., Junankar, P.R. and Dulhunty, A.F. (1995) Cytoplasmic Ca^{2+} inhibits the ryanodine receptor from cardiac muscle. *Journal of Membrane Biology* **147(1)**; 7-22

Lee, S.B., Varnai, P., Balla, A., Jalnik, K., Rhee, S. and Balla, T. (2004) The pleckstrin homology domain of phosphoinositide-specific phospholipase c delta 4 is not a critical determinant of the membrane localisation of the enzyme. *Journal of Biological Chemistry* **279**; 24362-24371

Lee, H.C. (1997) Mechanisms of calcium signalling by cyclic ADP-ribose and NAADP. *Physiological Reviews* **77(4)**; 1133-64

Leeb, T. and Brenig, B. (1998) cDNA cloning and sequencing of the human ryanodine receptor type 3 (RYR3) reveals a novel alternative splice site in the RYR3 gene. *Federation of European Biochemical Societies Letters* **423**; 367-370

Leenhardt, A., Lucet, V., Denjoy, I., Grau, F., Ngoc, D.D. and Coumel, P. (1995) Catecholaminergic polymorphic ventricular tachycardia in children. A 7-year follow-up of 21 patients. *Circulation* **91(5)**; 1512-9

Lehnart, S.E., Wehrens, X.H.T., Laitinen, P.J., Reiken, S.R., Deng, S., Cheng, Z., Landry, D.W., Kontula, K., Swan, H. and Marks, A.R. (2004) Sudden death in familial polymorphic

ventricular tachycardia associated with calcium release channel (ryanodine receptor) leak. *Circulation* **109**; 113-119

Leong, P. and MacLennan, D.H. (1998a) A 37-amino acid sequence in the skeletal muscle ryanodine receptor interacts with the cytoplasmic loop between domains II and III in the skeletal muscle dihydropyridine receptor. *Journal of Biological Chemistry* **273(14)**; 7791-4

Leong, P. and MacLennan, D.H. (1998b) The cytoplasmic loops between domains II and III and domains III and IV in the skeletal muscle dihydropyridine receptor bind to a contiguous site in the skeletal muscle ryanodine receptor. *Journal of Biological Chemistry* **273(45)**; 29958-64

Levitan, I.B. (1999) It is calmodulin after all! Mediator of the calcium modulation of multiple ion channels. *Neuron* **22(4)**; 645-8

Lewis, R.S. (2001) Calcium signalling mechanisms in T lymphocytes. *Annual Review of Immunology* **19**; 497-521

Li, D., Ahmad, F., Gardner, M.J., Weilbaecher, D., Hill, R., Karibe, A., Gonzalez, O., Tapscott, T., Sharratt, G.P., Bachinski, L.L. and Roberts, R. (2000) The locus of a novel gene responsible for arrhythmogenic right-ventricular dysplasia characterized by early onset and high penetrance maps to chromosome 10p12-p14. *American Journal of Human Genetics* **66(1)**; 148-56

Li, P. and Chen, S.R.W. (2001) Molecular basis of Ca^{2+} activation of the mouse cardiac Ca^{2+} release channel (ryanodine receptor). *Journal of General Physiology* **118**; 33-44

Li, Q., Liu, Y., Shen, P.Y., Dai, X.Q., Wang, S., Smillie, L.B., Sandford, R. and Chen, X.Z. (2003) Troponin I binds polycystin-L and inhibits its calcium-induced channel activation. *Biochemistry* **42(24)**; 7618-25

Li, Q., Shen, P.Y., Wu, G., and Chen, X.Z. (2003) Polycystin-2 interacts with troponin I, an angiogenesis inhibitor. *Biochemistry* **42(2)**; 450-7

Li, W., Llopis, J., Whitney, M., Zlokarnik, G. and Tsien, R.Y. (1998) Cell-permeant caged InsP3 ester shows that Ca^{2+} spike frequency can optimize gene expression. *Nature* **30**; 936-41

Li, Y., Kranias, G., Mignery, G.A. and Bers, D.M. (2002) Protein kinase A phosphorylation of the ryanodine receptor does not affect calcium sparks in mouse ventricular myocytes. *Circulation Research* **90**; 309-316

Lindner, M., Erdmann, E. and Beuckelmann, D.J. (1998) Calcium content of the sarcoplasmic reticulum in isolated ventricular myocytes from patients with terminal heart failure. *Journal of Molecular and Cellular Cardiology* **30(4)**; 743-9

Lindsay, A.R., Manning, S.D. and Williams, A.J. (1991) Monovalent cation conductance in the ryanodine receptor-channel of sheep cardiac muscle sarcoplasmic reticulum. *Journal of Physiology* **439**; 463-80

Lindsay, A.R. and Williams, A.J. (1991) Functional characterisation of the ryanodine receptor purified from sheep cardiac muscle sarcoplasmic reticulum. *Biochimica et Biophysica Acta* **1064**; 89-102

Lipp, P. and Niggli, E. (1998) Fundamental calcium release events revealed by two-photon excitation photolysis of caged calcium in Guinea-pig cardiac myocytes. *Journal of Physiology* **1**; 801-9

Liu, W. and Meissner, G. (1997) Structure-activity relationship of xanthines and skeletal muscle ryanodine receptor/Ca^{2+} release channel. *Pharmacology* **54(3)**; 135-43

Liu, Z., Zhang, J., Sharma, M.R., Li, P., Chen, W. and Wagenknecht, T. (2001) Three-dimensional reconstruction of the recombinant type 3 ryanodine receptor and localisation of its amino terminus. *Proceedings of the National Academy of Sciences of the United States of America* **98**; 6104-6109

Liu, Z., Zhang, J., Wang, R., Chen, S.R.W. and Wagenknecht, T. (2004) Location of divergent region 2 on the three-dimensional structure of cardiac muscle ryanodine receptor/calcium release channel. *Journal of Molecular Biology* **338**; 533-545

Lokuta, A.J., Meyers, M.B., Sander, P.R., Fishman, G.I. and Valdivia, H.H. (1997) Modulation of cardiac ryanodine receptors by sorcin. *Journal of Biological Chemistry* **272(40)**; 25333-8

Lokuta, A.J., Rogers, T.B., Lederer, W.J. and Valdivia, H.H. (1995) Modulation of cardiac ryanodine receptors of swine and rabbit by a phosphorylation-dephosphorylation mechanism. *Journal of Physiology* **487**; 609-22

Lopez-Lopez, J.R., Shacklock, P.S., Balke, C.W. and Wier, W.G. (1995) Local calcium transients triggered by single L-type calcium channel currents in cardiac cells. *Science* **268(5213)**; 1042-5

Lorenzon, N.M., Grabner, M., Suda, N. and Beam, K.G. (2001) Structure and targeting of RyR1: implications from fusion of green fluorescent protein at the amino-terminal. *Archives of Biochemistry and Biophysics* **388(1)**; 13-7

Luo, D., Broad, L.M., Bird, G. and Putney, J.W. (2001) Signalling pathways underlying muscarinic receptor-induced $[Ca^{2+}]_i$ oscillations in HEK293 cells. *Journal of Biological Chemistry* **276**; 5613-5621

Luo, D., Sun, H., Xiao, R.P. and Han, Q. (2005) Caffeine induced Ca^{2+} release and capacitative Ca^{2+} entry in human embryonic kidney (HEK293) cells. *European Journal of Pharmacology* **509(2-3)**; 109-15

Lyfenko, A.D., Goonasekera, S.A. and Dirksen, R.T. (2004) Dynamic alterations in myoplasmic Ca^{2+} in malignant hyperthermia and central core disease. *Biochemical and Biophysical Research Communications* **322**; 1256-1266

Lynch, P.J., Tong, J., Lehane, M., Mallet, A., Giblin, L., Heffron, J.J.A., Vaughan, P., Zafra, G. and MacLennan, D.H. (1999) A mutation in the transmembrane/luminal domain of the ryanodine receptor is associated with abnormal Ca^{2+} release channel function and severe central core disease. *Proceedings of the National Academy of Sciences of the United States of America* **96**; 4164-4169

Ma, G., Brady, W.J., Pollack, M., and Chan, T.C. (2001) Electrocardiographic manifestations: digitalis toxicity. *Journal of Emergency Medicine* **20(2)**; 145-52

Ma, J. (1993) Block by ruthenium red of the ryanodin-activated calcium release channel of skeletal muscle. *Journal of General Physiology* **102**; 1031-1056

Ma, J., Bhat, M.B. and Zhao, J. (1995) Rectification of skeletal muscle ryanodine receptor mediated by FK506 binding protein. Biophysical Journal **69(6)**; 2398-404

Ma, J. and Ptashne, M.A. (1987) A new class of yeast transcriptional activators. *Cell* **51(1)**; 113-9

Mack, W.M., Zimanyi, I., Pessah, I.N. (1992) Discrimination of multiple binding sites for antagonists of the calcium release channel complex of skeletal and cardiac sarcoplasmic reticulum. J Pharmacol Exp Ther **262(3)**; 1028-37

MacKinnon, R. (2003) Potassium channels. *Federation of European Biochemical Societies Letters* **555(1)**; 62-5

MacLennan, D.H., Abu-Abed, M. and Kang, C. (2002) Structure-function relationships in Ca^{2+} cycling proteins. *Journal of Molecular and Cellular Cardiology* **34**; 897-918

MacLennan, D.H. and Wong, P.T. (1971) Isolation of a calcium-sequestering protein from sarcoplasmic reticulum. *Proceedings of the National Academy of Sciences of the United States of America* **68(6)**; 1231-5

MacLennan, D.H., Zorzato, F., Fujii, J., Otsu, K., Phillips, M., Lai, F.A., Meissner, G., Green, N.M., Willard, H.F., Britt, B.A., Worton, R.G. and Korneluk, R.G. (1989) Cloning and localization of the human calcium release channel (ryanodine receptor) gene to the proximal long arm (cen-q13.2) of human chromosome 19. *American Journal of Human Genetics (Abstract)* **45 (supplement)**: A205

Mackrill, J.J. (1999) Protein-protein interactions in intracelular Ca^{2+}-release channel function. *Biochemical Journal* **337**; 345-361

Maier, L.S., Zhang, T., Chen, L., DeSantiago, J., Brown, J.H. and Bers, D.M. (2003) Transgenic CaMKIIdelta$_c$ overexpression uniquely alters cardiac myocyte Ca^{2+} handling. *Circulation Research* **92**; 904-911

Manunta, M., Rossi, D., Simeoni, I., Butelli, E., Romanin, C., Sorrentino, V. and Schindler, H. (2000) ATP-induced activation of expressed RyR3 at low free calcium. *Federation of European Biochemical Societies Letters* **471**; 256-260

Marban, E., Robinson, S.W.and Wier, W.G. (1986) Mechanisms of arrhythmogenic delayed and early afterdepolarizations in ferret ventricular muscle. *Journal of Clinical Investigation* **78(5)**; 1185-92

Marban, E. (2002) Cardiac channelopathies. *Nature* **415**; 213-218

Marcus, F.I., Fontaine, G.H., Guiraudon, G., Frank R., Laurenceau, J.L., Malergue, C. and Grosgogeat, Y. (1982) Right ventricular dysplasia: a report of 24 adult cases. *Circulation* **65(2)**; 384-98

Marcus, F., Towbin, J.A., Zareba, W., Moss, A., Calkins, H., Brown, M. and Gear, K. (2003) Arrhythmogenic right ventricular dysplasia/cardiomyopathy (ARVD/C): a multidisciplinary study: design and protocol. *Circulation* **107(23)**; 2975-8

Marengo, J.J., Hidalgo, C. and Bull, R. (1998) Sulfhydryl oxidation modifies the Ca^{2+} dependence of ryanodine-sensitive Ca^{2+} channels of excitable cells. *Biophysical Journal* **74**; 1263-1277

Mariot, P., Prevarskaya, N., Roudbaraki, M.M., Le Bourhis, X., Van Coppenolle, F., Vanoverberghe, K. and Skryma, R. (2000) Evidence of functional ryanodine receptor involved in apoptosis of prostate cancer (LNCaP) cells. *Prostate* **43(3)**; 205-14

Marks, A.R. (1996) Cellular functions of immunophilins. *Physiological Reviews* **76**; 631-650

Marks, A.R. (2000) Cardiac intracellular calcium release channels: role in heart failure. *Circulation Research* **87**; 8-11

Marks, A.R. (2001) Ryanodine receptors/calcium release channels in heart failure and sudden cardiac death. *Journal of Molecular and Cellular Cardiology* **33**; 615-524

Marks, A.R. (2002) Clinical implications of cardiac ryanodine receptor/calcium release channel mutations linked to sudden cardiac death. *Circulation* **106**; 8-10

Marks, A.R., Priori, S., Memmi, M., Kontula, K. and Laitinen, P.J. (2002a) Involvement of the cardiac ryanodine receptor/calcium release channel in catecholaminergic polymorphic ventricular tachycardia. *Journal of Cellular Physiology* **190**; 1-6

Marks, A.R., Reiken, S. and Marx, S.O. (2002b) Progression of heart failure: is protein kinase a hyperphosphorylation of the ryanodine receptor a contributing factor? *Circulation* **105(3)**; 272-5

Marks, A.R., Tempst, P., Hwang, K., Taubman, M.B., Inui, M., Chadwick, C., Fleischer, S. and Nadal-Ginard, B. (1989) Molecular cloning and characterization of the ryanodine receptor/junctional channel complex cDNA from skeletal muscle sarcoplasmic reticulum. *Proceedings of the National Academy of Sciences of the United States of America* **86**; 8683-8687

Marx, S.O., Ondrias, K. and Marks, A.R. (1998) Coupled gating between individual skeletal muscle Ca^{2+} release channels (ryanodine receptors). *Science* **281(5378)**; 818-21

Marx, S.O., Reiken, S., Hisamatsu, Y., Gaburjakova, M., Gaburjakova, J., Yang, Y., Rosemblit, N. and Marks, A. R. (2001) Phosphorylation-dependent regulation of ryanodine receptors: a novel role for leucine/isoleucine zippers. *Journal of Cell Biology* **153**; 699-708

Marx, S.O., Reiken, S., Hisamatsua, Y., Jayaraman, T., Burkhoff, D., Rosemblit, N. and Marks A.R. (2000) PKA phosphorylation dissociates FKBP12.6 from the calcium release channel (ryanodine receptor): Defective regulation in failing hearts. *Cell* **101**; 365-376

Masumiya, H., Li, P., Zhang, L. and Chen, S.R.W. (2001) Ryanodine sensitizes the calcium release channel (ryanodine receptor) to Ca^{2+} activation. *Journal of Biological Chemistry* **276**; 39727-39735

Masumiya, H., Wang, R., Zhang, J., Xiao, B. and Chen, S.R.W. (2003) Localization of the 12.6kDa FK506-binding protein (FKBP12.6) binding site to the NH_2-terminal domain of the cardiac Ca^{2+} release channel (ryanodine receptor). *Journal of Biological Chemistry* **278**; 3786-3792

Matsuda, Y., Saegusa, H., Zong, S., Noda, T. and Tanabe, T. (2001) Mice lacking Ca(v)2.3 (alpha1E) calcium channel exhibit hyperglycemia. *Biochemical and Biophysical Research Communications* **289**; 791-5

Matthews, K.P. and Moore, S.A. (2004) Multiminicore myopathy, central core disease, malignant hyperthermia susceptibility, and RyR1 mutations: one disease with many faces? *Archives of Neurology* **61**; 27-29

Mattson, M.P., Guo, Q., Furukawa, K. and Pedersen, W.A. (1998) Presenilins, the endoplasmic reticulum, and neuronal apoptosis in Alzheimer's disease. *Journal of Neurochemistry* **70**; 1-14

Matute-Bello, G., Liles, W.C., Steinberg, K.P., Kiener, P.A., Mongovin, S., Chi, E.Y., Jonas, M. and Martin, T.R. (1999) Soluble Fas ligand induces epithelial cell apoptosis in humans with acute lung injury (ARDS). *Journal of Immunology* **163(4)**; 2217-25

Maurer, A., Tanaka, M., Ozawa, T. and Fleischer, S. (1985) Purification and crystallization of the calcium binding protein of sarcoplasmic reticulum from skeletal muscle. *Proceedings of the National Academy of Sciences of the United States of America* **82(12)**; 4036-40

Mazhari, R., Greenstein, J.L., Winslow, R.L., Marban, E., Nuss, H.B. (2001) Molecular interactions between two long-QT syndrome gene products, HERG and KCNE2, rationalized by *in vitro* and *in silico* analysis. *Circulation Research* **89(1)**; 33-8

McCall, E., Li, L., Satoh, H., Shannon, T.R., Blatter, L.A. and Bers, D.M. (1996) Effects of FK-506 on contraction and Ca^{2+} transients in rat cardiac myocytes. Circulation Research **79(6)**; 1110-21

McCarthy, T.V., Quane, K.A. and Lynch, P.J. (2000) Ryanodine receptor mutations in malignant hyperthermia and central core disease. *Human Mutation* **15**; 410-417

McDonald, T.F., Pelzer, S., Trautwein, W. and Pelzer, D.J. (1994) Regulation and modulation of calcium channels in cardiac, skeletal and smooth muscle cells. *Physiological Reviews* **74(2)**; 365-507

McGarry, S.J. and Williams, A.J. (1993) Digoxin activates sarcoplasmic reticulum $Ca^{(2+)}$-release channels: a possible role in cardiac inotropy. *British Journal of Pharmacology* **108(4)**; 1043-50

McGrew, S.G., Wolleben, C., Siegl, P., Inui, M. and Fleischer, S. (1989) Positive cooperativity of ryanodine binding to the calcium release channel of sarcoplasmic reticulum from heart and skeletal muscle. *Biochemistry* **28(4)**; 1686-91

Meissner, G. (1984) Adenine nucleotide stimulation of Ca^{2+}-induced Ca^{2+} release in sarcoplasmic reticulum. *Journal of Biological Chemistry* **259**; 2365-2374

Meissner, G. (1994) Ryanodine receptor/Ca^{2+} release channels and their regulation by endogenous effectors. *Annual Review of Physiology* **56**; 485-508

Meissner, G. (2004) Molecular regulation of cardiac ryanodine receptor ion channel. *Cell Calcium* **35**; 621-628

Meissner, G. and el-Hashem, A. (1992) Ryanodine as a functional probe of the skeletal muscle sarcoplasmic reticulum Ca^{2+} release channel. *Molecular and Cellular Biochemistry* **114(1-2)**; 119-23

Meissner, G. and Henderson, J.S. (1987) Rapid calcium release from cardiac sarcoplasmic reticulum vesicles is dependent on Ca^{2+} and is modulated by Mg^{2+}, adenine nucleotide, and calmodulin. *Journal of Biological Chemistry* **262(7)**; 3065-73

Meissner, G., Rios, E., Tripathy, A. and Pasek, D.A. (1997) Regulation of skeletal muscle Ca^{2+} release channel (ryanodine receptor) by Ca^{2+} and monovalent cations and anions. *Journal of Biological Chemistry* **272**; 1628-1638

Mela T, Galvin, J.M. and McGovern, B.A. (2002) Magnesium deficiency during lactation as a precipitant of ventricular tachyarrhythmias. *Pacing and Clinical Electrophysiology* **25(2)**; 231-3

Meldolesi, J. and Pozzan, T. (1998) The endoplasmic reticulum Ca^{2+} store: a view from the lumen. *Trends in Biochemical Science* **23(1)**; 10-4

Meszaros, L.G., Bak, J. and Chu, A. (1993) Cyclic ADP-ribose as an endogenous regulator of the non-skeletal type ryanodine receptor Ca^{2+} channel. *Nature* **364(6432)**; 76-9

Meyers, M.B., Fischer, A., Sun, Y.J., Lopes, C.M., Rohacs, T., Nakamura, T.Y., Zhou, Y.Y., Lee, P.C., Altschuld, R.A., McCune, S.A., Coetzee, W.A. and Fishman, G.I. (2003) Sorcin regulates excitation-contraction coupling in the heart. *Journal of Biological Chemistry* **278(31)**; 28865-71

Meyers, M.B., Pickel, V.M., Sheu, S.S., Sharma, V.K., Scotto, K.W. and Fishman, G.I. (1995) Association of sorcin with the cardiac ryanodine receptor. *Journal of Biological Chemistry* **270(44)**; 26411-8

Michalak, M., Corbett, E.F., Mesaeli, N., Nakamura, K. and Opas, M. (1999) Calreticulin: one protein, one gene, many functions. *Biochemical Journal* **344 (2)**; 281-92

Mickelson, J.R. and Louis, C.F. (1996) Malignant hyperthermia: excitation-contraction coupling, Ca^{2+} release channel, and cell Ca^{2+} regulation defects. *Physiological Reviews* **76(2)**; 537-92

Mikami, A., Imoto, K., Tanabe, T., Niidome, T., Mori, Y., Takeshima, H., Narumiya, S. and Numa, S. (1989) Primary structure and functional expression of the cardiac dihydropyridine-sensitive calcium channel. *Nature* **340(6230)**; 230-3

Milnes, J.T. and MacLeod, K.T. (2001) Reduced ryanodine receptor to dihydropyridine receptor ratio may underlie slowed contraction in a rabbit model of left ventricular cardiac hypertrophy. *Journal of Molecular and Cellular Cardiology* **33(3)**; 473-85

Mohler, P.J., Schott, J., Gramolini, A., Dilly, K.W., Guatimosim, S., duBell, W.H., Song, L., Haurogne, K., Kyndt, F., Ali, M.E., Rogers, T.B., Lederer, W.J., Escande, D., Le Marec, H. and Bennet, V. (2003) Ankyrin-B mutation causes type 4 long-QT cardiac arrythmia and sudden cardiac death. *Nature* **421**; 634-639

Mohler, P.J., Splawski, I., Napolitano, C., Bottelli, G., Sharpe, L., Timothy, K., Priori, S.G., Keating, M.T. and Bennet, V. (2004) A cardiac arrythmia syndrome caused by loss of ankyrinB function. *Proceedings of the National Academy of Sciences of the United States of America* **101**; 9137-9142

Monnier, N., Romero, N.B., Lerale, J., Landrieu, P., Nivoche, Y., Fardeau, M. and Lunardi, J. (2001) Familial and sporadic forms of central core disease are associated with mutations in the C-terminal domain of the skeletal muscle ryanodine receptor. *Human Molecular Genetics* **10(22)**; 2581-92

Montero, M., Brini, M., Marsault, R., Alvarez, J., Sitia, R., Pozzan, T. and Rizzuto, R. (1995) Monitoring dynamic changes in free Ca2+ concentration in the endoplasmic reticulum of intact cells. *European Molecular Biology Organisation Journal* **14(22)**; 5467-75

Moore, R.A., Nguyen, H., Galceran, J., Pessah, I.N. and Allen, P.D. (1998) A transgenic myogenic cell line lacking ryanodine receptor protein for homologous expression studies: reconstitution of RyR1 protein and function. *Journal of Cell Biology* **140(4)**; 843-51

Moore, C.P., Zhang, J., and Hamilton, S.L. (1999) A role for cysteine 3635 of RyR1 in redox modulation and calmodulin binding. *Journal of Biological Chemistry* **274**; 36831-36834

Murayama, T., Oba, T., Latayama, E., Oyamada, H., Oguchi, K., Kobayashi, M., Otsuka, K. and Ogawa, Y. (1999) Further characterization of the type 3 ryanodine receptor (RyR3) purified from rabbit skeletal rabbit diaphragm. *Journal of Biological Chemistry* **274**; 17297-17308

Nakai, J., Dirksen, R.T., Nguyen, H.T., Pessah, I.N., Beam, K.G. and Allen, P.D. (1996) Enhanced dihydropyridine receptor channel activity in the presence of ryanodine receptor. *Nature* **380(6569)**; 72-5

Nakai, J., Goa, L., Xin, C., Pasek, D.A. and Meissner, G. (1999) Evidence for a role of C-terminus in Ca^{2+} inactivation of skeletal muscle Ca^{2+} release channel ryanodine receptor). *Federation of European Biochemical Societies Letters* **459**; 154-158

Nakai, J., Imagawa, T., Hakamat, Y., Shigekawa, M., Takeshima, H. and Numa, S. (1990) Primary structure and functional expression from cDNA of the cardiac ryanodine receptor/calcium release channel. *Federation of European Biochemical Societies Letters* **271**; 169-77

Nakai, J., Ogura, T., Protasi, F., Franzini-Armstrong, C., Allen, P.D. and Beam, K.G. (1997) Functional nonequality of the cardiac and skeletal ryanodine receptors. *Proceedings of the National Academy of Sciences of the United States of America* **94(3)**; 1019-22

Nakajima, T., Kaneko, Y., Taniguchi, Y., Hayashi, K., Takizawa, T., Suzuki, T. and Nagai R. (1997) The mechanism of catecholaminergic polymorphic ventricular tachycardia may be triggered activity due to delayed afterdepolarization. *European Heart Journal* **18(3)**; 530-1

Nava, A., Canciani, B., Daliento, L., Miraglia, G., Buja, G., Fasoli, G., Martini, B., Scognamiglio, R. and Thiene, G. (1988) Juvenile sudden death and effort ventricular tachycardias in a family with right ventricular cardiomyopathy. *International Journal of Cardiology* **21(2)**; 111-26

Nelson, M.T. and Herrera, G.M. (2002) Molecular physiology: protecting the heart. *Nature* **416(6878)**; 273-4

Nelson, T.E., Lin, M., Zapata-Sudo, G. and Sudo, R.T. (1996) Dantrolene sodium can increase or attenuate activity of skeletal muscle ryanodine receptor calcium release channel. Clinical implications. *Anesthesiology* **84(6)**; 1368-79

Neyroud, N., Tesson, F., Denjoy, I., Leibovici, M., Donger, C., Barhanin, J., Faure, S., Gary, F., Coumel, P., Petit, C., Schwartz, K. and Guicheney P. (1997) A novel mutation in the potassium channel gene KVLQT1 causes the Jervell and Lange-Nielsen cardioauditory syndrome. *Nature Genetics* **15(2)**; 186-9

Niggli, E. (1999) Ca^{2+} sparks in cardiac muscle: is there life without them? *News in Physiological Sciences* **14**; 129-134

Nimer, L.R., Needleman, D.H., Hamilton, S.L., Krall, J. and Movsesian, M.A. (1995) Effect of ryanodine on sarcoplasmic reticulum Ca^{2+} accumulation in nonfailing and failing human myocardium. *Circulation* **92(9)**; 2504-10

Oda, T., Yano, M., Yamamoto, T., Tokuhisa, T., Okuda, S., Doi, M., Ohkusa, T., Ikeda, Y., Kobayashi, S., Ikemoto, N. and Matsuzaki, M. (2005) Defective regulation of interdomain interactions within the ryanodine receptor plays a key role in the pathogenesis of heart failure. *Circulation* **111(25)**; 3400-10

Ogawa, Y. and Harafuji, H. (1990) Effect of temperature on [^{3}H]ryanodine binding to sarcoplasmic reticulum from bullfrog skeletal muscle. *Journal of Biochemistry (Tokyo)* **107(6)**; 887-93

Okuda, S., Yano, M., Doi, M., Oda, T., Tokuhisa, T., Kohno, M., Kobayashi, S., Yamamoto, T., Ohkusa, T. and Matsuzaki, M. (2004) Valsartan restores sarcoplasmic reticulum function with no appreciable effect on resting cardiac function in pacing-induced heart failure. *Circulation* **109(7)**; 911-9

Ono, K., Yano, M., Ohkusa, T., Kohno, M., Hisaoka, T., Tanigawa, T., Kobayashi, S., Kohno, M. and Matsuzaki, M. (2000) Altered interaction of FKBP12.6 with ryanodine receptor as a cause of abnormal Ca^{2+} release in heart failure. *Cardiovascular Research* **48(2)**; 323-31

Orchard, C.H., Smith, G.L. and Steele D.S. (1998) Effects of cytosolic Ca^{2+} on the Ca^{2+} content of the sarcoplasmic reticulum in saponin-permeabilized rat ventricular trabeculae. *Pflügers Archiv – European Journal of Physiology* **435**; 555-563

Orlova, E.V., Serysheva, I.I., van Heel, M., Hamilton, S.L. and Chiu, W. (1996) Two structural configurations of the skeletal muscle calcium release channel. *Nature Structural Biology* **3(6)**; 547-52

Otsu, K., Huntington, F.W., Khanna, V.K., Zorzato, F., Green, N.M. and MacLennan, D.H. (1990) Molecular cloning of cDNA encoding the Ca^{2+} release channel (ryanodine receptor) of rabbit cardiac muscle sarcoplasmic reticulum. *Journal of Biological Chemistry* **265**; 13472-13483

Otsu, K., Nishida, K., Kimura, Y., Kuzuya, T., Hori, M., Kamada, T. and Tada, M. (1994) The point mutation Arg^{615} to Cys in the Ca^{2+} release channel of skeletal sarcoplasmic reticulum Is responsible for hypersensitivity to caffeine and halothane in malignant hyperthermia. *Journal of Biological Chemistry* **269**; 9413-9415

Owen, V.J., Taske, N.L. and Lamb, G.D. (1997) Reduced Mg^{2+} inhibition of Ca^{2+} release in muscle fibers of pigs susceptible to malignant hyperthermia. *American Journal of Physiology* **272(1 Pt 1)**; C203-11

Ozil, J.P. and Swann, K. (1995) Stimulation of repetitive calcium transients in mouse eggs. *Journal of Physiology* **483**; 331-46

Palade, P. (1987) Drug-induced Ca^{2+} release from isolated sarcoplasmic reticulum. III. Block of Ca^{2+}-induced Ca^{2+} release by organic polyamines. *Journal of Biological Chemistry* **262(13)**; 6149-54

Pastore, J.M., Girouard, S.D., Laurita, K.R., Akar, F.G. and Rosenbaum, D.S. (1999) Mechanism linking T-wave alternans to the genesis of cardiac fibrillation. *Circulation* **99(10)**; 1385-94

Patterson, R.L., Boehning, D. and Snyder, S.H. (2004) Inositol 1,4,5-trisphosphate receptors as signal integrators. *Annual Review of Biochemistry* **73**; 437-65

Penner, R., Neher, E., Takeshima, H., Nishimura, S. and Numa, S. (1989) Functional expression of the calcium release channel from skeletal muscle ryanodine receptor cDNA. *Federation of American Societies for Experimental Biology Journal* **259(1)**; 217-21

Pessah, I.N., Stambuk, R.A. and Casida, J.E. (1987) Ca^{2+}-activated ryanodine binding: mechanisms of sensitivity and intensity modulation by Mg^{2+}, caffeine, and adenine nucleotides. *Molecular Pharmacology* **31(3)**; 232-8

Pessah, I.N., Waterhouse, A.L. and Casida, J.E. (1985) The calcium-ryanodine receptor complex of skeletal and cardiac muscle. *Biochemical and Biophysical Research Communications* **128**; 449-456

Pessah, I.N. and Zimanyi, I. (1991) Characterization of multiple [^{3}H]ryanodine binding sites on the Ca^{2+} release channel of sarcoplasmic reticulum from skeletal and cardiac muscle: evidence for a sequential mechanism in ryanodine action. *Molecular Pharmacology* **39(5)**; 679-89

Pelzer, T., Neumann, M., de Jager, T., Jazbutyte, V. and Neyses, L.. (2001) Estrogen effects in the myocardium: inhibition of NF-kappaB DNA binding by estrogen receptor-alpha and -beta. *Biochemical and Biophysical Research Communications* **286(5)**; 1153-7

Petroff, M.G.V., Kim, S.H., Pepe, S., Dessy, C., Marban, E., Balligand, J. and Sollot, S.J. (2001) Endogenous nitric oxide mechanisms mediate the stretch dependence of Ca^{2+} release in cardiomyocytes. *Nature Cell Biology* **3**; 867-873

Phillips, M.S., Fujii, J., Khanna, V. K., DeLeon, S., Yokobata, K., De Jong, P.J. and MacLennan, D.H. (1996) The structural organization of the human skeletal muscle ryanodine receptor (RYR1) gene. *Genomics* **34**; 24-41

Piacentino, V. 3rd, Dipla, K., Gaughan, J.P. and Houser, S.R. (2000) Voltage-dependent Ca^{2+} release from the SR of feline ventricular myocytes is explained by Ca^{2+}-induced Ca^{2+} release. *Journal of Physiology* **523 Pt 3**; 533-48

Pieske, B., Maier, L.S., Bers, D.M. and Hasenfuss, G. (1999) Ca^{2+} handling and sarcoplasmic reticulum Ca^{2+} content in isolated failing and nonfailing human myocardium. *Circulation Research* **85(1)**; 38-46

Plaster, N.M., Tawil, R., Tristani-Firouzi, M., Canun, S., Bendahhou, S., Tsunoda, A., Donaldson, M.R., Iannaccone, S.T., Brunt, E., Barohn, R., Clark, J., Deymeer, F., George, A.L. Jr, Fish, F.A., Hahn, A., Nitu, A., Ozdemir, C., Serdaroglu, P., Subramony, S.H., Wolfe, G., Fu, Y.H. and Ptacek, L.J. (2001) Mutations in Kir2.1 cause the developmental and episodic electrical phenotypes of Andersen's syndrome. *Cell* **105(4)**; 511-9

Pogwizd, S.M. and Bers, D.M. (2004) Cellular basis of triggered arrhythmias in heart failure. *Trends in Cardiovascular Medicine* **14**; 61-66

Pogwizd, S.M., McKenzie, J.P. and Cain, M.E. (1998) Mechanisms underlying spontaneous and induced ventricular arrhythmias in patients with idiopathic dilated cardiomyopathy. *Circulation* **98(22)**; 2404-14

Pogwizd, S.M., Schlotthauer, K., Li, L., Yuan, W. and Bers, D.M. (2001) Arrhythmogenesis and contractile dysfunction in heart failure: roles of sodium-calcium exchange, inward rectifier potassium current, and residual beta-adrenergic responsiveness. *Circulation Research* **8**; 1159-67

Postma, A.V., Denjoy, I., Hoorntje, T.M., Lupoglazoff, J., Da Costa, A., Sebillon, P., Mannens, M.M.A.M., Wilde, A.A.M. and Guicheney, P. (2002) Absence of calsequestrin 2 causes severe forms of catecholaminergic polymorphic ventricular tachycardia. *Circulation Research* **91**; e21-e26

Prasher, D.C., Eckenrode, V.K., Ward, W.W., Prendergast, F.G. and Cormier, M.J. Primary structure of the Aequorea victoria green-fluorescent protein. *Gene* **111(2)**; 229-33

Priori, S.G., Aliot, E., Blomstrom-Lundqvist, C., Bossaert, L., Breithardt, G., Brugada, P., Camm, A.J., Cappato, R., Cobbe, S.M., Di Mario, C., Maron, B.J., McKenna, W.J., Pedersen, A.K., Ravens, U., Schwartz, P.J., Trusz-Gluza, M., Vardas, P., Wellens, H.J. and Zipes, D.P. (2001a) Task Force on sudden cardiac death of the European Society of Cardiology. *European Heart Journal* **23(3)**; 257

Priori, S.G., Napolitano, C., Tiso, N., Memmi, M., Colombi, B., Drago, F., Gasparini, M., DeSimone, L., Corloti, F., Bloise, R., Keegan, R., Cruz Filho, F.E.S., Vignati, G., Benatar, A., DeLogu, A. (2002) Clinical and molecular characterization of patients with catecholaminergic polymorphic ventricular tachycardia. *Circulation* **106**; 69-74

Priori, S.G., Napolitano, C., Tiso, N., Memmi, M., Vignati, G., Bloise, R., Sorrentino, V. and Danieli, G.A. (2001b) Mutations in the cardiac ryanodine receptor gene (hRyR2) underlie catecholaminergic polymorphic ventricular tachycardia. *Circulation* **103**; 196-200

Priori, S.G., Napolitano, C. and Vincentini, A. (2003) Inherited arrythmia syndromes: applying the molecular biology and genetic to the clinical management. *Journal of Interventional Cardiac Electrophysiology* **9**; 93-101

Priori, S.G., Zuanetti, G. and Schwartz, P.J. (1988) Ventricular fibrillation induced by the interaction between acute myocardial ischemia and sympathetic hyperactivity: effect of nifedipine. *American Heart Journal* **116(1 Pt 1)**; 37-43

Proenza, C., O'Brien, J., Nakai, J., Mukherjee, S., Allen, P.D. and Beam, K.G. Identification of a region of RyR1 that participates in allosteric coupling with the alpha(1S) (Ca(V)1.1) II-III loop. *Journal of Biological Chemistry* **277(8)**; 6530-5

Protasi, F., Sun, X.H. and Franzini-Armstrong, C. (1996) Formation and maturation of the calcium release apparatus in developing and adult avian myocardium. *Developmental Biology* **173(1)**; 265-78

Querfurth, H.W., Haughey, N.J., Greenway, S.C., Yacono, P.W. and Golan, D.E. (1998) Expression of ryanodine receptors in human embryonic kidney (HEK293) cells. *Biochemical Journal* **334**; 79-86

Radermacher, M., Radermacher, V., Grassucci, R., Frank, J., Timerman, A.P., Fleischer, S., and Wagenknecht, T. (1994) Cryo-electron microscopy and three-dimensional reconstruction of the calcium release channel/ryanodine receptor from skeletal muscle. *Journal of Cell Biology* **127**; 411-423

Ramos-Franco, J., Galvan, D., Mignery, G.A. and Fill, M. (1999) Location of the permeation pathway in recombinant type I inositol 1,4,5-trisphosphate receptor. *Journal of General Physiology* **114**; 243-250

Rampazzo, A., Nava, A., Danieli, G.A., Buja, G., Daliento, L., Fasoli, G., Scognamiglio, R., Corrado, D. and Thiene, G. (1994) The gene for arrhythmogenic right ventricular cardiomyopathy maps to chromosome 14q23-q24. *Human Molecular Genetics* **3(6)**; 959-62

Rampazzo, A., Nava, A., Erne, P., Eberhard, M., Vian, E., Slomp, P., Tiso, N., Thiene, G. and Danieli, G.A. (1995) A new locus for arrhythmogenic right ventricular cardiomyopathy (ARVD2) maps to chromosome 1q42-q43. *Human Molecular Genetics* **4(11)**; 2151-4

Rampazzo, A., Nava, A., Miorin, M., Fonderico, P., Pope, B., Tiso, N., Livolsi, B., Zimbello, R., Thiene, G. and Danieli, G.A. (1997) ARVD4, a new locus for arrhythmogenic right ventricular cardiomyopathy, maps to chromosome 2 long arm. *Genomics* **45(2)**; 259-63

Rampazzo, A., Pivotto, F., Occhi, G., Tiso, N., Bortoluzzi, S., Rowen, L., Hood, L., Nava, A. and Danieli, G.A. (2000) Characterization of C14orf4, a novel intronless human gene containing a polyglutamine repeat, mapped to the ARVD1 critical region. *Biochemical and Biophysical Research Communications* **278(3)**; 766-74

Reiken, S., Gaburjakova, M., Gaburjakova, J., He, K., Prieto, A., Becker, E., Yi, G., Wang, J., Burkhoff, D. and Marks, A. (2001) Beta-adrenergic receptor blockers restore cardiac calcium release channel (ryanodine receptor) structure and function in heart failure. *Circulation* **104**; 2843-2848

Reiken, S., Lacampagne, A., Zhou, H., Kherani, A., Lehnart, S.E., Ward, C., Huanf, H., Gaburjakova, M., Gaburjakova, J., Rosemblit, N., Warren, M.S., He, K., Yi, G., Wang, J., Burkhoff, D., Vassort, G. and Marks A.R. (2003a) PKA phosphorylation activates the calcium release channel (ryanodine receptor) in skeletal muscle: defective regulation in heart failure. *Journal of Cell Biology* **160**; 919-928

Reiken, S., Wehrens, X.H.T., Vest, J.A., Barbone, A., Klotz, S., Mancini, D., Burkhoff, D. and Marks, A.R. (2003b) Beta-blockers restore calcium release channel function and improve cardiac muscle performance in human heart failure. *Circulation* **107**; 2459-2466

Reuter, H., Henderson, S.A., Han, T., Matsuda, T., Baba, A., Ross, R.S., Goldhaber, J.I. and Philipson, K.D. (2002) Knockout mice for pharmacological screening: testing the specificity of Na^{+}-Ca^{2+} exchange inhibitors. *Circulation Research* **91(2)**; 90-2

Roderick, H.L., Campbell, A.K. and Llewellyn, D.H. (1997) Nuclear localisation of calreticulin in vivo is enhanced by its interaction with glucocorticoid receptors. *Federation of European Biochemical Societies Letters* **405(2)**; 181-5

Rodney, G.G., Williams, B.Y., Strasburg, G.M., Beckingham, K., Hamilton, S.L. (2000) Regulation of RYR1 activity by Ca^{2+} and calmodulin. *Biochemistry* **39(26)**; 7807-12

Rodriguez, P., Bhogal, M.S. and Colyer, J. (2003) Stoichiometric phosphorylation of cardiac ryanodine receptor on serine 2809 by calmodulin-dependent kinase II and protein kinase A. *Journal of Biological Chemistry* **278**; 38593-38600

Romano, C., Gemme, G. and Pongiglione, R. (4963) Antmie cardiache rare in eta pediatrica. *La Clinica Pediatrica* **45**; 656–683

Rook, M.B., Bezzina Alshinawi, C., Groenewegen, W.A., van Gelder, I.C., van Ginneken, A.C., Jongsma, H.J., Mannens, M.M., Wilde, A.A.. (1999) Human SCN5A gene mutations alter cardiac sodium channel kinetics and are associated with the Brugada syndrome. *Cardiovascular Research* **44(3)**; 507-17

Rosen, M.R. and Danilo, P. Jr. (1980) Effects of tetrodotoxin, lidocaine, verapamil, and AHR-2666 on Ouabain-induced delayed afterdepolarizations in canine Purkinje fibers. *Circulation Research* **46(1)**; 117-24

Rossi, D., Simeoni, I., Micheli, M., Bootman, M., Lipp, P., Allen, P.D. and Sorrentino, V. (2002) RyR1 and RyR3 isoforms provide distinct intracellular Ca^{2+} signals in HEK 293 cells. *Journal of Cell Science* **115**; 2497-2504

Rousseau, E., Ladine, J., Liu, Q.Y. and Meissner, G. (1988) Activation of the Ca^{2+} release channel of skeletal muscle sarcoplasmic reticulum by caffeine and related compounds. *Archives of Biochemistry and Biophysics* **267(1)**; 75-86

Rousseau, E. and Meissner, G. (1989) Single cardiac sarcoplasmic reticulum Ca^{2+}-release channel: activation by caffeine. *American Journal of Physiology* **256**; 328-333

Rousseau, E., Smith, J.S., Henderson, J.S. and Meissner, G. (1986) Single channel and $^{45}Ca^{2+}$ flux measurements of the cardiac sarcoplasmic reticulum calcium channel. *Biophysical Journal* **50(5)**; 1009-14

Rousseau, E., Smith, J.S. and Meissner G. (1987) Ryanodine modifies conductance and gating behaviour of single Ca^{2+} release channel. *American Journal of Physiology* **253 (3 Pt 1)**; C364-8

Ruden, D.M. (1992) Activating regions of yeast transcription factors must have both acidic and hydrophobic amino acids. *Chromosoma* **101(5-6)**; 342-8

Ruden, D.M., Ma, J., Li, Y., Wood, K. and Ptashne, M. (1991) Generating yeast transcriptional activators containing no yeast protein sequences. *Nature* **350(6315)**; 250-2

Sagawa, T., Sagawa, K., Kelly, J., Tsushima, R.G. and Wasserstrom, J.A. (2002) Activation of cardiac ryanodine receptors by cardiac glycosides. *American Journal of Physiology. Heart and Circulatory Physiology* **282**; H1118-H1126

Sainte Beuve, C., Allen, P.D., Dambrin, G., Rannou, F., Marty, I., Trouve, P., Bors, V., Pavie, A., Gandgjbakch, I. and Charlemagne, D. (1997) Cardiac calcium release channel (ryanodine receptor) in control and cardiomyopathic human hearts: mRNA and protein contents are differentially regulated. *Journal of Molecular and Cellular Cardiology* **29(4)**; 1237-46

Saito, A., Iuni, M., Radermacher, M., Frank, J. and Fleischer, S. (1988) Ultrastructure of the calcium release channel of sarcoplasmic reticulum. *Journal of Cell Biology* **107**; 211-219

Sambrook, J., Fritshc, E.F. and Maniatis, T. (1989) Molecular cloning: a laboratory manual. Second edition. Cold Spring Harbour Laboratory press. NY, USA

Sambuughin, N., Sei, Y., Gallagher, K.L., Wyre, H.W., Madsen, D., Nelson, T.E., Fletcher, J.E., Rosenberg, H. and Muldoon, S.M. (2001) North American malignant hyperthermia population: screening of the ryanodine receptor gene and identification of novel mutations. *Anesthesiology* **95(3)**; 594-9

Samso, M. and Wagenknecht, T. (1998) Contributions of electron microscopy and single-particle techniques to the determination of the ryanodine receptor three-dimensional structure. *Journal of Structural Biology* **121**; 172-180

Samso, M., Wagenknecht, T., Allen, P.D. (2005) Internal structure and visualization of transmembrane domains of the RyR1 calcium release channel by cryo-EM. *Nature – Structural and Moecular Biology* **12(6)**; 539-44

Sanguinetti, M.C. (1999) Dysfunction of delayed rectifier potassium channels in an inherited cardiac arrhythmia. *Annals of the New York Academy of Science* **868**; 406-13

Santana, L.F., Cheng, H., Gomez, A.M., Cannell, M.B. and Lederer, W.J. (1996) Relation between the sarcolemmal Ca^{2+} current and Ca^{2+} sparks and local control theories for cardiac excitation-contraction coupling. *Circulation Research* **78(1)**; 166-71

Sato, Y., Ferguson, D.G., Sako, H., Dorn, G.W. 2nd, Kadambi, V.J., Yatani, A., Hoit, B.D., Walsh, R.A. and Kranias, E.G. (1998) Cardiac-specific overexpression of mouse cardiac calsequestrin is associated with depressed cardiovascular function and hypertrophy in transgenic mice. *Journal of Biological Chemistry* **273(43)**; 28470-7

Satoh, H., Blatter, L.A. and Bers, D.M. (1997) Effects of $[Ca^{2+}]_i$, SR Ca^{2+} load, and rest on Ca^{2+} spark frequency in ventricular myocytes. *American Journal of Physiology* **272(2 Pt 2)**; H657-68

Schreiber, S.L. and Crabtree, G.R. (1992) The mechanism of action of cyclosporin A and FK506. *Immunology Today* **13(4)**; 136-42

Schmitt, J.P., Kamisago, M., Asahi, M., Li, G.H., Ahmad, F., Mende, U., Kranias, E.G., MacLennan, D.H., Seidman, J.G. and Seidman, C.E. (2003) Dilated cardiomyopathy and heart failure caused by a mutation in phospholamban. *Science* **299(5611)**; 1410-3

Scoote, M. and Williams, A.J. (2002) The cardiac ryanodine receptor (calcium release channel): emerging role in heart failure and arrhythmia pathogenesis. *Cardiovascular Research* **56**; 359-372

Scoote, M. and Williams, A.J. (2004). Myocardial calcium signalling and arrhythmia pathogenesis. *Biochemical and Biophysical Research Communications* **322**; 1286-1309

Scott, B.T., Simmerman, H.K., Collins, J.H., Nadal-Ginard, B. and Jones, L.R. (1988) Complete amino acid sequence of canine cardiac calsequestrin deduced by cDNA cloning. *Journal of Biological Chemistry* **263(18)**; 8958-64

Seidler, T., Miller, S.L., Loughrey, C.M., Kania, A., Burow, A., Kettlewell, S., Teucher, N., Wagner, S., Kogler, H., Meyers, M.B., Hasenfuss, G. and Smith, G.L. (2003) Effects of adenovirus-mediated sorcin overexpression on excitation-contraction coupling in isolated rabbit cardiomyocytes. *Circulation Research* **93(2)**; 132-9

Serebriiskii, I.G. and Golemis, E.A. (2001) Two-hybrid system and false positives. Approaches to detection and elimination. *Methods in Molecular Biology* **177**; 123-34

Serysheva, I.I., Hamilton, S.L., Chiu, W. and Ludtke, S.J. (2005) Structure of Ca^{2+} release channel at 14 A resolution. *Journal of Molecular Biology* **345(3)**; 427-31

Serysheva, I.I., Orlova, E.V., Chiu, W., Sherman, M.B., Hamilton, S.L. and van Heel, M. (1995) Electron cryomicroscopy and angular reconstitution used to visualize the skeletal muscle calcium release channel. *Nature - Structural Biology* **2(1)**; 18-24

Shannon, T.R., Guo, T. and Bers, D.M. (2003) Ca^{2+} scraps: local depletions of free $[Ca^{2+}]$ in cardiac sarcoplasmic reticulum during contractions leave substantial Ca^{2+} reserve. *Circulation Research* **93(1)**; 40-5

Sharma, M.R., Jeyakumar, L.H., Fleischer, S. and Wagenknecht, T. (2000) Three-dimensional structure of ryanodine receptor isoform three in two conformational states as visualized by cryo-electron microscopy. *Journal of Biological Chemistry* **275**; 9485-9491

Sharma, M.R., Penczek, P., Grassucci, R., Xin, H., Fleischer, S. and Wagenknecht, T. (1998) Cryoelectron microscopy and image analysis of the cardiac ryanodine receptor. *Journal of Biological Chemistry* **273**; 18429-18434

Shibao, K., Hirata, K., Robert, M.E. and Nathanson, M.H. (2003) Loss of inositol 1,4,5-trisphosphate receptors from bile duct epithelia is a common event in cholestasis. *Gastroenterology* **125**; 1175-87

Shou, W., Aghdasi, B., Armstrong, D.L., Guo, Q., Bao, S., Charng, M.J., Mathews, L.M., Schneider, M.D., Hamilton, S.L. and Matzuk, M.M. (1998) Cardiac defects and altered ryanodine receptor function in mice lacking FKBP12. *Nature* **391(6666)**; 489-92

Sitsapesan, R., McGarry, S.J. and Williams, A.J. (1994) Cyclic ADP-ribose competes with ATP for the adenine nucleotide binding site on the cardiac ryanodine receptor Ca^{2+}-release channel. *Circulation Research* **75(3)**; 596-600
Sitsapesan, R. and Williams, A.J. (1990) Mechanisms of caffeine activation of single calcium-release channels of sheep cardiac sarcoplasmic reticulum. *Journal of Physiology* **423**; 425-39

Sitsapesan, R. and Williams, A.J. (1994) Gating of the native and purified cardiac sarcoplasmic reticulum Ca^{2+}-release channel with monovalent cations as permeant species. *Biophysical Journal* **67(4)**; 1484-94

Sitsapesan, R. and Williams, A.J. (1995) The gating of the sheep skeletal sarcoplasmic reticulum Ca^{2+}-release channel is regulated by luminal Ca^{2+}. *Journal of Membrane Biology* **146(2)**; 133-44

Smith, J.S., Coronado, R. and Meissner, G. (1985) Sarcoplasmic reticulum contains adenine nucleotide-activated Ca^{2+} channels. *Nature* **316**; 446-9

Smith, J.S., Imagawa, T., Ma, J., Fill, M., Campbell, K.P. and Coronado, R. (1988) Purified ryanodine receptor from rabbit skeletal muscle is the calcium-release channel of sarcoplasmic reticulum. *Journal of General Physiology* **92(1)**; 1-26

Song, L.S., Stern, M.D., Lakatta, E.G. and Cheng, H. (1997) Partial depletion of sarcoplasmic reticulum calcium does not prevent calcium sparks in rat ventricular myocytes. *Journal of Physiology* **505(3)**; 665-75

Sonnleitner, A., Conti, A., Bertocchini, F., Schindler, H. and Sorrentino, V. (1998) Functional properties of the ryanodine receptor type 3 (RyR3) Ca^{2+} release channel. *European Molecular Biology Organisation Journal* **17**; 2790-2798

Sonnleitner, A., Fleishcer, S. and Schindler, H. (1997) Gating of the skeletal calcium release channel by ATP is inhibited by protein phsophatatse 1 but not Mg^{2+} *Cell Calcium* **21**; 283-290

Splawski, I., Shen, J., Timothy, K.W., Lehmann, M.H., Priori, S., Robinson, J.L., Moss, A.J., Schwartz, P.J., Towbin, J.A., Vincent, G.M. and Keating, M.T. (2000) Spectrum of mutations in long-QT syndrome genes. KVLQT1, HERG, SCN5A, KCNE1, and KCNE2. *Circulation* **102(10)**; 1178-85

Splawski. I., Timothy, K.W., Decher, N., Kumar, P., Sachse, F.B., Beggs, A.H., Sanguinetti, M.C. and Keating, M.T. (2005) Severe arrhythmia disorder caused by cardiac L-type calcium channel mutations. *Proceedings of the National Academy of Sciences of the United States of America* **102(23)**; 8089-96

Splawski, I., Timothy, K.W., Sharpe, L., Decher, N., Kumar, P., Bloise, R., Napolitano, C., Schwartz, P., Joseph, R.M., Condouris, K., Tager-Flusberg, H., Priori, S.G., Sanguinetti, M.C., Keating, M.T. (2004) $Ca_v1.2$ calcium channel dysfunction causes a multisystem disorder including arrhythmia and autism. *Cell* **119**; 19-31

Splawski. I, Tristani-Firouzi. M,, Lehmann. M.H., Sanguinetti, M.C. and Keating, M.T. (1997) Mutations in the h*minK* gene cause long QT syndrome and suppress IKs function. *Nature Genetics* **17(3)**; 338-40

Stamler, J.S. and Hausladen, A. (1998) Oxidative modifications in nitrosative stress. *Nature Structural Biology* **5(4)**; 247-9

Stange, M., Xu, L., Balshaw, D., Yamaguchi, N. and Meissner, G. (2003) Characterization of recombinant skeletal muscle (Ser-2843) and cardiac muscle (Ser-2809) ryanodine receptor phosphorylation mutants. *Journal of Biological Chemistry* **278**; 51693-51702

Stern, M.D. (1992) Theory of excitation-contraction coupling in cardiac muscle. Biophysical Journal **63(2)**; 497-517

Stern, M.D. and Cheng, H. (2004) Putting out the fire: what terminates calcium-induced calcium release in cardiac muscle? *Cell Calcium* **35**; 591-601
Stewart, R., Zissimopoulos, S. and Lai, F.A. (2003) Oligomerization of the cardiac ryanodine receptor C-terminal tail. *Biochemical Journal* **376**; 795-799

Stoyanovsky, D., Murphy, T., Anno, P.R., Kin, Y. and Salama, G. (1997) Nitirc oxide activates skeletal and cardiac ryanodine receptors. *Cell Calcium* **21**; 19-29

Suarez, J., Belke, D.D., Gloss, B., Dieterle, T., McDonough, P.M., Kim, Y., Brunton, L.L. and Dillmann, W.H. (2004) *In vivo* adenoviral transfer of sorcin reverses cardiac contractile abnormalities of diabetic cardiomyopathy. *American Journal of Physiology - Heart and Circulatory Physiology* **286**; 68-75

Sun, J., Xin, C., Eu, J.P., Stamler, J.S. and Meissner, G. (2001) Cysteine-3635 is responsible for skeletal muscle ryanodine receptor modulation by NO. *Proceedings of the National Academy of Sciences of the United States of America* **98**; 11158-11162

Sun, J., Xu, L., Eu, J.P., Stamler, J.S. and Meissner, G. (2003) Nitric oxide, NOC-12, and S-Nitrosoglutathione modulate the skeletal muscle calcium release channel/ryanodine receptor by different mechanisms. *Journal of Bioogical. Chemistry* **278**; 8184-8189

Sun, X.H., Protasi, F., Takahashi, M., Takeshima, H., Ferguson, D.G. and Franzini-Armstrong, C. (1995) Molecular architecture of membranes involved in excitation-contraction coupling of cardiac muscle. *Journal of Cell Biology* **129(3)**; 659-71

Sutko, J.L. and Airey, J.A. (1996) Ryanodine receptor Ca^{2+} release channels: does diversity in form equal diversity in function? *Physiological Reviews* **76**; 1027-71

Sutko, J.L., Airey, J.A., Welch, W. and Ruest, L. (1997) The pharmacology of ryanodine and related compounds. *Pharmacological Reviews* **49**; 53-98

Sutko, J.L., Thompson, L.J., Kort, A.A. and Lakatta, E.G. (1986) Comparison of effects of ryanodine and caffeine on rat ventricular myocardium. *American Journal of Physiology* **250**(5 Pt 2); H786-95

Sutko, J.L. and Willerson, J.T. (1980) Ryanodine alteration of the contractile state of rat ventricular myocardium. *Circulation Research* **46**; 332 - 43

Swan, H., Laitinen, P., Kontula, K. and Toivonen, L. (2005) Calcium channel antagonism reduces exercise-induced ventricular arrhythmias in catecholaminergic polymorphic ventricular tachycardia patients with RyR2 mutations. *Journal of Cardiovascular Electrophysiology* **16**; 162-166

Swan, H., Piippo, K., Viitasalo, M., Heikkila, P., Paavonen, T., Kainulainen, K., Kere, J., Keto, P., Kontula, K. and Toivonen, L. (1999) Arrhythmic disorder mapped to chromosome 1q42-q43 causes malignant polymorphic ventricular tachycardia in structurally normal hearts. *Journal of the American College of Cardiology* **34(7)**; 2035-42

Szegedi, C., Sarkozi, S., Herzog, A., Jona, I. and Varsanyi, M. (1999) Calsequestrin: more than 'only' a luminal Ca^{2+} buffer inside the sarcoplasmic reticulum. *Biochemical Journal* **337** 19-22

Takasago, T., Imagawa, T., Furukawa, K., Ogurusu, T. and Shigekawa, M. (1991) Regulation of the cardiac ryanodine receptor by protein kinase-dependent phosphorylation. *Journal of Biochemistry* **109(1)**; 163-70

Takeshima, H. (1993) Primary structure and expression from cDNAs of the ryanodine receptor. *Annals of the New York Academy of Sciences* **707**; 165-77

Takeshima, H., Iino, M., Takekura, H., Nishi, M., Kuno, J., Minowa, O., Takano, H. and Noda, T. (1994) Excitation-contraction uncoupling and muscular degeneration in mice lacking functional skeletal muscle ryanodine-recpetor gene. *Nature* **369**; 556-9

Takeshima, H., Ikemoto, T., Nishi, M., Nishiyama, N., Shimuta, M., Sugitani, Y., Kuno, J., Saito, I., Saito, H., Endo, M., Iino, M., Noda, T. (1996) Generation and characterization of mutant mice lacking ryanodine receptor type 3. *Journal of Biological Chemistry* **271**; 19649-19652

Takeshima, H., Komazaki, S., Hirose, K., Nishi, M., Noda, T. and Iino, M. (1998) Embryonic lethality and abnormal cardiac myocytes in mice lacking ryanodine receptor type 2. *European Molecular Biology Organisation Journal* **17**; 3309-3316

Takeshima, H., Mishimura, S., Matsumoto, T., Ishida, H., Kangawa, K., Minamino, N., Matsuo, H., Ueda, M., Hanaoka, M., Hirose, T. and Numa, S. (1989) Primary structure and expression from complementary DNA of skeletal muscle ryanodine receptor. *Nature* **339**; 439-445

Takeshima, H., Yamazawa, T., Ikemoto, T., Takekura, H., Nishi, M., Noda, T. and Iino, M. (1995) Ca^{2+}-induced Ca^{2+} release in myocytes from dyspedic mice lacking the type-1 ryanodine receptor. *European Molecular Biology Organisation Journal* **14(13)**; 2999-3006

Tang, W., Ingalls, C.P., Durham, W.J., Snider, J., Reid, M.B., Wu, G., Matzuk, M.M. and Hamilton, S.L. (2004) Altered excitation-contraction coupling with skeletal muscle specific FKBP12 deficiency. *Federation of American Societies for Experimental Biology Journal* **18(13)**; 1597-9

Tang, T.S., Tu, H., Chan, E.Y., Maximov, A., Wang, Z., Wellington, C.L., Hayden, M.R. and Bezprozvanny, I. (2003) Huntingtin and huntingtin-associated protein 1 influence neuronal calcium signalling mediated by inositol-(1,4,5) triphosphate receptor type 1. *Neuron* **17**; 227-39

Terentyev, D., Cala, S.E., Houle, T.D., Viatchenko-Karpinski, S., Gyorke, I., Terentyeva, R., Williams, S.C. and Györke, S. (2005) Triadin overexpression stimulates excitation-contraction coupling and increases predisposition to cellular arrhythmia in cardiac myocytes. *Circulation Research* **96(6)**; 651-8

Terentyev, D., Viatchenko-Karpinski, S., Gyorke, I., Volpe, P., Williams, S.C. and Gyorke, S. (2003) Calsequestrin determines the functional size and stability of cardiac intracellular calcium stores: mechanism for hereditary arrhythmia. *Proceedings of the National Academy of Sciences of the United States of America* **100**; 11759-11764

Thastrup, O., Cullen, P.J., Drobak, B.K., Hanley, M.R. and Dawson, A.P. (1990) Thapsigargin, a tumor promoter, discharges intracellular Ca^{2+} stores by specific inhibition of the endoplasmic reticulum Ca^{2+}-ATPase. *Proceedings of the National Academy of Sciences of the United States of America* **87(7)**; 2466-70

Thomas, D., Toey, S.C., Collins, T.J., Bootman, M.J., Berridge, M.J. and Lipp, P. (2000) A comparison of fluorescent Ca^{2+} indicator properties and their use in measuring elementary and global Ca^{2+} signals. *Cell Calcium* **28**; 213-223

Timerman, A.P., Jayaraman, T., Wiederrecht, G., Onoue, H., Marks, A.R. and Fleischer, S. (1994) The ryanodine receptor from canine heart sarcoplasmic reticulum is associated with a

novel FK-506 binding protein. *Biochemical and Biophysical Research Communications* **198**; 701-706

Timerman, A P., Ogunbumni, E., Freund, E., Wiederrecht, G., Marks, A.R. and Fleischer, S. (1993) The calcium release channel of the sarcoplasmic reticulum is modulated by FK-506 binding protein. *Journal of Biological Chemistry* **268**; 22992-22999

Timerman, A.P., Onoue, H., Xin, H., Barg, S., Copello, J., Wiederrecht, G. and Fleischer, S. (1996) Selective binding of FKBP12.6 by the cardiac ryanodine receptor. *Journal of Biological Chemistry* **271**; 20385-20391

Tinker, A. and Williams, A.J. (1992) Divalent cation conduction in the ryanodine receptor channel of sheep muscle sarcoplasmic reticulum. *Journal of General Physiology* **100(3)**; 479-93

Tiso, N., Salamon, M., Bagattin, A., Danieli, G.A., Argenton, F. and Bortolussi, M. (2002) The binding of the RyR2 calcium channel to its gating protein FKBP12.6 is oppositely affected by ARVD2 and VTSIP mutations. *Biochemical and Biophysical Research Communications* **299**; 594-598

Tiso, N., Stephan, D.A., Nava, A., Bagattin, A., Devaney, J.M., Stanchi, F., Larderet, G., Brahmbhatt, B., Brown, K., Bauce, B., Muriago, M., Basso, C., Thiene, G., Danieli, G.A. and Rampazzo, A. (2001) Identification of mutations in the cardiac ryanodine receptor gene in families affected with arrhythmogenic right ventricular cardiomyopathy type 2 (ARVD2). *Human Molecular Genetics* **10**; 189-194

Tong, J., Du, G.G., Chen, S.R. and MacLennan, D.H. (1999a) HEK-293 cells possess a carbachol- and thapsigargin-sensitive intracellular Ca^{2+} store that is responsive to stop-flow medium changes and insensitive to caffeine and ryanodine. *Biochemical Journal* **343 (1)**; 39-44

Tong, J., McCarthy, T. and MacLennan, D. (1999b) Measurement of resting cytosolic Ca^{2+} concentrations and Ca^{2+} store size in HEK-293 cells transfected with malignant hyperthermia or central core disease mutant Ca^{2+} release channels. *Journal of Biological Chemistry* **274**; 693-702

Tong, J., Oyamada, H., Demaurex, N., Grinstein, S., McCarthy, T. and MacLennan, D. (1997) Caffeine and halothane sensitivity of intracellular Ca^{2+} release is altered by 15 calcium release channel (ryanodine receptor) mutations associated with malignant hyperthermia and/or central core disease. *Journal of Biological Chemistry* **272**; 26332-26339

Towbin, J.A. (2001) Molecular genetic basis of sudden cardiac death. *Cardiovascular Pathology* **10(6)**; 283-95

Toyoshima, C., Nakasako, M., Nomura, H. and Ogawa, H. (2000) Crystal structure of the calcium pump of sarcoplasmic reticulum at 2.6 A resolution. *Nature* **405(6787)**; 647-55

Trafford, A.W. and Eisner, D.A. (2003) No role for a voltage sensitive release mechanism in cardiac muscle. *Journal of Molecular and Cellular Cardiology* **35(2)**; 145-51

Treves, S., Larini, F., Menegazzi, P., Steinberg, T.H., Koval, M., Vilsen, B., Andersen, J.P. and Zorzato, F. (1994) Alteration of intracellular Ca^{2+} transients in COS-7 cells transfected with the cDNA encoding skeletal-muscle ryanodine receptor carrying a mutation associated with malignant hyperthermia. *Biochemical Journal* **301(Pt 3)**; 661-5

Treves, S., Pouliquin, P., Moccagatta, L. and Zorzato, F. (2002) Functional properties of EGFP-tagged skeletal muscle calcium-release channel (ryanodine receptor) expressed in COS-7 cells: sensitivity to caffeine and 4-chloro-m-cresol. *Cell Calcium* **31**; 1-12

Tripathy, A. and Meissner, G. (1996) Sarcoplasmic reticulum luminal Ca^{2+} has access to cytosolic activation and inactivation sites of skeletal muscle Ca^{2+} release channel. *Biophysical Journal* **70(6)**; 2600-15

Tristani-Firouzi, M., Jensen, J.L., Donaldson, M.R., Sansone, V., Meola, G., Hahn, A., Bendahhou, S., Kwiecinski, H., Fidzianska, A., Plaster, N., Fu, Y.H., Ptacek, L.J. and Tawil, R. (2002) Functional and clinical characterization of KCNJ2 mutations associated with LQT7 (Andersen syndrome). *Journal of Clinical Investigation* **110(3)**; 381-8

Tse, A., Tse, F.W., Almers, W. and Hille, B. (1993) Rhythmic exocytosis stimulated by GnRH-induced calcium oscillations in rat gonadotropes. *Science* **260**; 82-4

Tsien, R.W., Bean, B.P., Hess, P., Lansman, J.B., Nilius, B. and Nowycky, M.C. (1986) Mechanisms of calcium channel modulation by beta-adrenergic agents and dihydropyridine calcium agonists. *Journal of Molecular and Cellular Cardiology* **18**; 691-710

Tsugorka, A., Rios, E. and Blatter, L.A. (1995) Imaging elementary events of calcium release in skeletal muscle cells. *Science* **269(5231)**; 1723-6

Tunwell, R.E.A, Wickendum, C., Bertrand, B.M.A., Shevchenko, V.I., Walsh, M.B., Allen, P.D., and Lai, F.A. (1996) The human cardiac muscle ryanodine receptor - calcium release channel: Identification, primary structure and topological analysis. *Biochemical Journal* **318**; 477-487

Valdivia, H. H., Kaplan, J.H., Ellis-Davies, G.C. and Lederer, W.J. (1995) Rapid adaptation of cardiac ryanodine receptors: modulation by Mg^{2+} and phosphorylation. *Science* **267**; 1997-2000

Valente, M., Calabrese, F., Thiene, G., Angelini, A., Basso, C., Nava, A. and Rossi, L. (1998) *In vivo* evidence of apoptosis in arrhythmogenic right ventricular cardiomyopathy. *American Journal of Pathology* **152(2)**; 479-84

Vanden Abeele, F., Skryma, R., Shuba, Y., Van Coppenolle, F., Slomianny, C., Roudbaraki, M., Mauroy, B., Wuytack, F. and Prevarskaya, N. (2002) Bcl-2-dependent modulation of Ca^{2+} homeostasis and store-operated channels in prostate cancer cells. *Cancer Cell* **1**; 169-79

Varnava, A.M., Elliott, P.M., Baboonian, C., Davison, F., Davies, M.J. and McKenna, W.J. (2001) Hypertrophic cardiomyopathy: histopathological features of sudden death in cardiac troponin T disease. *Circulation* **104(12)**;1380-4

Varsanyi, M., Sarkozi, S., Szegedi, C., Herzog, A. and Jona, I. (2002) Troponin I converts the skeletal muscle ryanodine receptor into a rectifying calcium release channel. *Federation of European Biochemical Societies Letters* **515(1-3)**; 155-8

Vassilev, P.M., Guo, L., Chen, X.Z., Segal, Y., Peng, J.B., Basora, N., Babakhanlou, H., Cruger, G., Kanazirska, M., Ye, C.P., Brown, E.M., Hediger, M.A. and Zhou, J. (2001) Polycystin-2 is a novel cation channel implicated in defective intracellular $Ca^{(2+)}$ homeostasis in polycystic kidney disease. *Biochemical and Biophysical Research Communications* **23**; 341-50

Vatner, D.E., Sato, N., Kiuchi, K., Shannon, R.P. and Vatner, S.F. (1994) Decrease in myocardial ryanodine receptors and altered excitation-contraction coupling early in the development of heart failure. *Circulation* **90(3)**; 1423-30

Vatta, M., Dumaine, R., Varghese, G., Richard, T.A., Shimizu, W., Aihara, N., Nademanee, K., Brugada, R., Brugada, J., Veerakul, G., Li, H., Bowles, N.E., Brugada, P., Antzelevitch, C. and Towbin, J.A. (2002) Genetic and biophysical basis of sudden unexplained nocturnal death syndrome (SUNDS), a disease allelic to Brugada syndrome. *Human Molecular Genetics* **11(3)**; 337-45

Verkhratsky, A. (2005) Physiology and pathophysiology of the calcium store in the endoplasmic reticulum of neurons. *Physiological Reviews* **85**; 201-79

Viatchenko-Karpinski, S., Terentyev, D., Gyorke, I., Terenteyev, R., Volpe, P., Priori, S.G., Napolitano, C., Nori, A., Williams, S.C. and Gyorke, S. (2004) Abnormal calcium signalling and sudden cardiac death associated with mutation of calsequestrin. *Circulation Research* **94**; 471-7

Viskin, S. and Belhassen, B. (1998) Polymorphic ventricular tachyarrhythmias in the absence of organic heart disease: classification, differential diagnosis, and implications for therapy. *Prognosis in Cardiovascular Disease* **41(1)**; 17-34

Wagenknecht, T., Berkowitz, J., Grassucci, R., Timerman, A.P. and Fleischer, S. (1994) Localization of calmodulin binding sites on the ryanodine receptor from skeletal muscle by electron microscopy. *Biophysical Journal* **67(6)**; 2286-95

Wagenknecht, T., Grassucci, R., Frank, J., Saito, A., Inui, M. and Fleischer, S. (1989) Three-dimensional architecture of the calcium channel/foot structure of sarcoplasmic reticulum. *Nature* **338**; 167-70

Wagenknecht, T. and Radermacher, M. (1995) Three-dimensional architecture of the skeletal muscle ryanodine receptor. *Federation of European Biochemical Societies Letters* **369(1)**; 43-6

Wagenknecht, T. and Radermacher, M. (1997) Ryanodine receptors: structure and macromolecular interactions. *Current Opinion in Structural Biology* **7**; 258-265

Wagenknecht, T., Radermacher, M., Grassucci, R., Berkowitz, J., Xin, H. and Fleischer, S. (1997) Locations of calmodulin and FK506-binding protein on the three-dimensional architecture of the skeletal muscle ryanodine receptor. *Journal of Biological Chemistry* **272**; 32463-32471

Walev, I., Bhakdi, S.C., Hofmann, F., Djonder, N., Valeva, A., Aktories, K. and Bhakdi, S. (2001) Delivery of proteins into living cells by reversible membrane permeabilization with streptolysin-O. *Proceedings of the National Academy of Sciences of the United States of America* **98(6)**; 3185-90

Wang, J.P., Needleman, D.H., Seryshev, A.B., Aghdasi, B., Slavik, K.J., Liu, S.Q., Pedersen, S.E. and Hamilton, SL. (1996) Interaction between ryanodine and neomycin binding sites on Ca^{2+} release channel from skeletal muscle sarcoplasmic reticulum. *Journal of Biological Chemistry* **271(14)**; 8387-93

Wang, Q., Shen, J., Li, Z., Timothy, K., Vincent, G.M., Priori, S.G., Schwartz, P.J. and Keating M.T. (1995) Cardiac sodium channel mutations in patients with long QT syndrome, an inherited cardiac arrhythmia. *Human Molecular Genetics* **4(9)**;1603-7

Wang, S.Q., Stern, M.D., Rios, E. and Cheng, H. (2004) The quantal nature of Ca^{2+} sparks and in situ operation of the ryanodine receptor array in cardiac cells. *Proceedings of the National Academy of Sciences of the United States of America* **101**; 3979-3984

Ward, O.C. (1964) A new familial cardiac syndrome in children. *Journal of the Irish Medical Association* **54**; 103–106

Watkins, H., McKenna, W.J., Thierfelder, L., Suk, J., Anan, R., O'Donoghue, A., Spirito, P., Matsumori, A., Moravec, C.S. Seidman, J.G. and Seidman, C.E. (1995) Mutations in the genes for cardiac troponin T and alpha-tropomyosin in hypertrophic cardiomyopathy. *New England Journal of Medicine* **332(16)**; 1058-64

Watnick, T.J., Jin, Y., Matunis, E., Kernan, M.J. and Montell, C. (2003) A flagellar polycystin-2 homolog required for male fertility in Drosophila. *Current Biology* **13**; 2179-84

Wehrens, .H.T., Lehnart, S.E., Huang, F., Vest, J.A., Reiken, S.R., Mohler, P.J., Sun, J., Guatimosim, S., Song, L., Rosemblit, N., D'Aremiento, J.M., Napolitano, C., Memi, M., Priori, S.G., Lederer, W.J. and Marks, A.R. (2003) FKBP12.6 deficiency and defective calcium release channel (ryanodine receptor) function linked to exercise-induced sudden cardiac death. *Cell* **113**; 829-840

Wehrens, X.H.T., Lehnart, S.E., Reiken, S.R. and Marks, A.R. (2004a) Ca^{2+}/calmodulin-dependent protein kinase II phosphorylation regulates the cardiac ryanodine receptor. *Circulation Research* **94**; 61-70

Wehrens, X.H.T., Lehnart, S.E., Reiken, S.R., Seng, S., Vest, J.A., Cervantes, D., Coromilas, J., Landry, D.W. and Marks, A.R. (2004b) Protection from cardiac arrhythmia through ryanodine receptor - stabilizing protein calstabin2. *Science* **304**; 292-296

Wehrens, X.H.T. and Marks, A.R. (2004) Novel therapeutic approaches for heart failure by normalizing calcium cycling. *Nature Drug Discovery* **3**; 1-9

Wei, S.K., Hanlon, S.U. and Haigney, M.C. (2002) Beta-adrenergic stimulation of pig myocytes with decreased cytosolic free magnesium prolongs the action potential and enhances triggered activity. *Journal of Cardiovascular Electrophysiology* **13(6)**; 587-92

Williams, A. J. (1995) The measurement of the function of ion channels reconstituted into artificial membranes. In Ion Channels : A Practical Approach (ed. R. H. Ashley). Oxford: IRL Press

Williams, A.J., West, D.J. and Sitsapesan, R. (2001) Light at the end of the Ca^{2+}-release channel tunnel: structures and mechanisms involved in ion translocation in ryanodine receptor channels. *Quarterly Reviews of Biophysics* **34(1)**; 61-104

Wit, A.L. and Rosen, M.R. (1983) Pathophysiologic mechanisms of cardiac arrhythmias. *American Heart Journal* **106(4 Pt 2)**; 798-811

Witcher, D.R., McPherson, P.S., Kahl, S.D., Lewis, T., Bentley, P., Mullinnix, M.J., Windass, J.D. and Campbell, K.P. (1994) Photoaffinity labeling of the ryanodine receptor/Ca^{2+} release channel with an azido derivative of ryanodine. *Journal of Biological Chemistry* **269(18)**; 13076-9

Witcher, D.R., Kovacs, R.J., Schulman, H., Cefali, D.C. and Jones, L.R. (1991) Unique phosphorylation site on the cardiac ryanodine receptor regulates calcium channel activity. *Journal of Biological Chemistry* **266**; 11144-11152

Wong, P.W. and Pessah, I.N. (1996) Ortho-substituted polychlorinated biphenyls alter calcium regulation by a ryanodine receptor-mediated mechanism: structural specificity toward skeletal- and cardiac-type microsomal calcium release channels. *Molecular Pharmacology* **49(4)**; 740-51

Xiao, B., Jiang, M.T., Zhao, M., Yang, D., Sutherland, C., Lai, F.A., Walsh, M.P., Warltier, D.C., Cheng, H. and Chen, S.R. (2005) Characterization of a novel PKA phosphorylation site, serine-2030, reveals no PKA hyperphosphorylation of the cardiac ryanodine receptor in canine heart failure. *Circulation Research* **96(8)**; 847-55

Xiao, B., Sutherland, C., Walsh, M.P. and Chen, S.R.W. (2004) Protein kinase A phosphorylation ar Serine-2808 of the cardiac Ca^{2+}-release (ryanodine receptor) does not dissociate 12.6-kDa FK506-binding protein (FKBP12.6). *Circulation Research* **94**; 487-95

Xiao, R.P., Valdivia, H.H., Bogdanov, K., Valdivia, C., Lakatta, E.G. and Cheng, H. (1997) The immunophilin FK506-binding protein modulates Ca^{2+} release channel closure in rat heart. *Journal of Physiology* **500(2)**; 343-54

Xin, H., Senbonmatsu, T., Cheng, D., Wang, Y., Copello, J., Ji, G., Collier, M.L., Deng, K., Jeyakumar, L.H., Magnuson, M.A., Inagami, T., Kotlikoff, M.I. and Fleischer, S. (2002) Oestrogen protects FKBP12.6 null mice from cardiac hypertrophy. *Nature* **416**; 334-337

Xiong, L., Newman, R.A., Rodney, G.G., Thomas, O., Zhang, J., Persechini, A., Shea, M.A., and Hamilton, S.L. (2002) Lobe-dependent regulation of ryanodine receptor type 1 by calmodulin. *Journal of Biological Chemistry* **277**; 40862-40870

Xu, X., Bhat, M.B., Nishi, M., Takeshima, H. and Ma, J. (2000) Molecular cloning of cDNA encoding a drosophila ryanodine receptor and functional studies of the carboxyl-terminal calcium release channel. *Biophysical Journal* **78(3)**; 1270-81

Xu, L., Mann, G. and Meissner, G. (1996) Regulation of cardiac Ca^{2+} release channel (ryanodine receptor) by Ca^{2+}, H^{+}, Mg^{2+}, and adenine nucleotides under normal and simulated ischemic conditions. *Circulation Research* **79**; 1100-1109

Xu, L. and Meissner, G. (1998) Regulation of cardiac muscle Ca^{2+} release channel by sarcoplasmic reticulum lumenal Ca^{2+}. *Biophysical Journal* **75**; 2302-2312

Xu, L. and Meissner, G. (2004) Mechanism of calmodulin inhibition of cardiac sarcoplasmic reticulum Ca^{2+} release channel (ryanodine receptor). *Biophysical Journal* **86**; 797-804

Xu, L., Tripathy, A., Pasek, D.A. and Meissner, G. (1998) Potential for pharmacology of ryanodine receptor/calcium release channels. *Annals of the New York Academy of Sciences* **853**; 130-48

Xu, L., Tripathy, A., Pasek, D.A. and Meissner, G. (1999) Ruthenium red modifies the cardiac and skeletal muscle Ca^{2+} release channels (ryanodine receptors) by multiple mechanisms. *Journal of Biological Chemistry* **274(46)**; 32680-91

Yamaguchi, N., Xin, C. and Meissner, G. (2001) Identification of apocalmodulin and Ca^{2+}-calmodulin regulatory domain in skeletal muscle Ca^{2+} release channel, ryanodine receptor. *Journal of Biological Chemistry* **276(25)**; 22579-85

Yamaguchi, N., Xu, L., Pasek, D.A., Evans, K.E. and Meissner, G. (2003) Molecular basis of calmodulin binding to cardiac muscle Ca^{2+} release channel (ryanodine receptor). *Journal of Biological Chemistry* **278**; 23480-23486

Yamamoto, T., El-Hayek, R. and Ikemoto, N. (2000) Postulated role of interdomain within the ryanodine receptor in Ca^{2+} channel regulation. *Journal of Biological Chemistry* **275**; 11618-11625

Yamamoto, T. and Ikemoto, N. (2002) Peptide probe study of the critical regulatory domain of the cardiac ryanodine receptor. *Biochemical and Biophysical Research Communications* **291**; 1102-1108

Yamamoto, T., Yano, M., Kohno, M., Hisaoka, T., Ono, K., Tanigawa, T., Saiki, Y., Hisamatsu, Y., Ohkusa, T., Matsuzaki, M. (1999) Abnormal Ca^{2+} release from cardiac sarcoplasmic reticulum in tachycardia-induced heart failure. *Cardiovascular Research* **44**; 146-155

Yano, M., Kobayashi, S., Kohno, M., Doi, M., Tokuhisha, T., Okuda, S., Suetsugu, M., Hisaoka, T., Obauashi, M., Ohkusa, T., Kohno, M. and Matsuzaki, M. (2003) FKBP12.6-mediated stabilization of calcium-release channel (ryanodine receptor) as a novel therapeutic strategy against heart failure. *Circulation* **107**; 477-484

Yano, K. and Zarain-Herzberg, A. (1994) Sarcoplasmic reticulum calsequestrins: structural and functional properties. *Molelcular and Cellular Biochemistry* **135(1)**; 61-70

Yano, M., Ono, K., Ohkusa, T., Suetsugu, M., Kohno, M., Hisaoka, T., Kobayashi, S., Hisamatsu, Y., Yamamoto, T., Kohno, M., Noguchi, N., Takasawa, S., Okamoto, H. and

Matsuzaki, M. (2000) Altered stoichiometry of FKBP12.6 versus ryanodine receptor as a cause of abnormal Ca^{2+} leak through ryanodine receptor in heart failure. *Circulation* **102**; 2131-2136

Yin, C.C., Han, H., Wei, R. and Lai, F.A. (2005) Two-dimensional crystallisation of the ryanodine receptor Ca^{2+} release channel on lipid membranes. *Journal of Structural Biology* **149**; 219-224

Yin, C.C. and Lai, F.A. (2000) Intrinsic lattice formation by the ryanodine receptor calcium-release channel. *Nature Cell Biology* **2**; 669-671

Yoshinaga, M., Kamimura, J., Fukushige, T., Kusubae, R., Shimago, A., Nishi, J., Kono, Y., Nomura, Y. and Miyata, K. (1999) Face immersion in cold water induces prolongation of the QT interval and T-wave changes in children with nonfamilial long QT syndrome. *American Journal of Cardiology* **83(10)**; 1494-7

Zahradnikova, A., Minarovic, I., Venema, R.C. and Meszaros, L.G. (1997) Inactivation of the cardiac ryanodine receptor calcium release channel by nitric oxide. *Cell Calcium* **22**; 447-453

Zeng, W., Mak, D.O., Li, Q., Shin, D.M., Foskett, J.K. and Muallem, S. (2003) A new mode of Ca^{2+} signaling by G protein-coupled receptors: gating of IP_3 receptor Ca^{2+} release channels by $G_{\beta\gamma}$. *Current Biology* **13(10)**; 872-6

Zhang, L., Franzini-Armstrong, C., Ramesh, V. and Jones, L.R. (2001) Structural alterations in cardiac calcium release units resulting from overexpression of junctin. *Journal of Molecular and Cellular Cardiology* **33**; 233-247

Zhang, G., Gurtu, V. and Kain, S.R. (1996) An enhanced green fluorescent protein allows sensitive detection of gene transfer in mammalian cells. *Biochemical and Biophysical Research Communications* **227(3)**; 707-11

Zhang, L., Kelley, J., Schmeisser, G., Kobayashi, Y.M. and Jones, L.R. (1997) Complex formation between junctin, triadin, calsequestrin and the ryanodine receptor. *Journal of Biological Chemistry* **272**; 23389-23397

Zhang, T., Maier, L.S., Dalton, N.D., Miyamoto, S., Ross, J., Bers, D., Brown, J.H. (2003a) The $delta_C$ isoform of CaMKII is activated in cardiac hypertrophy and induces dilated cardiomyopathy and heart failure. *Circulation Research* **92**; 912-919

Zhang, J., Liu, Z., Masumiya, H., Wang, R., Jiang, D., Li, F., Wagenknecht, T. and Chen, S.R.W. (2003b) Three-dimensional localization of divergent region 3 of the ryanodine receptor to the clamp-shaped structures adjacent to the FKBP binding sites. *Journal of Biological Chemistry* **278**; 14211-14218

Zhang, H., Zhang, J., Danila, C.I. and Hamilton, S.L. (2003c) A noncontiguous, intersubunit binding site for calmodulin on the skeletal muscle Ca^{2+} release channel. *Journal of Biological Chemistry* **278**; 8348-8355

Zhao, F., Li, P., Chen, W., Louis, C. and Fruen, B.R. (2001) Dantrolene inhibition of ryanodine receptor Ca^{2+} release channels. *Journal of Biological Chemistry* **276**; 13810-13816

Zima, A.V., Copello, J.A. and Blatter, L.A. (2003) Differential modulation of cardiac and skeletal muscle ryanodine receptors by NADH. *Federation of European Biochemical Societies Letters* **547(1-3)**; 32-6

Zimanyi, I. and Pessah, I.N. (1991) Comparison of [^{3}H]ryanodine receptors and Ca^{2+} release from rat cardiac and rabbit skeletal muscle sarcoplasmic reticulum. Journal of Pharmacology and Experimental Therapeutics **256(3)**; 938-46

Ziolo, M.T., Katoh, H. and Bers, D.M. (2001) Expression of inducible nitric oxide synthase depresses Beta-adrenergic stimulated calcium release from the sarcoplasmic reticulum in intact ventricular myocytes. *Circulation* **104**; 2961-2966

Zissimopoulos, S. and Lai, F.A. (2005) Interaction of FKBP12.6 with the cardiac ryanodine receptor C-terminal domain. *Journal of Biological Chemistry* **280(7)**; 5475-85

Zolk, Q., Frohme, M., Maurer, A., Kluxen, F., Hentsch, B., Zubakov, D., Hoheisel, J.D., Zucker, I.H., Pepe, S. and Eschenhagen, T. (2002) Cardiac ankyrin repeat protein, a negative regulator of cardiac gene expression, is augmented in human heart failure. *Biochemical and Biophysical Research Communications* **293**; 1377-1382

Zorzato, F., Fujii, J., Otsu, K., Phillips, M., Green, N.M., Lai, F.A., Meissner, G. and MacLennan, D.H. (1990) Molecular cloning of çDNA encoding human and rabbit forms of the Ca^{2+} release channel (ryanodine receptor) of skeletal muscle sarcoplasmic reticulum. *Journal of Biological Chemistry* **265**; 2244-2256

Zorzato, F., Scutari, E., Tegazzin, V., Clementi, E. and Treves, S. (1993) Chlorocresol: an activator of ryanodine receptor-mediated Ca^{2+} release. *Molecular Pharmacology* **44(6)**; 1192-201

Zorzato, F., Yamaguchi, N., Xu, L., Meissner, G., Muller, C.R., Pouliquin, P., Muntoni, F., Sewry, C., Girard, T., Treves, S. (2003) Clinical and functional effects of a deletion in a COOH-terminal lumenal loop of the skeletal muscle ryanodine receptor. *Human Molecular Genetics* **12**; 379-388

Zucchi, R. and Ronca-Testoni, S. (1997) The sarcoplasmic reticulum Ca^{2+} channel/ryanodine receptor: Modulation by endogenous effectors, drugs and disease states. *Pharmacological Reviews* **49**; 1-51